MCEER
EARTHQUAKE ENGINEERING TO EXTREME EVENTS

U.S. Department of Transportation
Federal Highway Administration

Seismic Isolation of Highway Bridges

By

Ian Buckle, Michael Constantinou,
Murat Dicleli and Hamid Ghasemi

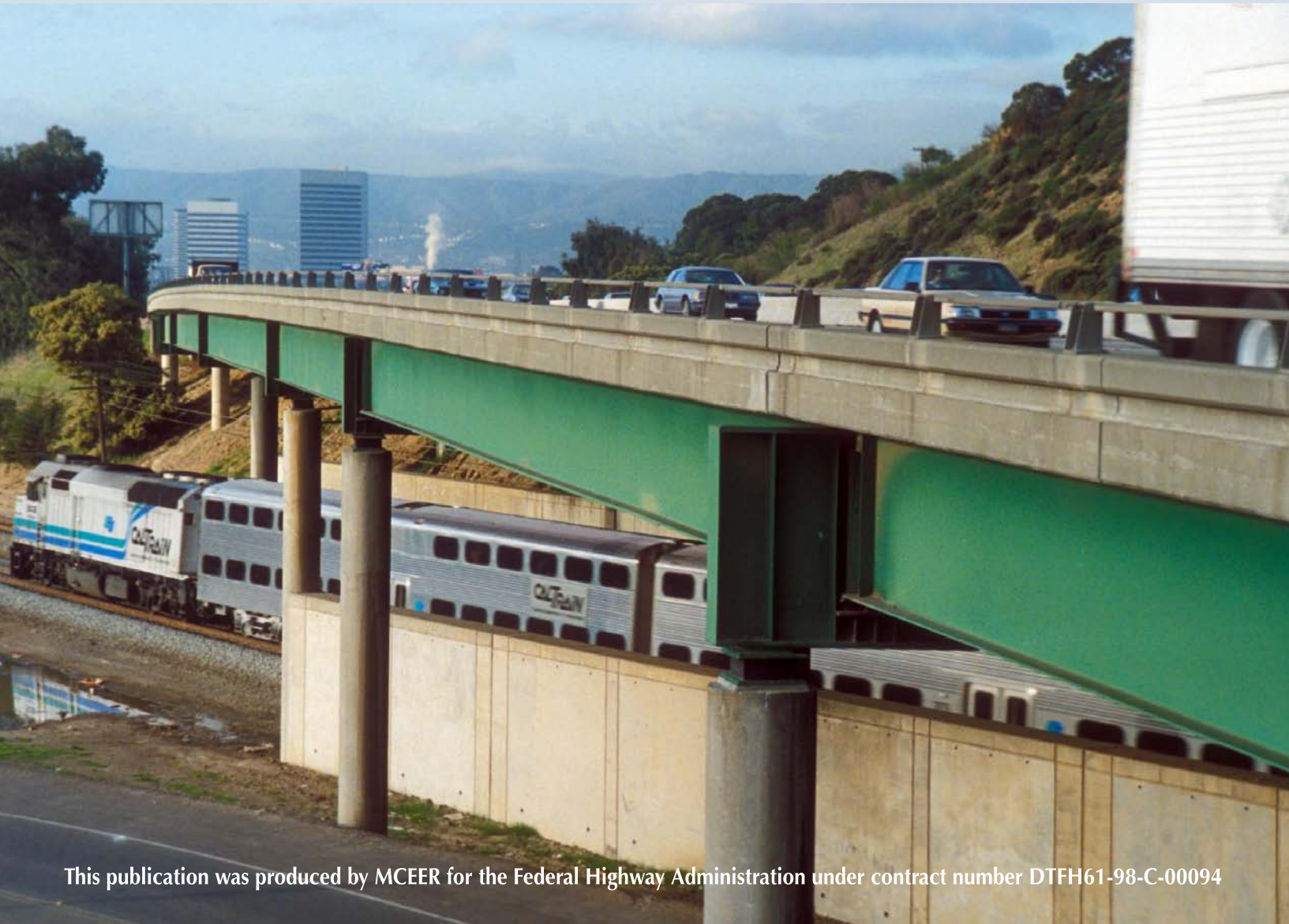

This publication was produced by MCEER for the Federal Highway Administration under contract number DTFH61-98-C-00094

MCEER is a national center of excellence dedicated to establishing disaster-resilient communities through the application of multidisciplinary, multi-hazard research. Headquartered at the University at Buffalo, State University of New York, the Center was originally established by the National Science Foundation (NSF) in 1986, as the National Center for Earthquake Engineering Research (NCEER).

Comprising a consortium of researchers from numerous disciplines and institutions throughout the United States, the Center's mission has expanded from its original focus on earthquake engineering to address a variety of other hazards, both natural and man-made, and their impact on critical infrastructure and facilities. The Center's goal is to reduce losses through research and the application of advanced technologies that improve engineering, pre-event planning and post-event recovery strategies. Toward this end, the Center coordinates a nationwide program of multidisciplinary team research, education and outreach activities.

Funded principally by NSF, the State of New York and the Federal Highway Administration (FHWA), the Center derives additional support from the Department of Homeland Security (DHS)/Federal Emergency Management Agency (FEMA), other state governments, academic institutions, foreign governments and private industry.

MCEER
EARTHQUAKE ENGINEERING TO EXTREME EVENTS

U.S. Department of Transportation
Federal Highway Administration

Seismic Isolation of Highway Bridges

by

Ian G. Buckle,[1] Michael C. Constantinou,[2]
Mirat Dicleli[3] and Hamid Ghasemi[4]

Publication Date: August 21, 2006

Special Report MCEER-06-SP07

Task Number 094-D-3.1

FHWA Contract Number DTFH61-98-C-00094
Contract Officer's Technical Representative: W. Phillip Yen, Ph.D., P.E. HRDI-7
Senior Research Structural Engineer/Seismic Research Program Manager
Federal Highway Administration

1 Department of Civil and Environmental Engineering, University of Nevada Reno
2 Department of Civil, Structural and Environmental Engineering, University at Buffalo, The State University of New York
3 Department of Engineering Sciences, Middle East Technical University
4 Turner Fairbanks Highway Research Center, Federal Highway Administration

MCEER
University at Buffalo, The State University of New York
Red Jacket Quadrangle, Buffalo, NY 14261
Phone: (716) 645-3391; Fax (716) 645-3399
E-mail: *mceer@buffalo.edu*; WWW Site: *http://mceer.buffalo.edu*

SI* (MODERN METRIC) CONVERSION FACTORS

APPROXIMATE CONVERSIONS TO SI UNITS

Symbol	When You Know	Multiply By	To Find	Symbol
		LENGTH		
in	inches	25.4	millimeters	mm
ft	feet	0.305	meters	m
yd	yards	0.914	meters	m
mi	miles	1.61	kilometers	km
		AREA		
in^2	square inches	645.2	square millimeters	mm^2
ft^2	square feet	0.093	square meters	m^2
yd^2	square yard	0.836	square meters	m^2
ac	acres	0.405	hectares	ha
mi^2	square miles	2.59	square kilometers	km^2
		VOLUME		
fl oz	fluid ounces	29.57	milliliters	mL
gal	gallons	3.785	liters	L
ft^3	cubic feet	0.028	cubic meters	m^3
yd^3	cubic yards	0.765	cubic meters	m^3
NOTE: volumes greater than 1000 L shall be shown in m^3				
		MASS		
oz	ounces	28.35	grams	g
lb	pounds	0.454	kilograms	kg
T	short tons (2000 lb)	0.907	megagrams (or "metric ton")	Mg (or "t")
		TEMPERATURE (exact degrees)		
°F	Fahrenheit	5 (F-32)/9 or (F-32)/1.8	Celsius	°C
		ILLUMINATION		
fc	foot-candles	10.76	lux	lx
fl	foot-Lamberts	3.426	candela/m^2	cd/m^2
		FORCE and PRESSURE or STRESS		
lbf	poundforce	4.45	newtons	N
lbf/in^2	poundforce per square inch	6.89	kilopascals	kPa

APPROXIMATE CONVERSIONS FROM SI UNITS

Symbol	When You Know	Multiply By	To Find	Symbol
		LENGTH		
mm	millimeters	0.039	inches	in
m	meters	3.28	feet	ft
m	meters	1.09	yards	yd
km	kilometers	0.621	miles	mi
		AREA		
mm^2	square millimeters	0.0016	square inches	in^2
m^2	square meters	10.764	square feet	ft^2
m^2	square meters	1.195	square yards	yd^2
ha	hectares	2.47	acres	ac
km^2	square kilometers	0.386	square miles	mi^2
		VOLUME		
mL	milliliters	0.034	fluid ounces	fl oz
L	liters	0.264	gallons	gal
m^3	cubic meters	35.314	cubic feet	ft^3
m^3	cubic meters	1.307	cubic yards	yd^3
		MASS		
g	grams	0.035	ounces	oz
kg	kilograms	2.202	pounds	lb
Mg (or "t")	megagrams (or "metric ton")	1.103	short tons (2000 lb)	T
		TEMPERATURE (exact degrees)		
°C	Celsius	1.8C+32	Fahrenheit	°F
		ILLUMINATION		
lx	lux	0.0929	foot-candles	fc
cd/m^2	candela/m^2	0.2919	foot-Lamberts	fl
		FORCE and PRESSURE or STRESS		
N	newtons	0.225	poundforce	lbf
kPa	kilopascals	0.145	poundforce per square inch	lbf/in^2

*SI is the symbol for the International System of Units. Appropriate rounding should be made to comply with Section 4 of ASTM E380.

(Revised March 2002)

EXECUTIVE SUMMARY

Seismic isolation is a response modification technique that reduces the effects of earthquakes on bridges and other structures. Isolation physically uncouples a bridge superstructure from the horizontal components of earthquake ground motion, leading to a substantial reduction in the forces generated by an earthquake. Improved performance is therefore possible for little or no extra cost, and older, seismically deficient bridges may not need strengthening if treated in this manner. Uncoupling is achieved by interposing mechanical devices with very low horizontal stiffness between the superstructure and substructure. These devices are called seismic isolation bearings or simply isolators. Thus, when an isolated bridge is subjected to an earthquake, the deformation occurs in the isolators rather than the substructure elements. This greatly reduces the seismic forces and displacements transmitted from the superstructure to the substructures.

More than 200 bridges have been designed or retrofitted in the United States using seismic isolation in the last 20 years, and more than a thousand bridges around the world now use this cost- effective technique for seismic protection.

This manual presents the principles of isolation for bridges, develops step-by step methods of analysis, explains material and design issues for elastomeric and sliding isolators, and gives detailed examples of their application to standard highway bridges. Design guidance is given for the lead-rubber isolator, the friction-pendulum isolator, and the Eradiquake isolator, all of which are found in use today in the United States. Guidance on the development of test specifications for these isolators is also given.

This document is intended to supplement the *Guide Specifications for Seismic Isolation Design* published by the American Association of State Highway and Transportation Officials, Washington, DC, in 1999. Every attempt is made with the procedures, descriptions and examples presented herein, to be compatible with these specifications. It is not intended that this Manual replace the Guide Specifications, but should, instead, be read in conjunction with these Specifications.

ACKNOWLEDGEMENTS

The authors are grateful for the financial support received from the Federal Highway Administration (FHWA) during the preparation of this Manual. This assistance was primarily provided through the Highway Project at the Multidisciplinary Center for Earthquake Engineering Research (MCEER) at the University at Buffalo. The FHWA Office of Infrastructure Research and Development at the Turner-Fairbank Highway Research Center was instrumental in the preparation of the design examples for the friction-pendulum isolator. The advice and encouragement of the MCEER Highway Seismic Research Council (an advisory committee to the Highway Project) is also gratefully acknowledged.

The content of this Manual closely follows that of the 1999 *AASHTO Guide Specification for Isolation Design*, and the authors wish to recognize the ground-breaking effort of the nine-member AASHTO panel that prepared this document under the T-3 Committee chairmanship of James Roberts and the panel chairmanship of Roberto LaCalle, both of Caltrans.

Technical assistance was also received from the Tun Abdul Razak Laboratory (formerly Malayasian Rubber Producers' Research Association), Dynamic Isolation Systems, California, Earthquake Protection Systems, California, and R.J. Watson, New York.

TABLE OF CONTENTS

TABLE OF CONTENTS (CONTINUED)

TABLE OF CONTENTS (CONTINUED)

TABLE OF CONTENTS (CONTINUED)

TABLE OF CONTENTS (CONTINUED)

LIST OF FIGURES

LIST OF FIGURES (CONTINUED)

LIST OF TABLES

LIST OF ACRONYMS

AASHTO	American Association of State Highway and Transportation Officials
ASCE	American Society of Civil Engineers
ASME	American Society of Mechanical Engineers
ATC	Applied Technology Council
Caltrans	California Department of Transportation
DIS	Dynamic Isolation Systems
DL	Dead Load
DOT	Department of Transportation
EDC	Energy Dissipated per Cycle
EPS	Earthquake Protection System
EQS	Eradiquake Bearing
FEMA	Federal Emergency Management Agency
FHWA	Federal Highway Administration
FPS	Friction Pendulum System
HDRB	High Damping Rubber Bearing
HITEC	Highway Innovative Technology Evaluation Center
IBC	International Building Code
LDRB	Low Damping Rubber Bearing
LL	Live Load
LRB	Lead Rubber Bearings
MER	Mass Energy Regulators
NEHRP	National Earthquake Hazard Reduction Program
NRB	Natural Rubber Bearing
PTFE	Polytetrafluoroethylene (Teflon)
RJW	RJ Watson
SEP	Seismic Energy Products
SPC	Seismic Performance Category
SRSS	Square Root of the Sum of the Squares

CHAPTER 1: INTRODUCTION

1.1 BASIC PRINCIPLES OF SEISMIC ISOLATION

Seismic isolation is a response modification technique that reduces the effects of earthquakes on bridges and other structures. Isolation physically uncouples a bridge superstructure from the horizontal components of earthquake ground motion, leading to a substantial reduction in the forces generated by an earthquake. Improved performance is therefore possible for little or no extra cost, and older, seismically deficient bridges may not need strengthening if treated in this manner. Uncoupling is achieved by interposing mechanical devices with very low horizontal stiffness between the superstructure and substructure as shown in figure 1-1. These devices are called seismic isolation bearings or simply isolators. Thus, when an isolated bridge is subjected to an earthquake, the deformation occurs in the isolators rather than the substructure elements. This greatly reduces the seismic forces and displacements transmitted from the superstructure to the substructures. More than 200 bridges have been designed or retrofitted in the United States using seismic isolation in the last 20 years, and more than a thousand bridges around world now use this cost- effective technique for seismic protection.

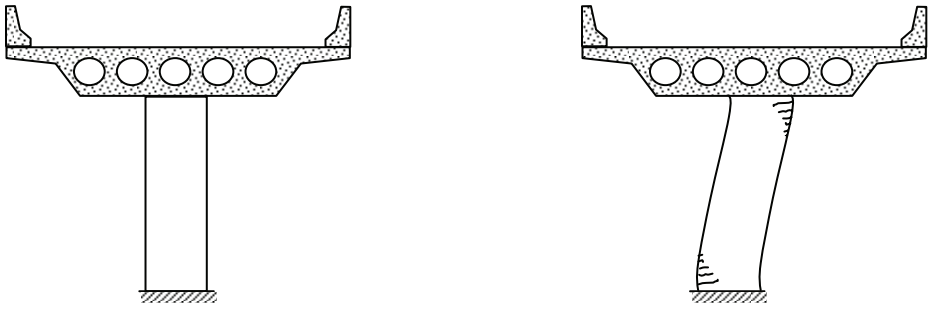

(a) Conventional bridge where deformation occurs in substructure.

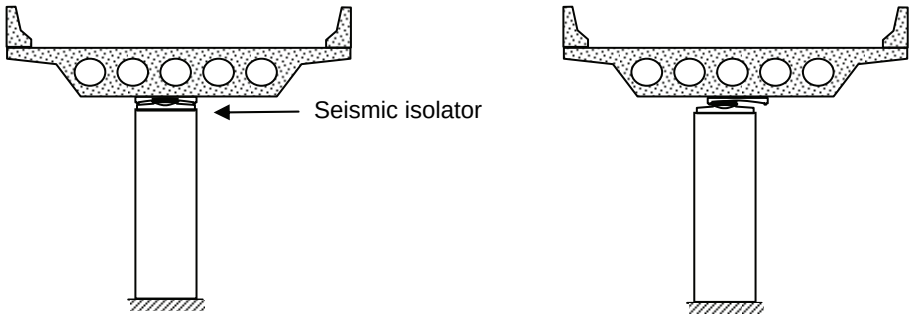

(b) Seismically isolated bridge where deformation occurs in the isolator.

Figure 1-1. Comparison of a Conventional and Seismically Isolated Bridge

As a minimum, a seismic isolator possesses the following three characteristics:

- Flexibility to lengthen the period of vibration of the bridge to reduce seismic forces in the substructure.
- Energy dissipation to limit relative displacements between the superstructure above the isolator and the substructure below.
- Adequate rigidity for service loads (e.g. wind and vehicle braking) while accommodating environmental effects such as thermal expansion, creep, shrinkage and prestress shortening.

1.1.1 FLEXIBILITY

The low horizontal stiffness of a seismic isolator changes the fundamental period of a bridge and causes it to be much longer than the period without isolation (the so-called 'fixed-base' period). This longer period is chosen to be significantly greater than the predominant period of the ground motion and the response of the bridge is reduced as a result. The effect of isolator flexibility on bridge response is illustrated in figure 1-2. The figure shows the AASHTO (1999) acceleration response spectrum (or seismic response coefficient) for stiff soil conditions (Soil Type II) and 5 percent damping. The spectrum is normalized to the peak ground acceleration. It is seen that a period shift from 0.5 to 1.5 second, due to the flexibility of the isolation system, results in a 60 percent reduction (approximately) in the seismic forces (the normalized spectral acceleration drops from 2.5 to 1.0).

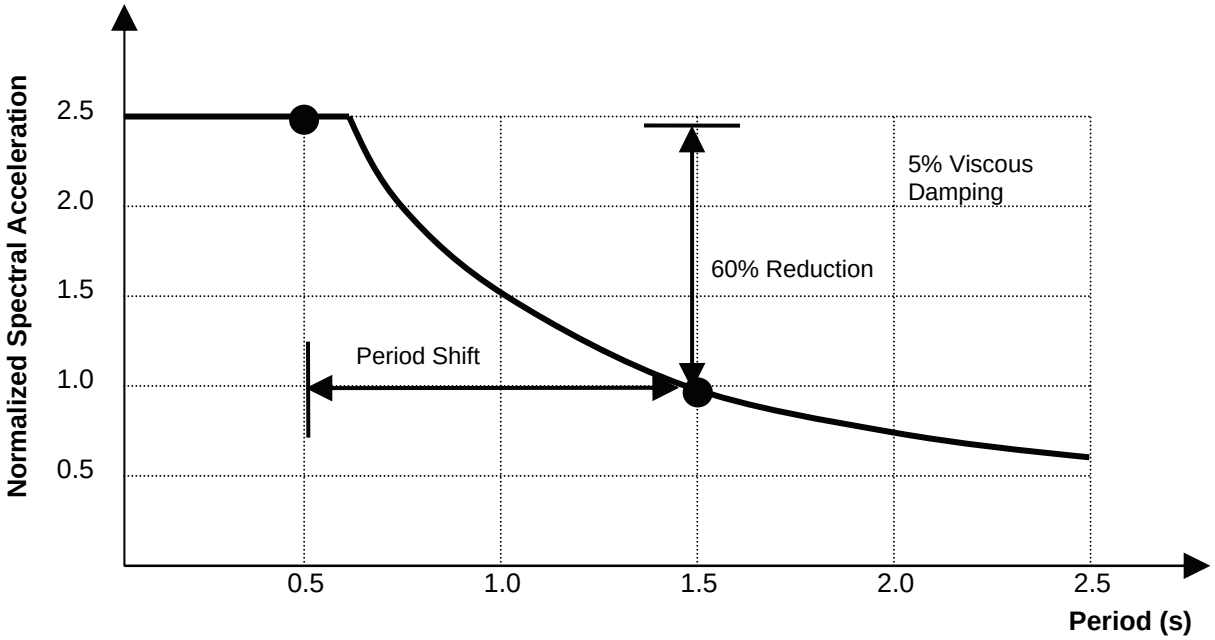

Figure 1-2. Effect of Isolator Flexibility on Bridge Response

1.1.2 ENERGY DISSIPATION

Although the low horizontal stiffness of seismic isolators leads to reduced seismic forces, it may result in larger superstructure displacements. Wider expansion joints and increased seat lengths may be required to accommodate these displacements. As a consequence, most isolation systems include an energy dissipation mechanism to introduce a significant level of damping into the bridge to limit these displacements to acceptable levels. These mechanisms are frequently hysteretic in nature, which means that there is an offset between the loading and unloading force-displacement curves under reversed (cyclic) loading. Energy, which is not recovered during unloading, is mainly dissipated as heat from the system. For instance, energy may be dissipated by friction in a mechanism that uses sliding plates. Figure 1-3 shows a bilinear force-displacement relationship for a typical seismic isolator that includes an energy dissipator. The hatched area under the curve is the energy dissipated during each cycle of motion of the isolator.

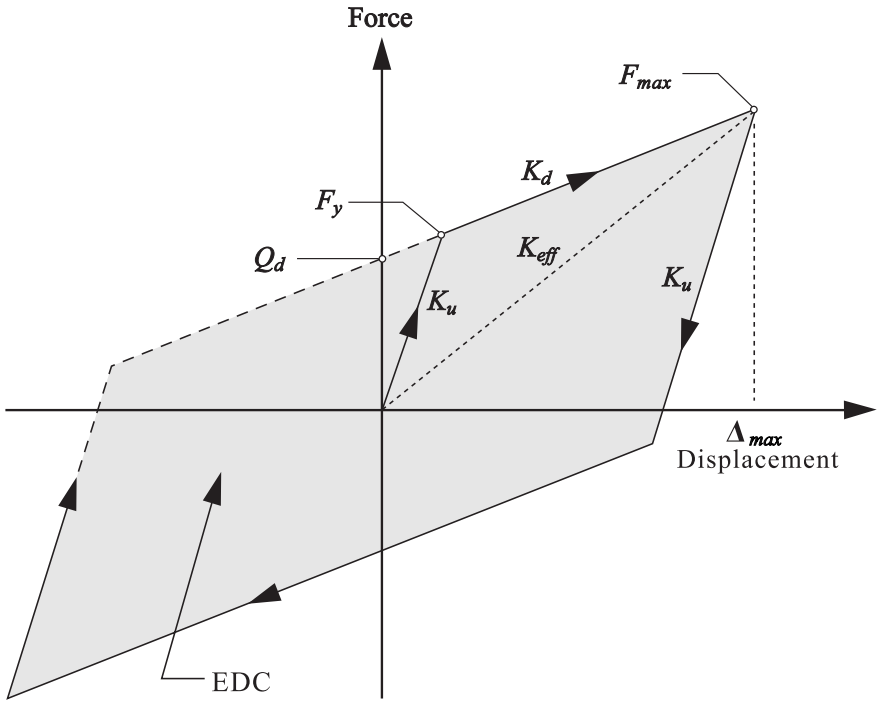

Q_d = Characteristic strength
F_y = Yield force
F_{max} = Maximum force
K_d = Post-elastic stiffness
K_u = Elastic (unloading) stiffness
K_{eff} = Effective stiffness
Δ_{max} = Maximum bearing displacement
EDC = Energy dissipated per cycle = Area of hysteresis loop (shaded)

Figure 1-3. Bilinear Hysteresis Loop (AASHTO 1999)

Analytical tools for these nonlinear systems are available using inelastic time-history structural analysis software packages. But these tools can be cumbersome to use and not always suitable for routine design office use. Simplified methods have therefore been developed which use effective elastic properties and an equivalent viscous dashpot to represent the energy dissipation. The effective stiffness (k_e) is defined in figure 1-3. The equivalent viscous damping ratio (β_e) is calculated as explained below.

The equivalent viscous damping ratio, β_e, is calculated such that the energy dissipated in each cycle of motion of the dashpot is the same as that for the hysteretic device. This is achieved by setting the area under the force-displacement loop of figure 1-4, which represents the energy dissipated due to viscous damping, equal to the area under the hysteresis curve of figure 1-3. It can then be shown that:

$$\beta_e = \frac{Hysteretic\,Energy\,Dissipated}{2\pi k_e D_{\max}^2} \tag{1-1}$$

where k_e and D_{max} are the effective elastic stiffness and maximum displacement of the isolation system as shown in figure 1-3.

Not only are displacements reduced with the increase in damping, but seismic forces are also reduced, compared to say the forces given by a 5 percent-damped spectrum. Figure 1-5 illustrates this effect. The solid and dashed curves represent the 5 percent- and 30 percent-damped AASHTO (1999) acceleration response spectra respectively, for stiff soil conditions (Soil Type II). The increased level of damping, due to the energy dissipated by the isolation system, leads to a further reduction in the seismic forces. It is seen that the 60 percent reduction at a period of 1.5 secs, due to flexibility, may increase to 77 percent when the damping increases from 5 percent to 30 percent.

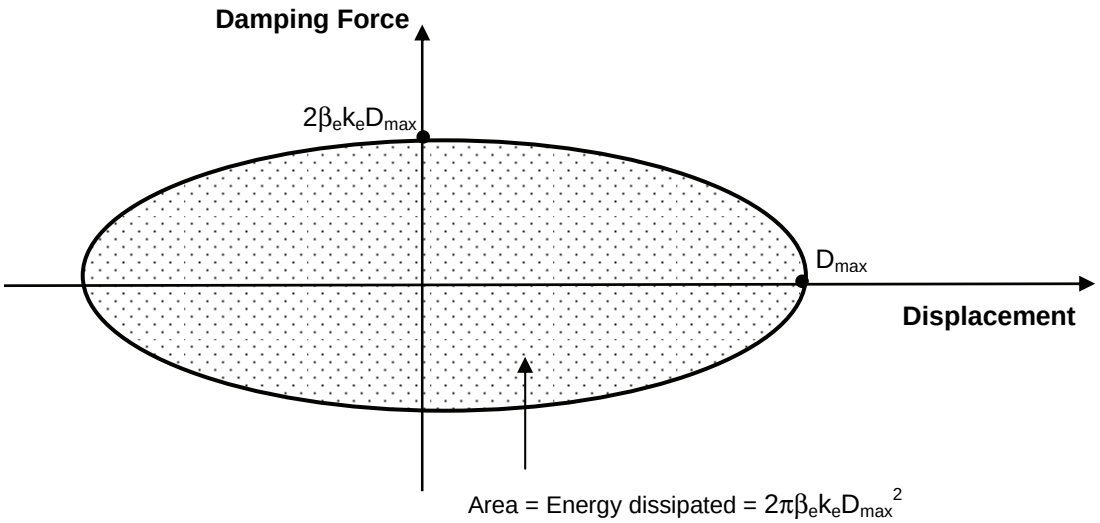

Figure 1-4. Force-displacement Loop for Viscous Damper Excited at a Frequency Equal to Natural Frequency of Isolated Bridge

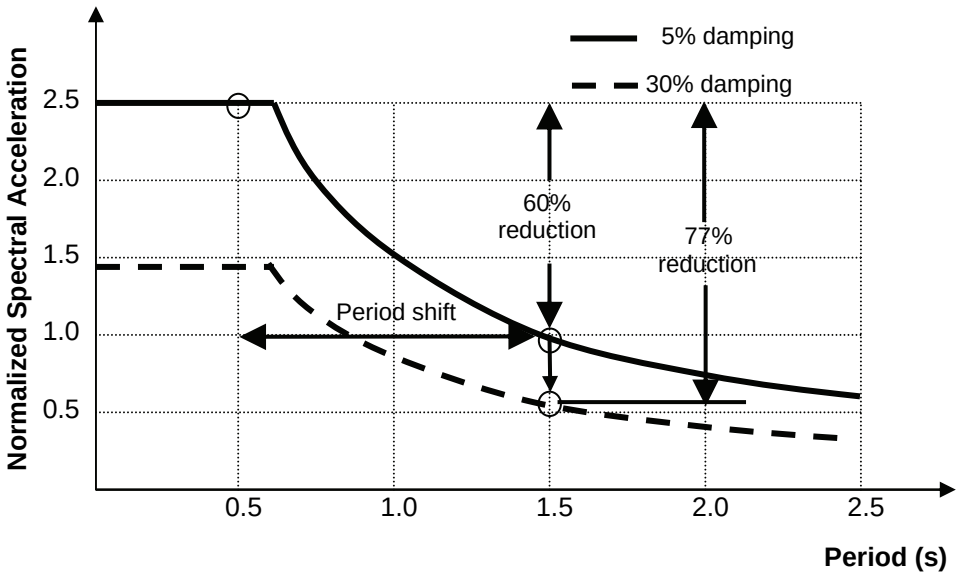

Figure 1-5. Effect of Damping on Bridge Response

1.1.3 RIGIDITY UNDER SERVICE LOADS

The lateral flexibility of a seismic isolator may allow the superstructure to move unacceptably under service loads, such as wind or vehicle braking forces. Resistance to these forces is important and the dual requirement of rigidity for service loads and flexibility for earthquake loads is accommodated in a variety of ways. For example, devices that are elastic for wind loads but yield under seismic loads are commonly used. For the same reason, friction devices are popular because the friction coefficient can be adjusted to resist wind load without sliding. It follows that if the wind load is greater than the earthquake load, isolation will not be practical. This is rarely the case in bridge applications but can occur for high-rise buildings.

1.2 SEISMIC ISOLATORS

Seismic isolators may generally be classified in one of two categories: those that use elastomeric components and those that use sliding components. The majority of bridge isolators in the United States are elastomeric-based, with or without a lead core for energy dissipation. These are the so-called lead-rubber bearings (LRB). Sliding isolators are also used and the most common types are the friction pendulum and the Eradiquake bearing. The former is the FPS isolator and uses friction as the energy dissipator. The latter (also known as the EQS isolator) and also uses friction as the dissipator. Figure 1-6 shows schematic details of these three isolator types.

The selection of isolator type is an important decision and should involve careful consideration of a number of factors. These include:

- Axial load to be carried (sliding systems generally have greater capacity than elastomeric devices for axial loads).

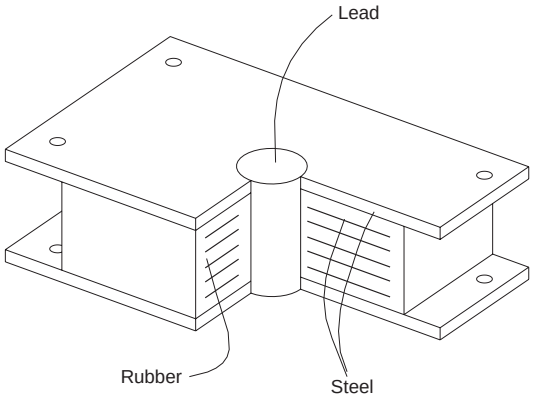

(a) Lead-Rubber Isolator

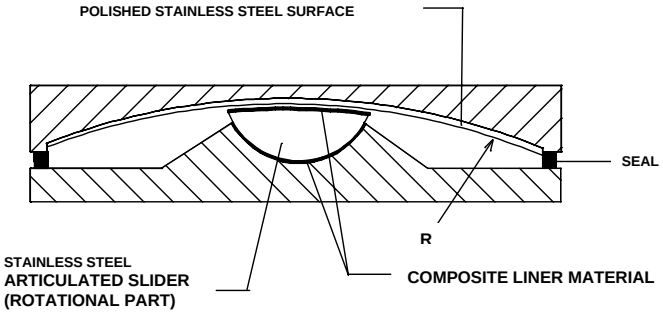

(b) Friction Pendulum Isolator

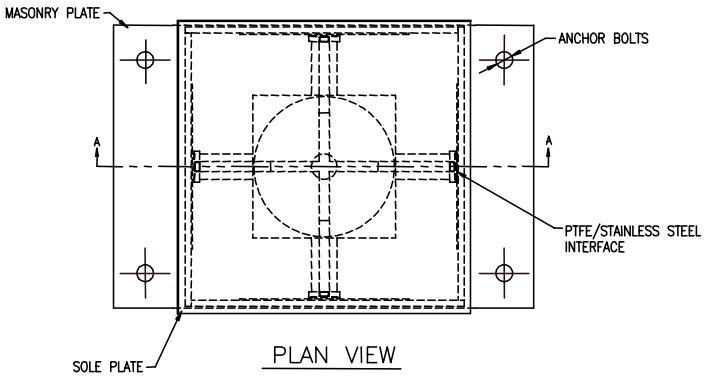

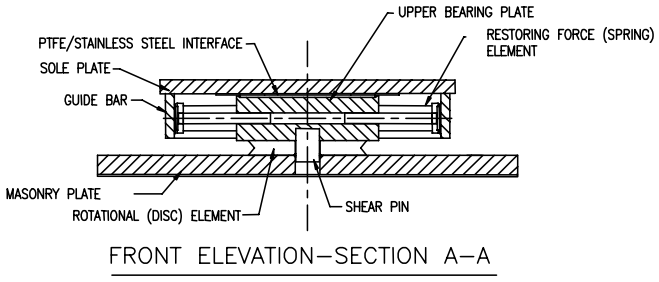

(c) Eradiquake Isolator

Figure 1-6. Three Types of Seismic Isolators used for the Earthquake Protection of Bridges

- Available clearances (isolators with higher damping ratios, such as lead-rubber bearings, have smaller displacement demands).
- Available space (sliding systems generally have lower profiles than elastomeric devices which may be important in retrofit situations).
- Service loads to be resisted and environmental movements to be accommodated (wind, vehicle braking, thermal expansion, creep, shrinkage…).
- Reliability (stability of properties under adverse field conditions over long periods of time).

With regard to the last two bullets, an isolator must be stiff enough to provide resistance to lateral loads due to wind and vehicle braking. In addition to the elasto-plastic and friction devices noted above, lock-up devices and elastomers which soften with increasing shear strain, have been used to resist service loads.

At the same time, the movement of the superstructure due to temperature variations, creep, shrinkage and the like, must be accommodated without over-stressing the substructures. This requires stable properties under adverse field conditions for long periods of time and this fact alone can determine the choice of isolator. The ideal isolator is maintenance free, does not require precise field tolerances to operate successfully, and is constructed from materials that are chemically inert and resistant to atmospheric pollutants, ultra-violet radiation, and de-icing salts.

Assurance that an isolator will perform in an earthquake, as intended by the designer, is also crucial. It may be many years before the design earthquake occurs, and stable isolator properties are required for this reason as well as the environmental issues noted above. Guidance is available (e.g., AASHTO 1999) to help the designer consider the effects of aging, temperature, wear, contamination, and scragging on isolator performance.

1.3 SCOPE OF MANUAL

This Manual is based on the *Guide Specifications for Seismic Isolation Design* published by the American Association of State Highway and Transportation Officials, Washington DC (AASHTO 1999). The material presented herein is intended to be compatible with these specifications. It is not intended that this Manual replace the Guide Specifications but should, instead, be read in conjunction with these Specifications.

The scope of the manual includes information on the principles of isolation, the benefits to be expected for new and existing bridges, a summary of applications to bridges in the United States, simplified methods of analysis for isolated bridges, detailed information on elastomeric and sliding isolators, guidance on testing specifications for the manufacture of isolators, and detailed design examples for the three commonly available isolators in the United States: the lead-rubber isolator, the friction pendulum isolator and the Eradiquake isolator.

CHAPTER 2: APPLICATIONS

2.1 EARLY APPLICATIONS

2.1.1 SOUTH RANGITIKEI RAIL BRIDGE, NEW ZEALAND

One of the earliest applications of 'modern' isolation was to the South Rangitikei Rail Bridge in New Zealand. Constructed in 1974, this 315 m long six span bridge carries a single track of the main north-south rail line across the South Rangitikei River gorge using rocking piers that average 70 m in height. The superstructure is a continuous prestressed box girder supported monolithically on slender, double stem, reinforced concrete piers (figure 2-1). The location is highly seismic and the designers had difficulty meeting the requirements of the current code, i.e., to provide adequate capacity for the bending moments and shears at the base of the piers, during a transverse earthquake.

It became apparent that an alternative design strategy was required and the most attractive option was to allow the structure to rock (or step) transversely, thereby reducing the moments and shears to be resisted. By allowing the piers to step, with each leg lifting vertically off the pile cap, one-at-a-time, the rocking period became considerable longer than the fixed base period, and the induced seismic forces were correspondingly reduced. In this way, the piers could remain elastic, reinforcing steel could be reduced, and the pier cross sections could be smaller, with consequential cost savings.

The arguments in favor of isolating the bridge (by allowing it to rock) were compelling and justified the investigation of the engineering implications of isolating this bridge, the first bridge of its type in New Zealand.

An essential element in the design was to control the transverse movements of the superstructure during rocking to prevent the structure overturning. The solution was to add a pair of mild steel torsion bar dissipators at the base of each pier leg. These devices act to dampen the upward movements of the legs and provide an ultimate stop against excessive vertical travel of the leg. Gravity loads are transferred to the pile cap by pairs of elastomeric pads. It is expect that wind loads may activate the dissipators but only in their elastic range. Their high initial stiffness will keep deflections to acceptable limits under in-service conditions. Twenty torsion bars have been installed, each with a characteristic yield strength of 400 kN and a total stroke of 80 mm.

Factors favoring the isolation of this bridge include the:

- Isolation mechanism is very simple and judged to be reliable with minimum maintenance requirements, and no mechanical parts that need precise alignment or regular servicing.
- Dampers use conventional mild steel, a proven material with well-established yield properties.
- Several full scale prototype dampers were tested during feasibility design, to study their strain-hardening characteristics and low-cycle fatigue behavior.

- Extensive analysis of the stepping bridge was carried out using nonlinear numerical simulation tools to gain confidence in the design and understand potential limit states.
- Significant cost savings were possible compared to a conventional capacity design approach.

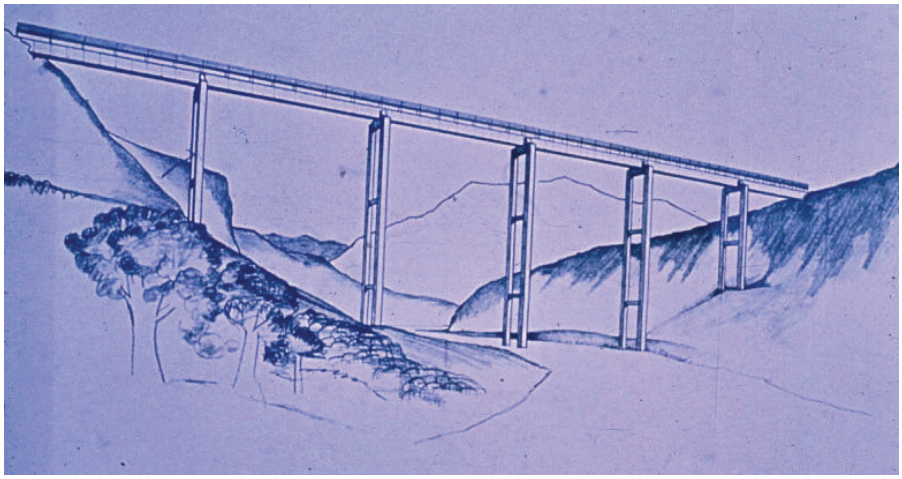

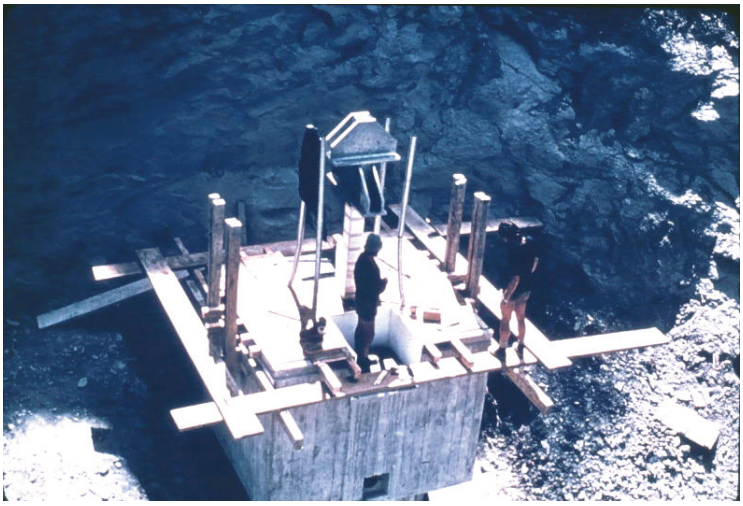

(a) Above Left: Schematic view

(b) Above: Elevation of stepping pier

(c) Left: Construction of pile cap and installation of torsion bar dissipator

Figure 2-1. South Rangitikei Rail Bridge, Mangaweka, New Zealand

2.1.2 SIERRA POINT OVERHEAD, CALIFORNIA

The first bridge to be isolated in the United States was the Sierra Point Overhead on US 101 near San Francisco. This highly skewed structure consists of 10 simply supported spans of steel girders with concrete slabs, seated on stand-alone, 3 ft diameter, reinforced concrete columns. The spans range from 26 to 100 ft. This bridge was constructed in the 1950's and had nonductile columns and inadequate seat widths at the girder supports. Isolation was chosen as the preferred retrofit scheme and existing steel bearings were replaced by 15 in-square lead-rubber isolators at the tops of all the columns and on the abutment seats. The reduction in seismic loads, due to the isolation, was sufficiently great that no column jacketing or foundation strengthening was necessary, for the 'design' earthquake ground motions. The bridge was isolated in 1985 and was subject to shaking during the Loma Prieta earthquake in 1989. Although instrumented with four strong motion instruments, records were inconclusive due to high frequency 'noise' in the steel superstructure. The bridge was however undamaged with no visible signs of distress (cracking or residual displacement).

(a) Above: Single column with existing steel bearing before retrofit.

(b) Left: Replacement of existing steel bearing with lead-rubber isolator.

(c) Above: Isolator installation on single column substructures

Figure 2-2. Sierra Point Overhead US 101, near San Francisco

2.2 RECENT APPLICATIONS

It is believed that the number of isolated bridges in North America is in excess of 200. Since a central registry is not maintained, this number is not known with certainty. Aiken and Whittaker compiled a list in 1996 and working from their database and soliciting new entries from the manufacturers of isolation bearings in the United States, an updated list has been compiled and given in appendix A. Based on this information, there are at least 208 isolated bridges in North America (United States, Canada, Mexico, and Puerto Rico). This number includes completed bridges but excludes those under construction or still in design. Twenty-five states have isolated bridges and six of these states have more than 10 such bridges, accounting for about 60 percent of the population of isolated bridges. Table 2-1 lists these six states and the number of isolated bridges in each. As might be expected, California, with its high seismic risk, leads the list with 13 percent of the total number of applications. But of interest is the fact that about 40 percent of the applications are in the four eastern states of New Jersey, New York, Massachusetts and New Hampshire, states with relatively low seismic risk.

Table 2-1. States with More Than Ten Isolated Bridges (April 2003)

STATE	Number of isolated bridges	Percentage of total number of isolated bridges in North America[1]
California	28	13%
New Jersey	23	11%
New York	22	11%
Massachusetts	20	10%
New Hampshire	14	7%
Illinois	14	7%
TOTAL	121	59%

NOTE **1.** United States, Canada, Mexico and Puerto Rico

About three-quarters of the isolated bridges in the U.S. use lead-rubber isolators, and a little under one-quarter use the EradiQuake isolator. Table 2-2 gives the breakdown of applications by isolator type**.**

2.2.1 TRENDS IN SEISMIC ISOLATORS

In the last decade there has been a marked increase in the size and capacity of isolators being manufactured and used in bridge design and retrofitting. Most of these applications have been to major structures and some notable examples are summarized in table 2-3. A decade ago, the largest elastomeric isolator in the U.S. was limited by the fabricator's know-how, to units that

Table 2-2. Bridge Applications by Isolator Type

ISOLATOR	Applications (percent of total number of isolated bridges in North America)
Lead-rubber isolator	75%
Eradiquake isolator	20%
Other: Friction pendulum system, FIP isolator, High damping rubber, Natural rubber bearing	5%

were about 24 inches square. Today the upper limit seems to be in the 45-55 inch range with load capacities approaching 2,500 K. Some very long structures have also been isolated with large numbers of moderate-to-large size isolators being used. For example the JFK Airport Light Rail access structure in New York is an isolated viaduct, 10 miles in length with 1300 lead-rubber isolators ranging up to 900 K capacity (figure 2-3).

Figure 2-3. Lead-rubber Isolators being Installed in the JFK Airport Light Rail Viaduct, New York

Even greater load capacities are possible with sliding isolators. For example a set of 13-foot diameter friction pendulum isolators have been installed in the Benecia-Martinez bridge in California which have an axial capacity of 5,000 K (figure 2-4). Another example is the set of isolators provided for a pair of bridges over the Corinth Canal in Greece (Constantinou 1998). As shown in figure 2-5, each of these bridges consists of a continuous prestressed concrete box girder supported on abutments by six elastomeric bearings, and at each of two piers by a single sliding bearing. The design was complicated by the fact that the site is in an area of high seismicity, has geological faults in close vicinity and the banks of the canal were of uncertain stability.

Figure 2-4. Friction Pendulum Isolator being Installed in the Benecia-Martinez Bridge, California

A preliminary design called for straight bridges and piers placed as close as possible to the banks so as to reduce the length of the middle span and consequentially the depth of the girder section. By placing the piers at a distance of 110 m apart, designing a deep

Table 2-3. Examples of Bridges with Large Isolators

BRIDGE	No. of Isolators and Type[1]	Isolator Dimensions	Axial Load capacity	Remarks
JFK Airport Light Rail Elevated Structure, NY	1300 LRB	18 - 29 in dia	300 – 900 K	600 spans 10 miles total length
Coronado San Diego, CA	54 LRB	41.5 in dia	1,550 K	11 in dia lead core 25 in displ capacity
Benecia-Martinez I-680 Crossing San Francisco Bay, CA	22 FPS	13 ft dia	5,000 K	10 spans Weight 40K / isolator 53 in displ capacity 5 sec isolated period
Memphis I-40 Crossing Mississippi R	18 FPS and LRB		1,000 K	3 miles total length 2, 900ft spans isolated with FPS 24 in displ capacity 4-5 sec isolated period 7 spans isolated with LRB
Boones Bridge, Clackamas Co, OR	32 EQS	37 - 50 in sq	375 - 950 K	5 spans 1137 ft total length
Regional Road 22 / Highway 417 Ontario Canada	6 EQS	36 – 45 in sq	650 -1,500 K	2 spans 240 ft total length
Corinth Canal, Greece	4 flat sliding isolators 12 elastomeric isolators		13,300 K 1,102 K	Pair curved, 3-span bridges Single large sliding isolator at each pier 3 elastomeric isolators at each abutment

NOTE: 1. LRB = Lead-rubber isolator, FPS = Friction-pendulum isolator, EQS = Eradiquake isolator

foundation and utilizing an isolation system, a satisfactory design was achieved. This early design used a lead-rubber isolation system with four such bearings at each pier location. During the final design, it was decided to use two rather than four bearings at each pier due, primarily, to uncertainties in the distribution of axial load on the bearings. With further refinement in the analysis, it became apparent that the combination of transverse seismic loading and vertical earthquake could cause uplift to one of the two pier bearings and significant overloading of the other bearing. Accordingly, a decision was made to use a single bearing at each pier, provide the bridge with curvature and utilize counterweights in order to completely eliminate bearing uplift problems at the abutment bearings under all possible loading combinations. The maximum design load was 13,300 K (60,400 kN) for the sliding bearings and 1,012 K (4,600 kN) for the elastomeric bearings.

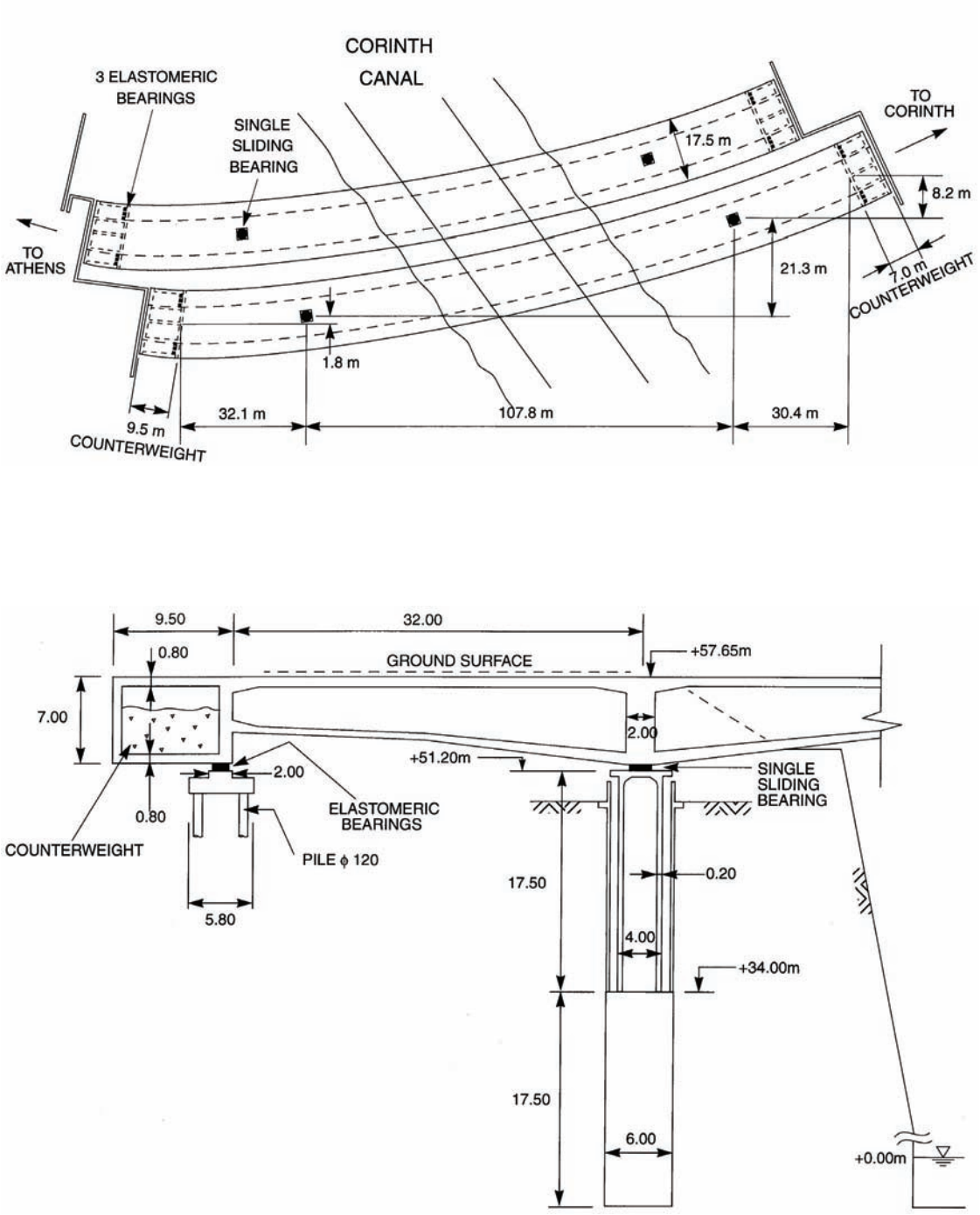

Figure 2-5. Plan and Elevation of Corinth Canal Highway Bridges

2.3 PERFORMANCE OF ISOLATED BRIDGES IN RECENT EARTHQUAKES

There is a general lack of field data quantifying the performance of full-scale isolated structures (buildings and bridges) during strong earthquakes. The evidence available to date is generally for low-to-moderate shaking and performance has either been as expected, or the results have been inconclusive. See for example, section 2.1.2 for a note on the performance of the Sierra Point Overhead during the Loma Prieta Earthquake near San Francisco in 1989. The one known exception to this statement about satisfactory performance, is the response of the Bolu Viaduct during the Duzce Earthquake in Turkey in 1999. This behavior is described in the next section.

2.3.1 BOLU VIADUCT, TURKEY

The Bolu Viaduct comprises two parallel bridges on the Trans European Motorway in central Turkey, At the time of the Duzce earthquake in November 1999, it was structurally complete but not open to traffic (figure 2-6). About 2.3 km in total length, one bridge has 58, 39 m spans and the other has 59 spans. Pier heights range from 10 to 49 m. The superstructure is constructed in 10 span segments, each with seven prestressed concrete hollow box-beams, set on pot sliding bearings with stainless steel / PTFE sliders.

Steel energy dissipating units are used at each pier, in parallel with the sliding bearings, to comprise a seismic isolation system for the viaduct. These dissipators contain yielding steel crescent-shaped elements (figure 7-2) and some have shock transmission units that act as longitudinal shear keys during extreme motions. Transverse shear keys are also provided. Essentially the isolation system comprises a set of flat sliders in parallel with a number of hysteretic steel dampers, but without a strong restoring force mechanism.

Figure 2-6. Bolu Viaduct, Trans European Motorway, Turkey

During the Ducze earthquake (M=7.2), fault rupture occurred directly beneath the bridge at an oblique angle between piers 45 and 47. The offset has been estimated at 1.5 m in the fault parallel direction, and peak accelerations and velocities, based on near-field theoretical models, have been estimated at 0.5g and 60 cm/sec, respectively.

No span collapsed during this strong shaking, but the isolators and dissipators were severely damaged or destroyed and have since been replaced. Several spans shifted on their pier caps and many of the shear keys failed (figure 2-7). Post-earthquake evaluations have since indicated that excessive displacements of the superstructure, relative to the piers, exhausted the capacity of the bearings. These bearings had less than 50 percent of the displacement capacity of the adjacent

dissipators and shear keys, and their failure led to the distortion and eventual collapse of many of the dissipators in the segment crossing the fault. Although severely damaged, the shear keys are credited with keeping the superstructure in place.

Figure 2-7. Damage Sustained by the Bolu Viaduct during Duzce Earthquake 1999

Three of the most important lessons to be learned from this experience are as follows:

1. Even a poorly designed isolation system can provide a measure of protection to a bridge. Fault rupture was not anticipated in the design of the viaduct, but despite higher than expected ground motions, the bridge did not collapse and no pier was significantly damaged. Damage was confined to the isolators and shear keys, with some spans experiencing permanent offset.
2. Performance would have been greatly improved if either (a) generous capacity had been provided for displacements in the sliding isolators, or (b) a strong restoring force, capable of re-centering the isolators, had been provided. This experience confirms the prudence behind the contentious provision in the AASHTO 1991 Isolation Guide Specifications (AASHTO 1991), which required isolators to have capacity for three times the design displacement in the absence of an adequate restoring force. This provision was replaced in the 1999 Guide Specifications (AASHTO 1999) by the requirement that all isolators must have a re-centering capability and a minimum restoring force.
3. Ground motions that are greater than those anticipated during design, are always possible and the provision of a backup load path is prudent so that, should the isolation system fail, the bridge is not lost. Such systems are not currently required in AASHTO 1999.

In summary, the over-arching lesson to be learned is the need to use an isolation system with either a strong restoring force or generous displacement capacity and preferably both. Backup devices (shear keys and the like) should be provided in all designs in the event of greater-than-expected ground motions.

CHAPTER 3: ANALYSIS

3.1 INTRODUCTION

Since most isolation systems are nonlinear, it might appear at first sight that only nonlinear methods of analysis can be used in their design (such as a nonlinear time history method). However, if the nonlinear properties can be linearized, equivalent linear (elastic) methods may be used, in which case many methods are suitable for isolated bridges. These methods include:

- Uniform Load Method
- Single Mode Spectral Method
- Multimode Spectral Method
- Time-History Method

The first three methods are elastic methods. The time history method may be either elastic or inelastic. It is used for complex structures or where explicit modeling of energy dissipation is required to better represent isolation systems with high levels of hysteretic damping (equivalent viscous damping > 30 percent).

All of the above methods are described in AASHTO 1998 and AASHTO 1999. Special care is required when modeling the isolators for use in these methods as shown in section 8.

A variation of the uniform load method is the displacement-based method of analysis which is particularly useful for performing initial designs, and checking the feasibility of isolation for a particular bridge. It may be used as a starting point in design, followed by more rigorous methods as the design progresses. This method is briefly described in section 3.2 and two examples are given of its use. In some publications, this method is also called the capacity-spectrum method.

3.2 DISPLACEMENT-BASED ANALYSIS METHOD (MODIFIED UNIFORM LOAD METHOD)

3.2.1 ASSUMPTIONS

1. The bridge superstructure acts as a diaphragm that is rigid in-plane and flexible-out-of -plane. Compared to the flexibility of the isolators, bridge superstructures are relatively rigid and this assumption is applicable to a wide range of superstructure types (e.g., box-girders, plate girders with cross-frames, slab and girders with diaphragms and the like).
2. The bridge may be modeled as a single-degree-of-freedom system. The uniform load and single mode spectral analysis methods in conventional seismic design make this same assumption, and is subject to the same limitations on applicability.
3. The displacement response spectrum for the bridge site is linearly proportional to period within the period range of the isolated bridge (i.e., the spectral velocity is constant and the spectral acceleration is inversely proportional to the period in this range).
4. The lateral force-displacement properties of seismic isolators may be presented by bilinear hysteretic loops.

5. Hysteretic energy dissipation can be represented by equivalent viscous damping.
6. The design response spectrum may be scaled for different viscous damping ratios by damping factors which are independent of period.

3.2.2 BASIC EQUATIONS FOR BRIDGES WITH STIFF SUBSTRUCTURES

If all the isolators supporting the superstructure experience the same displacement D, the properties of individual isolators may be lumped into a single, equivalent, 'system' isolator. This will be true when a single mode of vibration dominates response (Assumption 1 above) and for bridges with stiff substructures. In this section, stiff substructures are assumed and the properties of individual isolators are lumped into a single system isolator. The theory for bridges with flexible substructures is presented in section 3.2.5.

3.2.2.1 Effective Stiffness

From figure 1-3, the effective stiffness K_{eff}, of a bilinear isolator at displacement D, is given by:

$$K_{eff} = F / D = (Q_d + K_d D) / D = Q_d / D + K_d \quad (3\text{-}1)$$

where F = total lateral force in isolator at displacement D
Q_d = characteristic strength of isolator (force in isolator at zero displacement), and
K_d = post yield stiffness of isolator.

3.2.2.2 Effective Period

The effective period T_{eff}, of single-degree-of-freedom system of mass W/g, and stiffness K_{eff}, at displacement D, is given by:

$$T_{eff} = 2\pi\sqrt{W / g K_{eff}} \quad (3\text{-}2)$$

where W = weight of bridge superstructure.

3.2.2.3 Equivalent Viscous Damping Ratio

The hysteretic energy dissipated in a single cycle of a bilinear isolator is given by the area of the hysteresis loop as follows:

$$\text{Area} = 4Q_d(D - D_y) \quad (3\text{-}3a)$$

where D_y = yield displacement of the isolator.

Substituting this area into equation 1-1, gives the equivalent viscous damping ratio β, as follows:

$$\beta = 2 Q_d (D - D_y) / \pi K_{eff} D^2 \quad (3\text{-}3b)$$

3.2.2.4 Superstructure Displacement

The displacement D, of single-degree-of-freedom system with period T_{eff} and viscous damping ration β, is given by (AASHTO 1999)[1]:

$$D = 10\ A\ S_i\ T_{eff} / B \text{ (inches)} \quad (3\text{-}4a)$$
$$= 250\ A\ S_i\ T_{eff} / B \text{ (mm)} \quad (3\text{-}4b)$$

where A = acceleration coefficient for the site
S_i = site coefficient for isolated structures (table 3-1)
T_{eff} = effective period at displacement D (equation 3-2), and
B = damping factor (a scale factor for displacement based on the viscous damping ratio β, table 3-2)

Derivation of this expression is given in AASHTO 1999.

Table 3-1. Site Coefficient for Seismic Isolation, S_i (AASHTO 1999)

	Soil Profile Type[1]			
	I	II	III	IV
S_i	1.0	1.5	2.0	2.7

Note: 1. Soil profile types are defined in AASHTO 1998, 2002.

3.2.2.5 Total Base Shear and Individual Isolator Forces

The total lateral force in the system isolator at displacement D is given by:

$$F = K_{eff}\ D \quad (3\text{-}5)$$

This force is the total base shear for the bridge. Individual isolator forces may be found by dividing this quantity by the number of isolators (if all isolators have identical properties), or in proportion to their individual stiffnesses.

Some isolation systems have viscous dampers in place of, or in addition to, the hysteretic dampers, and in such cases the forces in the dampers will be out of phase with those in the bearings (elastomeric or sliding). To find the governing design force, seismic forces should be calculated for three cases and the maximum chosen for design. These cases are:

a. at maximum bearing displacement (i.e., zero velocity and therefore zero damper force)
b. at maximum bearing velocity (i.e., zero displacement), and
c. at maximum superstructure acceleration.

[1] Recent research has shown that a better estimate of the displacement D is given by D = 10 Si S1 T_{eff} / B (inches) or 250 Si S1 T_{eff} / B (mm), where Si is the site soil coefficient (table 3-1) and S1 is the spectral acceleration at 1.0 second period for the ground motion. Values of S1 are available from USGS web site *http://eqhazmaps.usgs.gov*.

Table 3-2. Damping Coefficient, B (AASHTO 1999)

	Damping ratio (percentage of critical), β[1]						
	< 2	5	10	20	30	40[2]	50[2]
B	0.8	1.0	1.2	1.5	1.7	1.9	2.0

Notes: 1. Damping factors for intermediate values of β may be found by linear interpolation.
2. The use of B-factors to scale response spectra is unreliable for hysteretically damped isolation systems with equivalent viscous damping ratios in excess of 30 percent. In these cases, a nonlinear time-history analysis is recommended using the actual hysteresis loop(s) rather than equivalent damping ratios and B-factors. If however the dampers are truly viscous, then B-factors greater than 1.7 may be used.

3.2.3 METHOD FOR BRIDGES WITH STIFF SUBSTRUCTURES

The methodology described here is an iterative one since many of the key parameters describing the properties of the bridge (K_{eff}, T_{eff}, and β) depend on the displacement of the bridge, which is not known at the beginning of the analysis. The method therefore begins by assuming a bridge displacement and iterating until convergence is achieved, usually within a few cycles. The steps are as follows:

Step 1. Assume a value for the superstructure displacement D.

Step 2. Calculate effective stiffness K_{eff}, from equation 3-1.

Step 3. Calculate effective period T_{eff}, from equation 3-2.

Step 4. Calculate equivalent viscous damping ratio β, from equation 3-3b.

Step 5. Obtain damping factor B, from table 3-2.

Step 6. Calculate displacement D, from equation 3-4a or 3-4b.

Step 7. Compare calculated value for displacement D, with that assumed in step 1. If in close agreement go to step 8; if otherwise repeat from step 2 using the value for displacement D, found in step 6.

Step 8. Calculate the total force in the isolator F, from equation 3-5. This force will be the total base shear in the bridge and may be divided by the number of isolators to find individual isolator forces (assuming the isolators have identical properties; otherwise distribute this force in proportion to the stiffnesses of the individual isolators).

3.2.4 EXAMPLE 3-1: BRIDGE WITH STIFF SUBSTRUCTURE

3.2.4.1 Problem

The superstructure of a two-span bridge weighs 533 K. It is located on a rock site (soil profile type I, S_i = 1.0, table 3-1), where the acceleration coefficient A is 0.55. Analyze the bridge for each situation described in (a) through (c) below. Neglect the flexibility of the center pier, i.e., assume a stiff substructure.

(a) If Q_d =0.075 W and that K_d = 13.0 K/in for the equivalent system isolator, calculate the total base shear (sum of all the isolator shears) and superstructure displacement in the longitudinal direction. (W = weight of superstructure = 533 K.)
(b) Calculate Q_d such that the displacement of the superstructure in the longitudinal direction does not exceed 5.0 ins (K_d =13.0 K/in).
(c) Calculate Q_d and K_d such that the displacement in the longitudinal direction does not exceed 6.0 ins and the total base shear does not exceed 110 K.

Use the displacement-based method described above for these analyses and assume the isolators have negligible yield displacements (D_y = 0).

3.2.4.2 Solution

An excel spreadsheet may be constructed to solve these three problems. Table 3-3 shows such a spreadsheet and solutions to (a), (b) and (c). Results may be summarized as follows:
(a) When Q_d = 0.075W and K_d = 13.0 K/in, the superstructure displacement is 5.98 in and the total base shear is 117.7 K (22.1 percent of the weight).
(b) To reduce the superstructure displacement to less than 5.0 ins while keeping K_d = 13.0 K/in, Q_d is increased to 0.10W.
(c) To reduce the base shear to less than 110.0 K while keeping the displacement less than 6.0 ins, K_d is reduced to 11.25 K/in and Q_d increased to 0.08W.

3.2.5 BASIC EQUATIONS FOR BRIDGES WITH FLEXIBLE SUBSTRUCTURES

When a bridge has flexible substructures, the isolators do not experience the same displacements, except in the unlikely event that all the substructures have the same flexibility. To apply the simplified displacement-based method, the effective stiffness of the bridge, used in step 2 above,

Table 3-3. Solution to Example 3-1

SIMPLIFIED DISPLACEMENT-BASED METHOD: (2-span bridge: W= 533K, A=0.55g)

BRIDGE AND SITE PROPERTIES		**Damping Factors, B**					
Acceleration coefficient, A	0.55	β	<2	5	10	20	30
Site Coefficient (table 3-1), Si	1.00	B	0.8	1.0	1.2	1.5	1.7
Superstructure weight, W	533.00						

(a) FIND BRIDGE RESPONSE FOR Qd = 0.075W and Kd = 13.0 K/in

Step	**Parameter**	**Trial 1**	**Trial 2**	**Trial 3**	**Trial 4**	
	Characteristic strength, Q_d	0.075	0.075	0.075	0.075	
	Post-yield stiffness, K_d	13.00	13.00	13.00	13.00	
1	Assumed displacement, D	5.00	5.60	6.00	5.98	
2	Effective stiffness, K_{eff}	20.995	20.138	19.663	19.685	
3	Effective period, T_{eff}	1.610	1.644	1.664	1.663	
4	Viscous damping ratio, β	0.242	0.226	0.216	0.216	
5	Damping factor, B	1.58	1.55	1.53	1.53	
6	Displacement, D (eq 3-4)	5.61	5.83	5.98	**5.98**	Answer
8	Total base shear, F	117.70	117.50	117.63	**117.69**	Answer
	Base shear / weight				**22.08%**	Answer

(b) FIND Qd for D< 5.0 ins (Kd = 13.0 K/in)

Step	**Parameter**	**Trial 1**	**Trial 2**	**Trial 3**	**Trial 4**	
	Characteristic strength, Q_d	0.075	0.090	0.120	**0.100**	Answer
	Post-yield stiffness, K_d	13.00	13.00	13.00	13.00	
1	Assumed displacement, D	5.00	5.00	5.00	5.00	
2	Effective stiffness, K_{eff}	20.995	22.594	25.792	23.660	
3	Effective period, T_{eff}	1.610	1.552	1.453	1.517	
4	Viscous damping ratio, β	0.242	0.270	0.316	0.287	
5	Damping factor, B	1.58	1.64	1.70	1.67	
6	Displacement, D (eq 3-4)	5.61	5.21	4.70	5.00	
8	Total base shear, F	117.70	117.63	121.25	118.21	
	Base shear / weight				22.18%	

(c) FIND Qd and Kd for D< 6.0 ins and F < 110 K

Step	**Parameter**	**Trial 1**	**Trial 2**	**Trial 3**	**Trial 4**	
	Characteristic strength, Q_d	0.050	0.075	0.075	**0.080**	Answer
	Post-yield stiffness, K_d	13.00	10.00	11.00	**11.25**	Answer
1	Assumed displacement, D	6.00	6.00	6.00	5.85	
2	Effective stiffness, K_{eff}	17.442	16.663	17.663	18.539	
3	Effective period, T_{eff}	1.767	1.808	1.756	1.714	
4	Viscous damping ratio, β	0.162	0.255	0.240	0.250	
5	Damping factor, B	1.35	1.61	1.58	1.60	
6	Displacement, D (eq 3-4)	7.20	6.18	6.11	5.89	
8	Total base shear, F	125.56	102.90	107.96	109.22	
	Base shear / weight				20.49%	

must be modified to include the substructure flexibility. Once this has been done, the method follows the same steps, and uses the same basic equations, as for the case with stiff substructures.

3.2.5.1. Effective Stiffness of Bridge with Flexible Substructures

The effective stiffness of an isolated superstructure on flexible substructures is obtained by summing the effective stiffnesses of the individual substructures. Figure 3-1 shows an idealized substructure with an isolator supported on a flexible column. The isolator is assumed to have bilinear properties and the column is assumed to be elastic.

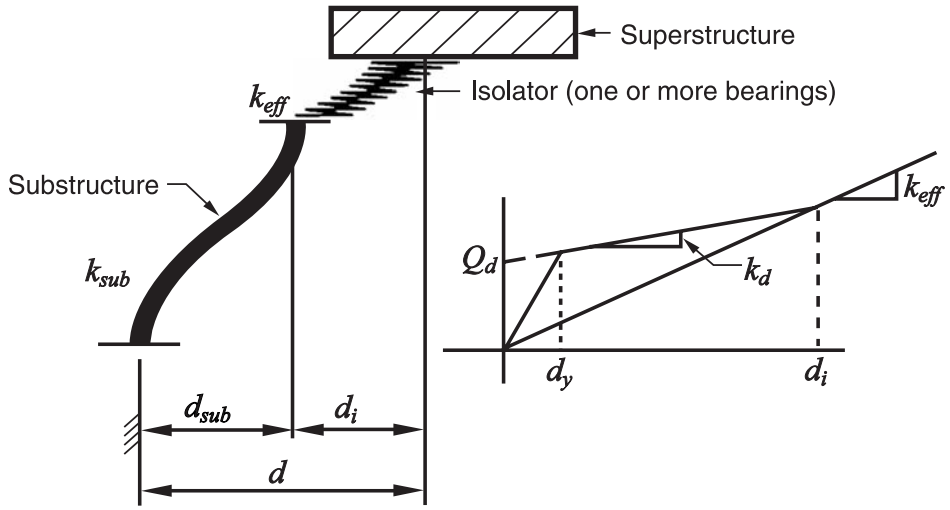

$$\beta = \frac{Energy\ Dissipated}{2\pi K_{eff} d^2} = \frac{Total\ Dissipated\ Energy}{2\pi \sum_j (K_{eff,j} d^2)}$$

$$\beta = \frac{2Q_d(d_i - d_y)}{\pi (d_i + d_{sub})^2 K_{eff}} = \frac{2\sum_j [Q_d(d_i - d_y)]}{\pi \sum_j [K_{eff,j}(d_i + d_{sub})^2]}$$

Note: These equations exclude damping from the substructure.

Figure 3-1. Idealized Deformations in an Isolated Bridge with Flexible Substructures (AASHTO 1999)

The effective stiffness of the substructure j ($K_{eff,j}$) is calculated as follows:

$$K_{eff,j} = \alpha K_{sub} / (1 + \alpha) \quad (3\text{-}6)$$

where $\alpha = K_{isol} / K_{sub}$

$$= (K_d D + Q_d) / (K_{sub} D - Q_d) \quad (3\text{-}7)$$

K_{isol} = effective stiffness of the isolators supported on substructure at displacement D_{isol}

$$= Q_d / D_{isol} + K_d$$

K_{sub}= stiffness of substructure in direction under consideration (e.g. $3EI/h^3$ for a single cantilever column of height h and flexural rigidity EI)

D_{isol} = isolator displacement

$= D / (1 + \alpha)$ (3-8)

and D = assumed displacement of superstructure (step 1)

It follows that the effective stiffness K_{eff} for the complete bridge with N substructures is given by:

$$K_{eff} = \sum_{1}^{N} K_{eff,j} \quad (3\text{-}9)$$

3.2.5.2 Substructure and Isolator Forces

The force in any substructure is given by:

$$F_{sub} = K_{sub} D_{sub} \quad (3\text{-}10)$$

where D_{sub} = substructure displacement

$$= D - D_{isol} \quad (3\text{-}11)$$

The force in the isolators supported by the substructure is given by:

$$F_{isol} = K_{isol} D_{isol} \quad (3\text{-}12)$$

It is noted that these two forces should be the same since both the isolator and substructure 'see' the same shear force due to the serial nature of the load path.

3.2.6 METHOD FOR BRIDGES WITH FLEXIBLE SUBSTRUCTURES

The method described here is essentially the same as for stiff substructures but is repeated here in its entirety for completeness. As above, it is an iterative method since many of the key parameters describing the properties of the bridge (K_{eff}, T_{eff}, and β) depend on the displacement of the bridge D, which is not known at the beginning of the analysis. The method therefore begins by assuming a displacement for the bridge superstructure (D) and iterating until convergence is achieved, usually within a few cycles. The steps are as follows:

Step 1. Assume a value for the superstructure displacement D.

Step 2. Calculate effective stiffness of the bridge K_{eff}, from equation 3-9.

Step 3. Calculate effective period T_{eff}, from equation 3-2.

Step 4. Calculate equivalent viscous damping ratio β, from equation 3-3b.

Step 5. Obtain damping factor B, from table 3-2.

Step 6. Calculate displacement D, from equation 3-4a or 3-4b.

Step 7. Compare calculated value for displacement D, with that assumed in step 1. If in close agreement go to step 8; otherwise repeat from step 2 using the value for displacement D, found in step 6.

Step 8. Calculate the total base shear F, from equation 3-5, or by summing individual substructure forces given by equation 3-10. Isolator forces are equal to the substructure forces or may be found from equation 3-12. Isolator and substructure displacements are given by equations 3-8 and 3-11 respectively.

3.2.7 EXAMPLE 3-2: BRIDGE WITH FLEXIBLE SUBSTRUCTURE

3.2.7.1 Problem

The superstructure of a two-span bridge weighs 533 K. It is located on a rock site (soil profile type I, $S_i = 1.0$, table 3-1), where the acceleration coefficient A is 0.55. The center pier is a single 36-inch diameter reinforced concrete column, 25 ft high, fixed at the base and pinned at the top. The elastic modulus for the concrete is 3,000 ksi. The lateral stiffness of each abutment is 10,000 K/in. The bridge is isolated with bearings at the abutments and over the pier. Total values for Q_d and K_d summed over all the isolators are 0.075 W (= 40 K) and 13.0 K/in, respectively. Isolator properties and the weight carried at each substructure are given in table 3-4.

Table 3-4. Isolator Properties for Bridge in Example 3-2

Substructure	Weight carried (K)	Qd (K)	Kd (K/in)
North Abutment	100	7.50	2.44
Pier	333	25.00	8.12
South Abutment	100	7.50	2.44
Totals	**533**	**40.00**	**13.00**

(a) Calculate seismic response of the bridge. In particular, find the displacement of the superstructure, the total base shear, and the distribution of this shear to the three substructures (two abutments and pier).
(b) If the shear capacity of the pier is only five percent of the weight of the bridge, redistribute the isolator properties between the abutments and pier to satisfy this limitation.

Use the displacement-based method described above for these analyses and assume the isolators have negligible yield displacements ($D_y = 0$).

3.2.7.2 Solution

As for the previous example, an excel spreadsheet may be constructed to solve these two problems. Table 3-5 shows such a spreadsheet and a solution for (a) and (b). The approach is the same as for the previous example except that the calculation of the effective stiffness for the complete bridge system (step 2) requires the summation of the effective stiffnesses of each substructure. This is shown in table 3-5 in a separate section of the table. This section is entered

Table 3-5. Solution to Example 3-2

SIMPLIFIED DISPLACEMENT-BASED METHOD: (2-span bridge with central pier: W= 533K, A=0.55g)

BRIDGE AND SITE PROPERTIES		PIER PROPERTIES			Damping Factors, B						
Acceleration coefficient, A	0.55	E	3,000.00	Ksi	β	<2	5	10	20	30	40	50
Site Coefficient (table 3-1), Si	1.00	I	82,445.53	in^4	B	0.8	1.0	1.2	1.5	1.7	1.9	2.0
Superstructure weight, W	533.00	h	300.00	in								
		3EI/h^3	27.48	K/in								

(a) FIND BRIDGE RESPONSE FOR Qd = 0.075W and Kd = 13K/in

Step	Parameter	Solution1
	Characteristic strength, Q_d	0.075
	Post-yield stiffness, K_d	13
1	Assumed displacement, D	6.26
2	Effective stiffness, K_{eff}	16.623
3	Effective period, T_{eff}	1.810
4	Viscous damping ratio, β	0.245
5	Damping factor, B	1.59
6	Displacement, D (eq 3-4)	**6.26**
8	Total base shear, F	**104.13**
	Base shear / weight	**19.54%**

Step 2. Effective stiffness of bridge Isolation system, Keff

D 6.26

Substruc	Wsub	Qd	Kd	Ksub	α	Keff	Disol	Dsub	Fsub	Fsub %
N. Abut	100.00	7.50	2.44	10,000.00	0.0004	3.63	6.258	0.002	22.75	21.87%
Pier	333.00	25.00	8.13	27.48	0.5159	9.35	4.129	2.131	58.55	56.27%
S. Abut	100.00	7.50	2.44	10,000.00	0.0004	3.63	6.258	0.002	22.75	21.87%
Totals	**533.00**	**40.00**	**13.00**			**16.62**			**104.06**	100.00%

(b) REDISTRIBUTE Qd and Kd such that maximum shear in center pier < 26.65K (5% total weight)

Step	Parameter	Solution1
	Characteristic strength, Q_d	0.075
	Post-yield stiffness, K_d	13
1	Assumed displacement, D	6.04
2	Effective stiffness, K_{eff}	19.025
3	Effective period, T_{eff}	1.692
4	Viscous damping ratio, β	0.221
5	Damping factor, B	1.54
6	Displacement, D (eq 3-4)	**6.03**
8	Total base shear, F	**114.73**
	Base shear / weight	**21.53%**

Step 2. Effective stiffness of bridge Isolation system, Keff

D 6.04

Substruc	Wsub	Qd	Kd	Ksub	α	Keff	Disol	Dsub	Fsub	Fsub %
N.Abut	100.00	20.00	4.33	10,000.00	0.0008	7.64	6.035	0.005	46.15	40.16%
Pier	333.00	0.00	4.33	27.48	0.1577	3.74	5.217	0.823	22.61	19.67%
S. Abut	100.00	20.00	4.33	10,000.00	0.0008	7.64	6.035	0.005	46.15	40.16%
Totals	**533.00**	**40.00**	**13.00**			**19.02**			**114.91**	100.00%

with an estimate of the displacement (6.26 in) and the effective stiffness is calculated for that displacement (16.62 K/in). This value is then used in step 3 to calculate the effective period and the solution proceeds as before. The solution shown in table 3-5 is the final trial after convergence has been obtained. Intermediate trials are not shown. It will be seen that the section that calculates effective stiffness, also calculates the displacements in the isolators and substructures, and the shears in the substructures both in absolute terms and as a percentage of the total base shear.

Results for the two cases are summarized as follows:

(a) Superstructure displacement = 6.26 in
Total base shear = 104.1 K (19.5 percent W)
North abutment shear = 22.8 K (21.9 percent total base shear, 4.3 percent W)
Pier shear = 58.5 K (56.2 percent total base shear, 11.0 percent W)
South abutment shear = 22.8 K (21.9 percent total base shear, 4.3 percent W)
Isolator and substructure displacements:
- at north abutment: 6.26 in (isolator), 0 in (abutment)
- at pier: 4.13 in (isolator), 2.13 in (pier)
- at south abutment: 6.26 in (isolator), 0 in (abutment)

Comparing these results with those obtained for part (a) of example 3-1where the substructure was considered stiff, the effect of the flexible pier is to increase the displacements by about 5 percent (from 5.98 to 6.26 in) and to reduce the total base shear by about 12 percent (from 118 K to 104 K). It is seen that the assumption of a stiff substructure gives a conservative estimate of base shear but underestimates the superstructure displacement (slightly). The main reason for this behavior is the lengthening of the effective period due to the increased flexibility of the bridge when the single-column pier is introduced (from 1.66 sec to 1.81 sec).

(b) Since the strength of the pier is so low (5 percent W), the strategy adopted in this solution is to soften the isolators above the pier and stiffen the ones at the abutments to draw lateral load away from the pier and to the abutments. Hence Q_d for the pier isolators is set to zero and the abutment values increased accordingly to maintain the total required value of 0.075W. Also the K_d values at the pier are reduced and the abutment values increased to provide a total value of 13.0 K/in as required. In this solution, it will be seen that K_d has been equally divided between all three substructures but this is not the only approach that will lead to a successful result. There are in fact many solutions to this problem and the optimal one will be determined when actual isolators (lead-rubber, friction pendulum or Eradiquake) are designed to meet these Q_d and K_d values while simultaneously supporting the weight of the bridge and providing the period shift.
Superstructure displacement = 6.04 in
Total base shear = 114.9 K (21.5 percent W)
North abutment shear = 46.2 K (40.2 percent total base shear, 8.7 percent W)
Pier shear = 22.6 K (19.6 percent total base shear, 4.2 percent W)
South abutment shear = 46.2 K (40.2 percent total base shear, 8.7 percent W)
Isolator and substructure displacements:
- at north abutment: 6.04 in (isolator), 0.0 in (abutment)
- at pier: 5.22 in (isolator), 0.82 in (pier)
- at south abutment: 6.04 in (isolator), 0.0 in (abutment)

3.3 SINGLE MODE AND MULTIMODE SPECTRAL ANALYSIS METHODS

These methods are essentially the same as those described in AASHTO 2002 with two modifications. First, to find the equivalent linear properties of the isolators for inclusion in a structural model of the bridge, an estimate of the design displacement must be made, followed by iteration if the estimate is significantly in error. Second, the 5 percent damped response spectrum is modified to recognize higher levels of damping in the 'isolated' modes, i.e., those modes that involve deflections in the isolators. This is done by scaling the spectrum by the damping coefficient B, for periods greater than 0.8 T_{eff}. The five percent damped spectrum is used for all other modes in the multimode method. As for conventional bridges, the analysis is performed in two orthogonal directions and the results combined according to article 3.9 of AASHTO 2002. These two directions are usually taken as the longitudinal (span-wise) and transverse directions. For a curved bridge, the longitudinal direction may be taken as the chord joining the two abutments.

3.4 TIME HISTORY ANALYSIS METHOD

The time history method may use either nonlinear or equivalent linear properties for the isolators and is suitable for complex structures where the above modal methods are inappropriate, or where explicit modeling of the energy dissipators is required to more accurately represent isolation systems with high levels of damping (> 30 percent). In both approaches, ground motion time histories are required and these may be either site-specific or spectrum-compatible. In both cases, no less than three pairs (one N-S and one E-W component) of time histories should be used in the analysis. Each pair is applied simultaneously to a three-dimensional model of the bridge and the maximum displacement of the isolation system is obtained by the vectorial sum of the orthogonal displacements at each time step. Design actions of interest (e.g., a shear force at the base of a column) are calculated for each time history. If three time history analyses are performed, the maximum response of the action of interest is used in design. If seven or more time history analyses are performed, the average value is used.

If site-specific ground motions are not available, spectrum-compatible time histories may be generated by frequency-scaling recorded ground motions of past earthquakes such that their spectra closely match the design spectrum for the site (figure 1-2). The duration of the recorded motions selected for scaling should be consistent with the magnitude and source characteristics of the design-basis earthquake. The following procedure is recommended to obtain spectrum-compatible time histories:

1. Calculate the five percent response spectrum for each component of ground motion of each selected earthquake.
2. Calculate the SRSS spectrum for each earthquake by taking the square root of the sum of the squares (SRSS) of the spectra of the two orthogonal components.
3. Calculate the average spectrum by taking the average of the SRSS spectra for each earthquake.
4. Compare the average spectrum with the design spectrum and scale it such that it does not fall below 1.3 times the 5-percent design-basis spectrum in the range 0.5 T_{eff} to 1.5 T_{eff}.
5. Scale the individual components of the recorded ground motions by the factor found in previous step.

CHAPTER 4: DESIGN

4.1 STRATEGY: BRIDGE AND SITE SUITABILITY

Seismic isolation should be considered whenever improved seismic performance, or reduction of cost, or both, may be achieved. Such benefits can be evaluated on a case-by-case basis using simplified analytical tools such as those described in section 3.2.

Factors affecting bridge and site suitability include superstructure type, site soil conditions and substructure flexibility. These factors are described in this section

4.1.1 LIGHTWEIGHT SUPERSTRUCTURES

Bridges with lightweight superstructures may present difficulties for effective seismic isolation. Such bridges include those with steel girders and concrete deck slabs, and those with precast concrete tee sections. These bridges usually have multiple lines of girders (5 and higher) and placement of an isolator under each girder means that the load carried per isolator is low. Consequentially, the ratio of mass-to-isolator stiffness is also low and it may be difficult to obtain a sufficiently large period shift (figure 1-2) to justify isolation.

Two options might be considered in such circumstances. The first is to use an isolator with a period that is independent of the weight carried (e.g., the friction pendulum isolator). The second is to use a cross beam (diaphragm) at the abutments and piers connecting the girder lines at their bearing locations and supported on, say, 2 or 3 isolators at each abutment seat and pier cap. The larger load per isolator improves the mass-to-stiffness ratio and meaningful period shifts become feasible. There are however consequential implications on the distribution of gravity loads to the girders due to the flexibility of the cross beam and the AASHTO live load distribution factors may not apply in such cases. This same flexibility may lead to high-cycle fatigue problems in the connections of the diaphragms to the girders. Both issues can be mitigated by using very stiff cross beams.

4.1.2 SOFT SOIL SITES

Ground motions at the surface of soft soil sites have significant long-period components. Lengthening the period of a bridge on such a site, by introducing a flexible isolation system, may not be desirable due to the possibility of increased forces, and it may not be practical due to much larger displacements at the abutment seats. Advanced analytical tools and procedures are available when assessing the effectiveness of isolation in such circumstances, and these should be used in lieu of the approximate methods in section 3.

Seismic isolation hardware may be used for any purpose that is shown by analysis to provide benefits. For example, engineers in Japan have successfully used seismic isolators for the protection of bridges on soft soil sites by using isolators to redistribute forces (rather than reduce them) among various substructures, and dissipate energy to limit displacements. Called *menshin* design, this approach has been widely used in Japan (Civil Engineering Research Center, 1992;

Sugita and Mahin, 1994). This technique is called *partial isolation* in the United States and has been shown to be an effective retrofit tool for existing bridges on stiff sites with inadequate seat widths at abutments and pier caps (Buckle and Mayes, 1990). In these situations, it is not the period shift that is important but the energy dissipation.

4.1.3 FLEXIBLE STRUCTURES

It is often stated that flexible structures may not be suitable for seismic isolation, usually in reference to buildings above a certain number of stories in height. The statement implies that, while the use of an isolation system increases the fundamental period, the increase for structures that are already flexible may not be sufficient to affect the dynamic response in a significant way.

This is also true for bridges, but not to the same extent. The outcome depends on the ratio of the isolator flexibility to the substructure flexibility. If this ratio is greater than unity, favorable response should be found when using isolation. If it is less than unity, the benefit of isolation will be negligible. For typical bridge situations, this ratio is almost always greater than unity.

As shown in section 3.2.5, the Uniform Load Method may be used to explore this effect in bridges being considered for isolation.

4.2 SEISMIC AND GEOTECHNICAL HAZARDS

4.2.1 ACCELERATION COEFFICIENT

The analysis methods described in section 3 depend on the availability of the following seismic and geotechnical data:

1. Peak ground acceleration (A) and site coefficient (S_i) when the Uniform Load Method and the Single Mode Spectral Analysis Method are used (sections 3.2 and 3.3).
2. 5%-damped response spectra for various site conditions, when the Multimode Spectral Analysis Method is used (sections 3.3).
3. Time histories of ground motion for site specific conditions, when the Time-History Method is used (section 3.4).

The acceleration coefficient (A) represents the design level of ground motion shaking, and is obtained from maps that are given in AASHTO 2002. The reader is referred to the AASHTO 2002 Commentary for an extensive discussion on earthquake ground motions and their use in design. It is important to note the following:

1. The AASHTO 2002 maps are identical to the maps of the 1998 NEHRP Recommended Provisions for horizontal accelerations in rock that have 10-percent probability of being exceeded in 50 years. Earthquake excitation with this probability of exceedance is often termed the *design earthquake*.
2. The AASHTO maps of acceleration are based on a definition of seismic hazard that provides for a uniform likelihood that the design ground motion would not be exceeded throughout the United States. However, this definition does not ensure a uniform margin of failure for bridges designed for the *design earthquake*. In contrast, standards, codes and

provisions such as the 2000 NEHRP Recommended Provisions (Federal Emergency Management Agency, 2001), the 2000 IBC-International Building Code (International Code Council, 2000) and the ASCE 7-98 Standard (American Society of Civil Engineers, 2000) define the seismic hazard in terms of the *maximum considered earthquake*, which for most regions of the United States has a two-percent probability of being exceeded in 50 years. This definition of seismic hazard provides for a uniform margin of failure of bridges designed for the *design earthquake*, which is now defined, on the basis of experience, as the ground shaking that is 2/3 of the *maximum considered earthquake* ground shaking. It should be noted that the definition of the *design earthquake* in the 2000 NEHRP Provisions, the 2000 IBC and the ASCE 7-98 Standard is not the same as the definition of the *design earthquake* in AASHTO 2002.

3. The design of seismically-isolated buildings (in accordance with 2000 NEHRP, 2000 IBC or ASCE 7-98) and of seismically-isolated bridges (in accordance with AASHTO) differs in the following ways:
    a. For buildings, the part of the structure above the isolation system is designed for the effects of the *design earthquake*, whereas the isolation system is designed and tested for the effects of the *maximum considered earthquake*. These effects are explicitly calculated.
    b. For bridges, the structure and isolation system are designed for the effects of the *design earthquake* except that isolation bearings are tested to a peak displacement equal to 1.25 times the total design displacement, d_t, and that bearings are designed to be stable at displacements equal to 1.5 d_t when $A>0.19$, and equal to 2.0 d_t when $A\leq 0.19$. The multipliers of 1.25, 1.5 and 2.0 on d_t are included as a rudimentary approach at estimating the effects of the *maximum considered earthquake* in lieu of explicit analysis. The differentiation on the value of the multiplier depending on the acceleration coefficient denotes the significant differences that are recognized between the *design earthquake* (defined with 10-percent probability of being exceeded in 50 years) and the *maximum considered earthquake* (defined with 10-percent probability of being exceeded in 250 years) in regions of high and low seismicity.

4.2.2 SITE COEFFICIENT

The site coefficient accounts for the effects of soil conditions on the response spectra and, accordingly, on the seismic coefficient. The site condition is described by the soil profile type, which is described in AASHTO 1998, 2002.

It is noted that the site coefficient for the four Soil Profile Types I, II, III, and IV has values of 1.0, 1.5, 2.0 and 2.7, respectively, when used for seismic isolation design (table 3-1), whereas it has values of 1.0, 1.2, 1.5 and 2.0 when used for conventional design. The AASHTO 1999 Commentary states that the values of 1.0, 1.5, 2.0 and 2.7 are used for retaining compatibility between the uniform load method and the spectral method of analysis which uses ground spectra. For this compatibility, the spectral shapes shown in figure 4-1 (from the AASHTO 2002 Commentary) should have, in the long period range, ratios of 2.7 to 2.0 to 1.5 to 1.0. However, a

careful inspection of these spectral shapes reveals a relation that more closely follows the ratios 2.2 to 1.5 to 1.2 to 1.0.

When response spectra are used for the analysis of seismically-isolated bridges, the five-percent damped spectra (figure 1-2) are constructed by multiplying the normalized response spectra of figure 4-1 by the acceleration coefficient, A. The value of the spectral acceleration need not exceed 2.0 (units of g) for Soil Profile Type III or IV when A≥ 0.30. The spectra may be extended to periods greater than 3.0 sec by using the fact that the spectra are inversely proportional to the period.

Site-specific response spectra may be used when desired by the Owner or the Owner's representative, and are recommended for bridges located on Soil Profile Type IV when A≥0.3. Studies for the development of site-specific spectra should account for the regional geology and seismicity, location of the site with respect to known faults and source zones, the expected rates of recurrence of seismic events, and the soil conditions.

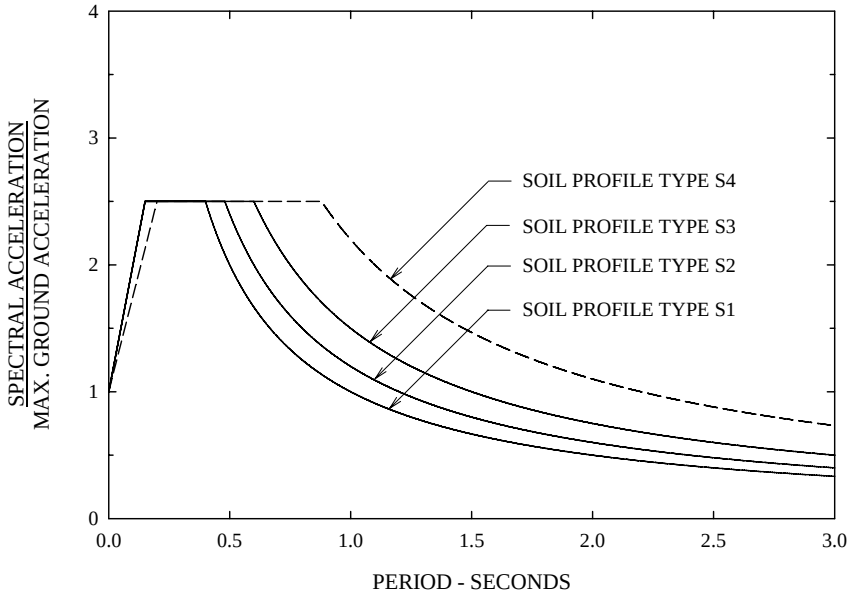

Figure 4-1. AASHTO Normalized Response Spectra

4.3 RESPONSE-MODIFICATION FACTOR

Response-modification factors (or R-factors) are used to calculate the design forces in structural components from the elastic force demand. That is, the demand is calculated on the assumption of elastic structural behavior and subsequently the design forces are established by dividing the elastic force demand by the R-factor. Illustrated in figure 4-2 is the structural response of an inelastic system. The elastic force demand is F_e, whereas the yield force of an idealized representation of the system is F_y. The design force is F_D so that

$$F_D = \frac{F_e}{R} \tag{4-1}$$

where R = response modification factor and has two components:

$$R = \frac{F_e}{F_D} = \frac{F_e}{F_y} . \frac{F_y}{F_D} = R_\mu . R_o \tag{4-2}$$

where R_μ = ductility-based portion of the factor, and
R_o = overstrength factor.

The ductility-based portion is the result of inelastic action in the structural system. The overstrength factor is due to the additional strength that exists between the design strength and the actual ultimate strength of the system.

When a strength design approach is followed, the design force corresponds to the level at which the first plastic hinge develops and the structural response deviates from linearity (as illustrated in figure 4-2). In this case, the overstrength factor results from structural redundancies, material overstrength, oversize of members, strain hardening, strain rate effects and code-specified minimum requirements related to drift, detailing, and the like.

When an allowable stress design approach is followed, the design force corresponds to a level of stress which is less than the nominal yield stress of the material. Accordingly, the R-factor (which is designated as R_w) contains an additional component which is the product of the ratio of the yield stress to the allowable stress and the shape factor (ratio of the plastic moment to moment at initiation of yield). This factor is often called the allowable stress factor, R_y, and has a value of about 1.5. That is,

$$R_w = R_\mu . R_o . R_y \tag{4-3}$$

There are numerous sources of information on response modification factors, such as Uang (1991), Uang (1993), Miranda and Bertero (1994), Applied Technology Council (1995), and Rojahn et al. (1997).

Model codes (such as the International Building Code), Specifications (such as the AASHTO 2002) and Resource Documents (such as the NEHRP Provisions) specify values of the R - factor which are empirical in nature. In general, the specified factor is dependent only on the structural system without consideration of the other affecting factors such as the period, framing layout, height, ground motion characteristics, etc.

The AASHTO 1991 Guide Specifications specified the response modification factors for isolated bridges to be the same as those for non-isolated bridges. For substructures (piers, columns and column bents) this factor has values in the range of 2 to 5.

While not explicitly stated in the 1991 Guide Specifications, it is implied that the use of the same R-factors would result in comparable seismic performance of the substructure of isolated and non-isolated bridges. Accordingly, the 1991 Guide Specifications recommended the use of lower R-factors when lower ductility demand on the substructure of the isolated bridge is desired. The

assumption that the use of the same R-factor would result in comparable substructure seismic performance in isolated and non-isolated bridges appeared rational. However, it has been demonstrated by simple analysis (Constantinou and Quarshie, 1998) that when inelastic action commences in the substructure, the effectiveness of the isolation system diminishes and larger displacement demands are imposed on the substructure.

Accordingly, the allowable R-factors were reduced to the range 1.5 to 2.5, in AASHTO 1999. Further explanation of this change is given in the Preface and section C.6 of the AASHTO 1999.

This revision essentially eliminates inelastic action in the substructure of a seismically-isolated bridge. This intention is not the result of desire for better performance. Rather it is a necessity for proper performance of an isolated bridge.

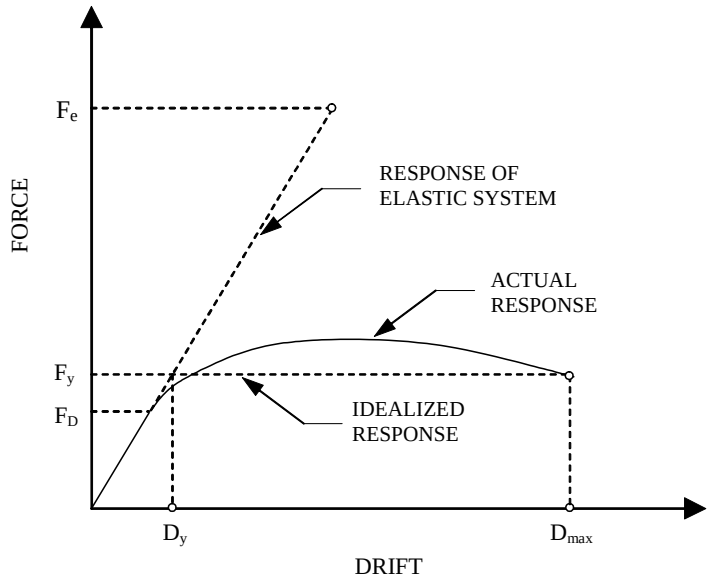

Figure 4-2. Structural Response of Inelastic System

4.4 DESIGN OF ISOLATED BRIDGE SUBSTRUCTURES AND FOUNDATIONS

AASHTO Specifications distinguish between the foundation of a bridge and the substructure of a bridge, which may consist of wall piers, pile bents, single columns or multi-column piers. Bridge analysis is typically performed assuming elastic substructures and foundations, whereas the isolation system is modeled either by a nonlinear hysteretic element or a linearized spring with equivalent viscous damping. Among several response quantities, the analysis determines the maximum lateral force, F_{max}, transmitted through the isolation system (figure 1-3). Also available are the yield force of the isolation system (F_y in figure 1-3), the friction force in a sliding isolation system (Q_d in figure 1-3), and the ultimate capacity of a sacrificial service restraint system, if used. For the purpose of the explanation below, these last three forces are denoted as Q.

The substructures of seismically-isolated bridges in Seismic Performance Categories (SPC) B, C and D should be designed for the effects of Q or F_{max}/R, whichever is largest, where R is one-half of the response modification factor of table 3.7 of AASHTO 2002, but not less than 1.5 (AASHTO 1999, articles 6 and 11).

The foundations of seismically-isolated bridges in SPC C and D should be designed for the effects of Q or F_{max} or the forces resulting from column hinging, whichever are the largest (AASHTO 1999, article 11).

The foundations of seismically-isolated bridges in SPC B should be designed for the effects of Q or F_{max} (AASHTO 1999, article 11). However, article 6.2.2 of AASHTO 2002 specifies the seismic force for foundation design to be $F_{max}/(R/2)$, where R is the response modification factor of the column or pier to which the foundation is attached (R/2 cannot be less than unity). Given that R factors for columns and piers of seismically-isolated bridges are reduced to values of 1.5 to 2.5, the requirement in article 6.2.2 (AASHTO 2002), that values of R/2 must be larger than or equal to unity, it is recommended that article 6.2.2 not be used in favor of the slightly more conservative requirements of AASHTO 1999, article 11 (i.e. design foundations using R = 1.0).

4.5 DESIGN PROPERTIES OF ISOLATION SYSTEMS

4.5.1 MINIMA AND MAXIMA

The properties of isolators inevitably vary due to a variety of reasons such as manufacturing differences, aging, wear, contamination, history of loading, and temperature. These variations may alter the effective period and equivalent damping of the isolation system, both of which will influence the dynamic response of the isolated structure. To adequately account for these variations, estimates should be made of minimum and maxima values for each quantity of interest and analyses made of bridge response with both sets of values. For example minimum and maximum values for effective stiffness should be calculated from minimum and maximum values of Q_d and K_d and the behavior of the bridge calculated using both values.

Minima and maxima for Q_d and K_d may be found using system property modification factors (λ) as follows:

$$K_{dmax} = \lambda_{maxKd} K_d \quad (4\text{-}4a)$$

$$K_{dmin} = \lambda_{minKd} K_d \quad (4\text{-}4b)$$

$$Q_{dmax} = \lambda_{maxQd} Q_d \quad (4\text{-}4c)$$

$$Q_{dmin} = \lambda_{minQd} Q_d \quad (4\text{-}4d)$$

where Q_d and K_d are nominal values (see section 4.5.2).

Development of the λ_{max} and λ_{min} values is discussed in the next section.

4.5.2 SYSTEM PROPERTY MODIFICATION FACTORS (λ-factors)

The minimum value of the system property modification factor λ_{min}, and is less than or equal to unity. Due to the fact that most values of λ_{min} proposed to date (Constantinou et al., 1999) are close to unity, λ_{min} is taken as unity (AASHTO 1999). That is, the lower bound of the system properties are considered to be the same as their nominal values. These nominal values are defined to be those determined for fresh and scragged (where appropriate) specimens under normal temperature conditions.

The maximum value of the λ-factor (λ_{max}) is calculated as the product of six component factors as follows:

$$\lambda_{max} = (\lambda_{max,t})(\lambda_{max,a})(\lambda_{max,v})(\lambda_{max,tr})(\lambda_{max,c})(\lambda_{max,scrag}) \quad (4\text{-}5)$$

where

$\lambda_{max,t}$ = maximum value of factor to account for the effect of temperature

$\lambda_{max,a}$ = maximum value of factor to account for the effect of aging (including corrosion)

$\lambda_{max,v}$ = maximum value of factor to account for the effect of velocity (established by tests at different velocities)

$\lambda_{max,tr}$ = maximum value of factor to account for the effect of travel and wear

$\lambda_{max,c}$ = maximum value of factor to account for the effect of contamination (sliding isolators)

$\lambda_{max,scrag}$ = maxiumum value of factor to account for the effect of scragging (elastomeric isolators)

Recommendations for λ_{max}-factors for elastomeric and sliding isolators are given in sections 6.6 and 7.7 respectively.

4.5.3 SYSTEM PROPERTY ADJUSTMENT FACTOR, (f_a-factors)

Adjustment factors (f_a) take into account the likelihood that maximum values for all of the component λ's (equation 4-5) will not occur at the same time. These are, in effect, reduction factors on the λ-factors and vary according to the importance of the bridge as shown in table 4-1. The adjusted factor (λ_{adj}) is given by

$$\lambda_{adj} = 1 + f_a(\lambda_{max} - 1) \quad (4\text{-}6)$$

where λ_{max} is given by equation 4-5.

Table 4-1. System Property Adjustment Factors

Bridge Importance	Adjustment Factor, fa
Critical	1.00
Essential	0.75
Other	0.66

4.6 MINIMUM RESTORING FORCE CAPABILITY

Seismic isolation systems that have been applied to buildings are characterized by strong restoring force capability. However, for bridge applications, two competing seismic isolation design strategies have been developed: (a) a strategy championed by engineers in New Zealand, the United States and Japan which requires strong restoring force in the isolation system, and (b) the Italian strategy in which the isolation system exhibits essentially elastoplastic behavior.

Specifications in the United States presume that the isolation system has, excluding any contribution from viscous devices, a bilinear hysteretic behavior characterized by the zero-force intercept or characteristic strength and the post-elastic stiffness. The International Building Code (International Code Council, 2000) specifies a minimum required second slope (K_d) such that:

$$K_d \geq 0.05\ W/D \tag{4-7}$$

which is equivalent to requiring that the period T_d, calculated on the basis of the post-elastic stiffness K_d, satisfies:

$$T_d \leq 28\left(\frac{D}{g}\right)^{1/2} \tag{4-8}$$

where W is the weight carried by the isolation system and D is the design displacement of the system. For example, at displacement D = 10 ins (250 mm), the period T_d must be les than or equal to 4.5 sec. It is noted that the International Building Code allows the use of systems with insufficient restoring force provided they are designed with a displacement capacity that is three times larger than the calculated demand (D).

The *AASHTO Guide Specification for Seismic Isolation Design* (AASHTO 1999) has a less stringent specification for minimum required second slope (Kd) i.e.,

$$K_d \geq 0.025\ W/D \tag{4-9}$$

but does not permit the use of systems which do not meet this requirement.

This requirement for K_d is equivalent to requiring that the period T_d, calculated on the basis of the post-elastic stiffness K_d, satisfies:

$$T_d \leq 40\left(\frac{D}{g}\right)^{1/2} \tag{4-10}$$

In addition to equations 4-9 and 4-10, AASHTO 1999 caps T_d at 6.0 secs, and this limitation effectively restricts D to less than or equal to 9.0 ins.

It is noted that the minimum stiffness given by equation 4-9 is satisfied if the restoring force at displacement D is greater than the restoring force at displacement 0.5D by at least W/80.

Isolation systems with a constant restoring force need not satisfy these requirements provided the force in the isolation system is at least 1.05 times the characteristic strength Q_d.

Forces that are not dependent on displacement, such as viscous forces, cannot be used to meet the above requirements.

The design strategy of requiring a strong restoring force is based on the experience that bridge failures in earthquakes have primarily been the result of excessive displacements. By requiring a strong restoring force, cumulative permanent displacements are avoided and the prediction of displacement demand is accomplished with less uncertainty. By contrast, seismic isolation systems with low restoring forces ensure that the force transmitted by the bearing to the substructure is predictable with some certainty. However, this is accomplished at the expense of uncertainty in the resulting displacements and the possibility for significant permanent displacements. Tsopelas and Constantinou (1997) have demonstrated the potential for significant permanent displacements in shake table testing of bridge models with seismic isolation systems having weak restoring force capability.

4.7 ISOLATOR UPLIFT, RESTRAINERS AND TENSILE CAPACITY

Isolation bearings are subjected to varying axial loads during an earthquake due to the overturning effect of the resultant horizontal seismic load, which acts above the plane of the isolators in most bridges. Under certain conditions, these axial load variations may exceed the compression in the bearing due to the self weight of the bridge, and either uplift occurs (e.g., if sliding bearings and doweled rubber bearings are used) or the bearing experiences tension (e.g., if bolted rubber bearings are used).

Whereas this effect is present in all bridge superstructures, it is most pronounced when the depth:width ratio of the superstructure is high, such as in a long span, continuous, single cell, concrete box girder bridge with a high centroidal axis and relatively narrow cell width. In such cases, and especially over the pier, the centroidal axis (and center of mass) of the girder is sufficiently high that uplift may occur due to the lateral earthquake force. The likelihood of uplift is even greater if unfavorable vertical excitations are present. This situation may also arise in other types of bridges, as for example in the San Francisco-Oakland Bay Bridge. Isolators at the San Francisco abutment of this bridge are FPS devices constructed with an uplift restrainer, which is engaged after small upward movement of the isolator begins.

The consequences of tensile forces or uplift in isolation bearings may be either:

1. *catastrophic*, when the isolators rupture, can no longer support the vertical load and the structure overturns (unless the designer provides for an alternative load path, or
2. *problematic*, when significant uplift occurs without rupture, but the impact on the return half-cycle damages the isolator, or
3. *uneventful*, when the uplift is minor and measures have been taken in the design of the isolator and substructure for the resulting axial loads and shear forces.

Nevertheless, it is preferred to avoid both uplift and tensile forces out of concern for the behavior of the isolators under conditions that are not well understood nor easily analyzed. Particularly, the tensile capacity of elastomeric bearings is not yet well understood, as noted in section 6.8.

4.8 CLEARANCES

Adequate clearances should be provided at the abutments to allow the superstructure to move freely during an earthquake. This clearance should be provided in two orthogonal directions and should not be less than the greater of:

- The calculated superstructure design displacement, D (section 3),
- 8 A S_i T_{eff} / B (inches) or 200 A S_i T_{eff} / B (mm), or (4-11)
- 1 inch (25mm).

where A, S_i, T_{eff} and B are as defined for equations 3-4a and b.

The purpose of these minima is to ensure adequate capacity for movement regardless of the results of higher order analyses. They are a consequence of the many uncertainties in seismic design and particularly a lack of confidence in the frequency content, duration and intensity of the ground motions.

4.9 VERTICAL LOAD STABILITY

A high factor of safety against instability is recommended for all isolators when carrying dead plus live load but not laterally deformed (i.e. non-seismic load case). Article 12.3 AASHTO 1999 requires a factor of 3.0 in these conditions.

Stability is also required (Factor of Safety = 1.0) under either:

(1) 1.2 times dead load + axial load due to overturning caused by seismic loads while deformed to 1.5 times the total design displacement (D) for a 475-year event with accelerations greater than 0.19g, or 2.0 times the total design displacement (D) for a 475-year event with accelerations less than or equal to 0.19g, or

(2) 1.2 times dead load + axial load due to overturning caused by seismic loads while deformed to 1.1 times the total design displacement (D) for the maximum considered event.

4.10 NON-SEISMIC REQUIREMENTS

Isolation systems are required to resist all non-seismic lateral load combinations that are applied to the bridge superstructure. Resistance to forces such as wind, centrifugal acceleration, braking, and thermally induced effects should be provided by a rational means and be verifiable by test.

CHAPTER 5: TESTING ISOLATION HARDWARE

5.1 INTRODUCTION

Seismic isolation hardware consists of elastomeric bearings (including lead-rubber bearings), sliding bearings (flat without restoring force, flat with restoring force and spherically shaped), and fluid viscous dampers. These devices represent the hardware used or being proposed for use on bridge structures in the United States. It is generally acceptable that testing guidelines that are suitable for all types of isolation hardware are too generic to be of value. Accordingly, the presentation in this section will concentrate on isolation bearings that represent the hardware used on the vast majority of seismically isolated bridges. Information on the testing of fluid viscous dampers may be obtained from HITEC (1996 and 2002).

Testing of seismic isolation bearings should consist of the following:

1. Characterization tests performed for establishing databases of properties such as effect of velocity, effect of pressure, effect of cumulative travel, effect of temperature, etc. These tests may be used to establish system property modification factors, to characterize the longevity of the bearings, and to develop models of the bearings for analysis.

2. Prototype tests performed for each project prior to fabrication of production isolation bearings. These tests are used to establish key mechanical properties of the bearings for comparison to the values used by the engineer for the design of the isolation system. Typically, two full-size isolators of each type and size of isolation bearing proposed are tested.

3. Production tests performed on each produced bearing. These tests represent quality control tests and are typically performed together with other material quality control tests as specified by the engineer.

5.2 CHARACTERIZATION TESTS

Characterization tests should be conducted for establishing databases of properties of particular hardware. It is usually the responsibility of the manufacturer of the hardware to conduct such tests, although the HITEC program (HITEC 1996) conducted performance evaluations of isolation hardware, which consisted of selected characterization tests. Manufacturers may utilize the HITEC program data, test data from research projects, and test data from prototype and production testing to establish the database of properties of their hardware.

Characterization tests should include:

1. Tests to characterize the virgin (or unscragged) properties of isolators. Test specimens should not have been previously tested regardless of whether it is the practice to conduct such testing for quality control purposes.
2. Tests to characterize the effect of pressure (axial load).
3. Tests to characterize the effect of velocity or frequency.
4. Tests to characterize the effect of displacement, or strain.

5. Tests to characterize the effect of temperature.
6. Tests to characterize the effect of cumulative travel under slow, non-seismic conditions.

Testing procedures should follow the basic guidelines described in HITEC (2002). Properties to be measured in the testing should include the characteristic strength (zero displacement force intercept), the post-elastic stiffness, the effective stiffness and the energy dissipated per cycle (parameters Q_d, K_d, K_{eff} and EDC in figure 1-3). These properties may then be used to obtain material properties such as the coefficient of friction (for sliding bearings), the shear moduli (for elastomeric bearings) and the effective yield stress of lead (for lead-rubber bearings). The reader is referred to section C9.2.2 of Federal Emergency Management Agency (1997) for a presentation on the relation of bearing properties to basic bearing material properties. Moreover, a database of material properties for sliding interfaces may be found in Constantinou et al. (1999).

5.3 PROTOTYPE TESTS

Article 13.2 of AASHTO 1999 specifies the prototype tests described below. The tests must be performed in the prescribed sequence and for a vertical load on the tested bearing equal to the average dead load on the bearings of the tested type. While not mentioned in the AASHTO 1999, the tests must be performed at the normal temperature, which is usually specified as $20^oC \pm 8^oC$.

1. *Thermal test.* This test consists of three cycles of sinusoidal displacement with amplitude equal to the maximum thermal displacement and a peak velocity not less than 4.5 mm/sec. The purpose of this test is to determine the lateral force exerted by the bearing during thermal movement of the bridge. It is required that the measured force does not exceed the specified design value.

2. *Wind and braking test.* This test consists of twenty cycles of sinusoidal lateral force with amplitude equal to the calculated maximum service load (wind or braking load) and a frequency equal to or less than 0.5 Hz (duration not less than 40 sec). The cyclic test is followed by a monotonic push with force equal to the maximum service load for one minute. The purpose of the test is to measure the displacement resulting from the application of the maximum service load and to verify that it is within the specified limits.

3. *Seismic test no. 1.* This test consists of six different tests, each with three cycles of sinusoidal displacement of amplitude equal to 1.0, 0.25, 0.5, 0.75, 1.0 and 1.25 times the total design displacement. This displacement is the isolator displacement calculated for the design earthquake including the effects of torsion in the isolated bridge. These tests must be conducted in the prescribed sequence starting with the one at amplitude of 1.0 times the total design displacement in order to determine the virgin (or unscragged) properties of the tested bearing. The tests at amplitudes of 0.25, 0.5, 0.75 and 1.0 times the total design displacement are used to determine the scragged properties of the bearing. The test at amplitude of 1.25 times the total design displacement is used to determine the properties of the tested bearing in an earthquake stronger than the design earthquake. Note that the 1.25 multiplier on displacement does not result in the displacement in the maximum considered earthquake. Rather, multipliers of 1.5 for sites with $A>0.19$ and 2.0 for sites with $A\leq0.19$

(see section 4.2.1) are used to verify the stability of the bearings in the maximum considered event.

4. *Seismic test no. 2*. This test consists of 10 to 25 cycles (depending on the soil profile and the equivalent damping of the isolation system) of sinusoidal displacement with amplitude equal to the design displacement. The purpose of the test is to determine the properties of the tested bearing over the maximum number of cycles expected in the design earthquake. The equation used to determine the number of cycles, $15\ S_i/B$, tends to over-predict the equivalent number of cycles as determined in a recent study by Warn and Whittaker (2002). It is advisable that this test be conducted with five continuous cycles followed by idle time and then repeating until the specified total number of cycles is reached. The idle time should be sufficient for heating effects to dissipate, which usually takes only a few minutes (see Constantinou et al., 1999 for discussion of heating effects). In this way, the purpose of the test is to determine the properties of the bearing over a sequence of design-level earthquakes, and verify the survivability of the isolation system after a major earthquake.

5. *Repetition of wind and braking test.* This test is a repetition of test (2) in order to verify the service load performance of the tested bearing following several design earthquake events.

6. *Seismic performance verification test.* This test consists of three cycles of displacement at amplitude equal to the total design displacement. The purpose of the test is to determine the properties and verify the performance of the bearing following several design earthquake events.

7. *Stability test.* The stability test is conducted under vertical load of 1.2D + LLs+OT and 0.8D-OT, where D is the dead load, LLs is the seismic live load and OT is the additional load due to seismic overturning moment effects, and for one cycle of lateral displacement of amplitude equal to the offset displacement (due to creep, shrinkage and 50% thermal displacement) plus $1.5\ d_t$ if $A > 0.19$ or plus $2.0\ d_t$ if $A \leq 0.19$, where d_t is the total design displacement. The difference in the multiplier (1.5 vs 2.0) is due to the difference between the design earthquake and the maximum earthquake that depends on the seismicity of the site (see section 4.2.1). Moreover, in case d_t is calculated using the maximum earthquake, the amplitude should be the offset displacement plus $1.1\ d_t$.

The purpose of the stability test is to demonstrate that the bearing is stable under the combination of maximum or minimum axial load and maximum lateral displacement. AASHTO 1999 defines stability as the condition of non-zero applied lateral (shear) force when the maximum displacement is reached. However, this definition is inadequate because it defines a bearing with decreasing slope in its lateral force-lateral displacement curve as stable. For example, this is the case in dowelled bearings when the displacement exceeds the limit of rollover. Naeim and Kelly (1999) recommend that displacements should be limited to the rollover value of displacement even for bolted bearings, whereas AASHTO would have classified bearings as stable, at displacements that exceed the rollover limit.
The seismic prototype tests should be conducted at a frequency equal to the inverse of the effective period of the isolated bridge. This is an important specification given that the

mechanical properties of isolators are affected by heating during cyclic movement. Reduction of the frequency (or equivalently velocity) of testing, results in either reduction of the generated heat flux in sliding bearings or increase of the heat conduction in elastomeric bearings, both of which result in reduction in the rise of temperature of the tested isolator. The significance of heating, either frictional in sliding bearings or due to yielding of lead in lead-rubber bearings has been demonstrated in Constantinou et al. (1999), whereas the viscous heating in damping devices has been studied by Makris et al. (1998).

The engineer may reduce or waive the requirement for testing at a frequency equal to the inverse of the effective period provided that data exists or can be generated in the prototype testing program that establish the effect of frequency or velocity. This is best done through the use of system property modification factors for frequency or velocity as described in AASHTO 1999.

The AASHTO 1999 Guide Specifications also require the following:

1. The seismic performance verification test be performed at temperatures of -7, -15, -21 and -26^{o}C for low temperature zones A, B, C and D, respectively. The time of exposure to these temperatures should not be less than the maximum number of consecutive days below freezing in table 4.3.2 of AASHTO 2002. This duration is 3, 7, 14 and an unspecified number larger than 14 days for zones A, B, C and D, respectively.

2. The specified number of days of exposure to low temperature prior to testing may be excessive and needs to be re-evaluated. The reader is referred to section 6 and particularly figures 6-4 to 6-6 that show the effect of time of exposure on the low temperature properties, and the effect that two days of exposure at -26^{o}C have on the effective stiffness and energy dissipated per cycle. (For the bearing of figure 6-6, the increases are 40 and 50%, respectively, with respect to the values of properties at the temperature of 20^{o}C). It is noted that the results in figures 6-5 and 6-6 are for bearings used on a bridge in low temperature zone D. The engineer specified exposure to -26^{o}C for two days rather than the over-14 days figure in AASHTO 1999.

3. Bearings are tested under the design load and a cyclic displacement of peak velocity not less than 1mm/s for a cumulative travel of at least 1600 m (1 mile) and as much as the calculated travel due to traffic and thermal loadings for a period of at least 30 years. This test need not be performed for each project. It will be sufficient to perform this test for representative bearings and then utilize the results in the prediction of properties of similar bearings. The purpose of the test is to observe the effects of wear and fatigue on the mechanical properties of the bearing. While not specified in AASHTO 1999, the effects need to be quantified following the wear test by conducting some or all of the specified prototype tests. Moreover, this wear test may be used to measure wear rates for materials used in sliding bearings.

Acceptance criteria for tested prototype bearings in accordance with the 1999 AASHTO Guide Specifications are summarized in table 5-1. Satisfying these acceptance criteria may not be possible when one considers the results of low temperature tests. Also, some bearings may not meet the acceptance criteria of table 5-1 due to significant scragging effects or significant heating effects in high frequency (or high velocity) testing. In such cases, either the bearings are rejected

or, more appropriately, bounding analysis is performed within the context of system property modification factors and the engineer accordingly modifies the acceptance criteria. An example of such a testing specification and acceptance criteria is presented in section 5.5.

Table 5-1. Acceptance Criteria for Tested Prototype Isolators

Test	Article No.[1]	Acceptance Criterion [2]
All tests	13.2	Positive, incremental instantaneous stiffness
Seismic No. 1 at 1.0 d_t	13.2(b) (3)	Average K_{eff} of three cycles within 10% of design value
Seismic No. 1 at each amplitude	13.2(b) (3)	Minimum K_{eff} over three cycles not less than 80% of maximum K_{eff} over three cycles
Seismic No. 2	13.2(b) (4)	Minimum K_{eff} over all cycles not less than 80% of maximum K_{eff} over all cycles
Seismic No. 2	13.2(b) (4)	Minimum EDC over all cycles not less than 70% of maximum EDC over all cycles
Stability	13.2(b) (7)	Bearing remains stable

Notes: 1. 'Guide Specification for Seismic Isolation Design', AASHTO, Washington DC 1999, 76pp.

2. Notation: d_t = total design displacement
   K_{eff} = effective stiffness (force at maximum displacement divided by maximum displacement), and
   EDC = energy dissipated per cycle

5.4 PRODUCTION TESTS

Production (or proof) testing typically consists of the following two tests:

1. *Compression test.* This is a sustained, five-minute compression at 1.5 times the maximum dead plus live load. The engineer may enhance the specification by specifying that the compression be accompanied by a rotation at the angle of design rotation. (This is easily accomplished by supporting one side of the bearing by a beveled plate). The bearing is inspected for flaws such as rubber bulging and surface cracks in elastomeric bearings, and flow of PTFE and abnormal deformations in sliding bearings.

2. *Combined compression-shear test.* The bearing is subjected to compression at the average dead load for the bearings of the tested type and subjected to five cycles of sinusoidal displacement of amplitude equal to the total design displacement (but not less than 50% of the total rubber thickness for elastomeric bearings). The effective stiffness (K_{eff}) and

energy dissipated per cycle (EDC) are determined and compared to specified limits. AASHTO 1999 requires that:

a. For each bearing, the average five-cycle K_{eff} is within 20% of the design value.
b. For each bearing, the average five -cycle EDC is not less by more than 25% of the design value.
c. For each group of bearings, the average K_{eff} (over five cycles) is within 10% of the design value.
d. For each group of bearings, the average EDC (over five cycles) is not less by more than 15% of the design value.

It is noted that the design value is not necessarily a single value but it may be a range of values. If a single value is used, it is the nominal value (see section 4.5.2) assuming that natural variability (excluding the effects of aging, temperature, loading history, etc.) is not significant.

Production testing is rudimentary and intends to verify the quality of the product. It is quality control testing. The compression test must be conducted since it is most important for quality control. The combined compression-shear test is also important although under certain circumstances it may be acceptable to test only a portion of the bearings (say 50%) and implement a rigorous inspection program. A case in which reduced testing may be implemented is when testing may severely delay the delivery of bearings.

5.5 EXAMPLES OF TESTING SPECIFICATIONS

Two examples of specifications for prototype and production (proof) testing are presented. They are based on actual specifications used for seismically isolated bridges in the U.S.
The first specification is presented in appendix B and is based on the specifications used for a bridge in California. In this case, only nominal values of the isolator properties were used following a determination on the basis of simplified analysis that the effects of temperature, aging and history of loading did not result in significant changes in the calculated response (typically a change in response of not more than 15% is considered insignificant - for example see AASHTO 1999, article C8.2.1). The specification is primarily based on the AASHTO 1999 with the following changes:

a. The thermal, repetition of wind and braking, and the seismic performance verification tests were eliminated.
b. The stability test was specified to be conducted at larger displacement amplitude.
c. The acceptance criteria were modified to reflect what was considered in the design.
d. The production combined compression and shear test was specified to be conducted at half the maximum design displacement.

The second specification is also presented in appendix B and is based on the specifications used for a bridge in the Eastern United States in a low temperature zone C. The bridge is a critical link and bounding analysis in accordance with the AASHTO 1999 for seismic and for non-seismic loading conditions was performed. The nominal mechanical properties of the isolators under seismic and non-seismic conditions were determined to be within a range on the basis of available experimental data. Analysis was then performed for the likely upper and lower bound

values determined on the basis of the nominal properties and the effects of aging, low temperature and history of loading.

The testing specification includes only the tests that are important for this particular project. It also includes clear and simple performance criteria, which are based on the assumed range of properties for the design, and the acceptance criteria of AASHTO 1999.

CHAPTER 6: ELASTOMERIC ISOLATORS

6.1 INTRODUCTION

Elastomeric bearings have been used for more than 50 years to accommodate thermal expansion effects in bridges and allow rotations at girder supports. Extending their application to seismic isolation has been attractive in view of their high tolerance for movement and overload and minimal maintenance requirements. Three types of elastomeric isolators have evolved over the years to meet different requirements. These are:

- Lead-rubber isolator: natural rubber elastomeric bearing fitted with a lead core for energy dissipation.
- High-damping rubber isolator: natural rubber elastomeric bearing fabricated from high damping rubber for energy dissipation.
- Low-damping rubber isolator: natural rubber elastomeric bearing fabricated from low damping rubber (standard natural rubber) and used alongside a mechanical energy dissipator such as a viscous damper for energy dissipation.

In bridge applications, the most common elastomeric isolator is the lead-rubber isolator and this device is the focus of the material presented in this section.

6.2 LEAD-RUBBER ISOLATORS

Lead-rubber isolators are elastomeric bearings fitted with a central lead core to increase the dissipation of energy during lateral displacements. As with other bridge isolators, these devices are usually installed directly under the superstructure and are seated on the substructures, instead of conventional expansion bearings. A section through a typical circular lead-rubber bearing is shown in figure 6-1. The bearing is made from layers of vulcanized rubber sandwiched together between thin layers of steel (shims). In the middle of the bearing is a solid lead-core. The core is inserted into a pre-formed hole in the bearing and is sized so that it is an interference fit after installation. Steel plates are fitted to the top and bottom of the bearing to attach to the masonry and sole plates on the sub- and superstructures, respectively. The internal rubber layers provide flexibility in the lateral direction. The steel reinforcing plates provide confinement to the lead core, vertical stiffness and vertical load capacity. The lead core provides resistance to wind-induced and vehicle braking forces, to minimize the movement of the structure under service loads, but yields and dissipates energy under seismically induced lateral movements. Creep in the lead permits slowly applied environmental movements (such as thermal expansion) to be accommodated with minimal effect on the substructures. The cover rubber protects the steel layers from environmental effects. The bearing is very stiff and strong in the vertical direction, but flexible in the horizontal direction (once the lead core yields).

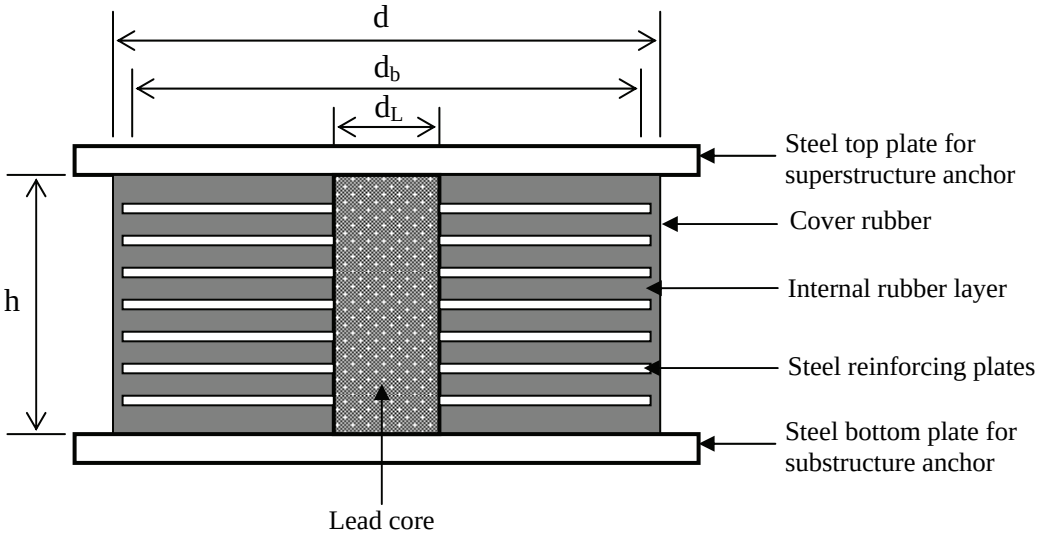

Figure 6-1. Sectional View of Lead-Rubber Isolator

6.2.1 MECHANICAL CHARACTERISTICS OF LEAD-RUBBER ISOLATORS

The mechanical characteristics of lead-rubber bearings with circular cross-section will be discussed here. The behavior of bearings with square or rectangular cross-section is similar. The combined lateral stiffness of the rubber layers and the lead core provide a large lateral elastic stiffness under service loads to control the movements of the structure. Under the effect of seismic loads, the steel reinforcing plates force the lead-core to deform in shear. The lead yields at a low shear stress of about 1.3 ksi (9.0 MPa). Once the yielding takes place, the lateral stiffness of the bearing is considerably reduced. The rubber layers then easily deform in shear providing the lateral flexibility to elongate the period of the bridge. Figure 6-2 shows the deformation of the bearing under lateral load. Figure 1-3 shows the idealized hysteretic behavior of the bearing.

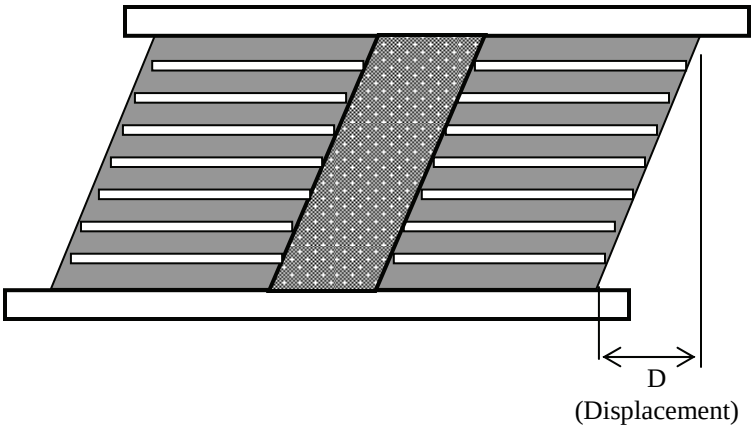

Figure 6-2. Shear Deformation in a Lead-Rubber Isolator

In the hysteresis loop of figure 1-3, Q_d is the characteristic strength of the bearing and F_y is yield strength. Since the elastomer is a low-damping, standard natural rubber, both Q_d and F_y are determined by the lead core alone as follows:

$$F_y = \frac{1}{\psi} f_{yL} \frac{\pi d_L^2}{4} \tag{6-1}$$

where f_{yL} = shear yield stress of the lead (1.3 ksi, 9.0 MPa)
d_L = diameter of the lead plug, and
ψ = load factor accounting for creep in lead
= 1.0 for dynamic (seismic) loads
= 2.0 for service loads (wind and braking loads)
= 3.0 for slowly applied loads (environmental effects such as thermal expansion).

The characteristic strength, Q_d is then given by

$$Q_d = F_y (1 - k_d/k_u) \tag{6-2}$$

where k_d = post elastic stiffness, and
k_u = elastic loading and unloading stiffness
= n k_d
n = 10 for dynamic (seismic) loads
= 8 for service loads (wind and braking loads)
= 5 for slowly applied loads (environmental effects such as thermal expansion)

For seismic loads, equation 6-2 becomes

$$Q_d = 0.9\ F_y \tag{6-3}$$

It follows from equations 6-1 and 6-3, that for f_{yL} = 1.3 ksi (9.0 MPa) and ψ = 1.0

$$Q_d \approx 0.9\ d_L^2 \quad \text{kips}, \quad d_L \text{ in inches} \tag{6-4a}$$
$$\approx 6.4\ d_L^2 \quad \text{N}, \quad d_L \text{ in millimeters} \tag{6-4b}$$

The post elastic stiffness k_d is primarily due to the stiffness of the rubber but is also influenced by the post-yield stiffness of the lead core. Thus

$$k_d = f\ k_r \tag{6-5}$$

where f is a factor to account for the contribution of the lead (generally taken equal to 1.1), and k_r is the elastic stiffness of the rubber material given by:

$$k_r = \frac{GA_b}{T_r} \tag{6-6}$$

where G = shear modulus of rubber
T_r = total thickness of rubber
A_b = net bonded area of rubber

The net bonded area A_b is the gross area the bearing less the area of the lead core. Thus:

$$A_b = \frac{\pi\left(d_b^2 - d_L^2\right)}{4} \tag{6-7}$$

where d_b is the diameter of bonded rubber.

From the hysteresis curve of figure 1-3, the total horizontal force F at displacement D is given by:

$$F = Q_d + k_d D \tag{6-8}$$

and the yield displacement, D_y, of the bearing is given by:

$$D_y = \frac{Q_d}{k_u - k_d} \tag{6-9}$$

The equivalent (linearized) properties of the lead-core isolator for use in elastic methods of analysis are the effective stiffness k_e and the equivalent viscous damping ratio β_e.

The effective stiffness is obtained by dividing the horizontal force, F, by the corresponding bearing displacement, D. Thus:

$$k_e = \frac{Q_d}{D} + k_d \tag{6-10}$$

The equivalent viscous damping ratio**,** β_e, is given by equation 3-3. Thus:

$$\beta_e = \frac{4Q_d(D - D_y)}{2\pi k_e D^2} = \frac{2Q_d(D - D_y)}{\pi D(Q_d + k_d D)} \tag{6-11}$$

An acceleration response spectrum with 5% damping is then modified for the actual damping, β_e and used for calculating the response of the isolated bridge (see section 3).

6.2.2 STRAIN LIMITS IN RUBBER

The bearing must be designed with adequate dimensions to accommodate the gravitational loads and corresponding rotations under large seismically induced lateral displacements. Accordingly, a set of strain limits in the elastomer must be satisfied. These limits are given in article 14.2 AASHTO 1999, and are as follows:

$$\gamma_c \le 2.5 \tag{6-12}$$

$$\gamma_c + \gamma_{s,s} + \gamma_r \le 5.0 \tag{6-13}$$

$$\gamma_c + \gamma_{s,eq} + 0.5\gamma_r \le 5.5 \tag{6-14}$$

where γ_c, $\gamma_{s,s}$, γ_r and $\gamma_{s,eq}$ are the shear strains respectively due to the effect of vertical loads, non-seismic lateral displacements, rotations imposed by vertical loads and seismic lateral displacements.

6.2.2.1 Compressive Strains

The maximum compressive strain in a rubber layer due to vertical load is given by:

$$\gamma_c = \frac{3SP}{2A_r G(1+2k'S^2)} \quad \text{for layers with small shape factors (S} \leq 15) \qquad (6\text{-}15a)$$

and

$$\gamma_c = \frac{3P(1+8Gk'S^2/K)}{4Gk'SA_r} \quad \text{for layers with large shape factors (S} > 15) \qquad (6\text{-}15b)$$

where P = vertical load resulting from the combination of dead load plus live load (including seismic live load, if applicable) using a load factor $\gamma = 1$

k' = material constant for elastomer (table 6-1)

K = bulk modulus of elastomer (table 6-1)

S = layer shape factor, defined for circular lead plug rubber bearings as:

$$S = \frac{d_b{}^2 - d_L^2}{4d_b t_i} \qquad (6\text{-}16)$$

t_i = thickness of elastomer layer i, and

A_r = the overlap area between the top-bonded and bottom-bonded elastomer areas of displaced bearing as given in figure 6-3.

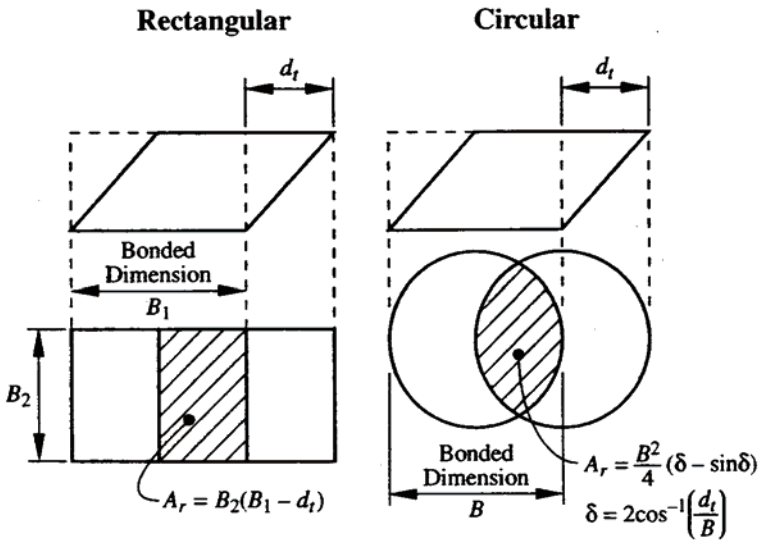

Figure 6-3. Overlap Area A_r Between Top-bonded and Bottom-bonded Areas of Elastomer in a Displaced Elastomeric Isolator (AASHTO 1999)

Table 6-1. Hardness and Elastic Moduli for a Conventional Rubber Compound[1]

Hardness	Elastic modulus, E[2]		Shear modulus, G[2]		Material constant, k[3]	Bulk modulus, K[4]	
IRHD / Shore A	psi	MPa	psi	MPa		psi	MPa
30	133	0.92	44	0.30	0.93	145,000	1000
35	171	1.18	49	0.37	0.89	145,000	1000
40	218	1.50	65	0.45	0.85	145,000	1000
45	261	1.80	78	0.54	0.80	145,000	1000
50	319	2.20	93	0.64	0.73	149,350	1030
55	471	3.25	117	0.81	0.64	158,050	1090
60	645	4.45	152	1.06	0.57	166,750	1150
65	862	5.85	199	1.37	0.54	175,450	1210
70	1066	7.35	251	1.73	0.53	184,150	1270
75	1363	9.40	322	2.22	0.52	192,850	1330

Notes: 1. Data in table are for a conventional, accelerated-sulphur, natural rubber compound, using SMR 5 (highest grade Standard Malayasian Rubber) and reinforcing black filler for hardnesses above 45. Tensile strength is 3,770 psi (26 MPa). Elongation at break is 730%. Values are taken from Lindley, 1978, and are reproduced with permission.

2. For an incompressible material (Poisson's ratio = 0.5), the elastic modulus is theoretically three times the shear modulus. Although rubber is virtually incompressible (Poisson's ratio = 0.4997), the ratio between these two moduli in the above table varies from 3.1 (at hardness= 30) to 4.2 (at hardness = 75). This is believed to be due to the effect of non-rubber fillers added to the compound to increase hardness (reinforcing black), improve resistance to environment (anti-oxidants), and assist with processing.
3. Material constant, k, is used to calculate compression modulus (Ec) of bonded rubber layers, i.e., $Ec = E(1 + 2kS^2)$, where S is the layer shape factor.
4. Bulk Modulus values are very sensitive to test method especially for samples with high shape factors. Other data (e.g., Wood and Martin (1964)) suggest values twice those listed above, particularly for parts with high shape factors.

6.2.2.2 Shear Strains

The shear strain, $\gamma_{s,s}$, due to non-seismic lateral displacement, Δ_s is given by:

$$\gamma_{s,s} = \frac{\Delta_s}{T_r} \tag{6-17}$$

The shear strain, $\gamma_{s,eq}$, due to seismic lateral design displacement, D, is given by:

$$\gamma_{s,eq} = \frac{D}{T_r} \tag{6-18}$$

The shear strain, γ_r, due to the design rotation, θ, that include the rotational effects of dead load, live load and construction is given by:

$$\gamma_r = \frac{d_b^2 \theta}{2 t_i T_r} \tag{6-19}$$

The shear strain γ_t, due to torsion ϕ, of the bridge superstructure is given by:

$$\gamma_t = \phi \cdot \frac{r}{h} \tag{6-20}$$

where r = radius of bearing (or half width of a square bearing), and
h = height of bearing.

Torsional rotations are typically very small and may be estimated on the basis of the simple procedure recommended in the International Building Code (International Code Council, 2000), i.e.:

$$\phi \cong \frac{12eD}{b^2 + d^2} \tag{6-21}$$

where e = eccentricity between the center of resistance of isolation and the center of mass
D = displacement of isolation system at the center of resistance, and
b, d = plan dimensions of superstructure.

Equation (6-21) gives rotations of the order of 0.01 rad, and since the radius r, is usually about equal to, or just more than the height h, the maximum shear strain due to torsion γ_t is of the order of 0.01, and is thus not significant.

In general, the torsional stiffness of individual bearings, and the stresses and strains resulting from torsion, are insignificant and may be neglected. If torsional stiffness is to be included in the analysis, equation 6-29 may used to calculate this property.

6.2.3 STABILITY OF LEAD-RUBBER ISOLATORS

Elastomeric bearings need to be checked against the possibility of instability in both the undeformed and deformed displaced states.

Instability is influenced by the installation details and there are two common types for these connections:

1. A moment-and-shear connection, such as a bolted connection to both the masonry and sole plates.
2. A shear-only connection, such as a doweled connection to the masonry and sole plates. Alternatively, keeper bars welded to both plates may be used, or the bearing located within recesses in both plates.

6.2.3.1 Stability in the Undeformed State

In the undeformed state and loaded only in the vertical direction, the buckling load of bearings installed in either of the above two configurations is theoretically the same.

For a bearing with moment of inertia I, cross-sectional area A, and total rubber thickness Tr, this load P_{cr}, is given by:

$$P_{cr} = \sqrt{\frac{\pi^2 E_c IGA}{3T_r^2}} \tag{6-22}$$

where G is the shear modulus, and E_c is the modulus of elasticity of the rubber in compression and is given by:

$$E_c = \frac{1}{\left(\frac{1}{6GS^2} + \frac{4}{3K}\right)} \tag{6-23}$$

If the bulk modulus *K*, is assumed to be infinite, then equation 6-23 gives $E_c = 6GS^2$ and for circular bearings with diameter B and layer thickness t, equation 6-22 becomes:

$$P_{cr} = 0.218\frac{GB^4}{tT_r} \tag{6-24a}$$

For square bearings with side B and layer thickness t, equation 6-22 becomes:

$$P_{cr} = 0.344\frac{GB^4}{tT_r} \tag{6-24b}$$

The factor of safety against buckling in the undeformed state is calculated by dividing P_{cr}, by the total load due to dead plus live load.

6.2.3.2 Stability in the Deformed State

In the deformed state the critical load depends on which of the above two configurations is used.

Case (1). For bolted connections, the critical load will be given by buckling as in the previous section, but modified to include the effect of the lateral deformation. However there is no simple rational theory that includes this effect and the following intuitive equation is used in lieu of a more rigorous solution (Buckle and Liu, 1994):

$$P'_{cr} = P_{cr}\frac{A_r}{A} \tag{6-25}$$

where P'_{cr} = buckling load in deformed state,

A = bonded elastomer area, and

A_r = effective column area defined as the area of the overlap between the top and bottom bonded areas of the deformed bearing (see figure 6-3).

Using values for A_r given in figure 6-3, it follows that:

$$P_{cr}' = P_{cr}(\delta - \sin\delta)/\pi \quad \text{for a circular bearing} \tag{6-26a}$$

and

$$P_{cr}' = P_{cr}(1 - d_t/B) \quad \text{for a square bearing} \tag{6-26b}$$

The factor of safety against buckling stability is calculated by dividing P'_{cr}, by the load due to dead plus seismic live load.

Case (2). During large lateral deformation, dowelled bearings and bearings recessed in keeper plates may experience partial uplift. At some critical lateral displacement, D_{cr}, the bearings roll-over or overturn. The critical value of this displacement is given by:

$$D_{cr} = \frac{PB - Q_d h}{P + k_d h} \tag{6-27}$$

where P = axial load on the bearing
B = plan dimension (e.g. diameter)
Q_d = characteristic strength
k_d = post-elastic stiffness, and
h = total height of bearing (total rubber thickness plus steel shims).

The factor of safety against this type of instability is given by dividing the rollover displacement D_{cr} by the design displacement D_d.

6.2.4 STIFFNESS PROPERTIES OF LEAD-RUBBER ISOLATORS

In addition to the effective lateral stiffness, k_e, the axial (compressive) and torsional stiffnesses of the isolators may be required for structural modeling of the bearings in a detailed seismic analysis. In the calculation of the axial stiffness of the bearing, the compressive stiffness of the steel reinforcing plates is neglected as it is much larger than that of the rubber. Thus, the axial stiffness, k_c, of the bearing, is determined by the stiffness of the rubber layers in compression and is given by:

$$k_c = \frac{E_c A_b}{T_r} \tag{6-28}$$

The axial stiffness is assumed to be independent of axial strain, i.e. it is linear for the range of strains encountered in practice.

Similarly, the torsional stiffness, k_T, of the bearings is calculated based on the properties of the rubber portion of the bearing conservatively assuming that the entire bearing is made of rubber. Thus:

$$k_T = \frac{GJ}{T_r} \tag{6-29}$$

where J is the polar moment of inertia of the entire bearing cross-section and given by:

$$J = \frac{\pi d^4}{32} \tag{6-30}$$

The torsional stiffness is assumed to be independent of torsional strain, i.e. it is linear for the range of strains encountered in practice.

6.3 PROPERTIES OF NATURAL RUBBER

Elastomeric isolators use either natural or synthetic rubbers and in the United States, the most commonly-used elastomer in seismic isolators is natural rubber. Whereas neoprene (a popular

synthetic rubber) has been used extensively in thermal expansion bearings for bridges, there have few if any applications of neoprene to isolation bearings. This is because very high shear strains can occur in isolation bearings under extreme seismic loads and natural rubber performs better under these conditions than neoprene (has higher elongation-at-break). Accordingly this section focuses on natural rubber. The notes below are adapted from Lindley (1978).

6.3.1 NATURAL RUBBER

Natural rubber is a polyisoprene and as such, is a member of a high-polymer family that includes silk, cellulose, wool, resins and synthetic plastics and rubbers. The distinguishing feature of this family is the long length of the molecular chain and, for the subdivision which contains natural and synthetic rubbers, the flexible nature of this chain and its ability to deform elastically when cross-linked. Raw rubber occurs as a latex beneath the bark of certain trees, notable *Hevea brasiliensis,* which is cultivated in the plantations of Malaysia and other tropical countries. To make practical use of this material it is first vulcanized, which is a chemical and mechanical process involving mastication while adding sulfur and various fillers, and applying heat. During this process the long chain molecules are chemically linked, usually by sulphur, forming an elastic compound with properties that depend on the curing conditions (temperature and time) and the additives.

6.3.1.1 Elastic Modulus, E

Vulcanized rubber is a solid three-dimensional network of crosslinked molecules. The more crosslinks there are in the network, the greater the resistance to deformation under stress. Certain fillers, notably reinforcing blacks (carbon), create a structure within the rubber which further increases both strength and stiffness. Load - deflection curves are approximately linear at small strains (less than a few percent) and values of the elastic modulus can be obtained from these linear regions. Values in tension and compression are approximately equal. Table 6-1 gives typical values for natural rubbers of varying hardness (amounts of carbon black filler).

6.3.1.2 Bulk Modulus, K

Typical values for the bulk modulus of rubber range from 1000 - 2000 MPa and are many times larger than corresponding values for elastic modulus (1 - 10 MPa). These very high numbers mean that rubber is virtually incompressible and Poisson's Ratio may be taken as 0.5. Table 6-1 gives typical values for natural rubbers of varying hardness (amounts of carbon black filler).

6.3.1.3 Shear Modulus, G

Theoretically, with a Poisson's ratio of 0.5, the shear modulus is one-third the elastic modulus. Test results show this to be true for soft gum rubbers (un-filled rubbers), but for harder (filled) rubbers that contain a reasonable proportion of non-rubber constituents, thixotropic and other effects reduce the shear modulus to about one-fourth of the elastic modulus. This can be seen in table 6-1 where the ratio between elastic and shear modulus increases from about 3 to more than 4 as the hardness increases from 30 to 75.

6.3.1.4 Hardness

Hardness measurements are generally used to characterize vulcanized rubber as seen in table 6-1. For rubber, hardness is essentially a measurement of reversible elastic deformation produced by a specially shaped indentor under a specified load and is therefore related to the elastic modulus of the rubber, unlike metal hardness which is ameasure of an irreversible plastic indentation. Readings using International Rubber Hardness degrees (IRHD) and the Shore Durometer A Scale are essentially the same.

Hardness is a relatively simple and easy number to obtain but is subject to some uncertainty ($\pm\ 2^0$ in table 6-1). Values for shear modulus are more accurate but less easily obtained.

6.3.1.5 Ultimate Strength and Elongation-at-Break

The tensile strength of a good quality natural rubber is in the range 2 – 4 ksi (14 - 28 MPa), based on the original cross-sectional area, and the strain at rupture (elongation-at-break) will be in the range 500 – 750 %. If the area-at-break is used to calculate the ultimate strength, it can be as high as 29 ksi (200 MPa). Compressive strengths are typically of the order of 23 ksi (160 MPa).

6.3.1.6 Fillers

Rubbers that contain only sulphur (and other chemicals necessary for vulcanization such as stearic acid and zinc oxide), protective agents, and processing aids, are known as gum rubbers, or unfilled rubbers. By far the majority of rubbers used in engineering applications also contain fillers such as carbon black which may comprise up to one-third of the vulcanizate compound. These black fillers fall into two groups: (1) ‘reinforcing’ blacks, which improve tear and abrasion properties, and increase elastic modulus, hysteresis and creep, and (2) ‘non-reinforcing’ blacks, which have little effect on tear and abrasion and give only moderate increases in modulus, hysteresis and creep. They can however be used in greater volumes than reinforcing blacks.

6.3.1.7 Hysteresis

Natural unfilled rubbers exhibit very little hysteresis but, as noted above, fillers can be used to increase this effect. The High-Damping Rubber (HDR) isolator is a device where fillers are added to increase the hysteresis to a level where the energy dissipation is sufficient to limit structure displacements in a cost-effective manner. However, uncertainty about creep and scragging effects have limited their application and few, if any, HDR isolators have been used in bridge applications. By contrast, natural rubbers with minimal amounts of filler (just sufficient for hardness and abrasion resistance), are used almost exclusively in bridge isolators in the U.S. In these cases, energy dissipation for displacement control is provided by a separate mechanical means, such as a lead core that yields or a friction device.

6.3.1.8 Temperature Effects

The physical properties of rubber are generally temperature dependent, but these effects are also fully reversible provided no chemical change has occurred within the rubber.

Below -5°F (-20°C), the stiffness (hardness) of a typical natural rubber begins to increase until, at about -75°F (-60°C), it is glass-like and brittle. This glass-hardening phenomenon is fully reversible and elasticity is recovered as the temperature is increased. Natural rubber will also crystallize and lose elasticity if it is held for several days at its crystallization temperature (about -15°F (-25°C) for a typical compound). Like glass-hardening, this effect also disappears quickly as the temperature is increased. The temperatures at which these two phenomena occur can be lowered by compounding the rubber specifically for low-temperature applications.

Typical rubbers can be used at sustained temperatures up to 140°F (60°C) without any deleterious effect (but see note below about susceptibility to oxygen, UV and ozone). Specially compounded rubbers are available for applications up to 212°F (100°C). At temperatures approaching those used for vulcanizing (about 285°F (140°C)), further vulcanization may occur resulting in increased hardness and decreased mechanical strength. At very high temperatures (above say 660°F (350°C)), rubber first softens as molecular breakdown occurs and then becomes resin-like, i.e., hard and brittle.

6.3.1.9 Oxygen, Sunlight and Ozone

Exposure to oxygen, ultra-violet (UV) radiation, and ozone generally results in a deterioration of physical properties and an increase in creep and stress relaxation. These effects are more pronounced in parts with thinner cross-sections, and/or subject to tensile strain. Elevated temperatures may also accelerate these effects. As a result, antioxidants are almost always added to natural rubber compounds intended for engineering applications, along with carbon black fillers for UV protection, and waxes for ozone resistance.

6.3.1.10 Chemical Degradation

Natural rubber is remarkably resistant to a wide range of chemicals from inorganic acids to alkalies. However, if a large volume of a liquid is absorbed, rubber will swell and lose strength. The extent of this swelling depends on the liquid and the nature of the rubber compound. Typical natural rubbers have excellent swelling resistance to water, alcohol, and vegetable oils, but are very susceptible to low-viscosity petroleum products such as gasoline. Whereas the occasional splashing of a rubber part with gasoline is not likely to be serious, immersion should be avoided. Such a situation is not anticipated in isolators intended for bridge applications but in the unlikely event that it did occur, due say to an overturned gasoline tanker, the large physical size of these devices is expected to give adequate time for clean-up before swelling becomes significant.

6.3.2 EXAMPLE OF A NATURAL RUBBER COMPOUND FOR ENGINEERING APPLICATIONS

A data sheet for a rubber compound that is suitable for use in an elastomeric isolator is shown in table 6-2. Developed by the MRPRA (now Tun Abdul Razak Laboratory) this compound has a shear modulus of 125 psi (0.86 MPa) at 50% shear strain. The compound is a conventional, accelerated-sulphur vulcanizate containing 40 parts per hundred by weight of FEF (N-550) carbon black. It is suitable for most engineering applications at moderate and low temperatures.

Other key properties that may be read from this sheet are:
Hardness = 60
Tensile strength = 3,770 psi (26 MPa)
Elongation at break = 560%
Shear modulus at low shear strain (2%) = 141 psi (0.97 MPa)
Shear modulus at moderate shear strain (50%) = 125 psi (0.86 MPa)
Bulk modulus (estimated) = 308,850 psi (2,130 MPa)
Viscous damping ratio at 1Hz, 50% shear strain, 73^0 F (23^0 C) = 2.9%

6.4 PROPERTIES OF LEAD

Pure lead has a yield stress in shear of about 1.3 ksi (8.96 MPa) which means that lead cores with reasonable sized dimensions can be designed such that wind and other service loads can be resisted within the elastic range. Nevertheless it is important that the core size is neither too small nor too large for the elastomeric bearing in which it is to be fitted. As a general rule, the core diameter (d_L) should fall within the following range:

$$B/6 < d_L < B/3 \qquad (6\text{-}31)$$

where B = bonded diameter if a circular bearing, or side dimension if square.

It is also important that the lead be tightly confined within the bearing, which means that the rubber layer thickness should not exceed 3/8 in (9 mm) and the ends of the core be sealed by end caps in the cover plate. These caps not only help confine the lead but also protect the ends of the core against damage during shipping and installation.

Pure lead recrystallizes at room temperature which means that after extrusion or shear deformation the elongated grains necessary to accommodate the deformation, regain their original shape almost instantaneously. Most metals exhibit recrystallization but few do so at room temperature. Lead therefore does not work-harden at room temperature and it is virtually impossible to cause lead to fail by fatigue. These characteristics apply only to chemically pure lead; the slightest contamination with antimony and other elements that occur naturally with lead, will elevate the recrystallization temperature leading to work-hardening at ambient temperatures.

Table 6-2a. Natural Rubber Engineering Data Sheet

Natural Rubber Engineering Data Sheet

1980

EDS 23

The Malaysian Rubber Producers' Research Association, Tun Abdul Razak Laboratory, Brickendonbury, Hertford SG13 8NL, England.
A Malaysian Rubber Research and Development Board Organization.

Natural Rubber engineering vulcanizate: 0·86MPa shear modulus (60 IRHD) Ref. no. MRPRA EDS 23

A conventional accelerated-sulphur vulcanizate containing 40 parts phr of FEF (N-550) carbon black.
Suitable for most engineering applications at moderate and low temperatures.
Similar stiffness to EDS 15, 25 and 27 which have the same formulation except for the carbon black filler.

Formulation

	parts by weight
Natural rubber, SMR CV60	100
Zinc oxide	5
Stearic acid	2
Carbon black, FEF (ASTM N-550)	40
Process oil[1]	4
Antioxidant/antiozonant, HPPD[2]	3
Antiozonant wax[3]	2
CBS[4]	0·6
Sulphur	2·5

1. Low viscosity naphthenic oil; Fina Process Oil 2059 (Petrofina) was used.
2. N-(1,3-dimethylbutyl)-N′-phenyl-p-phenylenediamine; Santoflex 13 (Monsanto) was used.
3. Sunproof Improved (Uniroyal) was used.
4. N-cyclohexylbenzothiazole-2-sulphenamide.

Where ingredients in MRPRA formulations are designated by trade names this indicates only that these were the materials used to develop the formulation and does not imply recommendation of specific trade materials. Chemically equivalent materials would normally be expected to give similar results.

Mix preparation and properties

Francis Shaw K2A Intermix, 33kg batch, 80°C, 50rev/min, 0·69MPa (100 lbf/in²) ram pressure, cooling water 150 l/min (2000 imp.gal/h). 0min: add rubber. 1min: add ZnO, StA, HPPD, wax. 2min: add black, oil. 3½min: discharge. Mix finalized on cold mill.

Mooney viscosity (ISO/R289), ML1+4, 100°C	34
Mooney scorch (ISO 667), t_5, 120°C, min	31·3
Monsanto Rheometer (ISO 3417), 140°C	
scorch, t_{s1}, min	9·7
time to 95% crosslinking, min	27·4

Vulcanizate properties

for press cure 45min at 140°C

Density (ISO 2781), Mg/m³	1·091
Hardness (ISO 48), IRHD	60
Tensile strength (*TS*) (ISO 37), MPa	26
Elongation at break (*EB*) (ISO 37), %	560
Modulus at 300% elongation(*M300*)(ISO 37),MPa	10·1
Relaxed modulus (*MR100*), MPa	1·80
Compression set (ISO 815)	
22h at 23°C, %	6
22h at 70°C, %	33
22h at 100°C, %	56
22h at 125°C, %	75
22h at 150°C, %	99
7 days at 23°C, %	8
7 days at 70°C, %	52
3 days at 100°C, %	65
Resilience, Lüpke (ISO 4662), %	73
Stress relaxation, bonded disk 13mm dia × 6·3mm	
20% compression, % per decade	2·8
Tear strength (ISO 34)	
trouser, kN/m	14
angle, without nick, kN/m	59
angle, with 1mm nick, kN/m	42
crescent (with 1mm nick), kN/m	89

Tension fatigue, ring test pieces, kc to failure

strain range	minimum strain 0%	12½%	25%	37½%
50%	1027	969	>2000	>2000
75%	314	335	702	>2000
100%	207	147	216	693
125%	87	84	116	213
150%	49	43	52	74

Goodrich Flexometer (ISO 4666)	
static stress 1MPa, stroke 5·71mm, 30Hz, 100°C	
temperature increase after 120min, degC	17
Abrasion loss, Akron (BS 903:A9) dusted, mg/1000 rev	105
Ozone resistance (ISO 1431), 40°C, 20% strain	
No cracks after 7 days at 100pphm ozone	
Resistance to liquids (ISO 1817), 70h at 100°C	
Oil No. 3, volume change, %	280
Water, volume change, %	5·1

Low temperature hardness (ISO 3387) IRHD

days	1	3	7	14	21	28
0°C	61	60	60	60	60	60
−10°C	61	61	61	62	63	62
−25°C	61	60	60	62	63	63
−40°C	62	63	63	63	62	63

Low temperature compression set (ISO 1653)
lubricated small disks, set after 30min recovery, %

days	1	3	7	14	21	28
0°C	13	13	15	15	17	19
−10°C	10	14	14	14	16	16
−25°C	21	22	26	32	35	31
−40°C	29	27	28	28	47	48

Impact brittleness (ISO 812), −40°C	no failures
Air-oven ageing resistance (ISO 188)	
increase in IRH, deg	
decrease in *TS* and *EB*, %	
increase in *M300* and *MR100*, %	

	IRH	*TS*	*EB*	*M300*	*MR100*
3 days at 70°C	0	2	6	11	10
4 ,, ,,	1	0	5	15	9
7 ,, ,,	1	2	6	18	8
14 ,, ,,	2	9	12	26	29
3 days at 100°C	−2	40	38	24	25
4 ,, ,,	−2	59	58	—	28
7 ,, ,,	−2	70	71	—	71
14 ,, ,,	2	75	84	—	—
1 day(s) at 125°C	−10	81	72	—	22
3 ,, ,,	−7	85	90	—	—
1 day at 150°C	−3	98	89	—	—

Table 6-2b. Natural Rubber Engineering Data Sheet (continued)

EDS 23

Stress-strain characteristics

Shear modulus	(0–2%)	0·97MPa
,,	(0–50%)	0·86MPa
Bulk modulus (calculated)		2130MPa

Static shear moduli

Chord modulus G_{ch} = stress/strain; tangent modulus G_{tan} = slope of stress-strain curve. Strain rate ~ 30%/min.

Strain, %		2	5	10	25	50	75	100	150	200	250	300	350
1st cycle	G_{ch}, MPa	1·13	1·10	1·07	0·98	0·90	0·87	0·86	—	—	—	—	—
	G_{tan}, MPa	1·12	1·06	1·00	0·85	0·81	0·82	0·92	—	—	—	—	—
10th cycle	G_{ch}, MPa	0·97	0·96	0·94	0·90	0·86	0·84	0·84	0·94	1·12	1·38	1·73	2·07
	G_{tan}, MPa	0·95	0·95	0·92	0·84	0·80	0·81	0·89	1·31	2·03	2·91	3·82	4·58

First nine cycles to 100% strain. Set at end of 9th cycle 5·2%.

Static compression moduli

Chord modulus E_{ch} = stress/strain; tangent modulus E_{tan} = slope of stress-strain curve. Strain rate 10–30%/min.

Diameter/thickness		2 (S = 0·5)				4 (S = 1)				8 (S = 2)			
Strain, %		5	10	15	20	5	10	15	20	5	10	15	20
1st cycle	E_{ch}, MPa	5·58	5·07	4·99	4·91	10·3	9·10	8·91	9·42	26·7	25·9	27·8	31·8
	E_{tan}, MPa	5·00	4·73	4·72	4·81	9·18	9·00	9·81	11·7	26·0	28·4	35·8	49·2
10th cycle	E_{ch}, MPa	5·22	5·01	4·92	4·88	8·75	8·76	8·95	9·22	23·6	22·6	24·4	28·9
	E_{tan}, MPa	4·76	4·71	4·64	4·87	8·67	8·73	9·50	11·3	21·8	24·8	28·9	49·6
Max strain on first cycle			33%				29%				32%		
Set at end of 9th cycle			1·7%				1·3%				2·1%		

Diameter/thickness		12 (S = 3)				20 (S = 5)				32 (S = 8)			
Strain, %		5	10	15	20	5	10	15	20	5	10	15	20
1st cycle	E_{ch}, MPa	51·8	53·4	61·6	76·3	128	147	188	—	305	383	—	—
	E_{tan}, MPa	52·5	65·0	97·0	150	136	218	416	—	367	662	—	—
10th cycle	E_{ch}, MPa	46·2	45·0	52·2	65·1	110	118	157	—	246	314	—	—
	E_{tan}, MPa	42·3	48·7	72·2	167	101	149	502	—	256	708	—	—
Max strain on 1st cycle			22%				16%				12%		
Set at end of 9th cycle			1·5%				1·1%				1·6%		

Dynamic shear moduli and phase angles

Shear modulus is the ratio of stress amplitude to strain amplitude. Mean strain is zero.

Frequency	0·1Hz			1Hz							15Hz		
Strain amplitude, %	2	10	50	1	2	5	10	20	50	100	2	5	10
Shear modulus, MPa													
150°C	0·91	0·84	0·64	1·00	0·95	0·88	0·87	0·79	0·66	0·62	1·01	0·95	0·94
125°C	1·12	1·04	0·91	1·21	1·17	1·10	1·07	1·02	0·93	0·84	1·22	1·15	1·12
100°C	1·19	1·13	1·00	1·26	1·23	1·18	1·16	1·12	1·03	0·96	1·29	1·22	1·20
70°C	1·24	1·12	0·93	1·34	1·29	1·20	1·17	1·08	0·97	0·91	1·36	1·25	1·21
50°C	1·28	1·17	0·95	1·41	1·32	1·23	1·21	1·11	0·97	0·92	1·39	1·28	1·27
23°C	1·47	1·28	0·96	1·68	1·54	1·39	1·32	1·13	0·99	0·94	1·64	1·47	1·40
0°C	1·63	1·36	0·98	1·92	1·71	1·51	1·42	1·19	1·01	0·93	1·93	1·67	1·56
–10°C	1·65	1·39	0·99	1·97	1·81	1·58	1·48	1·21	1·02	0·94	2·11	1·83	1·70
–25°C	1·93	1·52	1·07	2·46	2·15	1·88	1·70	1·45	1·18	1·02	3·30	2·78	2·43
–40°C	2·25	1·84	1·21	4·23	3·70	3·23	3·00	2·39	1·74	1·48	10·8	7·34	4·98
Phase angle, degrees													
150°C	3·3	2·5	2·5	3·0	3·3	3·2	2·8	2·5	3·0	2·8	4·0	3·3	3·3
125°C	2·8	2·0	1·8	2·5	2·8	2·7	2·2	2·0	1·5	1·7	2·5	2·7	2·5
100°C	3·0	2·2	2·0	2·3	2·0	2·3	2·3	2·3	2·5	1·8	2·5	2·7	2·3
70°C	4·5	3·0	2·6	3·3	4·2	3·8	2·8	2·3	2·3	2·5	4·3	3·8	3·0
50°C	5·3	3·8	2·7	4·0	4·5	4·2	3·0	3·2	2·5	2·3	4·2	4·0	3·3
23°C	5·7	4·0	3·0	4·3	5·5	4·7	4·2	3·5	3·3	3·0	6·0	5·7	5·0
0°C	6·7	5·2	4·3	5·5	5·8	6·0	5·7	5·5	4·5	4·3	8·8	8·8	8·5
–10°C	6·5	5·8	4·8	6·7	8·3	7·3	7·0	6·7	6·0	5·8	13	14	13
–25°C	9·0	7·8	6·7	11	12	13	12	13	12	11	27	28	27
–40°C	16	18	16	30	33	34	34	35	31	28	47	47	42

Further information

EDS 1 Test methods used for the natural rubber engineering vulcanizates in the EDS series
EDS 2 Properties given for the natural rubber engineering vulcanizates in the EDS series
EDS 3 Effect of compounding on the properties of natural rubber engineering vulcanizates

Lead also has a relatively high creep coefficient which means that slowly applied deformations, such as expansion and contraction due to seasonal temperature changes in the superstructure, can occur without significant resistance. Loads imposed on substructures due to these effects are correspondingly small.

The mechanical properties of lead are very stable with time and the system property modification for lead is set equal to 1.0 (table 6-4).

6.5 EFFECTS OF VARIABILITY OF PROPERTIES, AGING, TEMPERATURE, AND LOADING HISTORY ON PROPERTIES OF ELASTOMERIC ISOLATORS

The properties of isolators inevitably vary due to manufacturing differences, aging, wear, history of loading, temperature, and the like. These variations may alter the effective period and equivalent damping of the isolation system, both of which will influence the dynamic response of the isolated structure. The interested reader is referred to Constantinou et al. (1999) for a detailed description of these effects. They are briefly discussed below.

6.5.1 VARIABILITY OF PROPERTIES

The mechanical properties of seismic isolation hardware exhibit variability in values as a result of natural variability in the properties of the materials used and as a result of the quality of manufacturing. It is not unusual to have properties, such as the post-elastic stiffness or the characteristic strength in a particular cycle of reversed loading, differ by ± 25 percent from the average values among all tested isolators.

6.5.2 AGING

Aging is the degradation or change of properties with time. Herein, a brief description of the aging effects on the mechanical properties of characteristic strength and post-elastic stiffness of seismic isolation hardware is presented. Moreover, it should be recognized that aging may also have effects on the ability of the isolation hardware to sustain stress, strain, force or deformation, which also need to be considered in design.

Seismic isolation is a relatively new technology so the field observation of performance of seismic isolation hardware is limited to about 15 years. Actual data on the mechanical properties of seismic isolation bearings removed from structures and re-tested after years of service are limited to a pair of bearings but the results are inclusive given that the original condition of the bearings was not exactly known. However, there is considerable information collected from the field inspection of seismic isolation and other similar bearings, from testing of field-aged bearings in non-seismic applications, from laboratory studies and from theoretical studies. While this information is indirect, it is very useful and may be summarized as follows:

1. Aging in elastomeric bearings is dependent on the rubber compound and generally results in increases in both the stiffness and the characteristic strength. These increases are expected to be small, likely of the order of 10-percent to 20-percent over a period of 30 years, for the standard low damping, high shear modulus compounds (shear modulus of

about 0.5 to 1.0 MPa). However, the increases may be larger, and likely substantially larger, for improperly cured bearings and for materials compounded for either very high damping or very low shear modulus.

2. The continuous movement of bearings due to traffic loads in bridges may cause wear and fatigue. While AASHTO 1999 requires that tests be performed to evaluate the effects of cumulative movement of at least 1600 m (1 mile) , such tests have not been performed on elastomeric bearings. It is expected that such tests may reveal some but not significant change in properties.

6.5.3 TEMPERATURE

The effects of temperature on the mechanical properties of seismic isolation bearings may be discussed in two distinct ways: (a) the effect of heating (viscous, hysteretic or frictional) on the mechanical properties during cyclic movement of the bearings, and (b) the effect of ambient temperature (and particularly low temperature) and of the duration of exposure to this temperature on the mechanical properties.

6.5.3.1 Heating During Cyclic Movement

In elastomeric bearings without a lead core, heating results from energy dissipation in the entire volume of rubber. Constantinou et al. (1999) have shown that for typical conditions (pressure of 7MPa, shear strain of 150-percent), the rise in temperature is about 1^{o}C or less per cycle regardless of the speed of the cyclic movement. This figure is consistent with experimental results. The temperature rise is too small to have any significant effect on the mechanical properties of the bearings.

In lead-rubber bearings, the energy dissipation primarily takes place in the lead core which is substantially heated during cyclic movement. During the first couple of cycles, when the generated heat in the lead core is entirely consumed for the rise of its own temperature, rises of temperature of the order of 20 to 40^{o}C per cycle have been calculated (see Constantinou et al., 1999) for typical conditions (pressure of about 5.5 MPa, shear strain of 120-percent, velocity of up to 1 m/sec). Under these conditions, the mechanical properties of lead (e.g., ultimate strength and effective yield stress) reduce resulting in a noted reduction of energy dissipated per cycle.

6.5.3.2 Effect of Ambient Temperature

Low temperatures generally cause an increase in stiffness and characteristic strength (or friction in sliding bearings). For elastomeric bearings this increase is depicted in figure 6-4. As noted in section 6.3.1.8, elastomers exhibit almost instantaneous stiffening when exposed to low temperatures, which is followed by further time-dependent stiffening (Constantinou et al., 1999; Roeder et al., 1987). As an example, figure 6-5 compares loops recorded in testing of an elastomeric bearing (bonded area = 114,000 mm^2, rubber height = 195 mm, natural rubber grade 3, shore A hardness 45, tested at peak shear strain of about 60%). The substantial increase in stiffness and energy dissipated per cycle are evident following conditioning for 48 hours in a chamber at –26° temperature. Also, figure 6-6 compares loops recorded in the testing of a lead-

rubber bearing of identical construction as the previously described bearing but with a 70 mm diameter lead core. Note that in this case the increases in stiffness and energy dissipation per cycle at low temperature are due primarily to changes in the properties of the elastomer and not of the lead core.

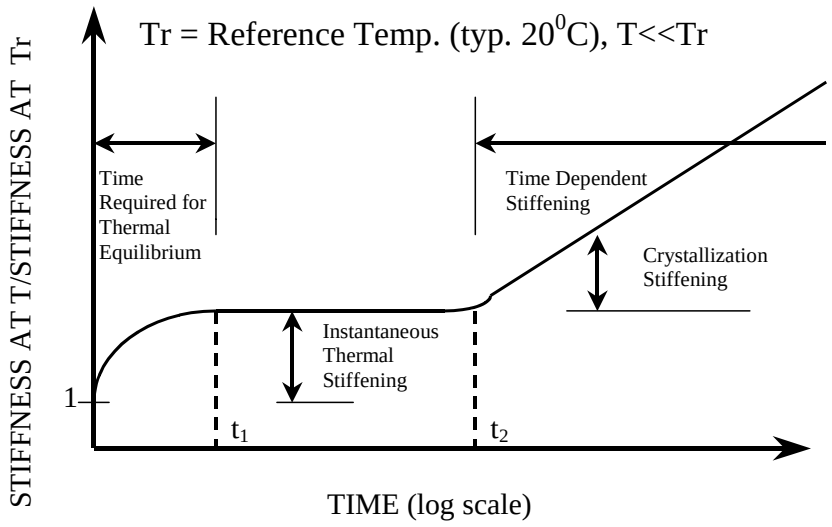

Figure 6-4. Time-dependent Low Temperature Behavior of Elastomers

6.5.4 LOADING HISTORY

The history of loading can have a marked effect on the mechanical properties of all types of bearings. Some of these effects have a profound impact, leading to significant error if disregarded. Two examples are discussed below: scragging effects in rubber, and cyclic loading in lead-rubber isolators. Cyclic loading effects in friction pendulum isolators are discussed in section 7.6.4.

Shown in figure 6-7 is the force-displacement relation of a high damping elastomeric bearing (Thompson et al., 2000). The bearing exhibits a substantially higher stiffness during the initial cycle than during the subsequent cycles of motion. The initial stiffness occurs at the unscragged state of the elastomer, that is, under virgin conditions. Following stretching and fracture of molecules of the elastomer during deformation, the bearing reaches the scragged state with stable properties. It has been assumed in the past that the elastomer cannot recover to the virgin state so that the initial high stiffness was disregarded in the analysis. However, recent experimental evidence (see Thompson et al., 2000 and Constantinou et al., 1999) demonstrated that recovery occurs within short period of time due likely to continuous chemical activity in the elastomer. Thompson et al. (2000) demonstrated that substantial differences between unscragged and scragged properties are possible in low shear modulus elastomers. It is essential that elastomeric bearings be tested in their virgin stage so that both the unscragged and scragged properties be determined.

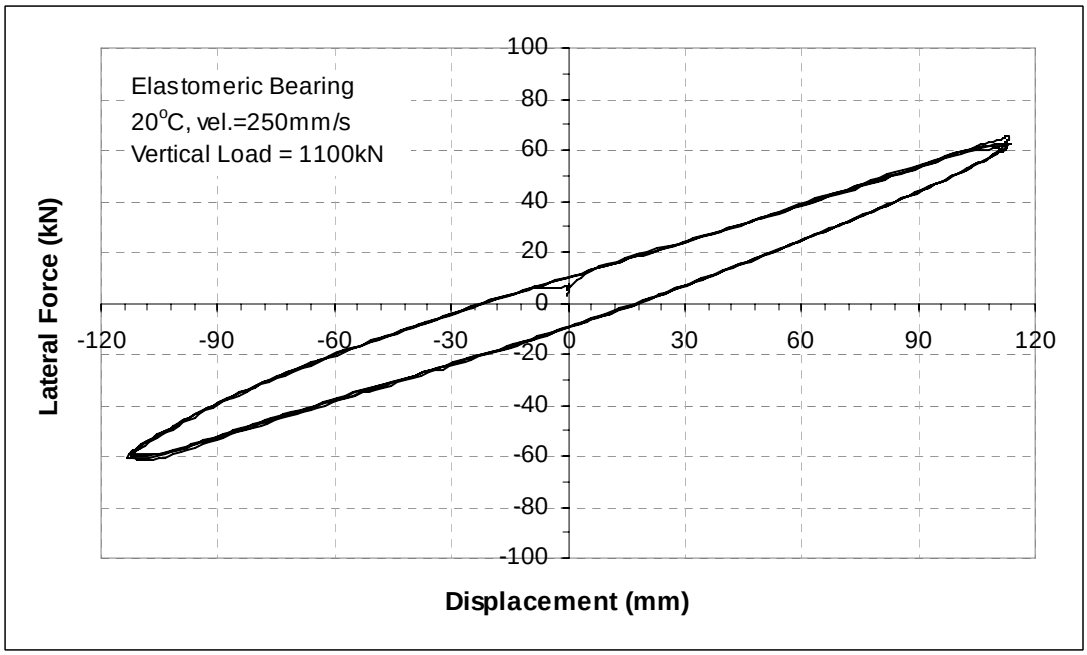

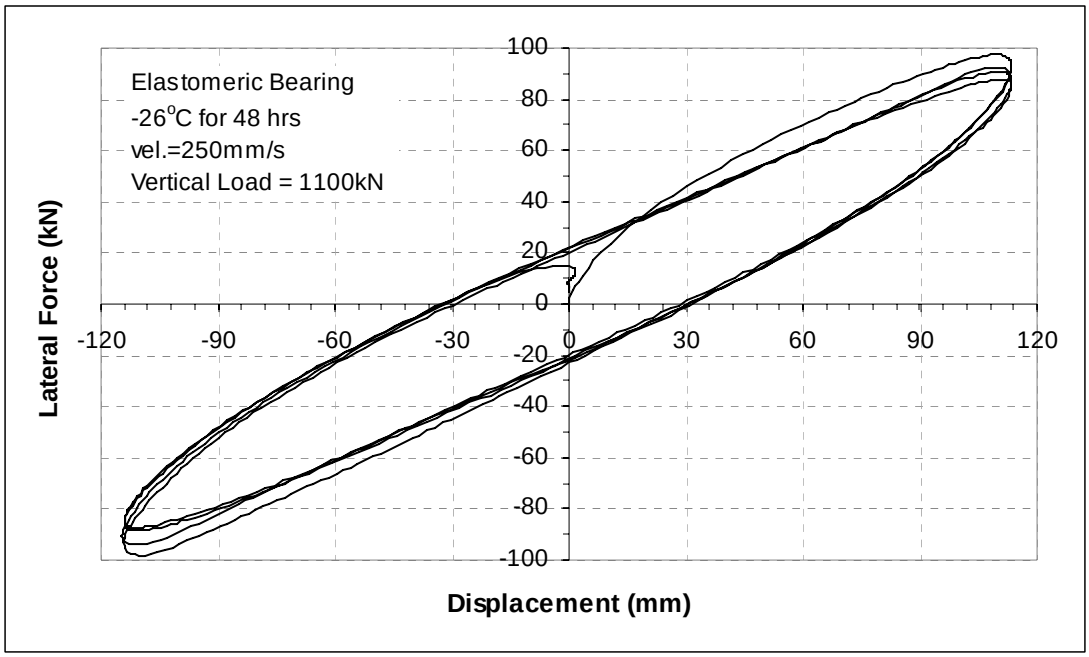

Figure 6-5. Force-displacement Relation of an Elastomeric Isolator at Normal and Low Temperatures

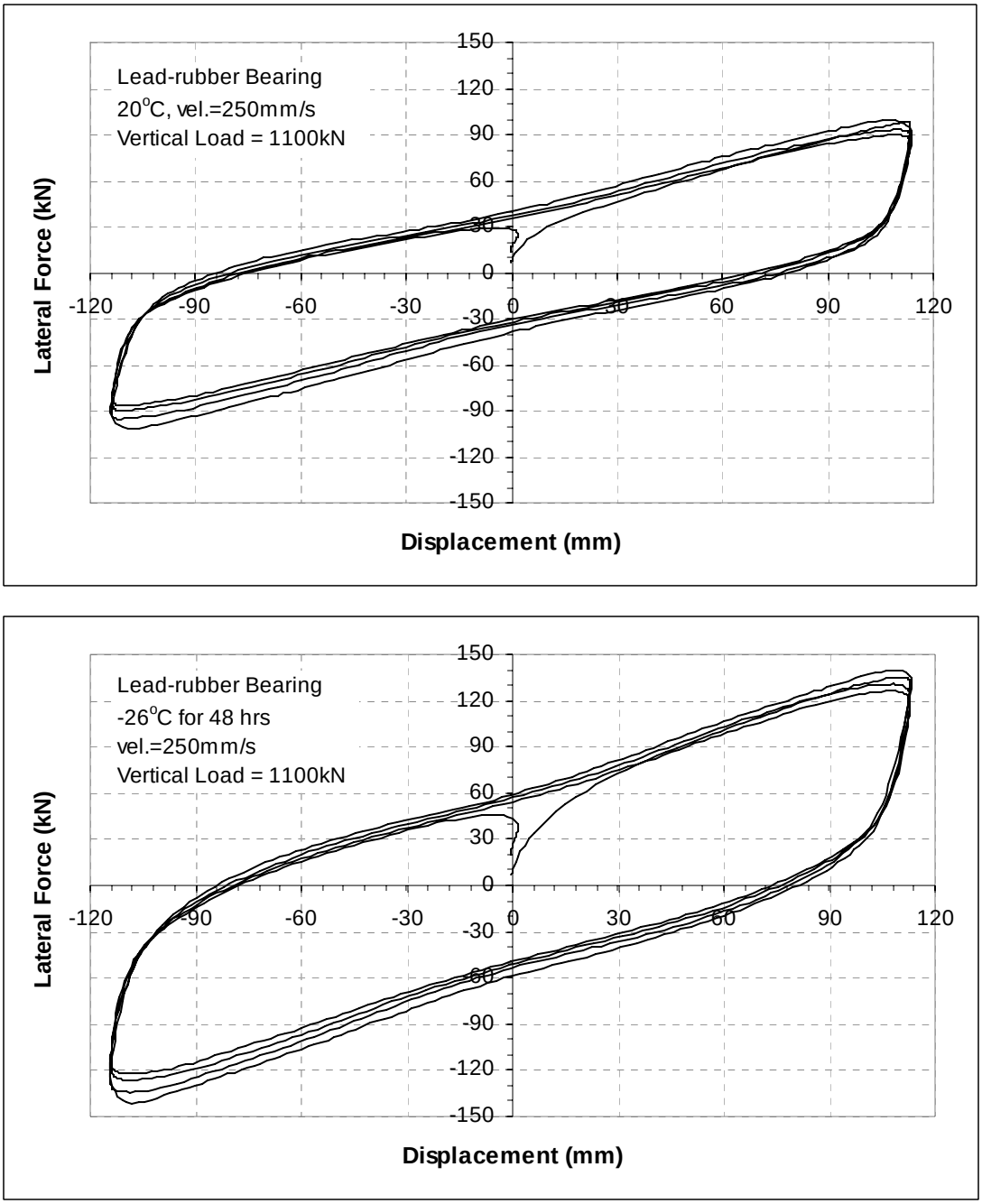

Figure 6-6. Force-displacement Relation of a Lead-Rubber Isolator at Normal and Low Temperatures

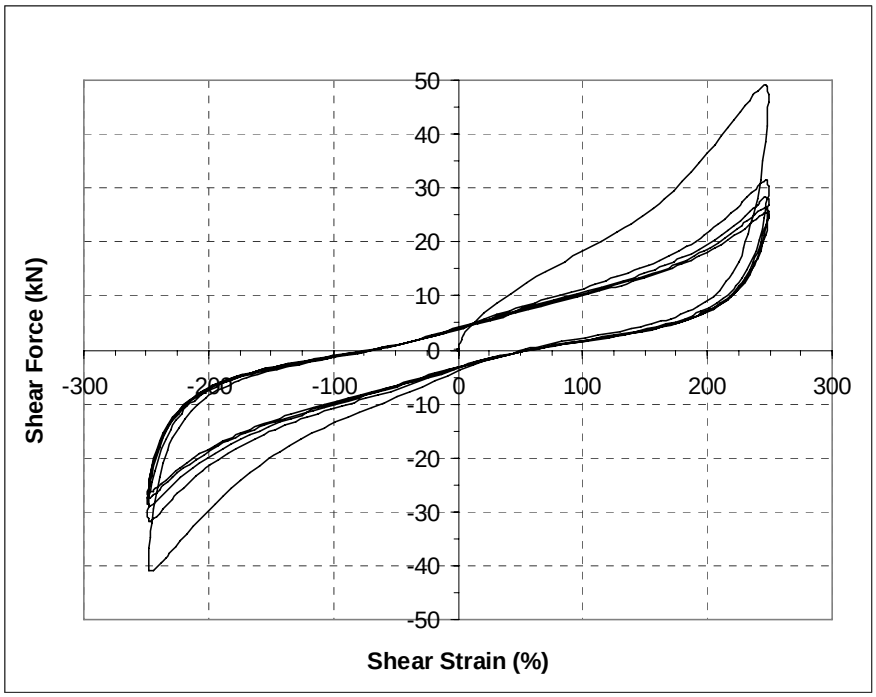

Figure 6-7. Force-displacement Relation for a Virgin (unscragged) High-damping Elastomeric Isolator (from Thompson et al., 2000)

Tests conducted on lead-core rubber isolators indicate that the characteristic strength Qd of these isolators may deviate from the average by about 20%-25%. In a test involving 3-5 cycles of displacement, the characteristic strength of the bearing in the first cycle is generally about 25% larger than the average characteristic strength from all the cycles. The average characteristic strength from all the cycles represents the target design characteristic strength of the bearing. Accordingly, the initial lower characteristic strength, Q_L, is set equal to the target design characteristic strength. The initial upper bound characteristic strength, Q_U, is then initially set equal to $1.25Q_L$ for design purposes. However, this should later be verified by the actual prototype testing of the bearings and the coefficient 1.25 may be modified accordingly. The initial lower and upper bound characteristic strengths of the bearing are then adjusted using the property modification factors defined below to obtain the minimum and maximum probable characteristic strengths for the isolators.

6.6 SYSTEM PROPERTY MODIFICATION FACTORS FOR ELASTOMERIC ISOLATORS

As described in section 4.5, system property modification factors are used to account for the likely variations in isolator properties over the life of an isolated bridge. In this approach, the minimum and maximum effective stiffness and equivalent damping of the isolation system are calculated using the minimum and maximum values of the post-elastic stiffness, K_d, and characteristic strength, Q_d, of each isolation bearing. These values of parameters are calculated as the product of (1) the nominal values of these parameters, and (2) the minimum and maximum values of the corresponding system property modification factors.

The minimum value of the system property modification factor (λ-factor) is denoted as λ_{min} and has values less than or equal to unity. Due to the fact that most values of λ_{min} proposed by Constantinou et al. (1999) are close to unity, the AASHTO Guide Specifications (AASHTO 1999) sets λ_{min} equal to unity. That is, the lower bound values of properties of the isolation systems are considered to be the nominal values. These values are defined to be those determined for fresh and scragged specimens under normal temperature conditions.

As noted in section 4.5.2, the maximum value of the λ-factor is calculated as the product of six component factors:

$$\lambda_{max} = (\lambda_{max,t})(\lambda_{max,a})(\lambda_{max,v})(\lambda_{max,tr})(\lambda_{max,c})(\lambda_{max,scrag}) \quad (6\text{-}32)$$

where

$\lambda_{max,t}$ = maximum value of factor to account for the effect of temperature (table 6-3)

$\lambda_{max,a}$ = maximum value of factor to account for the effect of aging (table 6-4)

$\lambda_{max,v}$ = maximum value of factor to account for the effect of velocity (= 1, unless established otherwise by test)

$\lambda_{max,tr}$ = maximum value of factor to account for the effect of travel and wear (= 1, unless established otherwise by test)

$\lambda_{max,c}$ = maximum value of factor to account for the effect of contamination (= 1 for elastomeric bearings)

$\lambda_{max,scrag}$ = maximum value of factor to account for the effect of scragging (table 6-5)

Values for the above factors are presented in tables 6-3 to 6-5 as noted above (AASHTO 1999, and Constantinou et al., 1999).

Table 6-3. Maximum Values for Temperature λ-factors for Elastomeric Isolators ($\lambda_{max,t}$)

Minimum Temperature For Design		Q_d			K_d		
°C	°F	HDRB-1	HDRB-2	LDRB	HDRB-1	HDRB-2	LDRB
21	70	1.0	1.0	1.0	1.0	1.0	1.0
0	32	1.3	1.3	1.3	1.2	1.1	1.1
-10	14	1.4	1.4	1.4	1.4	1.2	1.1
-30	-22	2.5	2.0	1.5	2.0	1.4	1.3

Note: HDRB-1 is High Damping Rubber Bearing with large difference (more than 25%) between scragged and unscragged properties
HDRB-2 is High Damping Rubber Bearing with small difference (less than or equal to 25%) between scragged and unscragged properties
LDRB is Low Damping Rubber Bearing (conventional natural rubber bearing)

Table 6-4. Maximum Values for Aging λ-factors for Elastomeric Isolators ($\lambda_{max,a}$)

Material	K_d	Q_d
Low Damping Natural Rubber (LDRB)	1.1	1.1
High Damping Rubber with large differences (>25%) between scragged and unscragged properties (HDRB-1)	1.3	1.3
High Damping Rubber with small differences (≤25%) between scragged and unscragged properties (HDRB-2)	1.2	1.2
Lead	-	1.0
Neoprene	3.0	3.0

Table 6-5. Maximum Values for Scragging λ-factors for Elastomeric Isolators ($\lambda_{max,scrag}$)

Material	Q_d	K_d
LDRB	1.0	1.0
HDRB-A	1.2	1.2
HDRB-B	1.5	1.8

Note: HDRB-A is High Damping Rubber Bearing with equivalent viscous damping ratio ≤0.15
HDRB-B is High Damping Rubber Bearing with equivalent viscous damping ratio >0.15

Recent studies on the scragging λ-factor (Thompson et al., 2000) concluded that the scragging factor values in table 6-5 should be increased and the shear modulus of the elastomer rather than the equivalent damping should be used to classify materials. Specifically, Thompson et al. (2000) recommend the following values of the λ-factor for scragging: (1) 1.5 for elastomers with shear modulus (at third cycle, at 100% strain) large than 0.7 MPa and (2) 2.0 for elastomers with shear modulus less than 0.7 MPa. This recommendation was based on experimental data from about 30 bearings with different elastomeric compounds which were produced by manufacturers in the United States, Japan, England and Italy. Figure 6-8 presents values of the scragging factor as reported by Thompson et al. (2000).

6.7 FIRE RESISTANCE OF ELASTOMERIC ISOLATORS

In general, the fire resistance of a bridge isolator is not the same concern as it is for a building application. Nevertheless the fire rating of these isolators should be consistent with that of the superstructure above and the substructure below.

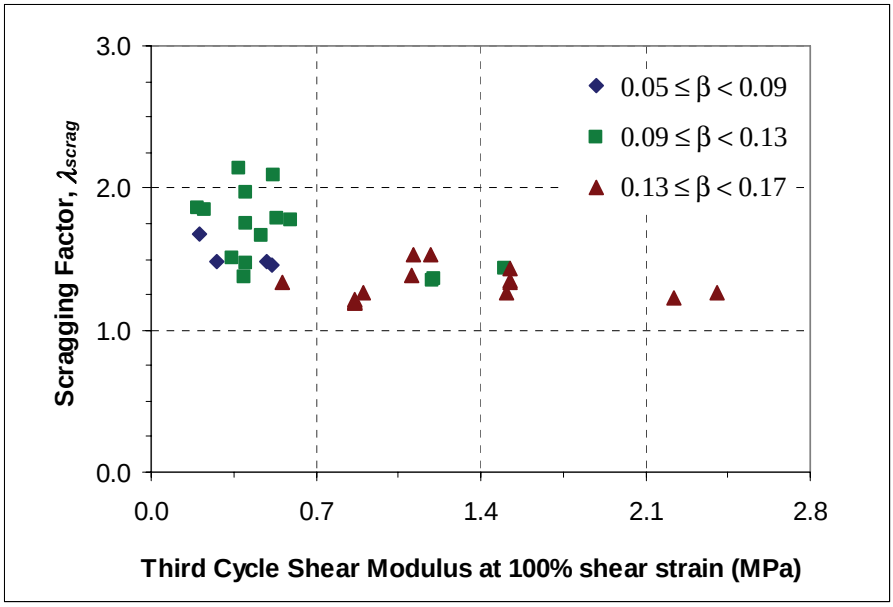

Figure 6-8. Values of the Scragging λ-factor for Elastomeric Isolators (from Thompson et al., 2000)

Fire tests conducted on elastomeric and lead-rubber isolators by the Architectural Institute of Japan and the Sumitomo Construction Co. in Japan, have demonstrated that properly insulated elastomeric bearings can safely support loads in a 1000°C fire for a period of 3 hours. The insulation consisted of either 50 mm thick ceramic fiber enclosure or a 100 mm thick silicone foam and seal enclosure. Fire tests without insulation in a 1000°C fire resulted in burning of the elastomer and loss of vertical load capacity. Such fires are unusual in bridge situations but may occur if, for example a gasoline tanker overturns beneath a bridge and catches fire. However, adding fire protection to isolators for this kind of extreme event only makes sense if the rest of the bridge is similarly protected.

6.8 TENSILE STRENGTH OF ELASTOMERIC ISOLATORS

The tensile capacity of elastomeric bearings is not yet well understood. Elastomeric bearings may fail in tension either due to loss of bond to steel, or due to elastomer cavitation. The former is typically the case in bearings of low quality of construction. The failure characteristics of elastomeric bearings in tension also depend on the size of the bearing since it affects its quality of construction, and the success and uniformity of vulcanization. Tensile capacities of large size elastomeric bearings are, in general, of the order of 1 MPa, whereas small size bearings may have much larger capacities (Skinner et al., 1993).

CHAPTER 7: SLIDING ISOLATORS

7.1 INTRODUCTION

Contemporary sliding seismic isolation systems may take a variety of forms. Flat sliding bearings may be combined with elastomeric bearings to form hybrid isolation systems with a range of energy dissipation capabilities and stiffnesses. The basic types of flat sliding bearings are shown in figure 7-1. They include pot, disk and spherical bearings. The three types differ in the construction of the rotational part, with the spherical bearing having the least rotational resistance and hence the most favorable distribution of pressure on the sliding interface.

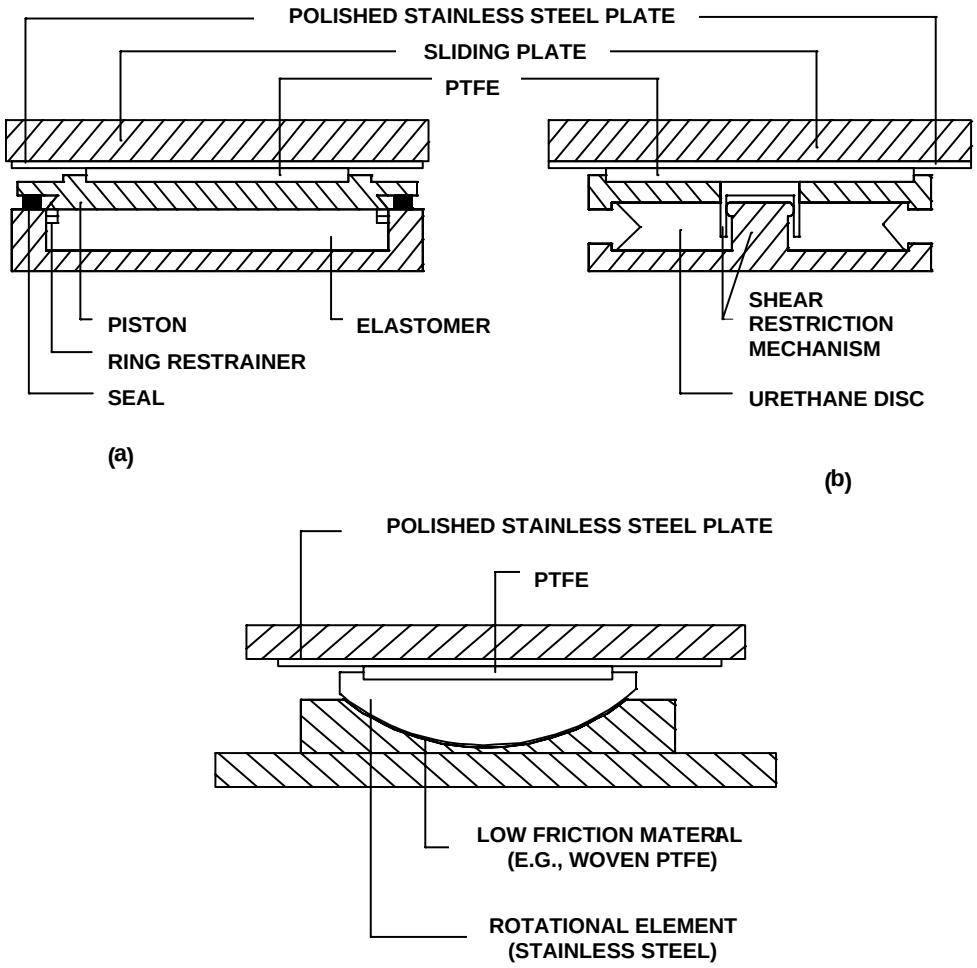

Figure 7-1. Flat Sliding Isolators: (a) Pot Isolator, (b) Disc Isolator, (c) Spherical Isolator

Materials used for the sliding interface of these bearings are typically austenitic stainless steel (either type 304 or preferably the most corrosion-resistant type 316 which contains molybdenum) in contact with unfilled PTFE. To achieve significant energy dissipation capability, the PTFE needs to be non-lubricated. Other materials have been used such as woven PTFE, PTFE-composites and bronze-lead composites, although bi-metallic interface are considered problematic (AASHTO 1999, Constantinou et al., 1999).

Lubricated flat sliding bearings have been used in combination with yielding steel elastoplastic devices, such as those depicted in figure 7-2 (Marioni 1997), in bridge seismic isolation systems. In these systems, lock-up devices (or shock transmission devices) are used to allow for unobstructed thermal movement of the bridge on the lubricated bearings. The devices lock-up in seismic excitation and engage the yielding steel devices, which dissipated energy and limit the seismic movement. However, such systems lack sufficient restoring force capability and thus may develop significant permanent displacements.

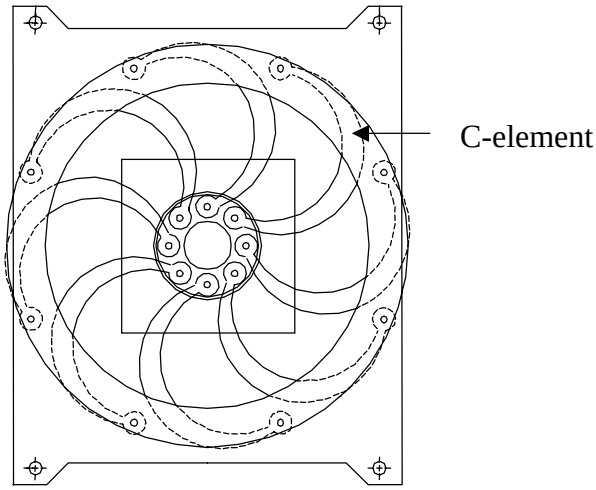

Figure 7-2. Elasto-plastic Yielding Steel Device used in Combination with Lubricated Sliding Isolators in Bridges

The Friction Pendulum (FPS) bearing (figure 7-3) is a spherical bearing (for the rotational part) with a spherical sliding interface. It very much acts like the spherical bearing of figure 7-1(c) but it has lateral stiffness as a result of the curvature of the sliding interface. These isolators are capable of carrying very large axial loads (see table 2-3) and can be designed to have long periods of vibration (5 seconds or longer) with large capacities for lateral displacement. Section 7.2 describes these isolators in more detail.

Another sliding seismic isolation bearing is the Eradiquake bearing. As shown in figure 7-4, it consists of a flat plate slider mounted on a disk bearing and fitted with orthogonally aligned, urethane springs as restoring force elements. Most of the applications to date have been in the low-to-moderate seismic zones of the central and eastern United States (see appendix B). (http://www.rjwatson.com).

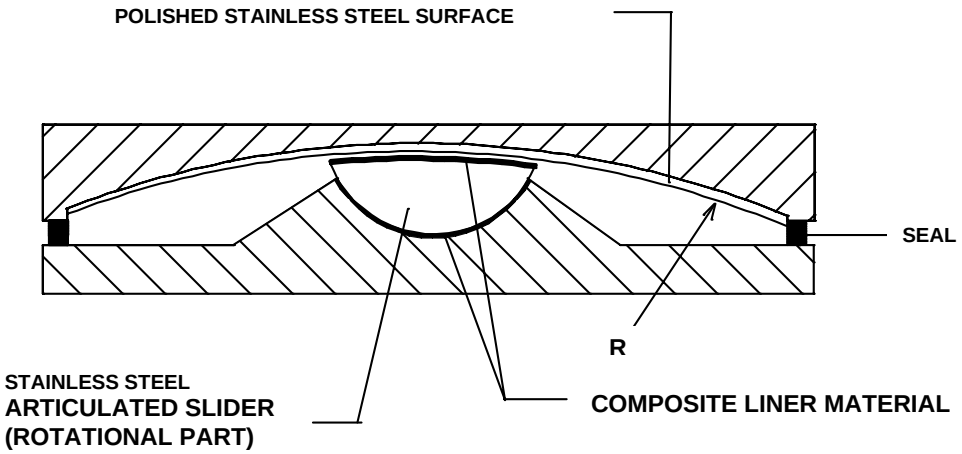

Figure 7-3. Friction Pendulum Isolator

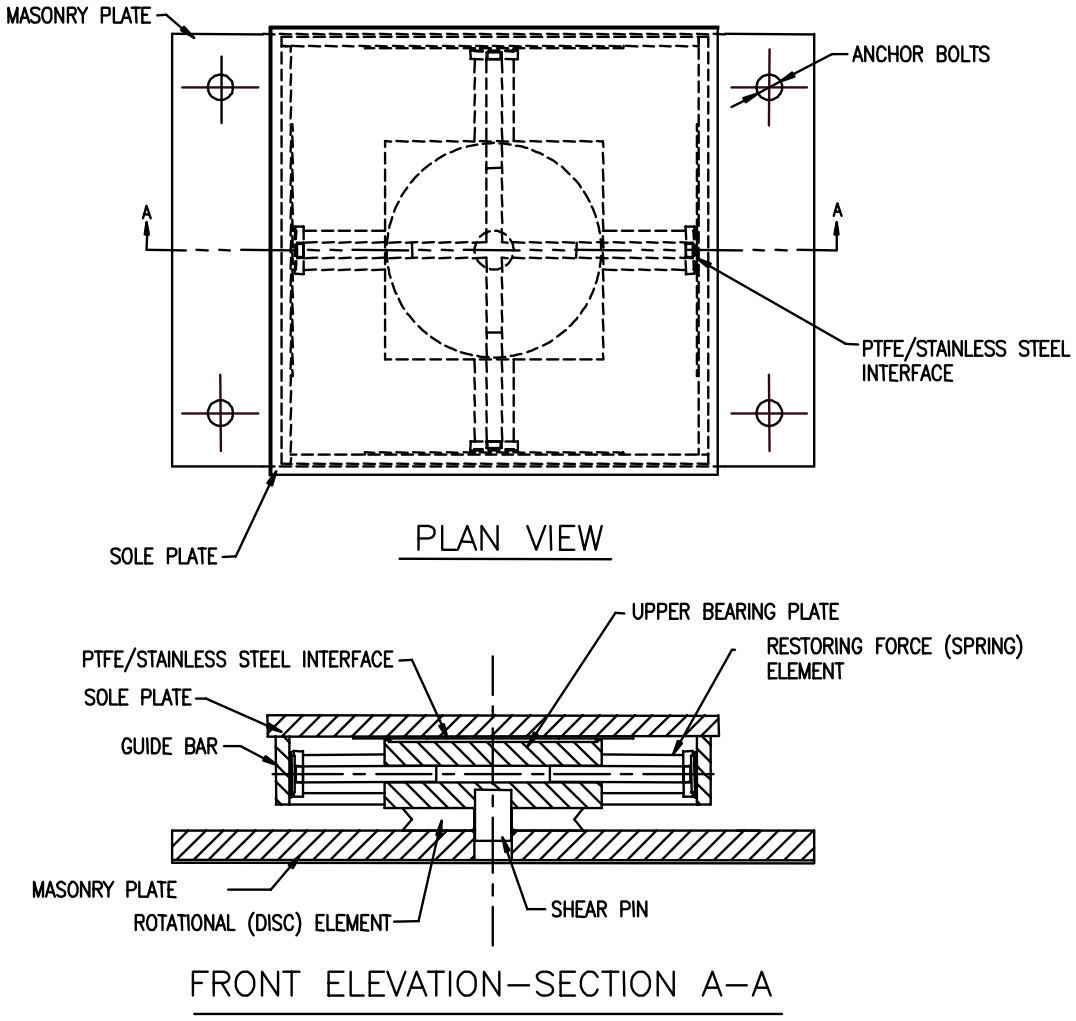

Figure 7-4. Eradiquake Isolator

7.2 FRICTION PENDULUM ISOLATORS

Friction pendulum bearings are sliding-based seismic isolators, which are installed between the superstructure and the substructures in application to bridges. A typical friction pendulum bearing used in the seismic design of the Mississippi River Bridge in Ontario, Canada is shown in figure 7-5. Sectional and plan views of the same bearing are illustrated in figure 7-6. The main components of friction pendulum bearings are a stainless steel concave spherical plate, an articulated slider and a housing plate as illustrated in figure 7-6. In the figure, the concave spherical plate is facing down. The bearings may also be manufactured to have the concave spherical plate facing up. The side of the articulated slider in contact with the concave spherical surface is coated with a low-friction composite material. The other side of the slider is also spherical but coated with stainless steel and sits in a spherical cavity also coated with low-friction composite material.

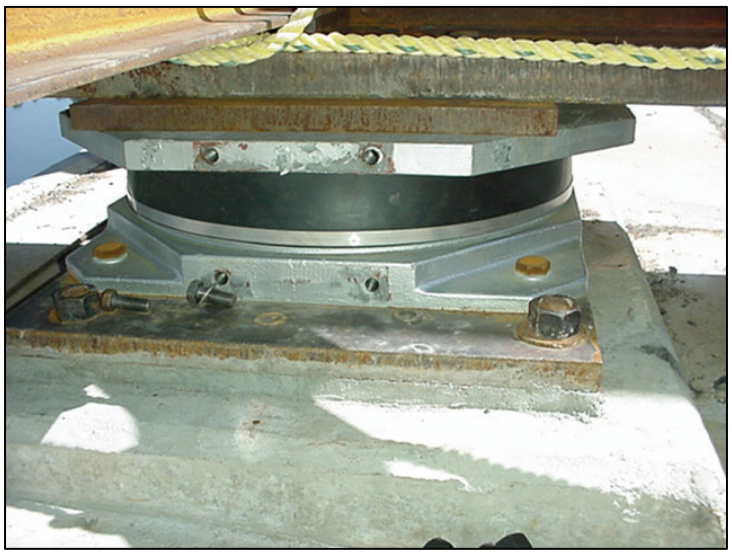

Figure 7-5. Typical Friction Pendulum Isolator

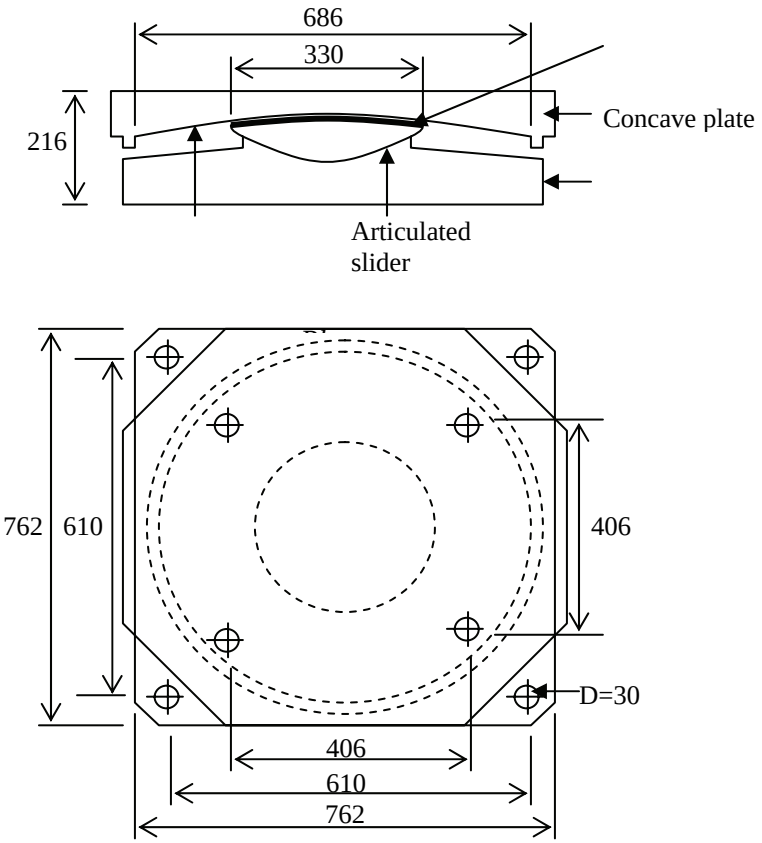

Figure 7-6. Section and Plan of Typical Friction Pendulum Isolator

7.2.1 MECHANICAL CHARACTERISTICS OF FRICTION PENDULUM ISOLATORS

Friction pendulum bearings are described by the same equation of motion as conventional pendulums and their period of vibration is directly proportional to the radius of curvature of the concave surface. Long period shifts are therefore possible with surfaces that have large radii of curvature. Friction between the articulated slider and the concave surface dissipates energy and the weight of the bridge acts as a restoring force, due to the curvature of the sliding surface (figure 7-7).

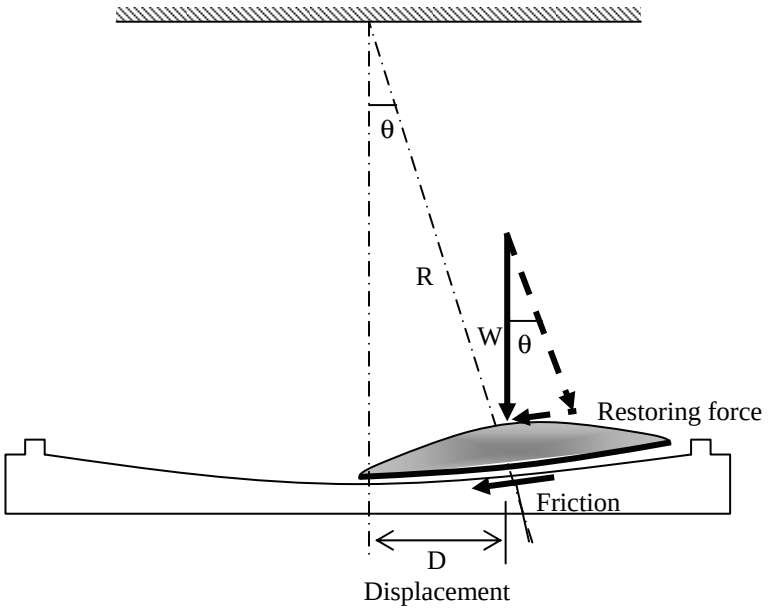

Figure 7-7. Operation of Friction Pendulum Isolator (Force Vectors Shown for Sliding to the Right)

7.2.1.1 Formulation of Isolator Behavior

The resistance of the bearing to horizontal forces that act to increase displacement, is provided by two different mechanisms. The first one is the frictional resistance, F_f, generated at the interface between the articulated slider and the concave surface as shown in figure 7-7. This force is equal to the product of the dynamic friction coefficient, μ, and the component of the weight normal to the concave surface. Thus:

$$F_f = \mu W \cos\theta \tag{7-1}$$

The second resistance mechanism is the restoring force generated by the tangential component of the weight acting on the bearing, also shown in figure 7-7. This force is given by:

$$F_f = W \sin\theta \tag{7-2}$$

If the displacement, D, of the bearing is small compared to the radius, R, of the concave surface, then:

$$\cos\theta = 1 \tag{7-3}$$

and

$$\sin\theta = \frac{D}{R} \tag{7-4}$$

Substituting equations 7-3 and 7-4 into equations 7-1 and 7-2 and summing up the results, the total horizontal resistance of the bearing to displacement is given by:

$$F = \mu W + \frac{W}{R} D \tag{7-5}$$

Setting $Q_d = \mu W$ and $k_d = W/R$ and substituting into equation 7-5 gives:

$$F = Q_d + k_d D \tag{7-6}$$

which is identical to equation 6-6 developed for elastomeric isolators.

It will be seen that the term W/R in equation 7-5 is the lateral stiffness produced by the tangential component of the weight. Using this stiffness and the weight acting on the bearing, the period while sliding is given by:

$$T = 2\pi\sqrt{\frac{R}{g}} \tag{7-7}$$

where g is the gravitational acceleration. The sliding period is seen to be simply determined by the radius, R.

The idealized force-displacement hysteresis loop for the friction pendulum isolator is shown in figure 7-8. The envelope of the loop is defined by equations 7-5 and 7-6.

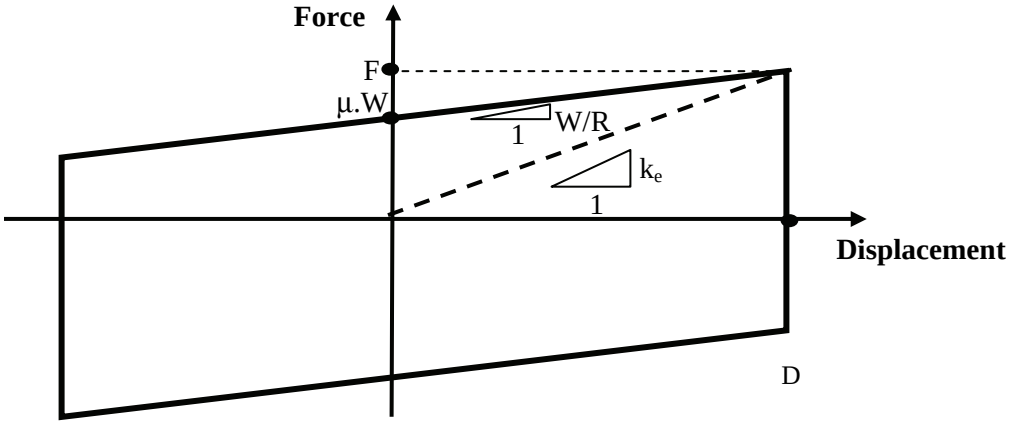

Figure 7-8. Idealized Force-displacement Hysteretic Behavior of a Friction Pendulum Isolator

Since the behavior of the isolator is nonlinear, equivalent linearized properties are needed if elastic methods of analysis are to be used (section 3). As with elastomeric isolators, these properties include the effective bearing stiffness and an equivalent viscous damping ratio to account for the effect of the hysteretic energy dissipation.

The effective bearing stiffness, k_e, is shown in figure 7-8, and is obtained by dividing the horizontal force, F, by the corresponding bearing displacement, D. Thus:

$$k_e = \frac{\mu W}{D} + \frac{W}{R} \tag{7-8}$$

Since the area of the hysteretic loop in figure 7-8 is given by:

$$\text{Area} = 4\mu WD \tag{7-9}$$

equation 1-1 gives the following expression for the equivalent viscous damping ratio**,** β_e:

$$\beta_e = \frac{2}{\pi}\left(\frac{\mu}{\mu + \frac{D}{R}}\right) \tag{7-10}$$

An acceleration response spectrum with 5% damping is then modified for the actual damping, β_e, and used for calculating the response of the isolated bridge (see section 3).

7.3 ERADIQUAKE ISOLATORS

7.3.1 MECHANICAL CHARACTERISTICS OF ERADIQUAKE ISOLATORS

As noted above the essential components of the Eradiquake isolator include a pair of flat sliding plates, a disc bearing to accommodate rotation when required, and a set of urethane springs, called Mass Energy Regulators, to provide a restoring force to re-center the bridge after an earthquake.

7.3.1.1 Formulation of Bearing Behavior

As with the Friction Pendulum Isolator, the resistance of the bearing to horizontal forces is provided by two different mechanisms. The first is frictional resistance, F_f, generated at the interface between the flat PTFE and stainless steel as shown in figure 7-4. The friction force is the product of the coefficient of friction, μ, and the weight acting on the bearing:

$$F_f = \mu W \tag{7-11}$$

The second mechanism is the restoring force generated by compression of the Mass Energy Regulators (MER) against the upper bearing plate. The MER is a polyether urethane cylinder that acts like a spring and provides a stiffness given as k_d. The restoring force F_r, is given by:

$$F_r = k_d D \tag{7-12}$$

The total horizontal resistance of the bearing is obtained by summing the friction and MER resistances to give:

$$F = \mu W + k_d D \tag{7-13}$$

The idealized force displacement hysteresis loop for an Eradiquake bearing is shown in figure 7-9.

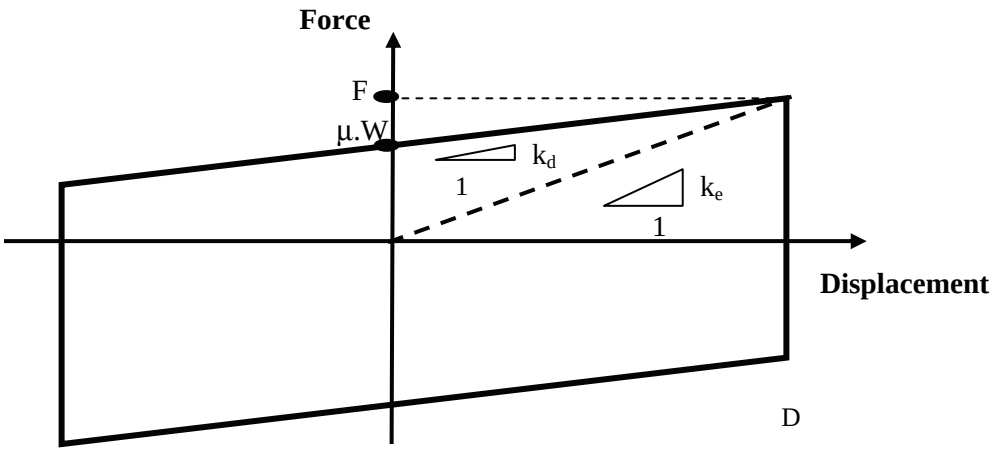

Figure 7-9. Idealized Force-displacement Hysteretic Behavior of an Eradiquake Isolator

Since the behavior of the isolator is nonlinear, equivalent linearized properties are needed if elastic methods of analysis are to be used (section 3). As with the FPS and elastomeric isolators, these properties include the effective bearing stiffness and an equivalent viscous damping ratio to account for the effect of the hysteretic energy dissipation.

The effective bearing stiffness, k_e, is shown in figure 7-9, and is obtained by dividing the horizontal force, F, by the corresponding bearing displacement, D. Thus:

$$k_e = \frac{\mu W}{D} + k_d \tag{7-14}$$

Since the area of the hysteretic loop in figure 7-9 is given by:

$$\text{Area} = 4\mu WD \tag{7-15}$$

equation 1-1 gives the following expression for the equivalent viscous damping ratio, β_e:

$$\beta_e = \frac{2}{\pi}\left(\frac{\mu}{\mu + \frac{k_d D}{W}}\right) \tag{7-16}$$

An acceleration response spectrum with 5% damping is then modified for the actual damping and used as the input spectrum for calculating the response of the isolated bridge. See section 3.

7.4 DESIGN OF SLIDING ISOLATORS

The design of a sliding isolator involves the following:

1. Selection of the materials for the sliding interface and the contact pressure in order to achieve the desired frictional characteristics.
2. Selection of the thickness of the stainless steel plate in order to avoid uplift or bow waves that may lead to rupture.
3. Selection of the thickness of PTFE or other mating material in order to meet the desired wear characteristics for the application.
4. Selection of thickness of the end plates to safely sustain stresses and to provide sufficient stiffness in order to avoid distortion of the sliding surface.
5. Selection of the size and stiffness of the rotational part in order to minimize edge stresses on the sliding interface. These stresses may lead to excessive wear.

The following geometric and material specifications are recommended in AASHTO 1999 and should be used as guidance in the design of sliding isolation bearings:

1. The useful thickness (thickness of part projecting out of recess or thickness of part capable of wearing out) of sheet and woven PTFE should be at least 1.6 mm after compression. By comparison, the European Standard EN 1337-1 (European 2000) relates the useful thickness (or protrusion) to the dimensions of the sheet and requires a minimum thickness of 2.2 mm in the unloaded condition.
2. The useful thickness of other bearing liners should either be 1.6 mm or be determined on the basis of wear tests for the conditions of application. For bridge applications, wear due to bearing movement caused by traffic may be the dominating factor for the selection of materials and thicknesses.
3. The stainless steel sliding surface should be polished to a high degree of reflectivity. AASHTO 1999 recommends a finish with an arithmetic average (R_a) surface roughness of not more than 0.8 micrometers. The commercially available mirror finish will result in an arithmetic average surface roughness (R_a) of about 0.05 micrometers per ANSI/ASME B46.1-1985 (ASME 1985).
4. The stainless steel should be austenitic and preferably of the 316 type conforming to ASTM A 240 (in the U.S.A.) or type 5 CrNiMo conforming to DIN 17440 (in Germany) or equivalent. Austenitic 304 type is also acceptable, although it is of lesser corrosion resistance.
5. The thickness of the stainless steel sliding plate should be at least 1.5 mm for surfaces having a maximum dimension of less than 300 mm, and at least 2.3 mm for surfaces having a maximum dimension of less than 900 mm. For larger dimensions the thickness of the stainless steel plate needs to be verified by testing of full size bearings at representative loads and velocities.
6. Materials other than corrosion-resistant austenitic stainless steel in contact with PTFE, woven PTFE, or other non-metallic liner materials are not recommended. Particularly, chrome-plated carbon steel and bi-metallic interfaces are known to either corrode or result in significant changes in friction (British Standards Institution 1979; Constantinou et al., 1999).
7. Lubricated bearings should be of the sheet PTFE type and dimpled. The dimples should have diameter not more than 8 mm and depth not more than 2 mm. Dimples shall cover 20

to 30-percent of the PTFE surface. The lubricant should be silicone grease effective to very low temperatures.

Sliding bearings must have rotational capability in order to accommodate rotation resulting from loading, construction tolerances and thermal effects. Furthermore, the FPS bearing needs to accommodate rotation, θ, resulting from lateral movement:

$$\theta = \sin^{-1}\left(\frac{D}{R}\right) \tag{7-17}$$

where D = lateral movement (displacement) and
R = radius of curvature.
Since typically $D/R \leq 0.2$, the rotation is about 0.2 rad or less.

The rotational resistance of sliding bearings is important in calculating the moment acting on the bearing and the associated additional edge stresses on the sliding interface. Roeder et al. (1995) presented experimental data on the rotational resistance of pot, disk and spherical bearings that may be used as guidance in calculating the rotational stiffness of sliding bearings.

Sliding bearings have insignificant torsional resistance and can typically accommodate very large torsional rotations.

Torsional rotations of bridge superstructures are typically very small and man be estimated on the basis of the simple procedure recommended in the International Building Code (International Code Council 2000), i.e.,

$$\phi \cong \frac{12eD}{b^2 + d^2} \tag{7-18}$$

where e = eccentricity between the center of resistance of isolation and the center of mass
D = displacement of isolation system at the center of resistance, and
b, d = plan dimensions of superstructure.

Torsional rotations given by equation 7-18 are usually of the order of 0.01 rad.

7.5 FRICTIONAL PROPERTIES OF SLIDING ISOLATORS

An attempt to summarize the state of knowledge on the nature of friction in sliding structural bearings has been presented by Constantinou et al. (1999). Herein it is sufficient to present representative and informative data on the frictional properties of unlubricated sheet PTFE in contact with highly polished stainless steel. The behavior of other materials such as woven PTFE and PTFE-based, non-metallic composites is similar.

The coefficient of friction of PTFE-polished stainless steel interfaces depends on a number of factors, of which the apparent bearing pressure, the velocity of sliding, and the temperature are the most important. In general, the behavior of these interfaces may be described as follows:

1. At initiation motion and under quasi-static condition, the interfaces exhibit a high value of coefficient of friction. It is termed static or breakaway and it is denoted as μ_B.

2. Following breakaway, and while moving at very low velocity, the coefficient of friction attains its minimum value, f_{min}, which is substantially less than the breakaway value.

3. The coefficient of friction increases with increasing velocity and attains a constant maximum value, f_{max}, at velocities beyond about 100 mm/sec.

4. In general, f_{min} is much less than μ_B or f_{max} and f_{max} is larger than μ_B, except for very low temperatures (about -40^oC and less) where μ_B becomes larger than f_{max}. This behavior is depicted in figures 7-10 and 7-11.

5. At intermediate values of velocity (v), the coefficient of friction may be expressed in terms of f_{min} and f_{max} as follows (Constantinou et al., 1990):

$$\mu = f_{max} - (f_{max} - f_{min})\, e^{-av} \qquad (7\text{-}19)$$

6. The breakaway value of the coefficient of friction appears to be independent of the duration of loading without movement. Rather, it appears to be maximum when the specimen is tested for the first time regardless of the duration of loading.

7. Temperature in the range of -30^oC to 50^oC has a rather mild effect on the maximum value of the coefficient of friction (f_{max}) as seen in figure 7-11. This phenomenon is the result of frictional heating at the sliding interface (see also section 7.6).

8. Cumulative travel has an effect on the coefficient of friction as shown in figure 7-12. Following small travel, the coefficient of friction drops to stabilize at a lower value that is maintained for travel of at least 500 m.

9. The effect of the degree of roughness of the stainless steel surface on the coefficient of friction is presented in figure 7-13. In this figure, data for roughness measured as arithmetic average of 0.03 μm R_a correspond to highly polished (mirror finish) surface. Data for roughness of 0.3 and 0.5 μm R_a correspond, respectively, to as-milled and to artificially roughened surfaces. They approximately represent the conditions at the surface of stainless steel following years of exposure that resulted in uniform rust stains. The results demonstrate substantial effects on the breakaway (μ_B) and the low velocity friction (f_{min}) and rather insignificant effects on the high velocity friction (f_{max}).

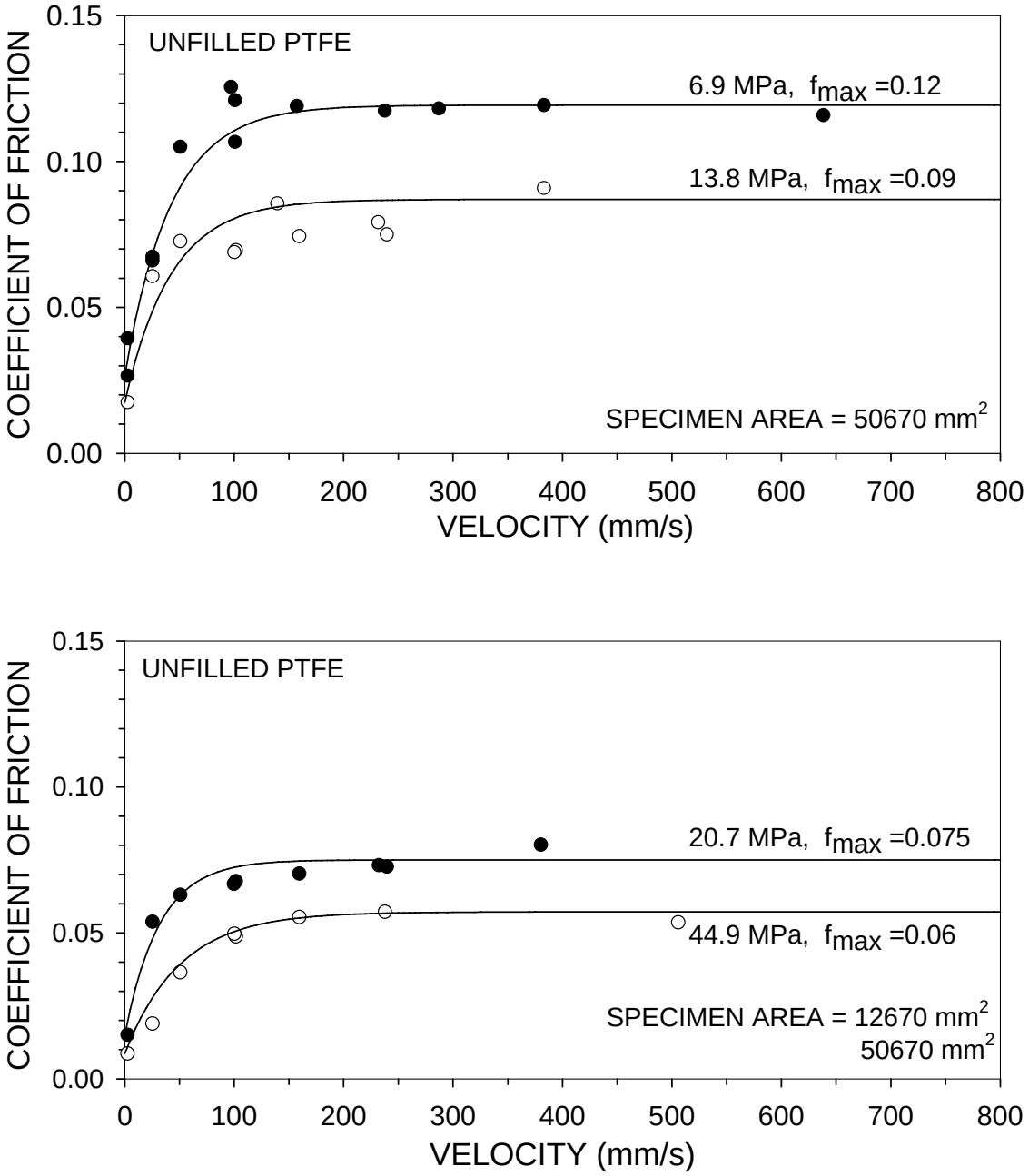

Figure 7-10. Coefficient of Sliding Friction of Unfilled PTFE-polished Stainless Steel Interfaces (Surface Roughness 0.03 μm Ra; Ambient Temperature about 20°C)

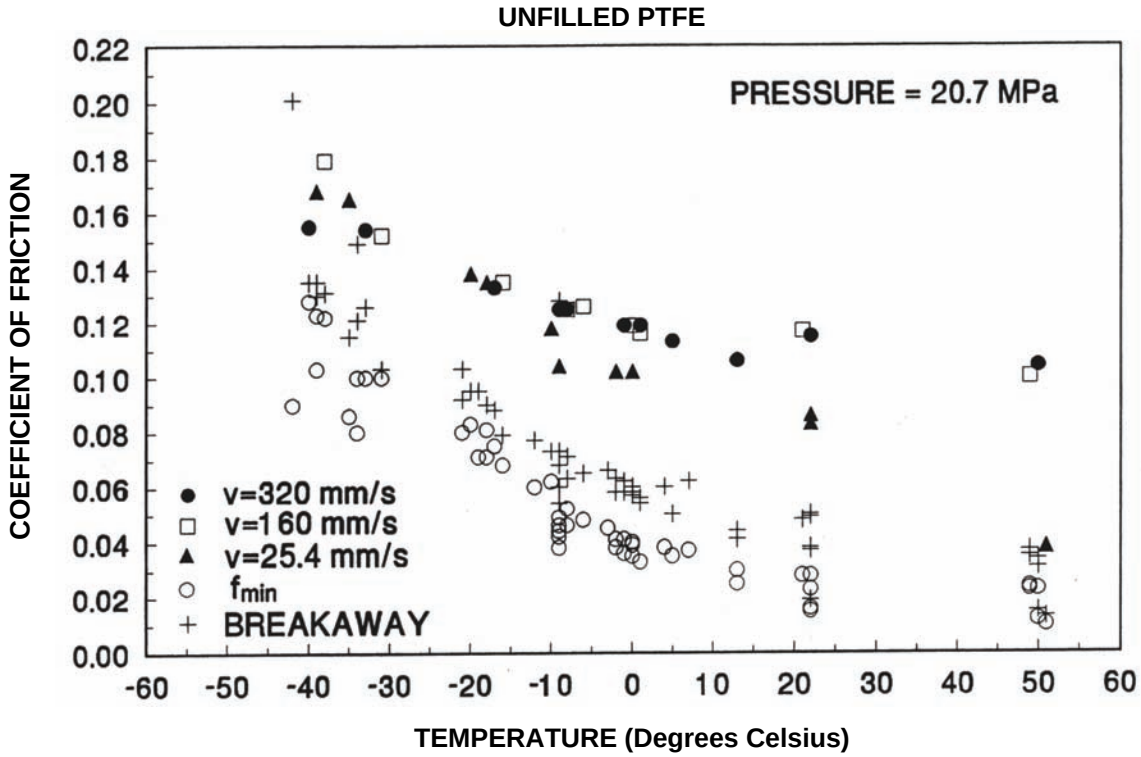

Figure 7-11. Coefficient of Friction of Unfilled PTFE-polished Stainless Steel Interfaces as Function of Temperature

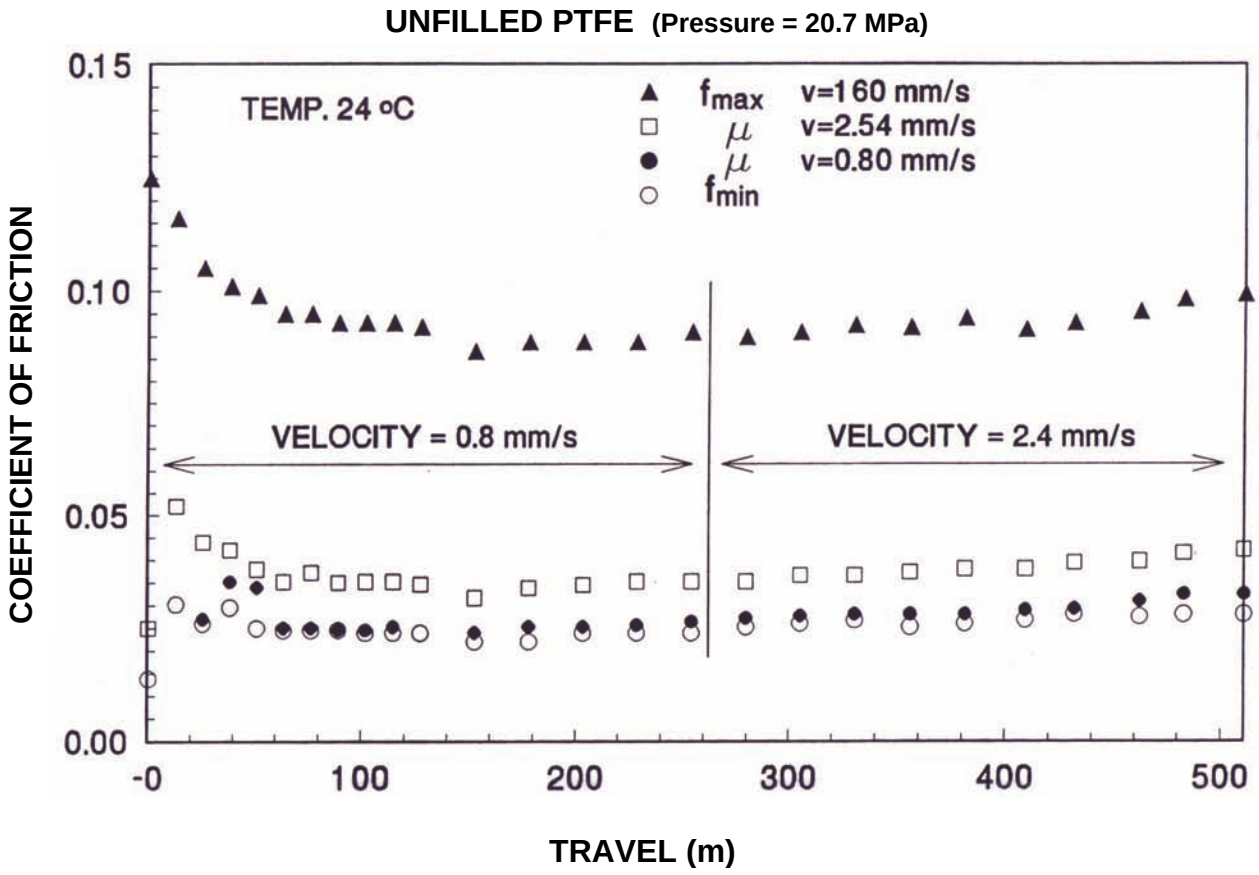

Figure 7-12. Effect of Cumulative Movement (Travel) on Sliding Coefficient of Friction of Unfilled PTE in Contact with Polished Stainless Steel

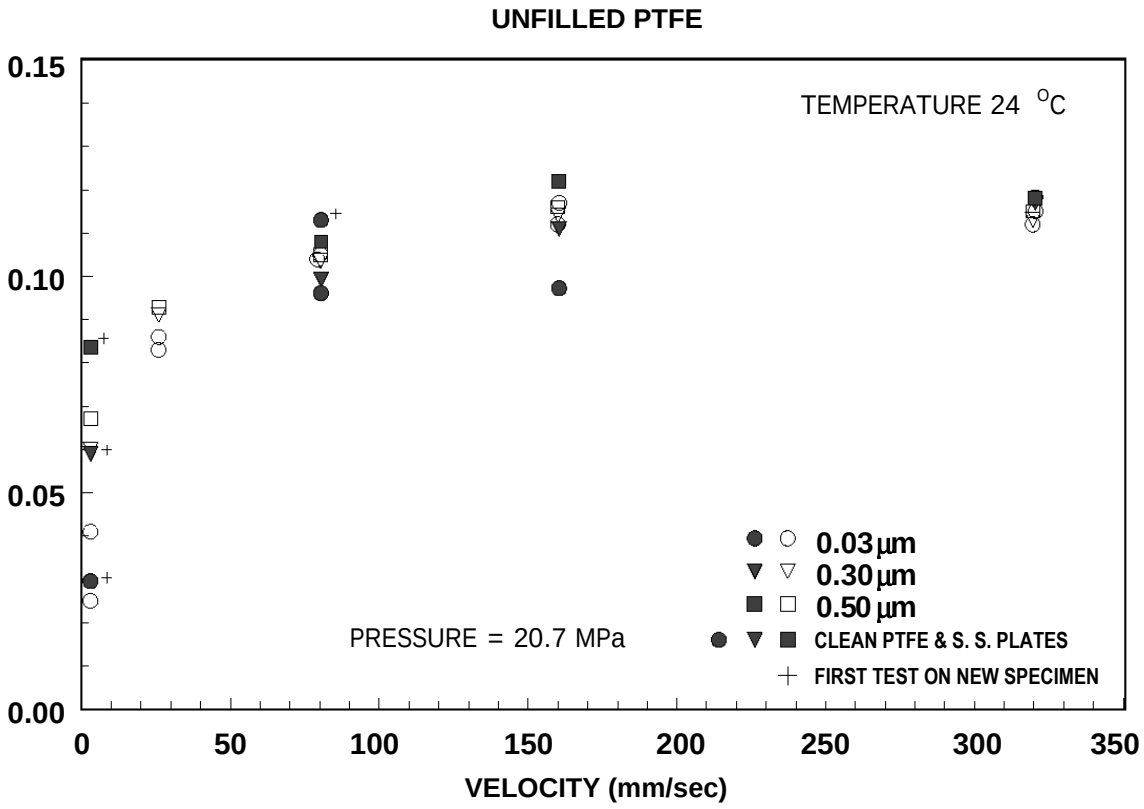

Figure 7-13. Effect of Surface Roughness of Stainless Steel on the Sliding Coefficient of Friction of Unfilled PTFE

7.6 EFFECTS OF VARIABILITY OF PROPERTIES, AGING, TEMPERATURE, AND LOADING HISTORY ON THE PROPERTIES OF SLIDING ISOLATORS

The properties of isolators inevitably vary due to manufacturing differences, aging, wear, history of loading, temperature, etc. These variations may alter the effective period and effective damping of the isolation system, either of which will influence the dynamic response of the isolated structure. The interested reader is referred to Constantinou et al. 1999 for a comprehensive discussion on the effects of the environment, temperature, aging, history of loading, etc. on the mechanical properties of isolators. These effects are briefly discussed in the following sections.

7.6.1 VARIABILITY OF PROPERTIES

The mechanical properties of seismic isolation hardware exhibit variability in values as a result of natural variability in the properties of the materials used and as a result of the quality of manufacturing. It is not unusual to have properties, such as the sliding stiffness or the coefficient of friction in a particular cycle of reversed loading, differ by ± 25 percent from the average values among all tested isolators.

7.6.2 AGING

Aging is the degradation or change of properties with time. Herein, a brief description of the aging effects on the mechanical properties of characteristic strength and post-elastic stiffness of seismic isolation hardware is presented. Moreover, it should be recognized that aging may also have effects on the ability of the isolation hardware to sustain stress, strain, force or deformation, which also need to be considered in design.

Seismic isolation is a relatively new technology so that the field observation of performance of seismic isolation hardware is limited to about 15 years. Actual data on the mechanical properties of seismic isolation bearings removed from structures and re-tested after years of service are limited to a pair of bearings but the results are inclusive given that the original condition of the bearings was not exactly know. However, there is considerable information collected from the field inspection of seismic isolation and other similar bearings, from testing of field-aged bearings in non-seismic applications, from laboratory studies and from theoretical studies. While this information is indirect, it is very useful and may be summarized as follows:

a. Aging in sliding bearings generally results in increases in the coefficient of friction. However, the origins of the increase are complex to describe and interpret, and they depend on the nature of the sliding interface. Aging may be due to corrosion of stainless steel, an increase in the true contact area following prolonged loading without movement, contamination, or loss of material at the sliding interface or any combination.

b. Corrosion of stainless steel is typically limited to light rust stains over small part of the surface following several years of service. Data extend up to 25 years in urban, chemical, industrial and marine environments. Insignificant corrosion was observed in austenitic,

type 316 stainless steel (which contains molybdenum). This type of stainless steel is mostly used in seismic isolation bearings.

2. Bi-metallic sliding interfaces tend to slowly creep under prolonged loading without movement, which results in an increase in the true contact area. This, in turn, results in substantial increases in friction even in the absence of corrosion. AASHTO 1999 severely penalizes the use of bi-metallic interfaces in sliding seismic isolation bearings. By contrast, experimental studies and theoretical considerations indicate that this phenomenon does not occur in interfaces consisting of PTFE, or PTFE composites in contact with highly polished stainless steel.

3. Contamination of sliding interfaces while under load (bearings in service) is preventable with proper installation and sealing of the bearings. AASHTO 1999 recommends installation of sealed bearings with the stainless steel surface facing down. All other types of installation are either penalized or prohibited. Moreover, it is important not to disassemble sliding bearings in the field. Also, grease-lubricated sliding bearings tend to be much more easily contaminated than non-lubricated bearings.

4. Continuous movement of sliding bearings due to primarily traffic loading in bridges results in wear and eventual loss of the softer material (PTFE or PTFE-composite) of the sliding interface. AASHTO 1999 requires evaluation of wear over the expected lifetime of the structure, including testing for cumulative travel of at least 1600 m (1 mile). Such tests have so far been performed only for friction pendulum bearings and PTFE / stainless sliding bearings.

7.6.3 TEMPERATURE

The effects of temperature on the mechanical properties of seismic isolation bearings may be discussed in two distinct ways: (a) the effect of heating (viscous, hysteretic or frictional) on the mechanical properties during cyclic movement of the bearings, and (b) the effect of ambient temperature (and particularly low temperature) and of the duration of exposure to this temperature on the mechanical properties.

7.6.3.1 Heating During Cyclic Movement

For sliding bearings, frictional heating has been described by Constantinou et al. (1999), where analytical and experimental results are presented. Due to the fact that frictional heating occurs at the sliding interface, which is very small in volume, the temperature at the siding interface increases substantially and in proportion to the velocity of sliding. While these high temperatures diffuse quickly in the surrounding medium, they cause wear and some reduction of the friction force. The reduction in the friction force is modest due to the fact that friction is due to a number of contributing mechanisms, each one of which is differently affected by elevated temperature. It appears that wear is the major result of frictional heating.

7.6.3.2 Effect of Ambient Temperature

Low temperatures generally cause an increase in friction in sliding bearings, as shown in figure 7-14. In general, the coefficient of friction of PTFE or related materials in contact with highly polished stainless steel exhibits a variation with the velocity of sliding as shown in this figure. The maximum value of the coefficient of friction occurs at velocities of sliding that, in general, exceed about 100 mm/sec (denoted as f_{max}). As temperature reduces, the friction values substantially increase at the initiation of movement but increase much less at high velocities of sliding. At temperature below about –40°C, the maximum value of the coefficient of friction occurs at initiation of motion (denoted as μ_B). As an example, figure 7-15 presents recorded normalized friction force vs. displacement loops of a sliding bearing (consisting of unfilled sheet PTFE in contact with highly polished stainless steel) at temperatures of 21°C and –38°C. Note that the tests were conducted with imposed sinusoidal displacement history of peak velocity equal to 125 mm/sec. Despite the modest velocity and the extremely low temperature, frictional heating is substantial so that the low temperature effects are mitigated.

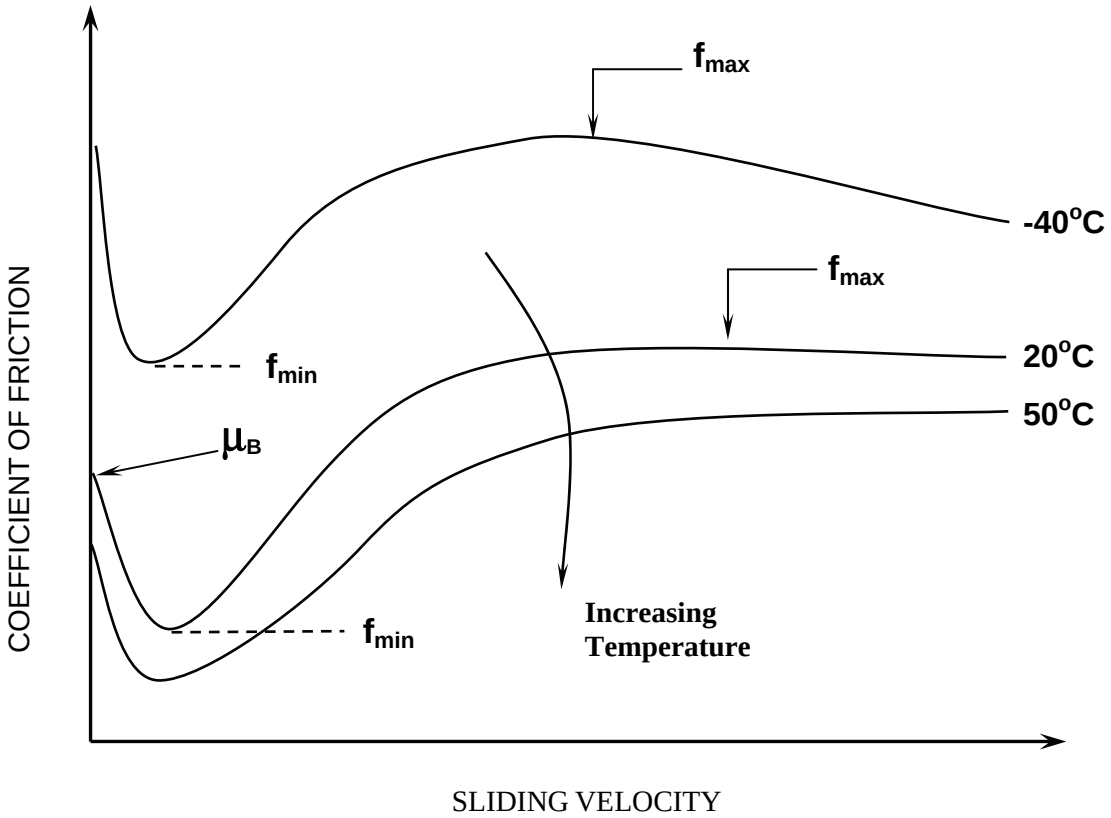

Figure 7-14. Effect of Temperature on the Frictional Properties of PTFE-polished Stainless Steel Interfaces

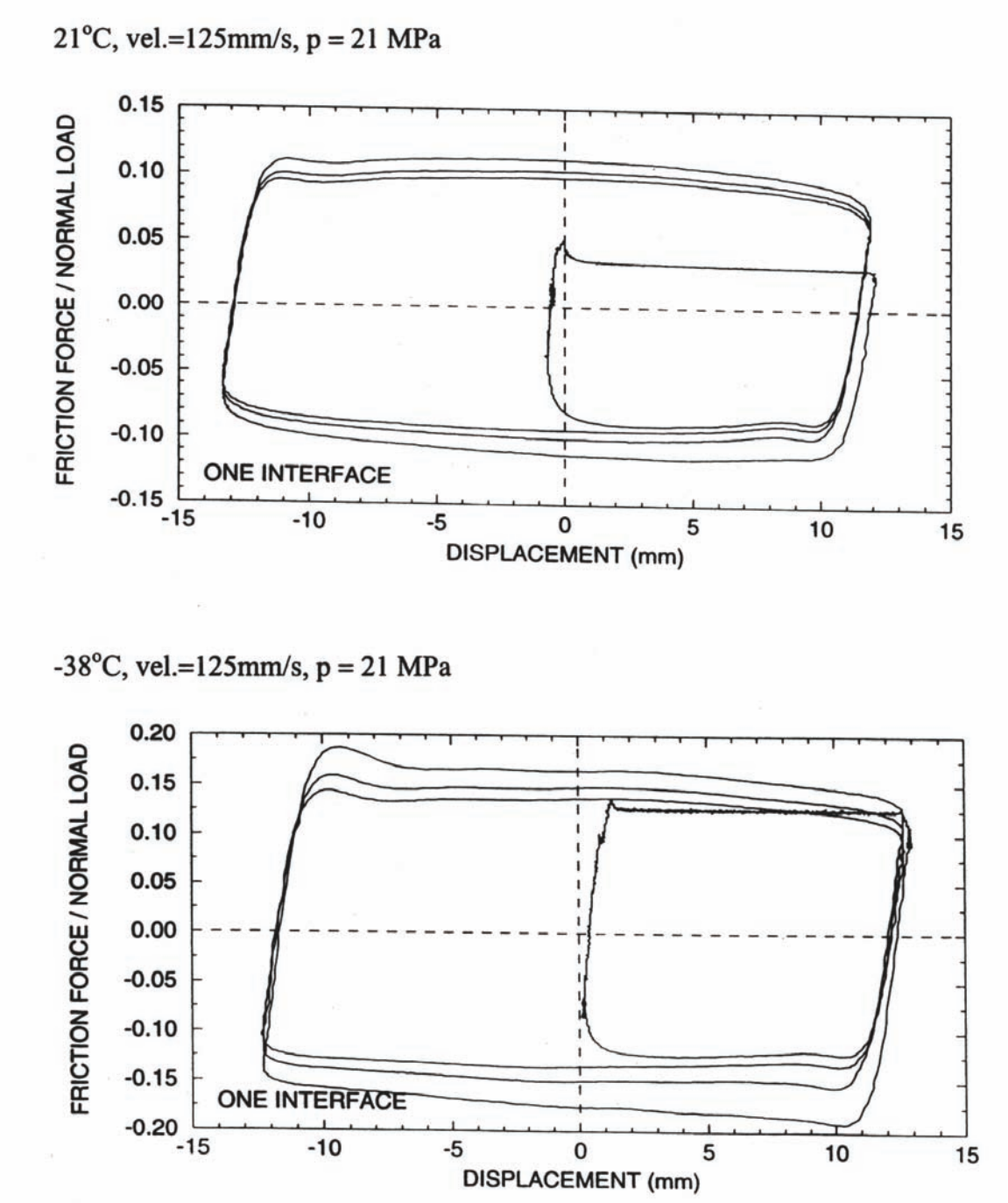

Figure 7-15. Normalized Force-displacement Relation of a Flat Sliding Isolator at Normal and Low Temperatures

7.6.4 LOADING HISTORY

The history of loading can have a marked effect on the mechanical properties of all types of bearings. Some of these effects have a profound impact, leading to significant error if disregarded. Loading history effects on elastomeric isolators are discussed in section 6.5.4. In this section cyclic loading effects in friction isolators are presented.

Tests conducted on friction pendulum isolators indicate that the dynamic friction coefficient from tests of full-size isolators should fall within 20% of the specified value. For conventional design applications, in a test involving 3-5 cycles of displacement, the coefficient of friction in the first cycle is generally about 20% higher than the average coefficient of friction from all the cycles. The average coefficient of friction from all the cycles represents the target design coefficient of friction. Accordingly, the initial lower bound friction coefficient, μ_L, is set equal to the target design coefficient of friction. The initial upper bound friction coefficient μ_U, is then initially set equal to $1.2\mu_L$ for design purposes. However, this should later be verified by the actual prototype testing of the bearings and the coefficient 1.2 may be modified accordingly. The initial lower and upper bound friction coefficients are then adjusted using the property modification factors to obtain the minimum and maximum probable friction coefficients for the isolators.

7.7 SYSTEM PROPERTY MODIFICATION FACTORS FOR SLIDING ISOLATORS

As described in section 4.5, system property modification factors are used to account for the likely variations in isolator properties over the life of a bridge. In this approach, the minimum and maximum effective stiffness and effective damping of the isolation system are calculated using the minimum and maximum values of the post-elastic stiffness, K_d, and characteristic strength, Q_d, of each isolation bearing. These values of parameters are calculated as the product of (1) the nominal values of these parameters, and (2) the minimum and maximum values of the corresponding system property modification factors.

The minimum value of the system property modification factor (λ-factor) is denoted as λ_{min} and has values less than or equal to unity. Due to the fact that most values of λ_{min} proposed by Constantinou et al. (1999) are close to unity, the AASHTO Guide Specifications (AASHTO 1999) sets λ_{min} equal to unity. That is, the lower bound values of properties of the isolation systems are considered to be the nominal values. These values are defined to be those determined for fresh and scragged specimens under normal temperature conditions.

As noted in section 4.5.2, the maximum value of the λ-factor is calculated as the product of six component factors:

$$\lambda_{max} = (\lambda_{max,t})(\lambda_{max,a})(\lambda_{max,v})(\lambda_{max,tr})(\lambda_{max,c})(\lambda_{max,scrag}) \qquad (7\text{-}20)$$

where

$\lambda_{max,t}$ = maximum value of factor to account for the effect of temperature (table 7-1)

$\lambda_{max,a}$ = maximum value of factor to account for the effect of aging (table 7-2)

$\lambda_{max,v}$ = maximum value of factor to account for the effect of velocity (= 1, unless established otherwise by test)

$\lambda_{max,tr}$ = maximum value of factor to account for the effect of travel and wear (table 7-3)

$\lambda_{max,c}$ = maximum value of factor to account for the effect of contamination (table 7-4)
$\lambda_{max,scrag}$ = maximum value of factor to account for the effect of scragging (= 1 for sliding isolators)

Values for the above factors are presented in tables 7-1 to 7-4 as noted above (AASHTO 1999, and Constantinou et al., 1999).

Table 7-1. Maximum Values for Temperature λ-factors for Sliding Isolators ($\lambda_{max,t}$)

Minimum Temperature for Design		Unlubricated PTFE	Lubricated PTFE	Bimetallic Interfaces
°C	°F			
21	70	1.0	1.0	To be established by test
0	32	1.1	1.3	
-10	14	1.2	1.5	
-30	-22	1.5	3.0	

Table 7-2. Maximum Values for Aging λ-factors for Sliding Isolators ($\lambda_{max,a}$)[1]

	Unlubricated PTFE		Lubricated PTFE		Bimetallic Interfaces[4]	
Environment/ Condition	Sealed	Unsealed[2]	Sealed	Unsealed[2]	Sealed	Unsealed[2]
Normal	1.1	1.2	1.3	1.4	2.0	2.2
Severe[3]	1.2	1.5	1.4	1.8	2.2	2.5

Notes: 1. Values are for 30-year exposure of stainless steel. For chrome-plated carbon steel, multiply values by 3.0.
2. Unsealed conditions assumed to allow exposure to water and salt, thus promoting further corrosion.
3. Severe environments include marine and industrial environments.
4. Values for bimetallic interfaces apply to stainless steel - bronze interfaces.

Table 7-3. Maximum Values for Travel and Wear λ-factors for Sliding Isolators ($\lambda_{max,tr}$)

Cumulative Travel		Unlubricated PTFE	Lubricated PTFE	Bimetallic Surfaces
Ft	M			
<3300	<1005	1.0	1.0	To be established by test
≤6600	≤2010	1.2	1.0	To be established by test
>6600	>2010	To be established by test	To be established by test	To be established by test

Table 7-4. Maximum Values for Contamination λ-factors for Sliding Isolators ($\lambda_{max,c}$)

	Unlubricated PTFE	Lubricated PTFE	Bimetallic Interfaces
Sealed with stainless steel surface facing down	1.0	1.0	1.0
Sealed with stainless surface facing up[1]	1.1	1.1	1.1
Unsealed with stainless surface facing down	1.1	3.0	1.1
Unsealed with stainless surface facing up	Not allowed	Not allowed	Not allowed

Note 1. Use factor of 1.0 if bearing is galvanized or painted for 30-year lifetime

7.8 FIRE RESISTANCE OF SLIDING ISOLATORS

In general, the fire resistance of an isolation bearing is not the same concern in a bridge application as it is in a building. Nevertheless the fire rating of these isolators should be consistent with that of the superstructure above and the substructures below.

Isolators consisting primarily of steel, such as sliding bearings without elastomeric parts, may meet fire-resistance requirements without special provisions due to their unique construction. But if insulation is required standard materials such as carbonate lightweight concrete may be used.

CHAPTER 8: EXAMPLE DESIGNS

Three design examples are presented in this section, which illustrate, in turn, the design and application of each of the three principal isolation systems to a standard highway bridge. In each case the same bridge is used. However, they are not designed for the same peak ground acceleration: the FPS and EQS examples assume an acceleration of 0.14 g, and the LRB example uses an acceleration of 0.3g. The three isolation systems are:

a. Friction pendulum isolators (FPS)
b. Lead-rubber isolators (LRB)
c. Eradiquake isolators (EQS)

8.1 DESCRIPTION OF THE BRIDGE

8.1.1 GENERAL

The bridge is located on Route 24, Section 44-4HB in Johnson County, Illinois. The structure number of the bridge is 044-0038. The bridge was constructed in 1970 to carry a westbound lane traffic over a roadway. The bridge has a relatively heavy slab-on-prestressed-concrete-girder superstructure and relatively lighter multiple column pier bents. The seismic isolation design of this bridge was performed as part of a retrofitting cost study (Dicleli and Mansour, 2003).

The plan view and elevation of the bridge is illustrated in figure 8-1. The total length of the bridge is 32.4 m and the width is 12.8 m. The bridge has three spans carrying two traffic lanes. The spans at the north and south ends of the bridge are 9.7 and the 8.2 m, respectively. The middle span is 14.5 m long and is located over a roadway. The bridge superstructure is continuous from one abutment to the other and supported by two piers in between. The expansion joint widths at the north and south abutments are respectively 38.1 and 25.4 mm.

8.1.2 SUPERSTRUCTURE

The bridge has a slab-on-girder superstructure where the deck is a prestressed concrete slab. Figure 8-1 shows the deck cross-section. There are six AASHTO Type II girders supporting a 191 mm thick reinforced concrete slab and are spaced at 2185-mm. A 75 mm thick asphalt pavement is provided on the deck surface.

8.1.3 PIERS

The piers of the bridge are reinforced concrete rigid frame bents typically used in Illinois bridges. The geometry and dimensions of Pier 1 and 2 are presented in figure 8-2. Each pier consists of a cap beam with a 864 x 915 mm cross-section and three circular columns spaced at 4267 mm. The columns have a diameter of 711 mm and are supported on a reinforced concrete wall. The height of the columns from the top of the wall to the bottom of the cap beam is 2591 mm in Pier 1 and 2324 mm in Pier 2. The heights of the walls are 1981 and 1943 mm respectively for Piers 1 and 2. Each wall is resting on a 610 mm thick spread footing.

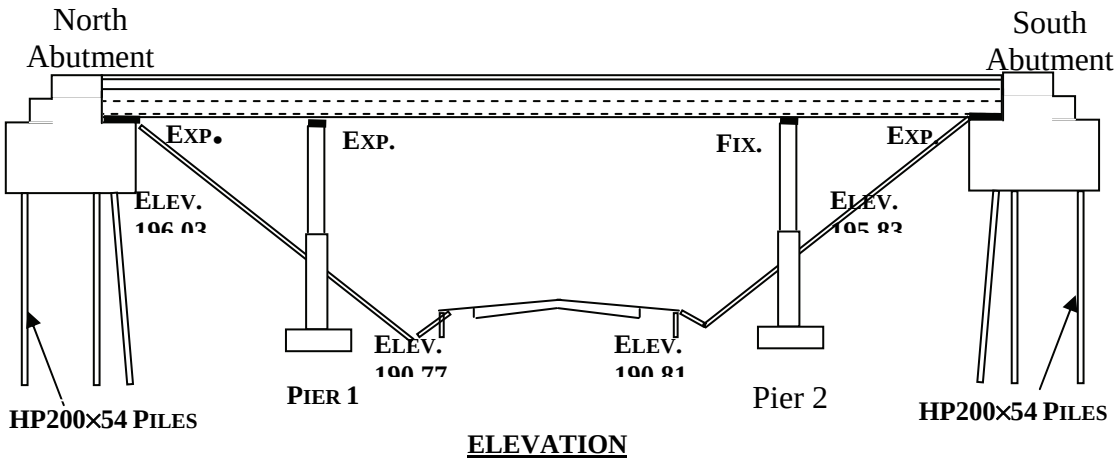

ELEVATION

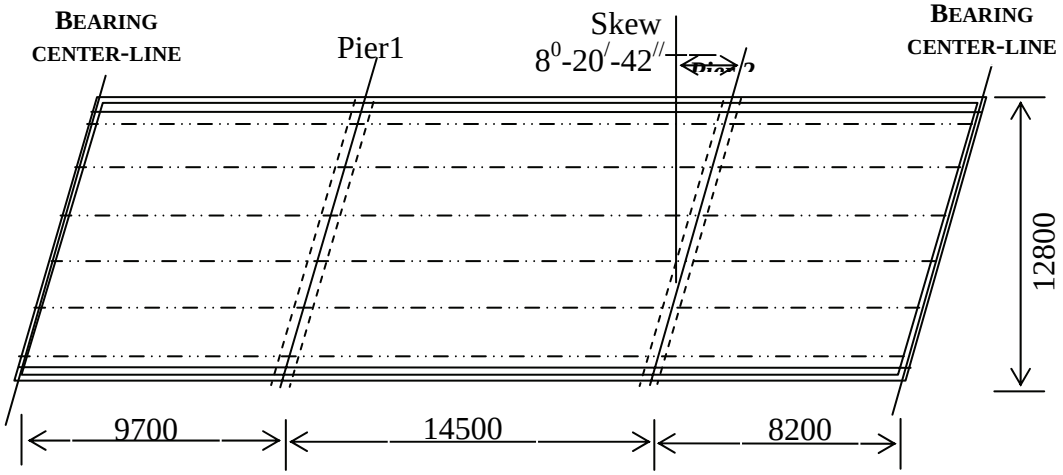

PLAN

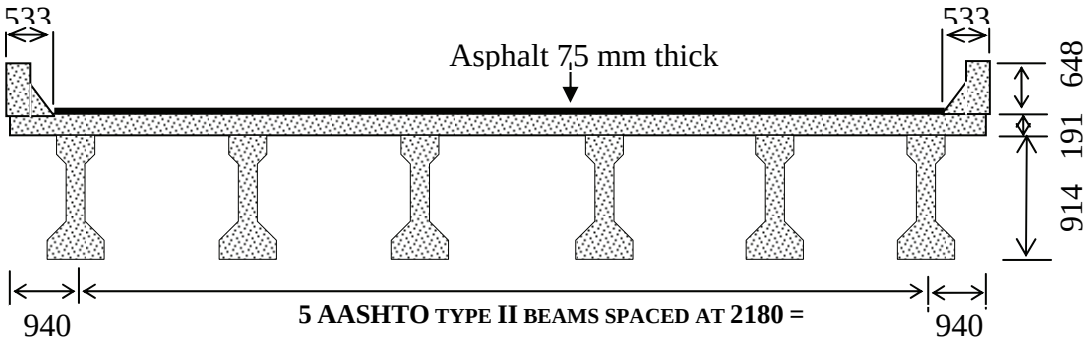

CROSS SECTION

Figure 8-1. General Layout of the Bridge

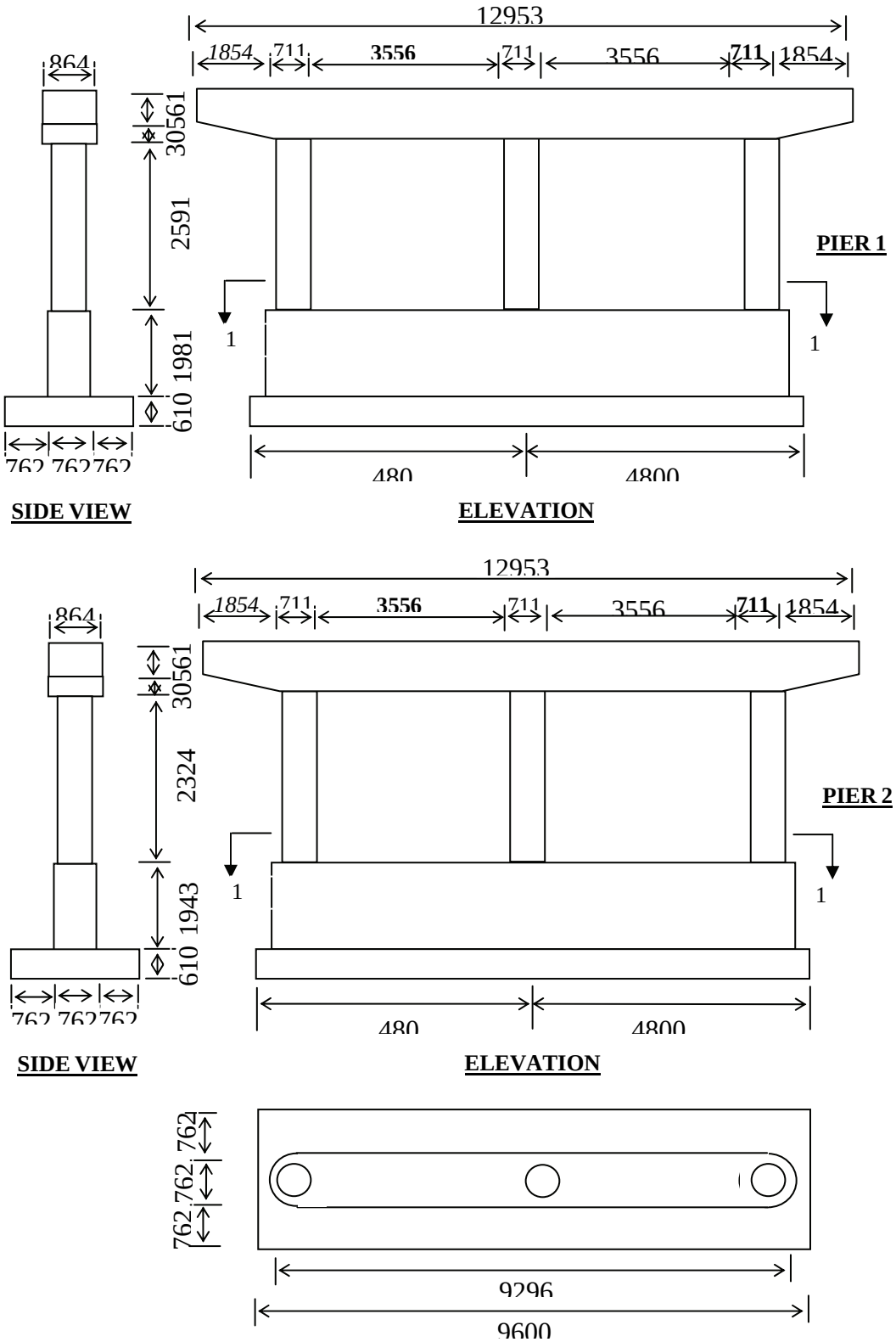

Figure 8-2. Bridge Piers

8.1.4 ABUTMENTS

Both the north and south abutments are seat type and are almost identical in geometry. The details of the abutments are illustrated in figure 8-3. The height and length of the abutments are respectively 1,854 and 12,940 mm. The thickness of the backwall is 458 mm and that of the breast wall is 1,372 mm. Two 305 mm thick wingwalls are connected perpendicular to the abutment and are extended 3500 mm to retain the backfill. The abutment and the wingwalls are directly supported on nine HP200X54 steel piles, seven of which support the abutment. The average length of the piles is 4.2 m at the north and 6.2 m at the south abutments. Three of the abutment piles are battered with a slope of 1:6. All the piles are embedded 305 mm into the abutments and wingwalls' footings. Additionally, a circular reinforced concrete encasement of 457-mm diameter is provided for the upper 914-mm length of the abutment piles.

8.1.5 SITE PROPERTIES

The results of geotechnical investigation for the bridge at the location of north abutment have indicated that the site soil profile consists of three separate layers of silty clay extending approximately 3.5 meters below the ground surface followed by hard brown sandstone. The base of the north abutment is placed approximately at the natural ground level.

The south abutment is placed approximately 1.7 m above the natural ground level. The fill material underneath the abutment is medium moist silty clay. Underneath the fill, there are two separate layers of silty clay extending 2.3 meters below the ground surface. The third layer of soil is roughly 1.5 meters thick and contains very stiff moist brown clay. The next layer consists of stiff brown clay shale.

Soil conditions near Pier 1 consists of three separate layers of silty clay extending for a depth of roughly 3 meters below the ground surface, followed by a layer of hard brown sandstone. The next layer consists of 1.5 meters thick very stiff moist brown clay followed by 2 meters thick hard gray mottled brown clay shale. The base of the pier footing is placed at approximately 4.7 m below the natural ground surface.

Soil conditions near pier 2 consist of three separate layers of silty clay extending approximately 2.5 meters below the ground level. The next layer is a very stiff moist brown mottled gray clay followed by a hard damped brown mottled gray clay shale layer extending for less than a meter down to the hard brown sandstone. The base of the pier footing is placed at approximately 3.4 m below the natural ground surface.

For the seismic analysis of the bridge, the bridge site is assumed to have stiff soil conditions (AASHTO soil type II). The acceleration coefficient for the site is obtained as 0.14 from a detailed seismic map of Illinois.

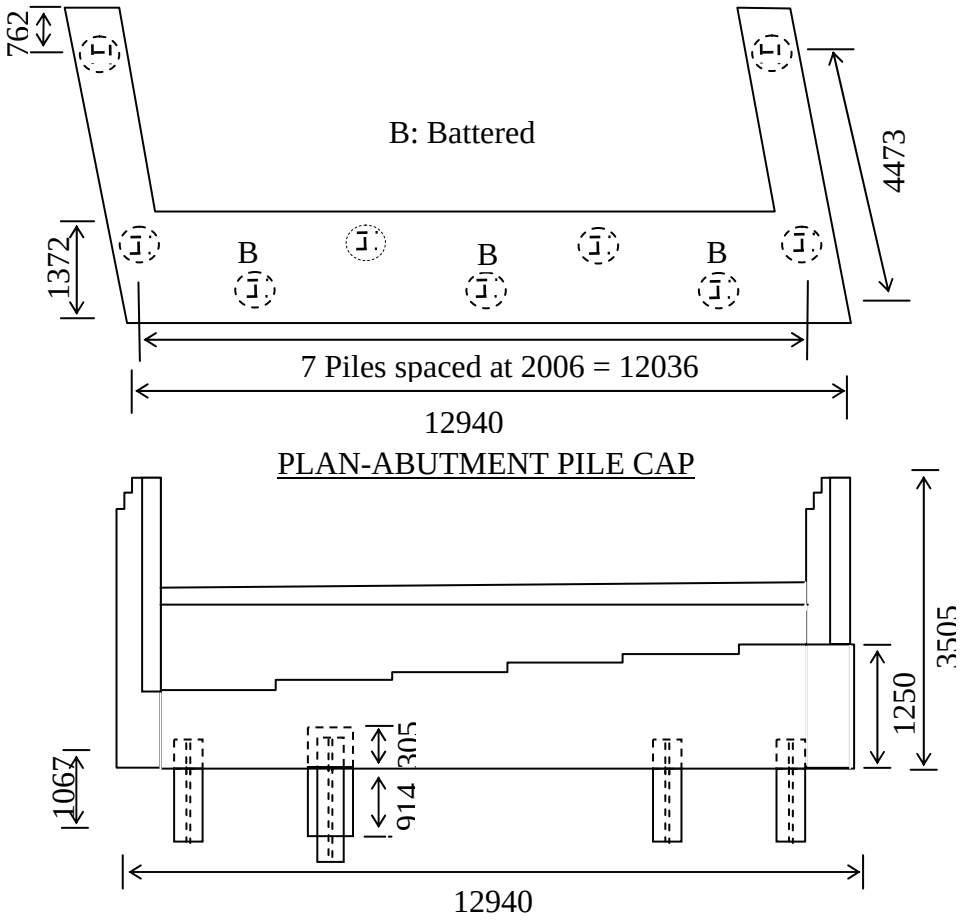

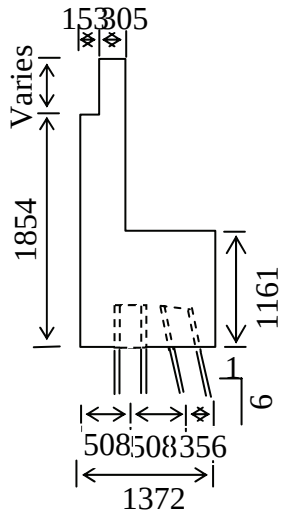

Figure 8-3. Bridge Abutments

8.1.6 SUPPORT REACTIONS

The superstructure loads due to the weight of the slab, girders, barrier walls, diaphragms and asphalt as well as the live load will be considered in the design of seismic isolation bearings. Tables 8-1, 8-2 and 8-3 present the superstructure dead load and live load reactions transferred to the substructures. The total weight and mass of the superstructure are 4354 kN and 444 x 10^3 kg respectively. The total weight of asphalt on the bridge and weight of the superstructure excluding asphalt are respectively 644 kN and 3710 kN.

Table 8-1. Bridge Superstructure Dead Load Reactions from a Typical Interior Girder

Member	Loads		Reactions (kN)			
	Uniformly Distributed (kN/m)	Point (kN)	North Abutment	Pier 1	Pier 2	South Abutment
Slab	9.73	N/A	32.80	136.00	127.75	24.42
Beam	5.59	N/A	18.83	78.15	73.4	14.00
Diaphragms at piers	N/A	26.13	0	26.13	26.13	0
Diaphragms in span	N/A	7.78	2.40	9.31	9.27	2.30
Asphalt	3.60	N/A	12.12	50.28	47.22	9.02
Total dead load			66.15	299.87	283.77	49.74

Table 8-2. Bridge Superstructure Dead Load Reactions from a Typical Exterior Girder

Member	Loads		Reactions (kN)			
	Uniformly Distributed (kN/m)	Point (kN)	North Abutment	Pier 1	Pier 2	South Abutment
Slab + Barrier Wall	14.25	N/A	48.12	199.60	187.50	35.84
Beam	5.59	N/A	18.83	78.15	73.40	14.00
Diaphragms at piers	N/A	13.08	0	13.08	13.08	0
Diaphragms in span	N/A	3.89	1.21	4.66	4.63	1.16
Asphalt	2.55	N/A	8.61	35.73	33.56	6.42
Total dead load			76.77	331.22	312.17	57.42

Table 8-3. Bridge Superstructure Average Dead Load Reactions per Girder Support and Total Load per Support

Load Type	Reaction (kN)			
	North Abutment	Pier 1	Pier 2	South Abutment
Per girder	70	310	293	52
Total load with asphalt	66	273	256	49
Total load w/out asphalt	352	1589	1504	265
Total load	418	1862	1760	314

8.2 SEISMIC ISOLATION DESIGN WITH FRICTION PENDULUM ISOLATORS

Seismic isolation design of the bridge primarily includes the determination of the properties of the isolation system. The following properties of friction pendulum isolators need to be determined as part of the design process so that the bearings can be ordered from the manufacturer.

1. Dynamic friction coefficient
2. Radius of concave surface
3. Displacement capacity

The design procedure for the example bridge is outlined below. It is based on a target isolator displacement and a targeted equivalent damping ratio.

8.2.1 Calculate the minimum required friction coefficient of the bearings
8.2.2. Calculate the minimum and maximum probable friction coefficient of the bearings
8.2.3 Calculate the radius of the concave surface of the bearings to ensure satisfactory performance of the isolated structure
8.2.4 Calculate the preliminary seismic displacement capacity of the bearings
8.2.5 Model the isolators for structural analysis
8.2.6 Perform structural analyses of the bridge to determine the seismic design displacements and substructure forces using respectively the minimum and maximum probable friction coefficients for the bearings
8.2.7 Calculate the required displacement capacity of the bearings including the additional displacements due to thermal variations.
8.2.8 Check the stability and rotation capacity of the bearings under gravitational loadings (not included as part of seismic isolation design)

8.2.1 DETERMINE MINIMUM REQUIRED FRICTION COEFFICIENT

To determine the design friction coefficient, μ, for friction pendulum isolators, the minimum friction coefficient required for resisting wind and braking forces need to be estimated. This will ensure that the bridge superstructure will not move under the effect of wind and braking forces. The larger of the friction coefficient obtained from wind and braking force is used to estimate the minimum friction coefficient. The design steps are presented below:

8.2.1.1 Calculate the wind force on structure [AASHTO 1998, article 3.8.1.2]
8.2.1.2 Calculate the wind force on vehicles [AASHTO 1998, article 3.8.1.3]
8.2.1.3 Calculate the braking force [AASHTO 1998, article 3.6.4]
8.2.1.4 Calculate the minimum required friction coefficient using the wind and braking forces calculated in steps 1-3 as well as load combinations and load factors presented in AASHTO (1998), table 3.4.1-1;
μ = max. factored horizontal load effect / min. factored weight of bridge deck
8.2.1.5 Decide if wind locking devices are required
8.2.1.6 Select minimum required friction coefficient

8.2.1.1 Calculate the wind force on structure [AASHTO 1998, Article 3.8.1.2]:

The horizontal wind force, WS, acting on the bridge is expressed as:

$$WS = \sum_{i=1}^{n} P_{Di} \times A_{Ei}$$

where P_{Di} is the design wind pressure for the i^{th} component of the bridge, and
A_E is the area of the i^{th} component of the bridge exposed to wind

The bridge elevation is less than 10 m above the ground level thus, the design wind pressure P_D is directly obtained from table 3.8.1.2.1-1 (AASHTO 1998). In the table, the design wind pressure is given for different components of the bridge. The design wind pressure for the girders is given as:
P_{D1} = 0.0024 MPa

The design wind pressure for the slab and barrier wall (large flat surfaces) is given as:
P_{D2} = 0.0019 MPa

Article 3.8.1.2.1 of AASHTO 1998 states that the wind force, f_W, per unit length of the bridge, shall not be taken as less than 4.4 N/mm on beam or girder components.

$f_W = P_D h_g$
where h_g is the height of the girder (914 mm from figure 8-1)

f_W = 0.0024 x 914 = 2.19 N/mm < 4.4 N/mm

Accordingly, use a larger wind pressure for the girder:
P_{D1} = 0.0024 x 4.4/2.19 = 0.0048 MPa

From figure 8-1:
Height of girder = 914 mm
Height of slab + barrier wall = 839 mm
Length of the bridge = 32,400 mm

$$WS = \sum_{i=1}^{n} P_{Di} \times A_{Ei} = 0.0048(914 \times 32{,}400) + 0.0019(839 \times 32{,}400) = 193{,}794 \text{ N}$$

WS = 193.8 kN

8.2.1.2 Calculate the wind force on vehicles [AASHTO 1998, Article 3.8.1.3]

The wind force on vehicles, WL, is taken as a uniformly distributed load of 1.46 N/mm. Accordingly, the total wind force on the vehicles on the bridge is calculated as:
WL = 1.46 x 32,400 = 47,304 N
WL = 47.3 kN.

8.2.1.3 Calculate the braking force [AASHTO 1998, Article 3.6.4]

The braking force, BR, is taken as 25 percent of the axle weights of the design truck or tandem per lane placed in all design lanes, which are carrying traffic headed in the same direction and is calculated as follows:

BR = BR_L m N_l

where BR_L is the braking force per lane, which is taken as 25 percent of the axle weights of the design truck or tandem
m is the multiple presence factor, and
N_l is the number of design lanes loaded in one direction

BR_L = 0.25 (35,000+145,000+145,000) = 81,250 N [AASHTO 1998, article 3.6.1.2.2]
BR_L = 81.25 kN

The number of design lanes is calculated as:

N_{dl} = (curb-to-curb clear width of the bridge in mm)/3600
= 11,735/3600 = 3.25
= 3 design lanes

Although the number of design lanes is calculated as 3, currently the bridge has only two traffic lanes. The number of traffic lanes is assumed to remain the same in the future. Thus, only one design lane is taken to be loaded in any one direction.

i.e., N_l = 1

m = 1.2 [AASHTO 1998, table 3.6.1.1.2-1]

BR = 81.25 x 1.2 x 1
= 97.5 kN

8.2.1.4 Calculate the minimum required friction coefficient

The calculation of the minimum required friction coefficient is done with reference to AASHTO 1998 load combinations and load factors (AASHTO 1998, table 3.4.1-1)

Limit state: STRENGTH-I, braking force effect
The factored braking load acting on the bridge superstructure is:
F_T = 1.75 BR = 1.75 x 97.5 = 170.6 kN

The total weight of the bridge is:
W = weight of components + weight of asphalt
= 3710 + 644 = 4354 kN

The factored weight of the bridge is:
W_F = 0.9(weight of components) + 0.65(weight of asphalt)
= 0.9 x 3710 + 0.65 x 644 = 3757.6 kN

The minimum required friction coefficient is then calculated as:
μ = 170.6/3757.6 = 0.045
= 4.5%

Limit state: STRENGTH-III, transverse wind load effect
The factored transverse wind load acting on the bridge superstructure is:

F_T = 1.40 WS = 1.40 x 193.8 = 271.3 kN

The minimum required friction coefficient is then calculated as:
μ = 271.3/3757.6 = 0.072
= 7.2%

Limit state: STRENGTH-V, transverse wind load effect combined with braking force
The factored transverse wind load acting on the bridge superstructure is:
F_T = 1.00 WS + 0.40 WL= 1.0 x 193.8 + 0.40 x 47.3= 212.7 kN

The factored braking load acting on the bridge superstructure is:
F_T = 1.35 BR = 1.35 x 97.5 = 131.6 kN

Total factored horizontal load is
$F = (F_T^2 + F_L^2)^{0.5} = (212.7^2 + 131.6^2)^{0.5}$ = 250.0 kN

The minimum required friction coefficient is then calculated as:
μ = 250.0/3757.6 = 0.067
= 6.7%

Selection of friction coefficient based on the results from above.
The minimum required friction coefficient calculated above is 7.2%.

8.2.1.5 Decide if wind locking devices are required

For a peak ground acceleration of 0.14g, a friction coefficient of 7.2% is relatively large and, if used, seismic performance may not be satisfactory. Therefore, wind-locking devices are recommended at the bearings to resist the transverse wind forces.

8.2.1.6 Select minimum required friction coefficient

The wind locking devices will resist the wind-induced forces. Therefore, the minimum required friction coefficient will be governed by the braking force. Accordingly, based on a 4.5% friction coefficient required to resist braking, a minimum friction coefficient of 5% will be used in the design.

8.2.2 DETERMINE MINIMUM AND MAXIMUM FRICTION COEFFICIENT

Minimum and maximum values for the friction coefficient need to be determined to account for variations due to loading history, temperature, aging, velocity, wear and contamination. The minimum value will be used to determine the maximum isolator displacements and the maximum value will be used to determine the loads transferred to the substructures. The steps are as follows:

8.2.2.1 Determine the initial lower and upper bound friction coefficients, μ_L and μ_U respectively per section 7.6.4.

8.2.2.2 Obtain the system property modification factors: λ_t, λ_a, λ_v, λ_{tr} and λ_c from section 7.7.

8.2.2.3 Obtain the system property adjustment factor, f_a per section 4.5.3 to account for the likelihood that the maximum λ-values do not all occur at the same time.

f_a = 1.00 for critical bridges
f_a = 0.75 for essential bridges
f_a = 0.66 for all other bridges

8.2.2.4 Apply the system property adjustment factor to the portion of system property modification factor deviating from unity to obtain adjusted system property modification factors: λ_{t1}, λ_{a1}, λ_{v1}, λ_{tr1} and λ_{c1}.

8.2.2.5 Calculate the minimum and maximum system property modification factors as:
$\lambda_{min} = 1.0$
$\lambda_{max} = \lambda_{t1}\,\lambda_{a1}\,\lambda_{v1}\,\lambda_{tr1}\,\lambda_{c1}$

8.2.2.6 Calculate the minimum and maximum probable friction coefficient as:
$\mu_{min} = \lambda_{min}\,\mu_L$
$\mu_{max} = \lambda_{max}\,\mu_U$

8.2.2.1 Determine initial lower and upper bound friction coefficients
μ_L = 5.0%
μ_U = 1.2 x 5 = 6.0%

8.2.2.2 Obtain the system property modification factors
From section 7.7, tables 7-1 to 7-4:
λ_t = 1.2 for a minimum air temperature of -18°C at bridge location.
λ_a = 1.1
λ_v = 1.0 (but needs to be verified from test results)
λ_{tr} = 1.0
λ_c = 1.0 (sealed bearings with the stainless steel surface facing down)

8.2.2.3 Obtain the system property adjustment factor
f_a = 0.66 for 'other' bridges (section 4.5.3, table 4-1]

8.2.2.4 Calculate the adjusted system property modification factors
λ_{t1} = 1.0 + (1.2 - 1.0)0.66 = 1.132
λ_{a1} = 1.0 + (1.1 - 1.0)0.66 = 1.066
λ_{v1} = 1.0
λ_{tr1} = 1.0
λ_{c1} = 1.0

8.2.2.5 Calculate the minimum and maximum system property modification factors
λ_{min} = 1.0
λ_{max} = 1.132 x 1.066 x 1.0 x 1.0 x 1.0 = 1.207

8.2.2.6 Calculate the minimum and maximum probable friction coefficient
μ_{min} = 1.0 x 5.0 = 5.0%
μ_{max} = 1.207 x 6.0 = 7.2%

8.2.3 DETERMINE RADIUS OF CONCAVE SURFACE

The determination of the surface radius is based on minimum lateral force requirements, the expected displacement and required damping ratio.

8.2.3.1 Minimum lateral restoring force (section 4.6)

In order to meet self-centering requirements, it is recommended that the difference between the magnitude of the restoring force at design displacement and at 50% of the design displacement should be larger than the weight acting on the bearings divided by a factor of 80. As shown in section 4.6 this recommendation means that the period of vibration when sliding must be less than that given by equation 4-10. Comparing equations 4-10 and 7-7, it can be seen that for a friction pendulum bearing, this criterion is satisfied when:

$$R \leq 40 D_d$$

where R is the radius of the concave surface, and

D_d is the design displacement of the bearing

Assuming a target design displacement of 40 mm, the maximum value for R is then calculated as:

R_{max} = 40 x 40 = 1600 mm.

Assuming a minimum target damping ratio of 30% and a design displacement of 40 mm, and using a friction coefficient of 5%, the minimum radius, R is back-calculated from equation 7-10 as:

R_{min} = 713 mm

The bearings are manufactured with a standard radius of 1020 and 1550 mm within the range of interest. Of the two choices, the bearing with the smaller radius will have the smaller displacement, since the period is less (equation 7-7), and is chosen here. Thus,

R = 1020 mm

The corresponding period is calculated using equation 7-7 as

$$T = 2\pi\sqrt{\frac{R}{g}} = 2\pi\sqrt{\frac{1020}{9810}} = 2 \text{ sec.}$$

This is less than the 6 second limit imposed by equation 4-10 and therefore, the selected radius of 1020 mm meets the minimum lateral restoring force requirements.

8.2.4 DETERMINE PRELIMINARY SEISMIC DESIGN DISPLACEMENT

The determination of preliminary design displacement is based on the simplified procedure described in section 3.2. This is done assuming that all the bearing displacements are the same and neglecting the effect of the substructure flexibility. Determination of the design displacement is an iterative procedure, which is as follows:

8.2.4.1 Assume a design displacement, D_d.

8.2.4.2 Calculate the effective stiffness, k_e, of the isolated superstructure from equation 7-8, substituting the weight of the bridge superstructure into the equation.

8.2.4.3 Calculate the equivalent viscous damping ratio, β_e from equation 7-10

8.2.4.4 Calculate the effective period, T_e of the isolated part of the bridge as

$$T_e = 2\pi\sqrt{\frac{W_s}{k_e g}}$$

where W_s is the weight of the bridge superstructure, and
g is gravitational acceleration

8.2.4.5 Obtain a new design displacement in mm using the equation 3-4b:
$D_d = 250AS_1T_e/B$
where A is the acceleration coefficient
S_1 is the site coefficient for seismic isolation (table 3-1), and
B is the damping coefficient corresponding to β_e (table 3-2).

8.2.4.6 Compare the new design displacement with the initial value. If they are sufficiently close, go to next step (section 8.2.5). Otherwise, set D_d equal to the new design displacement and go back to step 2 for next round of iteration.

8.2.4.1 Assume a design displacement

Assume a design displacement of 40 mm or 0.040 m (previously assumed for the determination of the bearings' radius of concave surface).

8.2.4.2 Calculate the effective stiffness of the structure (equation 7-8)

$$k_e = \frac{\mu W_s}{D_d} + \frac{W_s}{R} = \frac{0.05\times(4354\times10^3)}{40} + \frac{4354\times10^3}{1020} = 9711\ N/mm$$

8.2.4.3 Calculate the equivalent viscous damping ratio (equation 7-10)

$$\beta_e = \frac{2}{\pi}\left(\frac{\mu}{\mu + \frac{D_d}{R}}\right) = \frac{2}{\pi}\left(\frac{0.05}{0.05 + \frac{40}{1020}}\right) = 0.36$$

As noted in table 3-2, values for the damping factor, B, are unreliable when the damping ratio, β, exceeds 30% and a nonlinear time history analysis is recommended in these situations. For this example the equivalent damping ratio is taken at 30% and B is conservatively limited to 1.7.

8.2.4.4 Calculate the effective period of vibration

$$T_e = 2\pi\sqrt{\frac{W_s}{k_e g}} = 2\pi\sqrt{\frac{4354\times10^3}{9711\times9810}} = 1.34\ s.$$

8.2.4.5 Calculate the new design displacement (equation 3-4b)

A = 0.14
S_1 = 1.5, for AASHTO soil type II (table 3-1)
B = 1.7, for 30% equivalent damping ratio (table 3-2)
$D_d = 250AS_1T_e/B = 250 \times 0.14 \times 1.5 \times 1.34/1.7 = 41$ mm

8.2.4.6 Compare the new design displacement with the previous one

40 mm ~41 mm: sufficiently close.

D_d = 40 mm

The preliminary design displacement will be used as an initial displacement in the multi-mode response spectrum analysis of the bridge as described in the following sections

8.2.5 MODELING OF ISOLATORS FOR STRUCTURAL ANALYSIS

The iterative multi-mode response spectrum method is used in the analysis of the bridge. A 3-D structural model of the bridge is assembled and analyzed using the program SAP2000 (CSI 2002). Only the structural modeling of the bearings will be described here. Modeling of the complete bridge is outside the scope of this document.

In the structural model, each bearing is modeled as an equivalent single 3-D cantilever beam element connected between the superstructure and substructure at the girder locations as shown in figure 8-4. Pin connections are assumed at the joints linking the bearings to the substructures. The beam element is assigned section properties that match the calculated effective lateral stiffness of the bearing. The elastic modulus for concrete (E_c = 28,000 MPa) is taken as the modulus for these beam elements.

The moment of inertia, I_i, of the beam element representing bearing, i, is computed as:

$$I_i = \frac{k_{ei} h^3}{3E_c}$$

where h is the height of the bearing and k_{ei} is the effective stiffness of bearing i. The calculated moment of inertia will be adjusted throughout the iterative multimode response spectrum analysis procedure as the effective stiffness changes, as explained in the following section.

Since friction pendulum bearings are almost rigid in the vertical direction, a large cross-sectional area (A) of 1,000,000 mm^2 is arbitrarily assigned to each beam element.

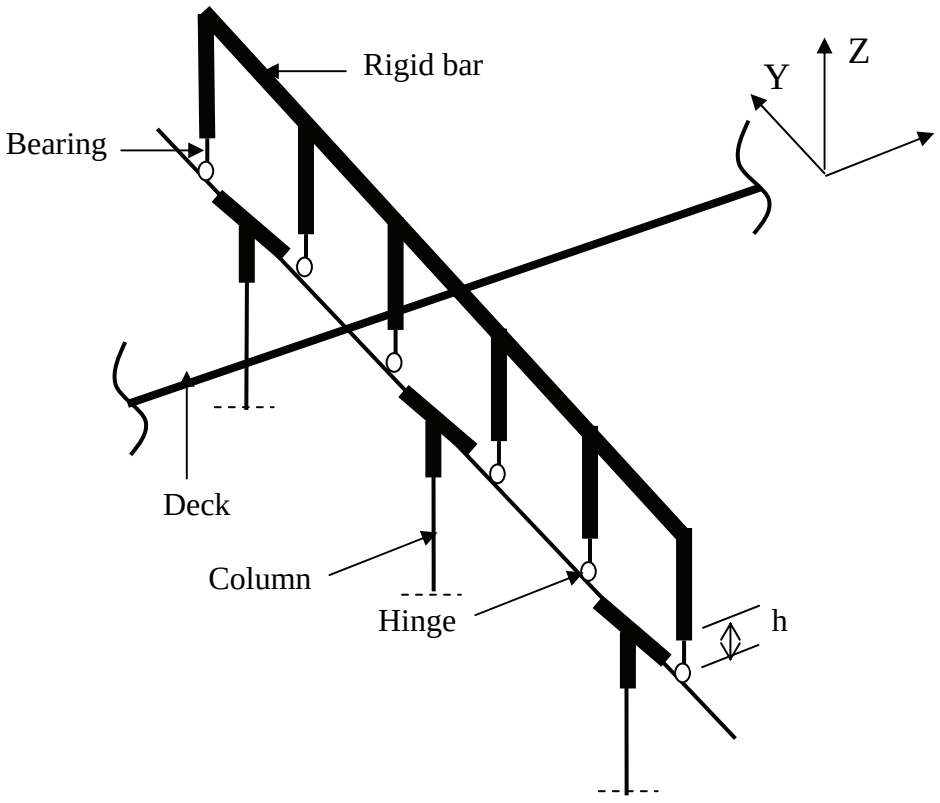

Figure 8-4. Structural Model of a Pier and Friction Pendulum Isolators

8.2.6 STRUCTURAL ANALYSIS OF THE BRIDGE

Two series of iterative multimode response spectrum analyses of the bridge need to be performed to determine the seismic design displacements and substructure forces. The first analysis is performed using the minimum probable friction coefficient to estimate the required displacement capacity of the bearings. The second analysis is performed using the maximum probable friction coefficient to estimate the forces in substructure members.

A seismically isolated bridge possesses vibration modes and periods associated with the movement of the seismic isolation system (isolated modes) and other structural members (structural modes). Five percent damping is assumed in the structural modes, and the calculated equivalent viscous damping ratio, β_e, is used in isolated modes to account for the hysteretic energy dissipated by the isolators. Accordingly, a hybrid design response spectrum is required with different levels of damping for the structural and isolated modes of vibration.

The hybrid spectrum used in this example is shown in figure 8-5. It was obtained by taking the AASHTO 1998, 1999 design spectra (which are calculated for 5% damping) and dividing the spectral values, at periods above 0.8 T_e, by the damping coefficient, B.

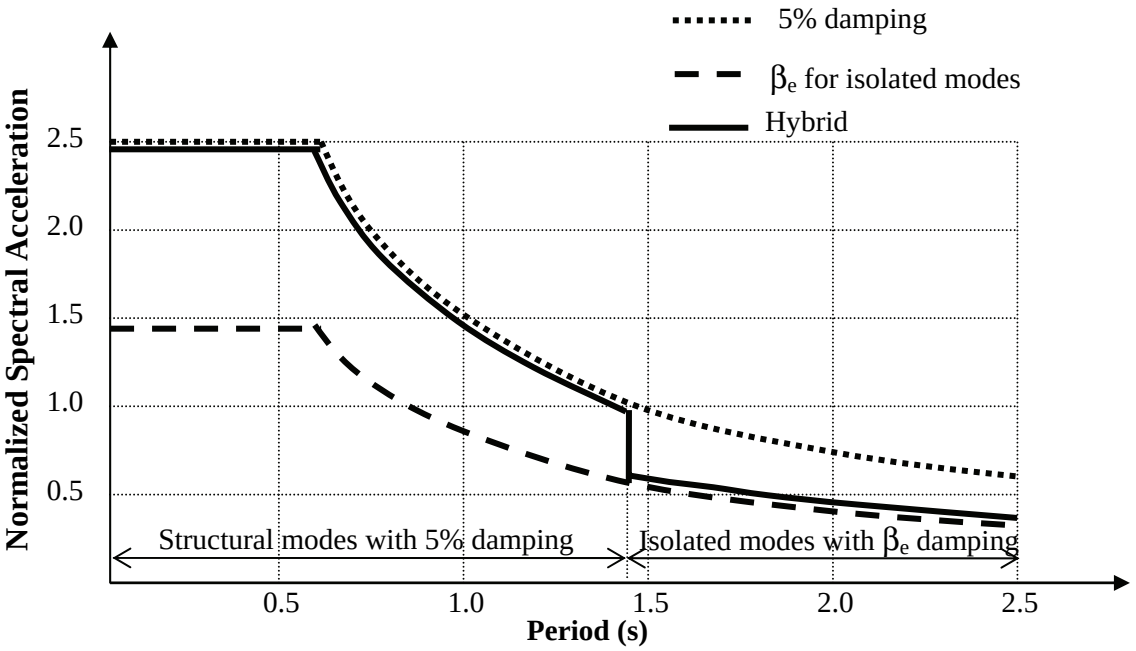

Figure 8-5. Hybrid Response Spectrum for Isolated Bridge

Using this hybrid design response spectrum, two series of iterative multimode response spectrum analyses of the bridge are performed to determine the design displacements and substructure forces. The first analysis is performed using the minimum probable friction coefficient to estimate the required seismic displacement capacity of the bearings. The second analysis is performed using the maximum probable friction coefficient to estimate the induced forces in substructure members. The analysis procedure is outlined below.

8.2.6.1 Assume a design displacement, D_{di} for each set of bearings over each support (Initially use the calculated preliminary design displacement for all the bearings in step 8.2.4.6)

8.2.6.2 Calculate the effective stiffness, k_{ei}, of each bearing by substituting the bearing displacement D_{di} and the dead load support reaction, W_i on the bearing into equation 7-8. Thus :

$$k_{ei} = \frac{\mu W_i}{D_{di}} + \frac{W_i}{R}$$

8.2.6.3 Neglecting the flexibility of the substructure, calculate the equivalent viscous damping ratio, β_e of the structure as:

$$\beta_e = \frac{2\sum_{i=1}^{n_b} \mu W_i D_{di}}{\pi \sum_{i=1}^{n_b} k_{ei} D_{di}^2}$$

where n_b is the number of isolation bearings.

8.2.6.4 Calculate the damping coefficient B, corresponding to β_e from table 3-2.

8.2.6.5 Calculate the section properties of the beam element representing the bearings as outlined in section 8.2.5 and implement the calculated properties into the structural model.

8.2.6.6 Perform a dynamic analysis of the bridge to determine the mode shapes and vibration periods of the isolated bridge. Generally, the first two modes of vibration are associated with the translation of the isolation system in both orthogonal directions of the bridge, and the third mode is associated with torsional motion of the superstructure about a vertical axis.

8.2.6.7 Based on the periods of the isolated modes calculated in the previous step, define a hybrid design spectrum that provides 5% damping for the non-isolated 'structural' modes of vibration and a higher damping level for the isolated modes.

8.2.6.8 Perform a multi-mode response spectrum analysis of the bridge to obtain a new design displacement for each bearing. Compare the new design displacements with the initially assumed design displacements. If they are sufficiently close, go to the next step (section 8.2.7). Otherwise, go to section 8.2.6.2 and repeat above calculations using the new design displacements.

The analysis procedure using $\mu = 0.05$ is outlined below.

8.2.6.1 Assume a design displacement, D_{di} for the bearings

D_{di} = 40 mm is assumed for all the bearings

8.2.6.2 Calculate the effective stiffness, k_{ei}, of each bearing

For the following calculations, the bearing reactions are obtained from table 8-3.

For each bearing over the north abutment:

$$k_{ei} = \frac{\mu W_i}{D_{di}} + \frac{W_i}{R} = \frac{0.05 \times 70 \times 10^3}{40} + \frac{70 \times 10^3}{1020} = 156\ N/mm$$

For each bearing over Pier 1:

$$k_{ei} = \frac{\mu W_i}{D_{di}} + \frac{W_i}{R} = \frac{0.05 \times 310 \times 10^3}{40} + \frac{310 \times 10^3}{1020} = 691\ N/mm$$

For each bearing over Pier 2:

$$k_{ei} = \frac{\mu W_i}{D_{di}} + \frac{W_i}{R} = \frac{0.05 \times 293 \times 10^3}{40} + \frac{293 \times 10^3}{1020} = 654\ N/mm$$

For each bearing over the south abutment:

$$k_{ei} = \frac{\mu W_i}{D_{di}} + \frac{W_i}{R} = \frac{0.05 \times 52 \times 10^3}{40} + \frac{52 \times 10^3}{1020} = 116\ N/mm$$

8.2.6.3 Calculate the equivalent viscous damping ratio, β_e of the structure

There are 6 bearings over each support and μ = 0.05 and D_{d1} = 40 mm for all the bearings:

$$\beta_e = \frac{2\sum_{i=1}^{n_b} \mu W_i D_{di}}{\pi \sum_{i=1}^{n_b} k_{ei} D_{di}^2} = \frac{2\times 6\times 0.05\times 40\times(70\times10^3 + 310\times10^3 + 293\times10^3 + 52\times10^3)}{\pi\times 6\times 40^2\times(156+691+654+116)} = 0.36$$

As before (section 8.2.4.3), to avoid being required to undertake a nonlinear time history analysis, the value of β_e is capped at 30%.

8.2.6.4 Calculate the damping coefficient, B

B= 1.7, for 30% equivalent damping ratio (table 3-2)

8.2.6.5 Calculate the section properties of the beam elements for the bearings

A_1 = 1,000,000 mm^2 for each bearing

To calculate the moment of inertia for each beam element that represents each bearing in the structural model, the beam element is assumed to have a height of 150 mm (typical height of a friction pendulum bearing). The moment of inertia of the beam elements over each support are then calculated as:

For each bearing over the north abutment:

$$I_i = \frac{k_{ei}h^3}{3E_c} = \frac{156\times150^3}{3\times28{,}000} = 6268\ mm^4$$

For each bearing over the Pier 1:

$$I_i = \frac{k_{ei}h^3}{3E_c} = \frac{691\times150^3}{3\times28{,}000} = 27763\ mm^4$$

For each bearing over the Pier 2:

$$I_i = \frac{k_{ei}h^3}{3E_c} = \frac{654\times150^3}{3\times28{,}000} = 26277\ mm^4$$

For each bearing over the south abutment:

$$I_i = \frac{k_{ei}h^3}{3E_c} = \frac{116\times150^3}{3\times28{,}000} = 4661\ mm^4$$

8.2.6.6 Perform the analysis of the bridge to determine isolated vibration periods

The periods of vibration for the two translational isolated modes are obtained as follows:

T_1 = 1.51 sec.

T_2 = 1.48 sec.

These modes are shown in figure 8-6.

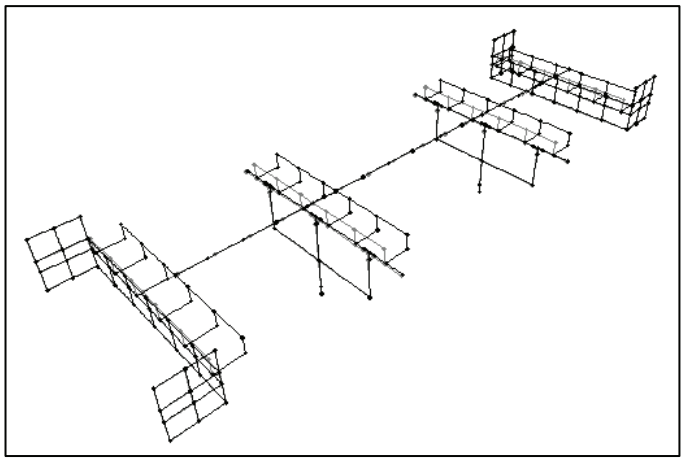

(a) First mode

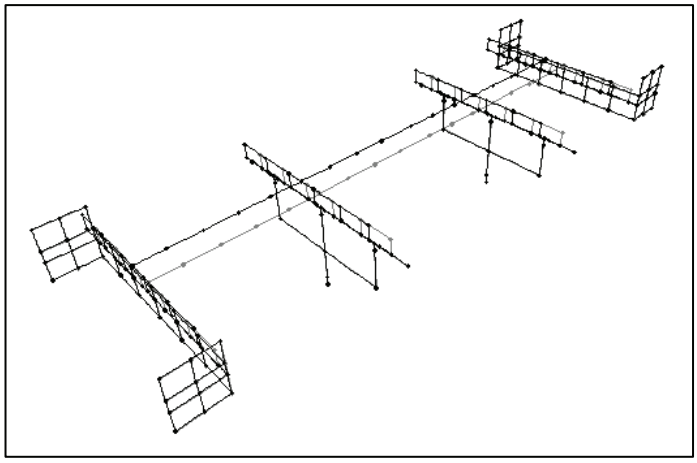

(b) Second mode

Figure 8-6. Isolated Vibration Modes of the Bridge

8.2.6.7 Determine hybrid response spectrum for the analysis

Based on the isolated periods of vibration, the hybrid response spectrum is obtained in compliance with article 7.3 of AASHTO 1999. The general equation for the normalized response spectrum with respect to the peak ground acceleration is given as:

$$C_{sm} = \frac{AS_i}{BT_e^{2/3}} \leq 2.5\frac{A}{B}$$

A = 0.14g, where g is the gravitational acceleration

S_1 = 1.5 for AASHTO Soil Type II (table 3-1)

B = 1.0 for 5% structural damping

B = 1.7 for 30% equivalent damping of the isolated modes

The hybrid spectrum is obtained by scaling spectral values for periods in excess of 0.8 T_e (0.8 x 1.48 = 1.18). Thus, the hybrid response spectrum is defined as:

For T_e < 1.18 sec

$$C_{sm} = \frac{0.14g \times 1.2}{T_e^{2/3}} \leq 2.5 \times 0.14g$$

For T_e > 1.18 sec

$$C_{sm} = \frac{0.14g \times 1.2}{1.7 \times T_e^{2/3}}$$

8.2.6.8 Perform the analysis of the bridge to obtain new bearing displacements

Following are the relative displacements of the bearings in the longitudinal direction:

For each bearing over the north abutment:
D_d = 41 mm

For each bearing over the Pier 1:
D_d = 38 mm

For each bearing over Pier 2:
D_d = 39 mm

For each bearing over the south abutment:
D_d = 41 mm

Similar results are obtained for the displacements in the transverse direction. The iteration is stopped here as the calculated bearing displacements are all close to the initially assumed displacement.

8.2.7 CALCULATE REQUIRED DISPLACEMENT CAPACITY OF THE ISOLATORS

8.2.7.1 Minimum required capacity

Section 4.8 requires that minimum clearances between the superstructure and abutments be provided to allow for unexpected movements in the bearings. These clearances imply that the displacement capacity of the isolator should not be less than:

25 mm or

$$\frac{200AS_iT_e}{B} = \frac{200 \times 0.14 \times 1.5 \times 1.51}{1.7} = 37.3\ mm$$

41 mm > 37.3 mm OK.

8.2.7.2 Allowance for thermal demand on bearings

The displacement at one end of the bridge relative to the midpoint due to uniform thermal expansion is calculated as:
$D_T = \alpha\ \Delta T\ (0.5L)$
where α is coefficient of thermal expansion (10×10^{-6}/ °C for concrete)

ΔT is design uniform temperature range, and
L is total length of the bridge (32,400 mm)

For the bridge site, the minimum and maximum design temperatures are specified as -18°C and 27°C respectively. Assuming a construction temperature of 15 °C, the negative and positive temperature ranges are respectively calculated as 15-(-18) = 33°C and 27-15 = 12°C. Thus, the design uniform temperature range is 33°C. Accordingly,

$D_T = 10 \times 10^{-6} \times 33 \times 0.5 \times 32{,}400 = 5.4$ mm

8.2.7.3 Required displacement capacity

To account for the unlikely event that the peak seismic demand will occur at the same time as the peak thermal demand, only 50% of the thermal demand is considered acting at the time of the earthquake.

Required displacement capacity of the bearing = 41 mm + 0.5 x 5.4 mm
= 43 mm
→ use 50 mm.

8.2.8 CHECK STABILITY AND ROTATION CAPACITY OF ISOLATORS

Checking the stability and rotation capacity of the friction pendulum bearings under gravity loads is beyond the scope of this document. However, in the case of friction pendulum bearings, stability is not usually a concern. Generally, once the bearing properties (friction coefficient, radius and displacement capacity) are determined, they can be ordered from the manufacturer.

8.2.9 FINAL ISOLATOR DESIGN

Final design values are:

- Nominal dynamic friction coefficient = 5.0%
- Upper-bound dynamic friction coefficient = 6.0%
- Upper-bound dynamic friction coefficient after modification for environmental effects = 7.2%
- Radius = 1020 mm
- Displacement capacity = 50 mm
- Wind locks to be used to resist transverse wind
- Stability of isolator not checked.

8.3 SEISMIC ISOLATION DESIGN WITH LEAD-RUBBER ISOLATORS

As with the previous example, the isolation design of a bridge with lead-rubber isolators primarily involves the determination of the properties of the isolators themselves. The following properties of the isolators need to be determined to complete the design so that the bearings can be ordered from the manufacturer:

1. Lead core diameter
2. Isolator diameter (or plan dimensions if square or rectangular)
3. Thickness and number of the rubber layers, and
4. Thickness and number of steel reinforcing plates (shims).

Note that for this example, a site peak ground acceleration of 0.30g is assumed.

The following material properties are assumed:
Effective yield stress of lead, f_{yL} = 11.4 MPa
Factor to account for effect of lead on post elastic stiffness of bearing, f = 1.1
Shear modulus of rubber, G_r = 0.62 MPa
Bulk modulus of rubber, K = 2000 MPa
Material constant for rubber, k' = 0.73 (section 6.3, table 6-1)

Maximum loads and rotations (live load effects are approximate)

At Pier 1 (most critical pier)	At North Abutment (most critical abutment)
P_D: Dead load = 300 kN	P_D: Dead load = 66 kN
P_L: Live load = 217 kN	P_L: Live load = 157 kN
P: Total load = 517 kN	P_L: Live load = 223 kN
Rotation = 0.00233	Rotation = 0.00274

The design procedure for the isolated bridge is as follows:

8.3.1 Calculate the minimum required diameter of the lead core
8.3.2 Set target values for effective period and damping ratio
8.3.3 Calculate the diameter of lead core and stiffness of rubber
8.3.4 Calculate the diameter and thickness of rubber
8.3.5 Calculate the thickness of rubber layers
8.3.6 Check the stability of the bearings
8.3.7 Check strain limits in the rubber
8.3.8 Calculate remaining properties and summarize
8.3.9 Calculate the system property adjustment factors for the bearings
8.3.10 Model the Bearings for structural analysis
8.3.11 Perform the structural analyses of the bridge to determine the seismic design displacements and substructure forces using respectively the minimum and maximum probable effective stiffness and characteristic strength of the bearings

8.3.1 CALCULATE MINIMUM REQUIRED DIAMETER OF LEAD CORE

To determine the diameter of the lead core, d_L, for seismic design, the minimum diameter required for resisting wind and braking forces need to be estimated first. This will ensure that

the bridge superstructure will not move under the effect of wind and braking forces. The larger of the diameters obtained from wind and braking forces is taken as the minimum core diameter. The design steps are as follows:

8.3.1.1 Calculate the wind force on structure [AASHTO 1998, article 3.8.1.2]
8.3.1.2 Calculate the wind force on vehicles [AASHTO 1998, article 3.8.1.3]
8.3.1.3 Calculate the braking force [AASHTO 1998, article 3.6.4]
8.3.1.4 Calculate the maximum combined horizontal service load effects using the wind and braking forces calculated in steps 1-3 as well as load combinations and load factors presented in AASHTO 1998, table 3.4.1-1.
8.3.1.5 Calculate the minimum required lead core diameter using the maximum of the combined load effects. Assuming that the same lead core diameter will be used for all the bearings, the required strength, Q is calculated as:
Q = maximum factored horizontal load effect / number of bearings
Next, from equations 6-1 and 6-3, the lead core diameter, d_L is calculated as:

$$d_{L\min} = \sqrt{\frac{4n\psi Q}{\pi(n-1)f_{yL}}}$$

8.3.1.1 Calculate the wind force on structure [AASHTO 1998, Article 3.8.1.2]:
The horizontal wind force, WS, acting on the bridge is expressed as:

$$WS = \sum_{i=1}^{n} P_{Di} \times A_{Ei}$$

where P_{Di} is the design wind pressure for the i^{th} component of the bridge, and
A_E is the area of the i^{th} component of the bridge exposed to wind

The bridge elevation is less than 10 m above the ground level thus, the design wind pressure P_D is directly obtained from table 3.8.1.2.1-1 (AASHTO 1998). In the table, the design wind pressure is given for different components of the bridge. The design wind pressure for the girders is given as:
P_{D1} = 0.0024 MPa

The design wind pressure for the slab and barrier wall (large flat surfaces) is given as:
P_{D2} = 0.0019 MPa

Article 3.8.1.2.1 of AASHTO 1998 states that the wind force, f_W, per unit length of the bridge, shall not be taken as less than 4.4 N/mm on beam or girder components.

$f_W = P_D h_g$
where h_g is the height of the girder (914 mm from figure 8-1)

f_W = 0.0024 x 914 = 2.19 N/mm < 4.4 N/mm

Accordingly, use a larger wind pressure for the girder:
P_{D1} = 0.0024 x 4.4/2.19 = 0.0048 MPa

From figure 8-1:

Height of girder = 914 mm
Height of slab + barrier wall = 839 mm
Length of the bridge = 32,400 mm

$$WS = \sum_{i=1}^{n} P_{Di} \times A_{Ei} = 0.0048(914 \times 32{,}400) + 0.0019(839 \times 32{,}400) = 193{,}794 \text{ N}$$

WS = 193.8 kN

8.3.1.2 Calculate the wind force on vehicles [AASHTO 1998, Article 3.8.1.3]

The wind force on vehicles, WL, is taken as a uniformly distributed load of 1.46 N/mm. Accordingly, the total wind force on the vehicles on the bridge is calculated as:
WL = 1.46 x 32400 = 47304 N
WL = 47.3 kN.

8.3.1.3 Calculate the braking force [AASHTO 1998, Article 3.6.4]

The braking force, BR, is taken as 25 percent of the axle weights of the design truck or tandem per lane placed in all design lanes, which are carrying traffic headed in the same direction and is calculated as follows:

$BR = BR_L \; m \; N_l$

where BR_L is the braking force per lane, which is taken as 25 percent of the axle weights of the design truck or tandem
m is the multiple presence factor, and
N_l is the number of design lanes loaded in one direction

BR_L = 0.25 (35,000+145,000+145,000) = 81,250 N [AASHTO 1998, article 3.6.1.2.2]
BR_L = 81.25 kN

The number of design lanes is calculated as:

N_{dl} = (curb-to-curb clear width of the bridge in mm)/3600
= 11,735/3600 = 3.25
= 3 design lanes

Although the number of design lanes is calculated as 3, currently the bridge has only two traffic lanes. The number of traffic lanes is assumed to remain the same in the future. Thus, only one design lane is taken to be loaded in any one direction.

i.e., N_l = 1

m = 1.2 [AASHTO 1998, table 3.6.1.1.2-1]

BR = 81.25 x 1.2 x 1
= 97.5 kN

8.3.1.4 Calculate the maximum combined horizontal service load effects

The maximum combined horizontal service load effects are calculated with reference to the AASHTO (1998) load combinations and load factors (AASHTO 1998, table 3.4.1-1)

The total weight of the bridge superstructure is:
W_s = weight of components + weight of asphalt
= 3710 + 644 = 4354 kN

Limit state: STRENGTH-I, braking force effect
The factored braking load acting on the bridge superstructure is:
F_T = 1.75 BR = 1.75 x 97.5 = 170.6 kN

Limit state: STRENGTH-III, transverse wind load effect
The factored transverse wind load acting on the bridge superstructure is:
F_T = 1.40 WS = 1.40 x 193.8 = 271.3 kN

Limit state: STRENGTH-V, transverse wind load effect combined with braking force
The factored transverse wind load acting on the bridge superstructure is:
F_T = 1.00 WS + 0.40 WL= 1.0 x 193.8 + 0.40 x 47.3= 212.7 kN

The factored braking load acting on the bridge superstructure is:
F_T = 1.35 BR = 1.35 x 97.5 = 131.6 kN

Total factored horizontal load is
$F = (F_T^2 + F_L^2)^{0.5} = (212.7^2 + 131.6^2)^{0.5} = 250.0$ kN

The maximum horizontal combined service load effect is therefore 271.3 kN (STRENGTH-III Limit State above)

8.3.1.5 Calculate the minimum required lead core diameter

Total number of bearings = 24
Q = 273.1 / 24 = 11.38 kN
ψ = 2.0; n = 8 for wind or braking force (section 6.2.1)
f_{YL} = 11.4 MPa (given section 8.3)

$$d_{L\min} = \sqrt{\frac{4n\psi Q}{\pi(n-1)f_{yL}}} = \sqrt{\frac{4\times8\times2\times11.38\times10^3}{\pi\times7\times10.3}} = 54\ mm$$

8.3.2 SET TARGET VALUES FOR EFFFECTIVE PERIOD AND DAMPING RATIO

For the bridge under consideration the following target effective period and damping values are assumed:
T_e = 1.00 sec, and
β_e = 0.30 (30% damping ratio)

8.3.3 CALCULATE LEAD CORE DIAMETER AND RUBBER STIFFNESS

The procedure outlined here is based on assuming target values for the effective period and equivalent damping of the isolated structure. To calculate the cross-sectional area of the lead core based on these assumed target values, the procedure below is followed:

8.3.3.1 Calculate the design displacement, D_d, using equation 3-4b:
8.3.3.2 Calculate the required effective stiffness of the bearings based on the assumed effective period.
8.3.3.3 Calculate the initial required characteristic strength (seismic resistance), Q_i, of the lead core.
8.3.3.4 Calculate diameter and check against minimum values required to resist service loads
8.3.3.5 Calculate the initial post elastic stiffness of the bearing using equation 6-10.
8.3.3.6 Calculate the final characteristic strength (seismic resistance) Q, of the lead core.
8.3.3.7 Calculate the final post elastic stiffness of the bearing using equation 6-10.
8.3.3.8 Check minimum lateral restoring force requirements (section 4.6).
8.3.3.9 Calculate the contribution of the rubber k_r, to the post-elastic stiffness, k_d

8.3.3.1 Calculate the design displacement using equation 3-4b

$D_d = 250AS_1T_e/B$

where A is the acceleration coefficient
S_1 is the site coefficient for seismic isolation (table 3-1), and
B is the damping coefficient corresponding to β_e from table 3-2.

$D_d = 250AS_1T_e/B = 250 \times 0.30 \times 1.5 \times 1.0/1.7 = 66$ mm

8.3.3.2 Calculate the required effective stiffness of the bearings

If all the bearings have the same effective stiffness, the effective stiffness of each individual bearing is given by:

$$k_e = \frac{W_s}{n_b g}\left(\frac{2\pi}{T_e}\right)^2$$

where W_s is the weight of the bridge superstructure
g is acceleration due to gravity, and
n_b is number of bearings.

$$k_e = \frac{W_s}{n_b g}\left(\frac{2\pi}{T_e}\right)^2 = \frac{4354\times10^3}{24\times9810}\left(\frac{2\pi}{1.0}\right)^2 = 730\ N/mm$$

8.3.3.3 Calculate the initial required characteristic strength (seismic resistance), Q_i, of the lead core.

From equation 6-11 and neglecting D_y, Q_i is approximated by:

$$Q_i = \frac{1}{2}\pi\beta_e k_e D_d = \frac{1}{2}\pi \times 0.30 \times 730 \times 66 = 22{,}704\ N$$

8.3.3.4 Calculate diameter and check against minimum values required to resist service loads

For earthquake loads, ψ = 1, n=10, and then:

$$d_L = \sqrt{\frac{4n\psi Q}{\pi(n-1)f_{yL}}} = \sqrt{\frac{4\times10\times1\times22704}{\pi\times9\times11.4}} = 53\,mm$$

Check if $d_L > d_{Lmin}$.

From section 8.3.1.5 $d_{Lmin} = 54$ mm $\approx d_L = 53$ mm

For design purposes, use an average $d_L = 60$ mm (use 50 mm for the 12 bearings at abutments and 70 mm for the 12 bearings at piers).

$$Q_i = \frac{n-1}{n\psi} f_{yL} \frac{\pi d_{L\min}^2}{4} = \frac{9}{10}\times11.4\times\frac{\pi\times60^2}{4} = 29{,}010N$$

8.3.3.5 Calculate the initial post-elastic stiffness of the bearing

From equation 6-10, the post elastic stiffness, k_d is calculated as:

$$k_{di} = k_e - \frac{Q_i}{D_d} = 730 - \frac{29{,}010}{66} = 289\ N/mm$$

8.3.3.6 Calculate the final characteristic strength (seismic resistance) Q, of the lead core

From equation 6-2, using n = 10 for seismic loading:

$$k_u = 10k_{di}$$

From equation 6-9:

$$D_y = \frac{Q_i}{k_u - k_d}$$

From equation 6-11:

$$Q = \frac{\pi\beta_e k_e D_d^2}{2(D_d - D_y)}$$

$$k_u = 10k_{di} = 10\times289 = 2890\ N/mm$$

$$D_y = \frac{Q_i}{k_u - k_d} = \frac{29{,}010}{2890 - 289} = 11.2\ mm$$

$$Q = \frac{\pi\beta_e k_e D_d^2}{2(D_d - D_y)} = \frac{\pi\times0.30\times730\times66^2}{2\times(66-11.2)} = 27{,}345\ N$$

Required value for Q (27,345 N) is close enough to that provided (29,010 N). Therefore use average core diameter of 60 mm (50 mm at abutments and 70 mm at piers).

8.3.3.7 Calculate the final post-elastic stiffness of the bearing

From equation 6-10, the post-elastic stiffness, k_p is calculated as:

$$k_d = k_e - \frac{Q_i}{D_d} = 730 - \frac{29{,}010}{66} = 289\ N/mm$$

8.3.3.8 Check minimum restoring force (section 4.6)

The minimum restoring force requirements in section 4.6 may be expressed by the following equation:

$$k_d \geq \frac{W_s}{40 n_b D_d}$$

where W_s is the weight of the superstructure (section 8.3.1.4).

The supplementary requirement that the period of vibration using the tangent stiffness must be less than 6 seconds, leads to the following equation:

$$k_d \geq \frac{4\pi^2 W_s}{36 n_b g}$$

(1) Check if:

$$k_d \geq \frac{W_s}{40 n_b D_d} = \frac{4354 \times 10^3}{40 \times 24 \times 66} = 68.7\ N/mm$$

K_d = 289 N/mm > 68.7 N/mm OK.

(2) Check if:

$$k_d \geq \frac{4\pi^2 W_s}{36 n_b g} = \frac{4\pi^2 \times 4354 \times 10^3}{36 \times 24 \times 9810} = 20.3\ N/mm$$

K_d = 289 N/mm > 20.3 N/mm OK

8.3.3.9 Calculate the contribution of the rubber k_r, to the post-elastic stiffness, k_d

Using the factor f that accounts for the effect of lead on post-elastic stiffness (f is generally taken as equal to 1.1), the contribution of the rubber k_r, is given by equation 6-5 as:

$k_r = k_d/f = 289/1.1 = 263$ N/mm

8.3.4 CALCULATE ISOLATOR DIAMETER AND RUBBER THICKNESS

To find the overall diameter of the isolator and the total rubber thickness, the procedure is as follows:

8.3.4.1 Calculate the bonded plan area, A_b, of the bearing (mm^2) per AASHTO 1998, article 14.7.5.3.2-1

8.3.4.2 Calculate the total thickness, T_r, of the rubber

8.3.4.1 Calculate the bonded plan area and diameter of the bearing

From AASHTO 1998, Art 14.7.5.3.2-1

$$A_b = \frac{P}{f_c} = \frac{517{,}000}{11} = 47{,}000\ mm^2$$

where P = total axial load (N)
and f_c = allowable compressive stress = 11.0 MPa (1.6 ksi)

The bonded diameter, d_b, of a rubber bearing with a central hole of diameter d_L for a lead core is given by:

$$d_b = \sqrt{\frac{4A_b}{\pi} + d_L^2}$$

Add the thickness of the rubber cover around the bearings to d_b to calculate the total diameter of the bearing as:

$d = d_b + 2$ cover (mm)

Pier Isolators:

$$d_b = \sqrt{\frac{4A_b}{\pi} + d_L^2} = \sqrt{\frac{4 \times 47000}{\pi} + 70^2} = 255\,mm$$

Use d_b = 340 mm (a larger diameter is chosen than minimum required to reduce possibility of instability at large horizontal displacements, see section 8.3.6)

$$A_b = \frac{\pi\left(d_b^2 - d_L^2\right)}{4} = \frac{\pi\left(340^2 - 70^2\right)}{4} = 86944\ mm^2$$

$d = d_b + 2$cover = 340 + (2 x 5) = 350 mm

Abutment Isolators:

$$A_b = \frac{P}{11} = \frac{223{,}000}{11} = 20273\,mm^2$$

$$d_b = \sqrt{\frac{4A_b}{\pi} + d_L^2} = \sqrt{\frac{4 \times 20273}{\pi} + 50^2} = 168\,mm$$

Use d_b = 240 mm (a larger diameter is chosen than minimum required to reduce the possibility of bearing instability at large horizontal displacements, see section 8.3.6)

$$A_b = \frac{\pi\left(d_b^2 - d_L^2\right)}{4} = \frac{\pi\left(240^2 - 50^2\right)}{4} = 43275\ mm^2$$

$d = d_b + 2$cover = 240 + (2 x 5) = 250 mm

8.3.4.2 Calculate the total thickness of the rubber

Total rubber thickness is given by

$$T_r = \frac{GA_b}{k_r}$$

Pier Isolators:

$$T_r = \frac{0.62 \times 86944}{263} = 205\ mm$$

To avoid the possibility of instability at large horizontal dispalcements under high axial loads, the slenderness of the bearing is reduced by limiting the rubber height to 150 mm.

Use T_r = 150 mm

Abutment Isolators:

$$T_r = \frac{0.62 \times 43275}{263} = 102\ mm$$

8.3.5 CALCULATE THICKNESS OF RUBBER LAYERS

Equations 6-15a and 6-15b are used to determine the shape factor that will satisfy the strain limits in equations 6-12, 6-13 and 6-14. The thickness of rubber layers will then be determined from the shape factor. The procedure is as follows:

8.3.5.1 Calculate A_r at design displacement using equations in figure 6-3
8.3.5.2 Calculate the required shape factor, S to satisfy limits on compression strain γ_c
8.3.5.3 Calculate the thickness of rubber layers

8.3.5.1 Calculate A_r at total design displacement

From figure 6-3:

$$A_r = \frac{d_b^2}{4}(\delta - \sin\delta)$$

where

$$\delta = 2\cos^{-1}\left(\frac{D_d}{d_b}\right)$$

Pier Isolators:

D_d = 66 mm
d_b = 340 mm

$$\delta = 2\cos^{-1}\left(\frac{D_d}{d_b}\right) = 2\cos^{-1}\left(\frac{66}{340}\right) = 2.751\ rad$$

$$A_r = \frac{d_b^2}{4}(\delta - \sin\delta) = \frac{340^2}{4}(2.751 - \sin 2.751) = 68{,}492\ mm^2$$

Abutment Isolators:

D_d = 66 mm
d_b = 240 mm

$$\delta = 2\cos^{-1}\left(\frac{D_d}{d_b}\right) = 2\cos^{-1}\left(\frac{66}{240}\right) = 2.584\ rad$$

$$A_r = \frac{d_b^2}{4}(\delta - \sin\delta) = \frac{240^2}{4}(2.584 - \sin 2.584) = 29{,}600\ mm^2$$

8.3.5.2 Calculate the required shape factor S, to satisfy limits on compression strain γ_c

The following equations are derived from equations 6-15a and 6-15b:

$$S = \frac{3P \pm \sqrt{9P^2 - 32(\gamma_c A_r G)^2 k'}}{8\gamma_c A_r G k'} \qquad \text{if } S \leq 15$$

$$S = \frac{\gamma_c A_r K}{12P} \pm \sqrt{\left(\frac{\gamma_c A_r K}{12P}\right)^2 - \frac{K}{8Gk'}} \qquad \text{if } S > 15$$

Also, from AASHTO 1998, equation 14.6.5.3.2.1:

$$S \geq \frac{P}{1.66GA_b}$$

Take γ_c = 2.0 (maximum shear strain due to compression, limit = 2.5, equation 6-12) and recall that (section 8.3):
K = 2000 MPa (bulk modulus)
K' = 0.73 (material constant)
G = 0.62 Mpa (shear modulus)

Pier Isolators:
A_b = 86,944
A_r = 68,492
P = 517,000 N

Assume S ≤ 15:

$$S = \frac{3P \pm \sqrt{9P^2 - 32(\gamma_c A_r G)^2 k'}}{8\gamma_c A_r G k'} = \frac{3\times 517000 \pm \sqrt{9\times 517000^2 - 32(2.0\times 68492x0.62)^2 \times 0.73}}{8\times 2.0\times 68492\times 0.62\times 0.73} = 6.14$$

$$S \geq \frac{P}{1.66GA} = \frac{517000}{1.66\times 0.62\times 86944} = 5.77$$

Minimum value for S is 6.14

Abutment Isolators:
A_b = 43,275
A_r = 29,600
P = 223,000 N

Assume S ≤ 15:

$$S = \frac{3P \pm \sqrt{9P^2 - 32(\gamma_c A_r G)^2 k'}}{8\gamma_c A_r G k'} = \frac{3\times 223000 \pm \sqrt{9\times 223000^2 - 32(2.0\times 29600x0.62)^2 \times 0.73}}{8\times 2.0\times 29600\times 0.62\times 0.73} = 6.13$$

$$S \geq \frac{P}{1.66GA} = \frac{223000}{1.66\times 0.62\times 43275} = 5.00$$

Minimum value for S is 6.13

8.3.5.3 Calculate the thickness of rubber layers

The maximum layer thickness is given by:

$$t_i = \frac{d^2 - d_L^2}{4dS}$$

Any thickness smaller than this value may be used, and still satisfy the minimum shape

factor values.

Pier Isolators:
Maximum layer thickness based on minimum required value for shape factor, S = 6.14

$$t_i = \frac{d^2 - d_L^2}{4dS} = \frac{350^2 - 70^2}{4 \times 350 \times 6.14} = 13.68\,mm$$

But to reduce possibility of instability at large horizontal displacements, a 6 mm layer thickness will be chosen. This will give a much higher layer shape factor and significantly improve the load capacity at large displacements (section 8.3.6).

Check that layer thickness is less than the maximum recommended thickness (9 mm) required for adequate confinement of the lead core (section 6.4). Ok

Hence use 24 layers of 6 mm thick rubber = 144 mm
For the top and bottom cover use 3 mm (total = 6 mm)

Total rubber thickness:
T_r = 150 mm

Abutment Isolators:
Maximum layer thickness based on minimum required value for shape factor, S = 6.13

$$t_i = \frac{d^2 - d_L^2}{4dS} = \frac{250^2 - 50^2}{4 \times 250 \times 6.13} = 9.79\,mm$$

For the same reason as the pier isolators, use 15 layers of 6 mm thick rubber = 90 mm
For the top and bottom cover layers use 3 mm (total = 6 mm)

Total rubber thickness:
T_r = 96 mm

8.3.6 CHECK ISOLATOR STABILITY

8.3.6.1 Calculate the critical buckling load, P_{cr}, of the bearing in the undeformed state using section 6.2.3.1.

8.3.6.2 Calculate the factor of safety against buckling instability

8.3.6.3 Calculate the critical buckling load, P'_{cr}, of the circular bearing in the deformed state (section 6.2.3.2) using equation 6-25.

8.3.6.4 Check isolator condition in deformed state as per section 4.9

8.3.6.1 Calculate the critical buckling load of the bearing in the undeformed state

Pier Isolators:
Using equations in section 6.2.3.1, the critical load, P_{cr}, in the undeformed state for a bearing with circular cross-section and 6 mm thick layers, is calculated as:

$$S = \frac{d^2 - d_L^2}{4dt_i} = \frac{350^2 - 70^2}{4 \times 340 \times 6} = 14$$

$$E_c = \frac{1}{\left(\frac{1}{6GS^2} + \frac{4}{3K}\right)} = \frac{1}{\left(\frac{1}{6 \times 0.62 \times 14^2} + \frac{4}{3 \times 2000}\right)} = 491\,MPa$$

$$I = \frac{\pi\left(d_b^4 - d_L^4\right)}{64} = \frac{\pi\left(340^4 - 70^4\right)}{64} = 654.8 \times 10^6\ mm^4$$

$$P_{cr} = \sqrt{\frac{\pi^2 E_c IGA}{3T_r^2}} = \sqrt{\frac{\pi^2 \times 491 \times 654.8 \times 10^6 \times 0.62 \times 86944}{3 \times 150^2}} = 1{,}591{,}874\ N$$

Abutment Isolators:

$$S = \frac{d^2 - d_L^2}{4dt_i} = \frac{250^2 - 50^2}{4 \times 250 \times 6} = 10$$

$$E_c = \frac{1}{\left(\frac{1}{6GS^2} + \frac{4}{3K}\right)} = \frac{1}{\left(\frac{1}{6 \times 0.62 \times 10^2} + \frac{4}{3 \times 2000}\right)} = 298\,MPa$$

$$I = \frac{\pi\left(d_b^4 - d_L^4\right)}{64} = \frac{\pi\left(240^4 - 50^4\right)}{64} = 162.6 \times 10^6\ mm^4$$

$$P_{cr} = \sqrt{\frac{\pi^2 E_c IGA}{3T_r^2}} = \sqrt{\frac{\pi^2 \times 298 \times 162.6 \times 10^6 \times 0.62 \times 43275}{3 \times 96^2}} = 681{,}241\ N$$

8.3.6.2 Calculate the factor of safety against buckling instability

FS = P_{cr}/P

where P is the total load due to dead load and live load

Check if FS > 3.0 per section 4.9. If not, revise the dimensions of the bearing

Pier Isolators:

FS = 1,591,874 / 517,000 = 3.08 > 3.0 OK.

Abutment Isolators:

FS = 681,241 / 223,000 = 3.06 > 3.0 OK.

8.3.6.3 Calculate the critical buckling load of the circular bearing in the deformed state

Since A=0.3g > 0.19g, the critical load must be calculated at a displacement equal to 1.5 D_d as per section 4.9.

Pier Isolators:

D_d = 66 mm

d_b = 340 mm

$$\delta = 2\cos^{-1}\left(\frac{1.5D_d}{d_b}\right) = 2\cos^{-1}\left(\frac{1.5 \times 66}{340}\right) = 2.551\,rad$$

$$A_r = \frac{d_b^2}{4}(\delta - \sin\delta) = \frac{340^2}{4}(2.551 - \sin 2.551) = 57{,}614\ mm^2$$

$$P'_{cr} = P_{cr}\frac{A_r}{A_b} = 1{,}591{,}874 \times \frac{57{,}614}{86{,}944} = 1{,}054{,}864\ N$$

Abutment Isolators:

D_d= 66 mm

d_b= 240 mm

$$\delta = 2\cos^{-1}\left(\frac{1.5D_d}{d_b}\right) = 2\cos^{-1}\left(\frac{1.5\times 66}{240}\right) = 2.291\ rad$$

$$A_r = \frac{d_b^2}{4}(\delta - \sin\delta) = \frac{240^2}{4}(2.291 - \sin 2.291) = 22{,}171\ mm^2$$

$$P'_{cr} = P_{cr}\frac{A_r}{A_b} = 681{,}241 \times \frac{22{,}171}{43{,}275} = 349{,}020\ N$$

8.3.6.4 Check isolator condition in deformed state per section 4.9

Since A = 0.3g > 0.19g, check if $P'_{cr} > 1.2P_D + P_{SL}$, at $1.5D_d$

Pier Isolators:

1,054,864 > 1.2 x 300,000 + 0 = 360,000 OK.

Abutment Isolators:

349,020 > 1.2 x 66,000 + 0 = 79,200 OK.

8.3.7 CHECK STRAIN LIMITS IN RUBBER

The procedure is as follows:

8.3.7.1 Calculate the maximum shear strain due to the effect of vertical loads using equation 6-15a or 6-15b.
8.3.7.2 Calculate the shear strain due to nonseismic lateral displacement using equation 6-17.
8.3.7.3 Calculate the shear strain due to seismic lateral design displacement using equation 6-18.
8.3.7.4 Calculate the shear strain due to design rotation, θ, using equation 6-19.
8.3.7.5 Check strain limits per equations 6-12, 6-13, and 6-14

8.3.7.1 Calculate the strain due to the effect of vertical loads

Using equation 6-15a for $S \leq 15$:

Pier Isolators:

$$\gamma_c = \frac{3SP}{2A_rG(1+2k'S^2)} = \frac{3\times 14\times 517{,}000}{2\times 68{,}492\times 0.62\times\left(1+2\times 0.73\times 14^2\right)} = 0.89$$

Abutment Isolators:

$$\gamma_c = \frac{3SP}{2A_r G(1+2k'S^2)} = \frac{3\times 10\times 223{,}000}{2\times 29{,}600\times 0.62\times\left(1+2\times 0.73\times 10^2\right)} = 1.24$$

8.3.7.2 Calculate the shear strain due to non-seismic lateral displacement

Pier Isolators:

The thermal expansion at Pier 1 (at 6400 mm from the centerline of the bridge) due to a thermal variation of 33°C is first calculated as:

$\Delta_s = \alpha \Delta T L$ = 10 x 10^{-6} x 33 x 6400 = 2.1 mm

The shear strain due to non-seismic lateral displacement is then calculated using equation 6-17:

$$\gamma_{s,s} = \frac{\Delta_s}{T_r} = \frac{2.1}{150} = 0.014$$

Abutment Isolators:

The thermal expansion at the abutments (at 16,200 mm from the centerline of the bridge) due to a thermal variation of 33°C is first calculated as:

$\Delta_s = \alpha \Delta T L$ = 10 x 10^{-6} x 33 x 16,200 = 5.4 mm

The shear strain due to non-seismic lateral displacement is then calculated using equation 6-17:

$$\gamma_{s,s} = \frac{\Delta_s}{T_r} = \frac{5.4}{96} = 0.056$$

8.3.7.3 Calculate the shear strain due to seismic lateral design displacement

Using equation 6-18:

Pier Isolators:

$$\gamma_{s,eq} = \frac{D_d}{T_r} = \frac{66}{150} = 0.44$$

Abutment Isolators:

$$\gamma_{s,eq} = \frac{D_d}{T_r} = \frac{66}{96} = 0.69$$

8.3.7.4 Calculate the shear strain due to design rotation

Using equation 6-19:

Pier Isolators:

$$\gamma_r = \frac{d_b^2\theta}{2t_i T_r} = \frac{340^2\times 0.00233}{2\times 6\times 150} = 0.15$$

Abutment Isolators:

$$\gamma_r = \frac{d_b^2\theta}{2t_i T_r} = \frac{240^2\times 0.00274}{2\times 6\times 96} = 0.14$$

8.3.7.5 Check strain limits per equations 6-12, 6-13 and 6-14

Pier Isolators:

$\gamma_c \leq 2.5$, 0.89 < 2.5, OK

$\gamma_c + \gamma_{s,s} + \gamma_r \leq 5.0$, 0.89 + 0.014 + 0.15 = 1.05 ≤ 5.0, OK

$\gamma_c + \gamma_{s,eq} + 0.5\gamma_r \leq 5.5$, 0.89 + 0.44 + (0.5 x 0.15) = 1.41 ≤ 5.5, OK

Abutment Isolators:

$\gamma_c \leq 2.5$, 1.24 < 2.5, OK

$\gamma_c + \gamma_{s,s} + \gamma_r \leq 5.0$, 1.24 + 0.056 + 0.14 = 1.44 ≤ 5.0, OK

$\gamma_c + \gamma_{s,eq} + 0.5\gamma_r \leq 5.5$, 1.24 + 0.69 + (0.5 x 0.14) = 2.00 ≤ 5.5, OK

8.3.8 CALCULATE REMAINING PROPERTIES AND SUMMARIZE

Pier Isolators:

Total height of pier isolator (excluding the anchor plates but including 25 x 1 mm thick internal shims) is 150 + (25 x 1) = 175 mm. Verify manufacturer can maintain tolerances with 1 mm plate, otherwise increase thickness to 2 or 3 mm.

Characteristic strength (seismic resistance):

$$Q_L = \frac{n-1}{n\psi} f_{yL} \frac{\pi d_{L\min}^2}{4} = \frac{9}{10} \times 11.4 \times \frac{\pi \times 70^2}{4} = 39{,}639\ N$$

Post-elastic stiffness:

$$k_d = \frac{f.GA_b}{T_r} = \frac{1.1 \times 0.62 \times 86{,}944}{150} = 395\ N/mm$$

Summary of properties of pier isolators:

Overall diameter, d = 350 mm
Bonded diameter, d_b = 340 mm
Total height, h = 175 mm
Total rubber thickness, T_r = 150 mm
Thickness of individual rubber layers, t_1 = 6 mm
Number of intermediate rubber layers, N_r = 24
Thickness of top and bottom rubber layers, t_c = 3 mm
Thickness of internal steel plates (shims), h_s = 1 mm
Number of internal steel plates (shims), N_s = 25
Characteristic strength (seismic resistance), Q = 39.64 kN
Post-elastic stiffness, k_d = 0.395 kN/mm

Abutment Isolators:
Total height of abutment isolator (excluding the anchor plates but including 16 x 1 mm thick internal shims) is 96 + (16 x 1) = 112 mm. Verify manufacturer can maintain tolerances with 1 mm plate, otherwise increase thickness to 2 or 3 mm.

Characteristic strength (seismic resistance):

$$Q_L = \frac{n-1}{n\psi} f_{yL} \frac{\pi d_{L\min}^2}{4} = \frac{9}{10} \times 11.4 \times \frac{\pi \times 50^2}{4} = 20{,}224\ N$$

Post-elastic stiffness:

$$k_d = \frac{f.GA_b}{T_r} = \frac{1.1 \times 0.62 \times 43{,}275}{96} = 308\ N/mm$$

Summary of properties of abutment isolators:
Overall diameter, d = 250 mm
Bonded diameter, d_b = 240 mm
Total height, h = 112 mm
Total rubber thickness, T_r = 96 mm
Thickness of individual rubber layers, t_1 = 6 mm
Number of intermediate rubber layers, N_r = 15
Thickness of top and bottom rubber layers, t_c = 3 mm
Thickness of internal steel plates (shims), h_s = 1 mm
Number of internal steel plates (shims), N_s = 16
Characteristic strength (seismic resistance), Q = 20.22 kN
Post-elastic stiffness, k_d = 0.308 kN/mm

8.3.9 CALCULATE SYSTEM PROPERTY ADJUSTMENT FACTORS

The minimum and maximum probable characteristic strength and post elastic stiffness for lead-plug rubber bearings need to be determined to account for the effect of loading history, temperature, aging, velocity, wear and scragging. The minimum properties will be used to determine the maximum isolator displacements and the maximum properties will be used to determine the loads transferred to the substructures. The steps are as follows:

8.3.9.1 Determine the initial lower and upper bound characteristic strength of the lead core, Q_L and Q_U respectively per section 6.5.4.
8.3.9.2 Obtain the system property modification factors: λ_t, λ_a, λ_v, λ_{tr} and λ_{sc} for the characteristic strength and post-elastic stiffness from section 6.6.
8.3.9.3 Obtain the system property adjustment factor, f_a per section 4.5.3 to account for the likelihood that the maximum properties do not occur at the same time.
8.3.9.4 Apply the system property adjustment factor to obtain adjusted system property modification factors (λ_{t1}, λ_{a1}, λ_{v1}, λ_{tr1} and λ_{sc1}) in accordance with equation 4-6.
8.3.9.5 Calculate the minimum and maximum system property modification factors as:
$\lambda_{min} = 1.0$
$\lambda_{max} = \lambda_{t1}\ \lambda_{a1}\ \lambda_{v1}\ \lambda_{tr1}\ \lambda_{c1}$

8.3.9.6 Calculate the minimum and maximum probable properties as:

$Q_{min} = \lambda_{min} Q_L$
$Q_{max} = \lambda_{max} Q_U$

$k_{d\text{-}min} = \lambda_{min} k_d$
$k_{d\text{-}max} = \lambda_{max} k_d$

8.3.9.1 Determine initial lower and upper bound yield strength of the lead core

Pier Isolators:

Q_L = 39,639 N
Q_U = 1.25 x 39,639 = 49,549 N

Abutment Isolators:

Q_L = 20,224 N
Q_U = 1.25 x 20,224 = 25,280 N

8.3.9.2 Obtain the system property modification factors (tables 4-3, 4-4 and 4-5)

For characteristic strength:

λ_t = 1.44 for a minimum temperature of -18°C at bridge location.
λ_a = 1.0 (Lead)
λ_{sc} = 1.0 (Low damping natural rubber bearing)

For post elastic stiffness:

λ_t = 1.18 for a minimum temperature of -18°C at bridge location.
λ_a = 1.1 (Low damping natural rubber bearing)
λ_{sc} = 1.0 (Low damping natural rubber bearing)

8.3.9.3 Obtain the system property adjustment factor

f_a = 0.66 for 'other' bridges (section 4.5.3)

8.3.9.4 Calculate the adjusted system property modification factors

For characteristic strength:

λ_{t1} = 1.0 + (1.44 - 1.0) x 0.66 = 1.290
λ_{a1} = 1.0
λ_{sc1} = 1.0

For post elastic stiffness:

λ_{t1} = 1.0 + (1.18 - 1.0) x 0.66 = 1.119
λ_{a1} = 1.0 + (1.1 - 1.0) x 0.66 = 1.066
λ_{sc1} = 1.0

8.3.9.5 Calculate the minimum and maximum system property modification factors

For characteristic strength:

λ_{min}= 1.0
λ_{max}= 1.290 x 1.0 x 1.0 =1.290

For post elastic stiffness:

λ_{min}= 1.0
λ_{max}= 1.119 x 1.066 x 1.0 =1.193

8.3.9.6 Calculate the minimum and maximum probable properties of the bearing

Pier Isolators:

Q_{min} = 1.0 x 39,639 = 39,639 N (39.6 kN)

Q_{max} = 1.29 x 49,549 = 63,912 N(63.9 kN)

$k_{d\text{-}min}$ = 1.0 x 359 = 359 N/mm (0.359 kN/mm)

$k_{d\text{-}max}$ = 1.193 x 359 = 428 N/mm (0.428 kN/mm)

Abutment Isolators:

Q_{min} = 1.0 x 20,224 = 20,224 N (20.2 kN)

Q_{max} = 1.29 x 25,280 = 32,611 N(32.6 kN)

$k_{d\text{-}min}$ = 1.0 x 280 = 280 N/mm (0.280 kN/mm)

$k_{d\text{-}max}$ = 1.193 x 280 = 333 N/mm (0.333 kN/mm)

8.3.10 MODELING OF THE ISOLATORS FOR STRUCTURAL ANALYSIS

The iterative multi-mode response spectrum method is used in the analysis of the bridge. A 3-dimensional structural model of the bridge is built and analyzed using the program SAP2000 (CSI 2002). Only the structural modeling of the bearings will be described here. Structural modeling of the complete bridge is outside the scope of this document, but detailed information can be found elsewhere (Dicleli and Mansour, 2003)

In the structural model, each bearing is modeled as an equivalent single 3-D fixed-ended beam element connected between the superstructure and substructure at the girder locations as shown in figure 8-7. The beam element is assigned section properties that match the calculated effective lateral stiffness of the bearing and other stiffness properties. The elastic and shear moduli for concrete (E_c = 28,000 MPa, G_c = 11,700 MPa) are taken as the moduli for these beam elements.

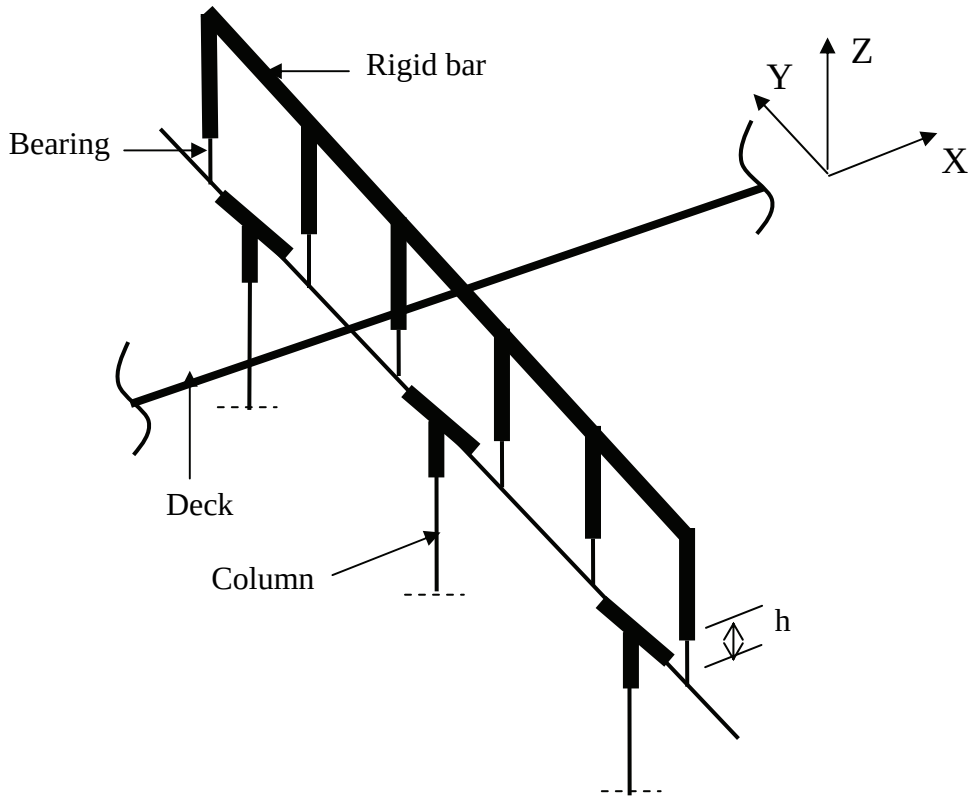

Figure 8-7. Structural Model of a Pier and Lead-rubber Bearings

First the vertical, k_v and torsional, k_T, stiffnesses of the lead-rubber bearings are calculated.

For the pier isolators,

$$k_v = \frac{E_c A_b}{T_r} = \frac{491 \times 86944}{150} = 284{,}597\ N/mm$$

$$J = \frac{\pi d^4}{32} = \frac{\pi 350^4}{32} = 1473 \times 10^6\ mm^4$$

$$k_T = \frac{GJ}{T_r} = \frac{0.62 \times 1473 \times 10^6}{150} = 6.09 \times 10^6\ N.mm/rad$$

For the abutment isolators,

$$k_v = \frac{E_c A_b}{T_r} = \frac{298 \times 43275}{96} = 134{,}333\ N/mm$$

$$J = \frac{\pi d^4}{32} = \frac{\pi 250^4}{32} = 384 \times 10^6\ mm^4$$

$$k_T = \frac{GJ}{T_r} = \frac{0.62 \times 384 \times 10^6}{96} = 2.48 \times 10^6 \ N.mm/rad$$

The stiffness properties of the lead-rubber bearings calculated above are then used to calculate the stiffness properties of the fixed-ended 3-D beam element used for representing the bearings.

Using the vertical stiffness, k_v, calculated above, the cross-sectional areas, A, of the beam elements at the piers and abutments are:

For the pier isolators:

$$A = \frac{k_v h}{E_c} = \frac{284{,}597 \times 174}{28{,}000} = 1769 \ mm^2$$

For the abutment isolators:

$$A = \frac{k_v h}{E_c} = \frac{134{,}333 \times 112}{28{,}000} = 537 \ mm^2$$

where h is the height of the bearing.

Using the torsional stiffness, k_T, calculated above, the polar moments of inertia, J, of the beam elements at the piers and abutments are :

For the pier isolators:

$$J = \frac{k_T h}{G_c} = \frac{6.09 \times 10^6 \times 174}{11{,}700} = 90569 \ mm^4$$

For the abutment isolators:

$$J = \frac{k_T h}{G_c} = \frac{2.48 \times 10^6 \times 112}{11{,}700} = 23740 \ mm^4$$

The moment of inertia, I_i, of the beam element representing bearing, i is:

$$I_i = \frac{k_{ei} h^3}{12 E_c}$$

where k_{ei} is the effective stiffness of bearing i. The calculated moment of inertia will be adjusted throughout the iterative multimode response spectrum analysis procedure as the effective stiffness changes, as explained in the following section.

8.3.11 STRUCTURAL ANALYSIS OF THE BRIDGE

Two series of iterative multimode response spectrum analyses of the bridge need to be performed to determine the seismic design displacements and substructure forces. The first analysis is performed using the minimum probable values for characteristic strength and post-elastic stiffness to estimate the required seismic displacement capacity of the bearings. The second analysis is performed using the maximum values for characteristic strength and post elastic stiffness to estimate the seismically induced forces in substructure members.

A seismically isolated bridge possesses vibration modes and periods associated with the movement of the seismic isolation system (isolated modes) and other structural members (structural modes). Five percent damping is assumed in the structural modes, and the calculated equivalent viscous damping ratio, β_e, is used in isolated modes to account for the hysteretic energy dissipated by the isolators. Accordingly, a hybrid design response spectrum is required with different levels of damping for the structural and isolated modes of vibration.

The hybrid spectrum used in this example is shown in figure 8-5. It was obtained by taking the AASHTO 1998, 1999 design spectra (which are calculated for 5% damping) and dividing the spectral values, at periods above 0.8 T_e, by the damping coefficient, B.

Using this hybrid design response spectrum, two series of iterative multimode response spectrum analyses of the bridge are performed to determine the seismic design displacements and substructure forces, as noted above. The first analysis is performed using Q_{min} and $k_{d\text{-}min}$, to estimate the required seismic displacement capacity of the bearings. The second analysis is performed using Q_{max} and $k_{d\text{-}max}$, to estimate the forces in substructure members. The analysis procedure is outlined below.

8.3.11.1 Assume a design displacement, D_{di} for each set of bearings over each support. In the absence of other information, use the calculated preliminary design displacement for all the bearings.

8.3.11.2 Calculate the effective stiffness, k_{ei}, of each bearing by substituting the bearing displacement D_{di}, the characteristic strength Q, and the post elastic stiffness k_d, of the bearing into equation 6-10. Thus:

$$k_e = \frac{Q}{D_d} + k_d$$

8.3.11.3 Neglecting the flexibility of the substructure, calculate the equivalent viscous damping ratio, β_e of the structure as:

$$\beta_e = \frac{2\sum_{i=1}^{n_b} Q_i (D_{di} - D_y)}{\pi \sum_{i=1}^{n_b} k_{ei} D_{di}^2}$$

where n_b is the number of isolation bearings and D_y is the yield displacement of the isolation bearing calculated using equation 6-9.

8.3.11.4 Calculate the damping coefficient B, corresponding to β_e from table 3-2.

8.3.11.5 Calculate the section properties of the beam element representing the bearings as outlined in section 8.3.10 and implement the calculated properties into the structural model.

8.3.11.6 Perform a dynamic analysis of the bridge to determine the mode shapes and vibration periods of the isolated bridge. Generally, the first two modes of vibration are associated with translation of the isolation system in both orthogonal directions of the bridge, and the third mode is associated with torsional motion of the superstructure about a vertical axis

8.3.11.7 Based on the periods of the isolated modes calculated in the previous step, define a new hybrid design spectrum that provides 5% damping for non-isolated 'structural' modes of vibration and a higher damping level for the isolated modes.

8.3.11.8 Perform the multi-mode response spectrum analysis of the bridge to obtain a new design displacement for each bearing. Compare the new design displacements with the initially assumed design displacements. If they are sufficiently close go to the next step. Otherwise, go to section 8.3.11.2 and repeat the above calculations using the new design displacements.

The analysis procedure is similar to that of the friction pendulum bearing example above and is not repeated here. Refer to section 8.2.6 for a description of the procedure.

8.4 SEISMIC ISOLATION DESIGN WITH ERADIQUAKE ISOLATORS

As with the previous examples, the isolation design of a bridge with Eradiquake (EQS) isolators primarily involves the determination of the properties of the isolators themselves. The following properties need to be determined to complete the design so that the bearings can be ordered from the manufacturer:

(1) Seismic and service coefficients of friction.
(2) Mass Energy Regulator (MER) size and quantity.
(3) Displacement capacity of the bearings.

The following information is taken from section 8.2:

A = 0.14 (acceleration coefficient)
S_1 = 1.5 (site coefficient for Type II soil, table 3-1)
W = 4,354 kN (total unfactored weight of bridge, section 8.2.1.4)
W_F = 3,757.6 kN (total factored weight of bridge, section 8.2.1.4)
D_T = 5.4 mm (total thermal expansion, section 8.2.7)

Abutments:
Number of bearings = 12 (6 per abutment)
PD = 70 kN per bearing
PL = 157 kN per bearing
Rotation = 0.02 radians per bearing

Piers:
Number of bearings = 12 (6 per pier)
PD = 310 kN per bearing
PL = 217 kN per bearing
Rotation = 0.02 radians per bearing

Total factored service load effects on superstructure:
FW = 271.3 kN (factored wind load, section 8.2.1.4)
FB = 170.6 kN (factored braking load, section 8.2.1.4)
FT = 250.0 kN (total factored horizontal load, section 8.2.1.4)

The isolation design procedure for the bridge is outlined below. It is based on a target isolator displacement and equivalent damping ratio.

8.4.1 Choose the service and seismic friction coefficients
8.4.2 Check if additional devices are required to resist service load effects
8.4.3 Calculate the minimum and maximum probable seismic friction coefficients
8.4.4 Determine the size and quantity of MER components
8.4.5 Determine the preliminary seismic design displacement
8.4.6 Model the isolation bearings for structural analysis
8.4.7 Perform the structural analysis of the bridge to determine the seismic design displacements and substructure forces using the minimum and maximum bearing properties
8.4.8 Calculate the required displacement capacity of the bearing including displacements due to thermal variations
8.4.9 Check the vertical load stability and rotation capacity of the bearings (not included as part of seismic isolation design)
8.4.10 Final EQS isolation bearing design values6

8.4.1 DETERMINE SERVICE AND SEISMIC FRICTION COEFFICIENTS

Using dry, unfilled PTFE mated with mirror finish stainless steel from the table below, based on the ratio of dead load to total vertical load on each bearing:

PD/PT	$\mu_{seismic}$	$\mu_{service}$
0.29	0.109	0.054
0.36	0.100	0.050
0.43	0.092	0.046
0.50	0.085	0.043
0.57	0.080	0.040
0.64	0.075	0.037
0.71	0.070	0.035
0.79	0.067	0.033
0.86	0.064	0.032
0.93	0.062	0.031

Abutments:
PD/PT = 70/227 = 0.3
Interpolate from table above, $\mu_{seismic}$ = 0.106, $\mu_{service}$ = 0.053

Piers:
PD/PT = 310/527 = 0.59
Interpolate from table above, $\mu_{seismic}$ = 0.078, $\mu_{service}$ = 0.039

8.4.2 CHECK IF ADDITIONAL DEVICES ARE REQUIRED TO RESIST SERVICE LOAD EFFECTS

Effective service load friction resistance of EQS bearings
= [12 x 0.053 + 12 x 0.039]/24 = 0.046

Total friction required to resist maximum wind forces without displacement across bearings:

FW/W_F = 271.3/3757.6 = 0.072

Since 0.072 > 0.046 wind locking devices are required at the bearings to prevent movement at the maximum wind force. As a cost effective alternative to wind locking devices, pre-compression of the MER's can be utilized allowing a small amount of displacement across the bearings at the maximum wind force.

Total friction required to resist maximum braking forces without displacement across bearings:

FB/W_F = 170.6/3757.6 = 0.045

Since 0.045 < 0.046 the chosen friction coefficients are sufficient to resist the maximum braking force.

8.4.3 CALCULATE THE MINIMUM AND MAXIMUM PROBABLE SEISMIC FRICTION COEFFICIENTS

Determine initial lower and upper bound friction coefficients (section 7.6.4):

Abutments:
$\mu_L = \mu_{seismic} = 0.106$
$\mu_U = 1.2\ \mu_{seismic} = 0.127$

Piers:
$\mu_L = \mu_{seismic} = 0.078$
$\mu_U = 1.2\ \mu_{seismic} = 0.094$

8.4.3.1 Obtain the system property modification factors (section 7.7)

λ_t = 1.2 for minimum air temperature of -18°C at bridge location
λ_a = 1.1
λ_v = 1.0 (to be verified by testing later)
λ_{tr} = 1.0
λ_c = 1.0 (sealed with stainless steel surface facing down)

8.4.3.2 Obtain the system property adjustment factor (section 4.5.3)

f_a = 0.66 for 'other bridges'

8.4.3.3 Calculate the adjusted system property modification factors

λ_{t1} = 1.0 + (0.2 x 0.66) = 1.132

$\lambda_{a1} = 1.0 + (0.1 \times 0.66) = 1.066$
$\lambda_{v1} = 1.0$
$\lambda_{tr1} = 1.0$
$\lambda_{c1} = 1.0$

8.4.3.3 Calculate the minimum and maximum system property modification factors

$\lambda_{min} = 1.0$
$\lambda_{max} = 1.132 \times 1.066 \times 1.0 \times 1.0 \times 1.0 = 1.207$

8.4.3.4 Calculate the minimum and maximum probably seismic friction coefficient

Abutments:
$\mu_{min} = \lambda_{min}\, \mu_L = 1.0 \times 0.106 = 0.106$
$\mu_{max} = \lambda_{max}\, \mu_U = 1.207 \times 0.127 = 0.153$

Piers:
$\mu_{min} = \lambda_{min}\, \mu_L = 1.0 \times 0.078 = 0.078$
$\mu_{max} = \lambda_{max}\, \mu_U = 1.207 \times 0.094 = 0.113$

8.4.4 DETERMINE THE SIZE AND NUMBER OF MER COMPONENTS

MER size and quantity are based on the recommended minimum restoring force recommendations of AASHTO 1999, as discussed in section 4.6.

Per section 4.6, to satisfy minimum restoring force requirements, $K_d > 0.025W/D_d$ where W is the total unfactored weight of the bridge.

Assume a target seismic displacement, D_d = 28 mm (iterate if necessary), and then
$K_d > 0.025 \times 4354/28 = 3.89$ kN/mm
K_d per bearing > 3.89/24 = 0.162 kN/mm

EQS bearings are typically manufactured with K_d = 0.53 to 1.59 kN/mm per MER. Typically there is one MER on each side of the bearing, four total per bearing. However, multiple MERs per side can be used as necessary, or omitted altogether.

Total K_d of 3.89 kN/mm is relatively low for this design, so increase total K_d to about 8.00 kN/mm to keep seismic displacements near initial estimate. Using K_d at 0.53 kN/mm per bearing, the number of bearings required with MERs = 8.00/0.53 = 15.1 bearings.

Use 16 bearings with MERs, K_d = 0.53 kN/mm, and the remaining 8 bearings will have only sliding surfaces (i.e., MERs will not be used in these bearings).

8.4.4.1 MER Size

MERs are polyurethane cylinders used in compression to act like a spring with stiffness K_r given by

$K_r = EA/L$

where E = compressive modulus = 41.4 MPa
A = cross-sectional area, and
L = length

Pre-compression of the MER is used to account for long term creep, provide ease of assembly, and resist service load movements. Including pre-compression, the post-elastic stiffness is given by:

$K_d = (1+ D_{pre}/D_d) K_r n$

where D_{pre} is the pre-compression displacement,
and n is the number of MERs on each side of the bearing.

Assume D_{pre} = 3 mm, n = 1 and solve for the MER stiffness K_r:

K_r = 0.53/[(1 + 3/28) x 1] = 0.479 kN/mm

The length L, is calculated based on strain limits. Recommended allowable compressive strains (ε) for polyurethane are as follows:

$\varepsilon_{seismic} \leq 0.40$, and $\varepsilon_{thermal} \leq 0.33$
Then
$L_{seismic} = D_d/0.40 = 28/0.40 = 70$ mm
$L_{thermal} = D_T/0.33 = 5.4/0.33 = 16.4$ mm

The minimum MER length is 70 mm + 6 mm pre compression = 76 mm.

The MER rides on a steel shaft inside the polyurethane cylinder. A minimum OD/ID ratio of 2.6 is required for proper performance. The cross-sectional area is given by:

$A = (\pi/4)(OD^2 - ID^2)$
where OD and ID are the outside and inside diameter of the MER cylinder.

Assuming the ID is 16 mm, the minimum OD = 2.6 x 16 = 41.6 mm.

$A = (\pi/4)(41.6^2 - 16^2) = 1158$ mm^2

Calculate the MER stiffness using the minimum length, 76 mm:

K_r = (41.4/1000) x 1158/76 = 0.631 kN/mm >> 0.479 kN/mm

The stiffness is too high, so increase the MER length to 100 mm:

K_r = (41.4/1000) x 1158/100 = 0.479 kN/mm ≈ 0.479 kN/mm … ok
K_d = (1 + 3/28) x 0.479 x 1 = 0.53 kN/mm

So the MER geometry is as follows:

OD = 41.6 mm
ID = 16 mm
L = 100 mm
D_{pre} = 3 mm
n = 1 per side of bearing

As discussed in section 4.6, AASHTO 1999 also requires that the restoring force be such that the period corresponding to the tangent stiffness of the isolation system (i.e., based on the restoring force alone) be less than 6 seconds.

Period using tangent stiffness, T_d $= 2\pi\sqrt{(W/K_d\, g)} = 2\pi\sqrt{(4354/0.53 \times 24 \times 9810)}$
$= 1.2$ sec < 6 sec ... ok

8.4.5 DETERMINE PRELIMINARY SEISMIC DESIGN DISPLACEMENT

A design displacement of 28 mm was assumed above when determining MER sizes. Use D_d = 28 mm again here with a uniform load analysis. Calculate the effective stiffness, k_{eff}, of the bearings:

Abutments:
with MERs -- $k_{eff} = Q_d/D_d + K_d = (\mu\, PD)/D_d + K_d = (0.106 \times 70)/28 + 0.53 = 0.795$ kN/mm
without MERs -- $k_{eff} = Q_d/D_d = (\mu\, PD)/D_d = (0.106 \times 70)/28 = 0.265$ kN/mm

Piers:
with MERs -- $k_{eff} = Q_d/D_d + K_d = (\mu\, PD)/D_d + K_d = (0.078 \times 310)/28 + 0.53 = 1.394$ kN/mm
without MERs -- $k_{eff} = Q_d/D_d = (\mu\, PD)/D_d = (0.078 \times 310)/28 = 0.864$ kN/mm

total $k_{eff} = 8 \times 0.795 + 4 \times 0.265 + 8 \times 1.394 + 4 \times 0.864 = 22.0$ kN/mm

Calculate the equivalent viscous damping:

total $Q_d = 12 \times 0.106 \times 70 + 12 \times 0.078 \times 310 = 379.2$ kN

$\beta = (2Q_dD_d)/(\pi D_d^2\, k_{eff}) = (2 \times 379.2 \times 28)/(\pi\, 28^2 \times 22.0) = 0.39$

A nonlinear time history analysis should be performed when the equivalent viscous damping is greater than 0.30. However, for this example, the equivalent viscous damping is conservatively taken as 0.30 and the uniform load method is used (section 3.2).

Calculate the effective isolated period of vibration:

$T_e = 2\pi\sqrt{(W/k_{eff}\, g)} = 2\pi\sqrt{(4354/22.0 \times 9810)} = 0.89$ sec

Calculate the new design displacement:
A = 0.14
S_1 = 1.5 (table 3-1, Type II)

B = 1.7 (table 3-2, β = 0.30)

$D_d = 250AS_1T_d/B = 250 \times 0.14 \times 1.5 \times 0.89/1.7 = 28$ mm ≈ 28 mm … ok

Comparing with the initial displacement estimate:

D_d = 28mm, no further iteration is required at this point. This can be used as the initial displacement in a more rigorous structural analysis that utilizes a method such as the multi-mode spectral analysis method.

8.4.6 MODEL THE ISOLATION BEARINGS FOR STRUCTURAL ANALYSIS

The modeling method is similar to that of the friction pendulum bearings and is not repeated here. Refer to section 8.2.5 for discussion on modeling isolation bearings.

8.4.7 STRUCTURAL ANALYSIS OF THE BRIDGE

The analysis procedure is similar to that of the friction pendulum bearings and is not repeated here. Refer to section 8.2.6 for description of the numerical procedure.

8.4.8 CALCULATE REQUIRED DISPLACEMENT CAPACITY OF ISOLATORS

The calculation method is similar to that of the friction pendulum bearings and is not repeated here. Refer to section 8.2.7 for details.

D_T = 5.4 mm (total thermal expansion)

The required displacement capacity of the EQS bearings is:
28 mm + 0.5 x 5.4 = 31 mm → use 32 mm.

8.4.9 CHECK STABILITY AND ROTATION CAPACITY OF ISOLATORS

Checking the vertical load stability and rotation capacity of the EQS bearings is beyond the scope of this document. However, EQS bearings tend to be low in profile leading to excellent stability. In addition, the vertical load and rotation element of an EQS bearing is an unconfined polyurethane disc which is able to accommodate rotations well beyond design values. With the bearing design values summarized below, the bearings can be ordered from the manufacturer.

8.4.10 FINAL EQS ISOLATION BEARING DESIGN VALUES

Abutments:
Nominal seismic coefficient of friction = 0.106
Upper bound seismic coefficient of friction = 0.127
Upper bound seismic coefficient of friction (modified for environmental effects) = 0.153
Piers:
Nominal seismic coefficient of friction = 0.078

Upper bound seismic coefficient of friction = 0.094
Upper bound seismic coefficient of friction (modified for environmental effects) = 0.113

MER Geometry:
OD = 41.6 mm
ID = 16 mm
L = 100 mm
D_{pre} = 3 mm
n = 1 per side of bearing
16 bearings with MERs, 8 bearings without MERs, arrange symmetrically throughout structure.
Displacement capacity = 32 mm
Wind locks required to resist transverse wind.
Stability not checked

CHAPTER 9: REFERENCES

AASHTO (1991) “Guide Specifications for Seismic Isolation Design”, American Association of State Highway and Transportation Officials, Washington, DC.

AASHTO (1998) “LRFD Bridge Design Specifications”, Second Edition, American Association of State Highway and Transportation Officials, Washington, DC.

AASHTO (1999 and 2000 Interim) “Guide Specifications for Seismic Isolation Design”, American Association of State Highway and Transportation Officials, Washington, DC.

AASHTO (2002) “Standard Specifications for Highway Bridges, Div I-A Seismic Design”, 17th Ed., American Association of State Highway and Transportation Officials, Washington, DC.

ASCE (2000) “Minimum Design Loads for Buildings and Other Structures”, Standard ASCE 7-98, American Society of Civil Engineers, Reston, Virginia.

ASME (1985) “Surface Texture (Surface Roughness, Waviness and Lay)”, ANSI/ASME B46.1-1985, American Society of Mechanical Engineers, New York.

ATC (1995) “Structural Response Modification Factors”, Report No. ATC-19, Applied Technology Council, Redwood City, California.

BSI (1979) “Commentary on Corrosion at Bi-metallic Contacts and Its Alleviation,” BSI Standard PD 6484, Confirmed March 1990, British Standards Institution, London.

Buckle, I.G. and Mayes, R.L. (1990) “Seismic Retrofit of Bridges Using Mechanical Energy Dissipators”, Proc. Fourth U.S. National Conference on Earthquake Engineering, Vol. 3, Earthquake Engineering Research Institute, Oakland, CA, pp 305-314.

Buckle, I.G., and Liu, H. (1994) “Critical Loads of Elastomeric Isolators at High Shear Strain”, Proc. 3rd US-Japan Workshop on Earthquake Protective Systems for Bridges”, Report NCEER-94-0009, National Center for Earthquake Engineering Research, Buffalo, NY.

Building Seismic Safety Council-BSCC (2001) “NEHRP Recommended Provisions for Seismic Regulations for New Buildings and Other Structures”, 2000 Edition Report Nos. FEMA 368 and 369, Federal Emergency Management Agency, Washington, DC.

Civil Engineering Research Center-CERC (1992) “Temporal Manual of Design Method for Base-Isolated Highway Bridges”, Japan (in Japanese).

Constantinou, M.C. (1998) “Application of Seismic Isolation Systems in Greece”, Proceedings of ’98 Structural Engineers World Congress, Paper T175-3, San Francisco, CA.

Constantinou, M.C., Mokha, A. and Reinhorn, A.M. (1990) “Teflon Bearings in Base Isolation II: Modeling,” Journal of Structural Engineering, ASCE, Vol. 116, No. 2, pp. 455-474.

Constantinou, M.C. and Quarshie, J.K. (1998) "Response Modification Factors For Seismically Isolated Bridges", Report No. MCEER-98-0014, Multidisciplinary Center for Earthquake Engineering Research, Buffalo, NY.

Constantinou, M.C., Tsopelas, P., Kasalanati, A. and Wolff, E.D. (1999) “Property Modification Factors for Seismic Isolation Bearings”, Report No. MCEER-99-0012, Multidisciplinary Center for Earthquake Engineering Research, Buffalo, NY.

CSI (2002) “SAP2000: Structural Analysis Program,” Computers & Structures Inc, Berkeley CA.

Dicleli, M. and Mansour, M. (2003) “Seismic Retrofitting of Highway Bridges in Illinois Using Friction Pendulum Seismic Isolation Bearings and Modeling Procedures”, Engineering Structures, Elsevier Science, Vol. 25, No. 9, pp 1139-1156.

European Committee for Standardization (2000) “Structural Bearings”, European Standard EN 1337-1, Brussels.

Federal Emergency Management Agency (1997) “NEHRP Guidelines and Commentary for the Seismic Rehabilitation of Building,” Reports FEMA 273 and FEMA 274, Washington, D.C.

Federal Emergency Management Agency (2001) “NEHRP Recommended Provisions for Seismic Regulations for New Buildings and Other Structures, 2000 Edition, Part 1: Provisions and Part 2: Commentary,” Reports FEMA 368 and 369, Washington, D.C.

HITEC (1996) “Guidelines for the Testing of Seismic Isolation and Energy Dissipation Devices,” CERF Report HITEC 96-02, Highway Innovative Technology Evaluation Center, Washington, D.C.

HITEC (2002) “Guidelines for the Testing of Large Seismic Isolator and Energy Dissipation Devices,” CERF Report 40600, Highway Innovative Technology Evaluation Center, Washington, D.C.

Imbsen, R.A. (2001) “Use of Isolation for Seismic Retrofitting Bridges,” Journal of Bridge Engineering, Vol. 6, No. 6, 425-438.

International Code Council (2000) “International Building Code”, Falls Church, Virginia.

Lindley, P.B. (1978) “ Engineering Design with Natural Rubber”, Malaysia Rubber Producers Research Association, now Tun Abdul Razak Laboratory, Hertford, England, 48pp.

Makris, N., Y. Roussos, A. S. Whittaker, and J. M. Kelly (1998) “Viscous Heating of Fluid Dampers II: Large-Amplitude Motions,” J. of Eng. Mechanics, ASCE, Vol. 124, No. 11.

Marioni, A. (1997) “Development of a New Type of Hysteretic Damper for the Seismic Protection of Bridges,” Proc. Fourth World Congress on Joint Sealants and Bearing Systems for Concrete Structures, SP-1-164, Vol. 2, American Concrete Institute, 955-976.

Miranda, E., Bertero, V.V. (1994) “Evaluation of Strength Reduction Factors for Earthquake-Resistant Design”, Earthquake Spectra, 10 (2), pp. 357-379.

Naeim, F. and Kelly, J.M. (1999) “Design of Seismic Isolated Structures”, J. Wiley & Sons, New York, NY.

Roeder, C.W., Stanton, J.F. and Campbell, T.I. (1995) “Rotation of High Load Multirotational Bridge Bearings”, Journal of Structural Engineering, ASCE, Vol. 121, No. 4, pp. 746-756.

Roeder, C.W., Stanton, J.F., and Taylor, A.W. (1987) “Performance of Elastomeric Bearings”, Report No. 298, National Cooperative Highway Research Program, Transportation Research Board, Washington, D.C.

Rojahn, C., Mayes, R., Anderson, D.G., Clark, J., Hom, J.H., Nutt, R.V., O’Rourke, M.J. (1997) “Seismic Design Criteria for Bridges and Other Highway Structures”, Technical Report NCEER-97-0002, National Center for Earthquake Engineering Research, Buffalo, NY.

Roussis, P.C., Constantinou, M.C., Erdik, M., Durukal, E. and Dicleli, M. (2002) “Assessment of Performance of Bolu Viaduct in the 1999 Duzce Earthquake in Turkey”, MCEER-02-0001, Multidisciplinary Center for Earthquake Engineering Research, Buffalo, NY.

Skinner, R.I. Robinson, W.H., and McVerry, G.H. (1993) “An Introduction to Seismic Isolation”, J. Wiley, Chichester, UK.

Sugita, H. and Mahin, S.A. (1994) “Manual for Menshin Design of Highway Bridges: Ministry of Construction, Japan”, Report No. UCB/FERC-94/10, Earthquake Engineering Research Center, University of California Berkeley.

Thompson, A.C.T., Whittaker, A.S., Fenves, G.L. and Mahin, S.A. (2000) “Property Modification Factors for Elastomeric Seismic Isolation Bearings”, Proc. 12th World Conference on Earthquake Engineering, New Zealand.

Tsopelas, P. and Constantinou, M.C., (1997) “Study of Elastoplastic Bridge Seismic Isolation System”, Journal of Structural Engineering, ASCE, 123 (4) pp 489-498.

Uang, Chia-Ming (1991) “Establishing R (or R_W) and C_d Factors for Building Seismic Provisions”, Journal of Structural Engineering, ASCE, 117 (1) pp 19-28.

Uang, Chia-Ming (1993) “An Evaluation of Two-Level Seismic Design Procedure”, Earthquake Spectra, 9 (1), pp. 121-135.

Warn, G. and Whittaker, A. S. (2002) “Performance Estimates in Seismically Isolated Bridges,” Proceedings, 4th US-China-Japan Conference on Lifeline Earthquake Engineering, Qingdao, PRC, October.

Wood, L.A., and Martin, G.M. (1964) “Compressibility of Natural Rubber at Pressures Below 500 kg/cm^2 ”, Rubber Chemistry and Technology, 37, pp 850-856.

APPENDIX A: LIST OF SEISMICALLY ISOLATED BRIDGES IN NORTH AMERICA

Listed below are highway bridges in North America (United States, Canada, Mexico and Puerto Rico) known to use seismic isolation for earthquake protection. Bridges are listed chronologically by state, province, or country (MX = Mexico). Discussion of this data is given section 2.

This list is based on material first assembled by Ian Aiken[1] and Andrew Whittaker[2] in 1995, and updated in May 2002 and again in April 2003 by Ian Buckle[3], with assistance from Steve Bowman[4], Greg Lawson[5], Anoop Mokha[6], and Ron Watson[7]. Although care has been taken when compiling this list, it is not necessarily complete. When data is uncertain or unknown, the entry has been left blank. Only completed bridges as of April 2003 are included in this list. Bridges under bid, or being constructed, are excluded. Abbreviations are defined at the end of the table.

BRIDGE	DATE	LOCATION		OWNER	ISOLATORS
Kodiak-Near Island Bridge		AK	Kodiak Island	AKDOT	FPS (EPS)
Dog River Bridge	**1992**	AL	Mobile Co.	Alabama Highway Dept.	LRB (DIS)
Fortuna Railroad Overpass	**1998**	AZ	Yuma, AZ	AZDOT	EQS (RJW)
Hwy 99 / Deas Slough Bridge	**1990**	BC	Richmond	British Columbia Ministry of Transportation and Highways	LRB (DIS)
Burrard St / False Creek	**1993**	BC	Vancouver	City of Vancouver	LRB (DIS)
Queensborough Bridge / Nth Arm Fraser River	**1994**	BC	New Westminster	British Columbia Ministry of Transportation and Highways	LRB (DIS)
Granville Bridge	**1996**	BC	Vancouver	-	FIP
Roberts Park Overhead / BC Rail	**1997**	BC	Vancouver	Vancouver Port Corp.	LRB (DIS)

[1] Seismic Isolation Engineering, Oakland CA
[2] University at Buffalo, Buffalo NY
[3] University of Nevada Reno, Reno NV
[4] Seismic Energy Products, Athens TX and Alameda CA
[5] Dynamic Isolation Systems, Lafayette CA and Sparks NV
[6] Earthquake Protection Systems, Richmond CA
[7] R.J. Watson, Buffalo NY

Second Narrows Bridge	**1998**	BC	Vancouver	British Columbia Ministry of Transportation and Highways	LRB (DIS)
Tamarac Bridge #3090	**1998**	BC	Vancouver	British Columbia Ministry of Transportation and Highways	LRB (SEP)
Lions Gate Bridge	**2000**	BC	Vancouver	British Columbia Ministry of Transportation and Highways	LRB (DIS)
White River Bridge	**1997**	YU	Yukon	Government of the Yukon	FPS (EPS)
US 101 Sierra Point Overhead	**1985**	CA	South San Francisco	Caltrans	LRB (DIS)
Santa Ana River Bridge	**1986**	CA	Riverside	Metropolitan Water District of Southern California	LRB (DIS)
US 101 / Eel River Bridge	**1987**	CA	Rio Dell	Caltrans	LRB (DIS)
Main Yard Vehicle Access Bridge, Long Beach Freeway	**1987**	CA	Long Beach	Los Angeles County Metropolitan Transportation Agency	LRB (DIS)
I-8 / All-American Canal Bridge	**1988**	CA	Winterhaven, Imperial Co.	Caltrans	LRB (DIS)
23rd St / Carlson Blvd Bridge	**1992**	CA	Richmond	City of Richmond	LRB (DIS)
SR 24 / I-680 Olympic Boulevard Separation	**1993**	CA	Walnut Creek	Caltrans	LRB (DIS)
I-280 / US 101 Alemany IC	**1994**	CA	San Francisco	Caltrans	LRB (DIS)
SR 242 SB / I-680 Separation	**1994**	CA	Concord	Caltrans	LRB (DIS)
US 101 / Bayshore Blvd	**1994**	CA	San Francisco	Caltrans	LRB (DIS)
1st Street / Figuero	**1995**	CA	Los Angeles	City of Los Angeles	LRB (DIS)
Colfax Avenue / L.A. River	**1995**	CA	Los Angeles	City of Los Angeles	LRB (DIS)
Chapman Avenue Bridge	**1997**	CA	Laguna Beach	-	LRB (DIS)
3-Mile Slough Bridge	**1997**	CA	-	Caltrans	LRB (Skellerup)
Rio Hondo Busway Bridge	**1997**	CA	El Monte	Caltrans	FPS (EPS)
American River Bridge	**1997**	CA	Lake Natoma, Folsom	City of Folsom	FPS (EPS)

Golden Gate Bridge North Viaduct	**1997**	CA	San Francisco	Golden Gate Bridge Hway Transportation District	LRB (DIS)
Atlantic Boulevard	**1998**	CA	Los Angeles	City of Los Angeles	LRB (DIS)
Benicia-Martinez Bridge	**1998**	CA	Carquinez Straits, San Francisco Bay	Caltrans	FPS (EPS)
Rte 242 / I-680 Separation	**1999**	CA	Concord	Caltrans	LRB (DIS)
Carquinez Bridge	**1999**	CA	Contra Costa / Solano Counties	Caltrans	NRB (SEP)
Coronado Bridge	**2000**	CA	San Diego Bay	Caltrans	LRB (DIS)
Rio Vista Bridge	**2000**	CA	Rio Vista Sacramento River	Caltrans	LRB (DIS)
Richmond-San Rafael Bridge	**2001**	CA	Richmond	Caltrans	LRB (DIS)
Golden Gate Bridge South Approach	**2001**	CA	San Francisco	Golden Gate Bridge Hway Transportation District	LRB (SEP)
North Fork Feather River	**2002**	CA	Tobin	Caltrans	LRB (DIS)
Mococo Overhead	**2002**	CA	Martinez	Caltrans	LRB (DIS)
Bayshore Blvd Expansion	**2002**	CA	San Francisco	City and County Of San Francisco	LRB (DIS)
I-95 / Saugatuck River Bridge	**1994**	CT	Westport	Conn DOT	LRB (DIS)
I-95 / Lake Saltonstall Bridge	**1994**	CT	E. Haven & Branford	Conn DOT	LRB (DIS)
Rte 15 Viaduct	**1996**	CT	Hamden	Conn DOT	EQS (RJW)
I-95/Yellow Mill Channel	**1997**	CT	Bridgeport	Conn DOT	LRB (SEP)
I-95/Metro North RR	**1997**	CT	Greenwich	Conn DOT	LRB (SEP)
I-95 / Rte 8&25 / Yellow Mill	**1998**	CT	Bridgeport	Conn DOT	LRB (SEP)
SR 661 / Willimantic River	**1999**	CT	Windham	Conn DOT	LRB (SEP)
I-95 at Bridgeport	**2001**	CT	Bridgeport	Conn DOT	LRB & NRB (SEP)
Church St South Extension	**2001**	CT	New Haven	Conn DOT	LRB (SEP)

SR 3 / Sexton Creek Bridge	**1990**	IL	Alexander Co.	ILDOT	LRB (DIS)
SR 3 / Cache River Bridge	**1991**	IL	Alexander Co.	ILDOT	LRB (DIS)
SR 161/ Dutch Hollow Bridge	**1991**	IL	St. Clair Co.	ILDOT	LRB (DIS)
I-55/70/64 Poplar St East Approach, Bridge #082-0005	**1992**	IL	East St. Louis	ILDOT	LRB (DIS)
Chain-of-Rocks Rd / FAP 310	**1994**	IL	Madison Co.	ILDOT	LRB (DIS)
Poplar Street East Approach Roadway B	**1994**	IL	East St. Louis	ILDOT	LRB (DIS)
Poplar Street East Approach Roadway C	**1995**	IL	East St. Louis	ILDOT	LRB (DIS)
St. Clair County	**1996**	IL	Freeburg	ILDOT	EQS (RJW)
Rte 13 Bridge	**1996**	IL	Near Freeburg	ILDOT	EQS (RJW)
Damen Ave. Bridge	**1998**	IL	Chicago	City of Chicago	EQS (RJW)
FAI Rte 70.Sec 82-(1,4) R5#70	**1999**	IL	St Clair Co.	ILDOT	LRB (SEP)
FAI Rte 70.Sec 82-(1,4) R6#71	**1999**	IL	St Clair Co.	ILDOT	LRB (SEP)
FAI Rte 70.Sec 82-5HB R#102	**1999**	IL	St Clair Co.	ILDOT	LRB (SEP)
FAI Rte. 57 over Rte 3	**2002**	IL	Alexander Co.	ILDOT	EQS (RJW)
US 40 / Wabash River Bridge	**1991**	IN	Terra Haute, Vigo Co.	INDOT	LRB (DIS)
RT 41 / Pigeon Creek	**1993**	IN	Evanville	INDOT	EQS (RJW)
US 51 / Minor Slough	**1992**	KY	Ballard Co.	KTC	LRB (DIS)
I-75 / Kentucky R. Bridge	**1995**	KY	Clays Ferry	KTC	LRB (DIS)
US 51 / Willow Slough	**1997**	KY	Ballard Co.	KTC	LRB & NRB (SEP)
KY 51 / Green River	**1998**	KY	McLean Co.	KTC	LRB & NRB (SEP)
SR 1 / Main Street Bridge	**1993**	MA	Saugus	Mass Hwy Department	LRB (DIS)

New Old Colony RR / Neponset River Bridge	**1994**	MA	Boston / Quincy	MBTA	LRB (DIS)
So. Boston Bypass Viaduct	**1994**	MA	South Boston	MHDCATP	LRB (DIS)
South Station Connector	**1994**	MA	Boston	MBTA	LRB (DIS)
Rte 6 / Acushnet River Swing Bridge	**1994**	MA	New Bedford-Fairhaven	Mass Hwy Department	EQS (RJW)
North Street Bridge No. K-26	**1995**	MA	Grafton	Mass Turnpike Authority	LRB (DIS)
Old Westborough Road Bridge No. K-27	**1995**	MA	Grafton	Mass Turnpike Authority	LRB (DIS)
Summer Street / Fort Point Channel Bridge	**1995**	MA	Boston	Mass Hwy Department	LRB (DIS)
I-93 / West Street	**1995**	MA	Wilmington	Mass Hwy Department	LRB (DIS)
Park Hill Ave. Rte. 20 / Mass. Pike (I-90)	**1995**	MA	Millbury	Mass Turnpike Authority	EQS (RJW)
Rte 6 Swing Bridge	**1995**	MA	New Bedford	Mass Hwy Department	EQS (RJW)
Mass Pike (I-90) Fuller & North Sts.	**1996**	MA	Ludlow	Mass Turnpike Authority	EQS (RJW)
Endicott Street / Rt.128 (I-95)	**1996**	MA	Danvers	Mass Hwy Department	EQS (RJW)
I-93 / I-90 Central Artery	**1996**	MA	South Boston	Mass Hwy Department	HDR (SEP)
Holyoke / Conn. R. / Canal St	**1996**	MA	South Hadley	Mass Hwy Department	LRB & NRB (SEP)
Aiken St / Merrimack River	**1997**	MA	Lowell	Mass Hwy Department	LRB (SEP)
Rte 112 / Westfield River	**1999**	MA	Huntington	Mass Hwy Department	LRB (SEP)
I-495 / Marston Bridge	**2001**	MA	Lawrence – North Andover	Mass Hwy Department	LRB (SEP)
School St Bridge	**2001**	MA	Lowell	Mass Hwy Department	LRB (SEP)
Calvin Coolidge Bridge	**2001**	MA	Northampton	Mass Hwy Department	LRB (DIS)
Metrolink Light Rail NB I-170	**1991**	MO	St. Louis	BSDA	LRB (DIS)
Metrolink Light Rail Ramp 26	**1991**	MO	St. Louis	BSDA	LRB (DIS)

Metrolink LR. Springdale New	**1991**	MO	St. Louis	BSDA	LRB (DIS)
Metrolink Light Rail SB I-170/EB I-70	**1991**	MO	St. Louis	BSDA	LRB (DIS)
Metrolink LR. UMSL Bridge	**1991**	MO	St. Louis	BSDA	LRB (DIS)
Metrolink Light Rail East Campus Drive Bridge	**1991**	MO	St. Louis	BSDA	LRB (DIS)
Metrolink Light Rail Geiger Rd Bridge	**1991**	MO	St. Louis	BSDA	LRB (DIS)
I-70 / 3rd Street	**1997**	MO	East St. Louis	MODOT	LRB (DIS)
E. Missoula / Bonner Bridge IM 90-(94)107, IM 90-2(95)110	**1998**	MO	Missoula	MODOT	EQS (RJW)
Eads Bridge	**1999**	MO	St Louis	City of St Louis Board of Public Service	LRB (SEP)
Kootenai River / Libby	**1999**	MT	Lincoln Co.	MTDOT	LRB (SEP)
Hidalgo-San Rafael Distributor	**1995**	MX	North Mexico City	MTB	LRB (DIS)
Infiernillo V Bridge	**2002**	MX	Michoacan State	Ministry of Communication and Transportation	EQS (RJW)
I-26 / Big Laurel Creek	**1999**	NC	Madison Co.	NCDOT	LRB & NRB (SEP)
US 176 / Green River	**1999**	NC	Henderson Co.	NCDOT	NRB (SEP)
Relocated NH Route 85 / 101	**1992**	NH	Exeter-Stratham, Rockingham Co.	NHDOT	LRB (DIS)
US 3 / Nashua River & Canal	**1994**	NH	Nashua	NHDOT	EQS (RJW)
NH 101 / Squamscott River Bridge	**1992**	NH	Exeter	NHDOT	LRB (DIS)
New Hampshire Route 85	**1993**	NH	Exeter-Stratham	NHDOT	LRB (DIS)
US 3 / Canal & River Bridges	**1994**	NH	Nashua	NHDOT	EQS (RJW)
Squamscott II	**1995**	NH	Exeter	NHDOT	LRB (DIS)
I-93 at Derby	**1997**	NH	Town of Derry	NHDOT	EQS (RJW)
I-93 / Fordway Ext.	**1997**	NH	Derry	NHDOT	EQS (RJW)

NH 3A / Sagamore Road	**1999**	NH	Nashua-Hudson	NHDOT	EQS (RJW)
Amoskeag Bridge	**1999**	NH	Manchester	City of Manchester	EQS (RJW)
US 3 / Broad Street	**1999**	NH	Nashua	NHDOT	EQS (RJW)
I-93 NB & SB	**2000**	NH	Manchester	NHDOT	EQS (RJW)
I-293 / Frontage Road	**2002**	NH	Manchester	NHDOT	EQS (RJW)
Portsmouth Naval Shipyard	**2002**	NH	Portsmounth	U.S. Navy	LRB (DIS)
I-287 / Pequannock R. Bridge	**1991**	NJ	Morris & Passaic Co.	NJDOT	LRB (DIS)
Foundry Street Overpass 106.68	**1993**	NJ	Newark	NJ Turnpike Authority	LRB (DIS)
Conrail Newark Branch Overpass E106.57	**1994**	NJ	Newark	NJ Turnpike Authority	LRB (DIS)
Wilson Avenue Overpass E105.79SO	**1994**	NJ	Newark	NJ Turnpike Authority	LRB (DIS)
E-NSO Overpass W106.26A	**1994**	NJ	Newark	NJ Turnpike Authority	LRB (DIS)
Rte 3 / Berry's Creek Bridge	**1995**	NJ	East Rutherford	NJ Turnpike Authority	LRB (Furon)
Conrail Newark Branch Overpass W106.57	**1995**	NJ	Newark	NJ Turnpike Authority	LRB (DIS)
Norton House Bridge	**1996**	NJ	Pompton Lakes Borough and Wayne Township, Passaic Co.	NJDOT	LRB (DIS)
Tacony-Palmyra Approaches	**1996**	NJ	Palmyra	Burlington County Bridge Commission	LRB (SEP)
Rt. 4 / Kinderkamack Rd	**1996**	NJ	Hackensack	NJDOT	LRB & NRB (SEP)
Baldwin St / Highland Ave/ Conrail	**1996**	NJ	Glen Ridge	NJDOT	LRB & NRB (SEP)
Main St / Passaic River	**1998**	NJ	Paterson	City of Paterson	LRB (SEP)
Rte 120 Pedestrian Bridge	**1999**	NJ	East Rutherford	NJ Sports and Exposition Authority	LRB (SEP)
Light Rail Transit Newport Viaduct (Flying Wye)	**1999**	NJ	Jersey City	NJ Transit	LRB (DIS)
Light Rail Transit Newport Viaduct (Area 3)	**1999**	NJ	Jersey City	NJ Transit	LRB (SEP)

East Ridgewood Ave / Rte 17	**2000**	NJ	New Jersey	NJ DOT	EQS (RJW)
Newark Airport Bridge N14 EWR 154.206	**2001**	NJ	Newark Airport	Port Authority of New York and New Jersey	EQS (RJW)
Rt 17 / Vreeland / Green / Pollifly	**2001**	NJ	Hackensack	NJDOT	LRB (SEP)
Hamilton Ave Station Pedestrian Bridge	**2001**	NJ	Trenton	NJ Transit	LRB (SEP)
Rte. 46 / Riverview Drive	**2002**	NJ	New Jersey	NJDOT	EQS (RJW)
Trumbull Street	**2002**	NJ	Elizabeth	NJDOT	LRB (DIS)
I-80 East / Green Street	**2002**	NJ	Hackensack	NJDOT	LRB (DIS)
I-80 / Truckee River Bridges B764E & W	**1992**	NV	Verdi	NDOT	LRB (DIS)
I-95 / West Street Overpass	**1991**	NY	Harrison	New York State Thruway Authority	LRB (DIS)
Aurora Expressway / Cazenovia Creek Bridge	**1993**	NY	Erie Co.	NYDOT	LRB (DIS)
Mohawk R & Conrail Bridge	**1993**	NY	Herkimer	New York State Thruway Authority	LRB (DIS)
Mohawk River Bridge	**1994**	NY	Herkimer	New York State Thruway Authority	LRB (DIS)
Moodna Creek Bridge	**1994**	NY	Orange Co.	New York State Thruway Authority	LRB (DIS)
Conrail Bridge	**1994**	NY	Herkimer	New York State Thruway Authority	LRB (DIS)
I-95 / Maxwell Ave	**1995**	NY	Rye	New York State Thruway Authority	EQS (RJW)
Maxwell Ave. Ramp over New England Thruway	**1996**	NY	-	New York State Thruway Authority	EQS (RJW)
John F. Kennedy Airport Terminal 1 Elevated Roadway	**1996**	NY	John F. Kennedy Airport	Port Authority of New York and New Jersey	LRB (DIS)
Buffalo Airport Viaduct	**1996**	NY	Buffalo-Niagara Intl Airport	Niagara Frontier Transportation Authority	EQS (RJW)
Yonkers Avenue Bridge	**1997**	NY	Yonkers Bronx River Parkway	NYDOT	EQS (RJW)
Buffalo-Niagara Intl Airport Departure Ramp	**1997**	NY	Buffalo-Niagara Intl Airport	Niagara Frontier Transportation Authority	EQS (RJW)
I-90 / Normanskill Creek	**1997**	NY	Albany Co.	New York State Thruway Authority	LRB (SEP)

Rte 9W / Washington St		NY	Rockland Co.	NYDOT	LRB & NRB (SEP)
I-87 / Sawmill R. Parkway	**2000**	NY	Westchester Co.	New York State Thruway Authority	LRB (SEP)
John F. Kennedy Airport Departure Ramp Terminal 4	**2000**	NY	John F. Kennedy Airport	Port Authority of New York and New Jersey	EQS (RJW)
John F. Kennedy Airport Arrival/ Departure Ramps Terminal 4	**2000**	NY	John F. Kennedy Airport	Port Authority of New York and New Jersey	EQS (RJW)
John F. Kennedy Airport Light Rail Viaduct	**2000**	NY	New York City	Port Authority of New York and New Jersey	LRB (DIS)
Kingston-Rhinecliff Bridge	**2000**	NY	New York State	NYS Bridge Authority	EQS (RJW)
John F. Kennedy Airport British Airways Terminal 7	**2001**	NY	John F. Kennedy Airport	Port Authority of New York and New Jersey	EQS (RJW)
American Airlines Terminal Access Ramps	**2001**	NY	John F. Kennedy Airport	American Airlines / Port Authority	LRB (DIS)
Stutson St / Genesee River	**2001**	NY	City of Rochester	Monroe Co. DOT	LRB (SEP)
Clackamas Connector	**1992**	OR	Milwaukee	ODOT	LRB (DIS)
Marquam Bridge	**1995**	OR	-	ODOT	FIP
Hood River Bridge	**1996**	OR	Hood River	ODOT	FIP
Hood River Bridge	**1996**	OR	Hood River	ODOT	NRB (SEP)
Sandy River Bridge	**1998**	OR	Sandy	ODOT	LRB (DIS)
Ferry Street Bridge	**1998**	OR	Eugene	ODOT	LRB (DIS)
Boones Bridge	**1999**	OR	Clackamas Co.	ODOT	EQS (RJW)
Grave Creek Bridge	**2000**	OR	Josephine Co.	ODOT	LRB (DIS)
E. Portland Fwy/Willamette R	**2000**	OR	Clackamas Co.	ODOT	LRB (SEP)
Frankport Viaduct	**2002**	OR	Near Ophir	ODOT	LRB (DIS)
Toll Plaza Rd Bridge, LR 145	**1990**	PA	Montgomery Co.	Pennsylvania Turnpike Commission	LRB (DIS)
Pennsylvania Turnpike	**1995**	PA	Chester Co.	-	LRB (DIS)

Penn DOT I-95	**1998**	PA	Bucks Co.	Penn DOT	EQS (RJW)
Schuykill River	**1999**	PA	Montgomery Co.	Pennsylvania Turnpike Commission	LRB (SEP)
Harvey Taylor Bridge	**2001**	PA	City of Harrisburg	Penn DOT	LRB (SEP)
Montebello Bridge	**1996**	PR	Puerto Rico	Puerto Rico Highway Authority	LRB & NRB (SEP)
Rio Grande Bridge	**1997**	PR	De Anansco	Puerto Rico Highway Authority	LRB & NRB (SEP)
Woonsocket Ind. Hwy / Blackstone R. Bridge	**1992**	RI	Woonsocket	RIDOT	LRB (DIS)
I-95 Providence Viaduct	**1992**	RI	Providence	RIDOT	LRB (DIS)
I-95 / Seekonk River Bridge	**1995**	RI	Pawtuckett	RIDOT	LRB (DIS)
I-295 to Rte 10, Bridges 662 & 663	**1996**	RI	Warwick / Cranston	RIDOT	LRB (SEP)
Court Street Bridge	**1999**	RI	Woonsocket	RIDOT	EQS (RJW)
Joseph Russo Mem. Bridge	**1999**	RI	Rhode Island	RIDOT	EQS (RJW)
Huntington Viaduct		RI	Rhode Island	RIDOT	EQS (RJW)
I-55 / Nonconnah Creek	**1999**	TN	Shelby Co.	TNDOT	LRB (SEP)
Fite Rd / Big Creek Canal	**2001**	TN	Shelby Co.	Shelby Co.	LRB (SEP)
I-40	**2001**	TN	Shelby Co.	Tennessee DOT	LRB (DIS)
I-40 Phase 2	**2002**	TN	Shelby Co.	Tennessee DOT	LRB (DIS)
I-15 Bridge 28	**1998**	UT	Salt Lake City	UDOT	LRB (DIS)
I-15 Bridge 26	**1999**	UT	Salt Lake City	UDOT	LRB (DIS)
US 1 / Chickahominy R.	**1996**	VA	Hanover-Hennico County Line	VDOT	LRB (DIS)
James River Bridge	**1999**	VA	-	VDOT	EQS (RJW)
Rte 5 / Ompompanoosuc R.	**1992**	VT	Norwich	Vermont Agency for Transportation	LRB (DIS)

I-405 / Cedar River Bridge	**1992**	WA	Renton	WSDOT	LRB (DIS)
Lacey V. Murrow Bridge, West Approach	**1992**	WA	Seattle	WSDOT	LRB (DIS)
SR 504 / Coldwater Creek Bridge No. 11	**1994**	WA	Mt. St. Helens Hwy	WSDOT	LRB (DIS)
SR 504 / East Creek Bridge No. 14	**1994**	WA	Mt. St. Helens Hwy	WSDOT	LRB (DIS)
Key Peninsula Hwy / Home Bridge	**1994**	WA	Home	Pierce Co. Public Works Road Dept.	LRB (DIS)
I-5 / Duwamish River Bridge	**1995**	WA	Seattle	WSDOT	LRB (DIS)
NE Carnation Farm Road / Snoqualmie River (Stossel Bridge)	**1996**	WA	Carnation	King County DOT	LRB (DIS)
Junita Drive NE / Sammamish River Bridge	**1996**	WA	West Kenmore	King County DOT	LRB (DIS)
University Bridge	**1997**	WA	Seattle	WSDOT	LRB (DIS)
Lakemount Blvd	**1997**	WA	Bellevue	City of Bellevue	LRB (SEP)
Bridge over County Road 3	**1993**	WV	Near Shinnston N. of Clarksburg	APSC	LRB (DIS)
West Fork River Bridge	**1994**	WV	Near Shinnston N. of Clarksburg	APSC	LRB (DIS)

Abbreviations

Caltrans California Department of Transportation
DIS Dynamic Isolation Systems
DOT Department of Transportation
EPS Earthquake Protection Systems
EQS EradiQuake Systems
FIP FIP-Energy Absorption Systems
FPS Friction Pendulum System
HDR High Damping Rubber
LRB Lead-Rubber Bearing
NRB Natural Rubber Bearing
RJW R. J. Watson
SEP Seismic Energy Products

APPENDIX B: EXAMPLES OF TESTING SPECIFICATIONS

B.1 EXAMPLE 1: PROTOTYPE AND PRODUCTION (PROOF) TESTING

Prototype and production (proof) test specimens of seismic isolation bearing systems shall be conditioned for 12 hours at 20° ± 8° C.

The following information shall be placed on prototype and proof tested seismic isolation bearings: production lot number, date of fabrication, design dead plus live load, and contract number.

The above information shall be stamped or etched on stainless steel plates and the plates shall be permanently attached to two of four sides of the bearing. The information may be stamped or etched directly to the sides of the metal portions of the bearing as long as markings are visible after, if required, surface is painted or galvanized.

Energy dissipators or other components in any bearing system which are permanently deformed during prototype and proof testing shall be replaced with identical dissipators or components.

B.1.1 Prototype Testing

A complete series of prototype tests shall be performed by the Contractor at the manufacturer's plant or at an approved laboratory in the presence of the Engineer, unless otherwise directed, on at least one full-sized specimen for each combination of maximum design lateral force or maximum design lateral displacement determined by the Engineer from the analysis and minimum energy dissipated per cycle (minimum EDC) shown on the plans. A total of at least two full-sized prototype specimens shall be constructed. Prototype tests may be performed on individual specimens or on pairs of specimens of the same size, at the Contractor's option. The prototype test bearings may be used in construction if they satisfy the project quality control tests after having successfully completed all prototype tests and upon the approval of the Engineer. Any prototype test bearings that fail any of the required tests shall be rejected and not incorporated into the work. For each cycle of tests the load, displacement, rotation, and hysteretic behavior of the prototype specimen shall be recorded.

Prototype Test 1. Twenty full reversed cycles of loads at the maximum non-seismic lateral load shown on the plans using a vertical load equal to dead load plus live load.

Prototype Test 2. Four full reversed cycles of loading at each of the following increments of the maximum design lateral displacement shown on the plans 1.0, 0.25, 0.50, 0.75, 1.0 and 1.1. The vertical load shall be the dead load.

Prototype Tests 3 and 4 shall be performed on seismic isolation bearing systems at a vertical load equal to the dead load as follows:

Prototype Test 3. Ten full reversed cycles at loadings not to exceed the maximum design lateral displacement shown on the plans.

Prototype Test 4. One full reversed cycle of loading at 1.5 times the maximum design lateral displacement shown on the plans.

A complete series of prototype tests shall satisfy the following conditions:

- The load-displacement plots of Prototype Tests 1, 2, 3 and 4 shall have a positive incremental lateral stiffness (load divided by displacement).
- At each displacement increment specified in Prototype Test 2, there shall be less than ±15 percent change from the average value of effective stiffness (K_{eff}) of the given test specimen over the required last three cycles of test. The energy dissipated per cycle (EDC), for each cycle, in Prototype Test 2 at 1.0 times the maximum design lateral displacement shown on the plans shall be equal to or greater than 90% of the value of the minimum EDC shown on the plans.
- The energy dissipated per cycle (EDC), for each cycle, in Prototype Test 3 shall be equal to or greater than 90% of the value of the minimum EDC shown on the plans.
- Specimens for Prototype Tests 1, 2 and 3 shall remain stable and without splits or fractures at all loading conditions.
- Specimens for Prototype Tests 4 shall remain stable at all loading conditions.

A complete series of prototype tests shall consist of either of the following combinations of prototype tests:

1. Prototype Tests 1, 2, 3, and 4, all performed on the same individual or pair of specimens.
2. Prototype Tests 1 and 3 performed on the same individual or pair of specimens combined with Prototype Tests 2 and 4 performed on another individual or pair of specimens.

If prototype tests are not performed at the period of vibration used in design of the seismic isolation bearing system, the Contractor shall perform additional physical tests in the presence of the Engineer, unless otherwise directed, to demonstrate that the requirements for hysteretic behavior are satisfied at the period of vibration used in design of the seismic isolation bearing system. The Contractor shall submit to the Engineer for approval a written procedure for performing the additional physical tests at least seven days prior to the start of prototype tests.

B.1.2 Proof Testing

Prior to installation of any seismic isolation bearing, the seismic isolation bearing systems shall be proof tested and evaluated by the Contractor at the manufacturer's plant or at an approved laboratory in the presence of the Engineer, unless otherwise directed, as follows:

Proof compression test: A five-minute sustained proof load test on each production bearing shall be required. The compressive load for the test shall be 1.5 times the maximum dead load plus live load at the design rotation. If bulging suggests poor laminate bond or the bearing demonstrates other signs of distress, the bearing will be rejected.

All seismic isolation bearing systems shall be proof tested in combined compression and shear as follows:

Each production bearing shall consist of the seismic isolation bearing systems designed for each combination of maximum design lateral displacement and associated minimum energy dissipated per cycle (minimum EDC). All the seismic isolation bearings to be used in the

work are to be proof tested. The tests may be performed on individual bearings or on pairs of bearings of the same size, at the Contractor's option.

Proof combined compression and shear test: The bearings shall be tested at a vertical load of 1.0 times the total of dead load plus live load shown on the plans and 5 full reversed cycles of loading at 0.5 times the maximum design lateral displacement as shown on the plans. The test results shall be within ±15 percent of values used in design of the seismic isolation bearing system.

Proof test seismic isolation bearing systems shall remain stable and without splits, fractures or other unspecified distress at all loading conditions.

The acceptance criteria for testing of a seismic isolation bearing system is as follows:

The seismic isolation bearing system shall satisfy all aspects of the prototype and proof tests.

The Contractor shall submit documentation indicating the replacement of any components which are replaced prior to final installation.

If a seismic isolation bearing that is prototype and proof tested fails to meet any of the acceptance criteria for testing as determined by the Engineer, then that seismic isolation bearing will be rejected and the Contractor shall modify the design or construction procedures and submit revised working drawings including these modifications and prototype test another seismic isolation bearing from the same system, or abandon the seismic isolation bearing system and test another prototype from another seismic isolation bearing system. Seismic isolation bearing prototype testing operations shall not begin until the Engineer has approved the revised working drawings in writing. No extension of time or compensation will be made for modifying working drawings and testing additional seismic isolation bearing systems.

B1.3 Test Submittals

At the completion of a prototype or proof test, the Contractor shall submit to the Engineer four copies of the complete test results for the seismic isolation bearings tested. Data for each test shall list key personnel, test loading equipment, type of seismic isolation bearing, location of test, complete record of load, displacement, rotation, hysteretic behavior and period of load application for each cycle of test. The seismic isolation bearing cyclic loadings for, first, the unscragged condition and then the scragged condition, as shown in the Prototype Test 2, shall be included in the test data.

B.2 EXAMPLE 2: PROTOTYPE AND PRODUCTION (PROOF) TESTING

B.2.1 General

Prototype and production test specimens of bearings shall be conditioned for 12 hours at 20 +/-8 degrees Celsius prior to testing, and the ambient temperature shall be maintained at 20 +/- 8 degrees Celsius during testing.

Bearings may be tested individually or in pairs. When tested in pairs, the test report shall identify the tested pairs and shall report the average results for each pair.
At the completion of a prototype or production test, the Contractor shall submit to the Engineer eight (8) copies of the complete test results for the bearings tested. Data for each test shall list location of test, key personnel, test loading equipment, type of bearing, complete record of load, displacement, hysteretic behavior and period of load application for each cycle of test.

During prototype and production tests, each bearing shall be closely inspected for lack of rubber to steel bond, laminate placement faults, and surface cracks wider or deeper than 0.08 inches. Any bearing showing such signs may be subject of rejection by the Engineer of Record.

The Engineer of Record or a representative of the Engineer, at the Contractor's expense, shall observe prototype tests unless the requirement is waived by the Engineer following the implementation of an acceptable test observation program.

Bearings used in prototype testing may be used for construction if they are tested and pass the production (proof) testing.

B.2.2 Prototype Testing

A series of tests shall be performed in the presence of the Engineer, unless otherwise directed, on at least two (2) full-sized specimens for each of the two bearing types designated in the Contract Plans. The bearings must satisfy the performance criteria shown in this document and as defined in the accepted working drawings and their supplements.

Prototype tests shall be performed on individual specimens. Depending on the capabilities of the testing machines, bearings may be tested in pairs and the average test results may be reported for the two bearings. However, in such a case four (4) full-sized bearings shall be tested.

The tests shall be performed at a laboratory approved by the Engineer. Such laboratories include:

1. Laboratory of the Supplier provided that the equipment, instruments, data acquisition systems, and testing methodologies are approved by the Engineer.
2. The Seismic Response Modification Device Testing Machine Laboratory at the University of California, San Diego, CA.
3. The Structural Engineering and Earthquake Simulation Laboratory at the University at Buffalo, State University of New York, Buffalo, NY.

Prototype testing shall consist of the following tests conducted in the sequence they are described:

1. Each of the two bearings of each type (or each of the four bearings of each type when part of testing is conducted in pairs) shall be compressed for five (5) minutes under load not less than 1.5 times the maximum dead (DL) plus maximum live load (LL) shown in the Contract Plans and in Table 1 herein. The bearing shall be observed for bulging and other signs of defects or distress. If bulging or other signs of distress or defects are observed, the bearing shall be rejected. When the bearing passes the proof compression tests, it shall be subjected to five (5) cycles of compressive load from zero to a value equal to the average dead load (DL) plus average seismic live load (LL) shown in table 1 herein, and then return to zero. The compressive load and average vertical displacement (based on measurements of vertical displacement at three or more points) of the bearing shall be recorded, plotted, and used to measure the compression stiffness of the bearing.

2. Each bearing (or each pair of bearings) of each type shall be subjected to the following combined compression and shear tests:
    a. Thermal Test as described in 13.2 (b) (1) of the 1999 AASHTO Guide Specifications for Seismic Isolation Design. The vertical load shall be the average dead load (DL) plus the average live load (LL) and the displacement amplitude shall be three (3) inch. The velocity of testing shall not exceed 0.04 in/sec, or the frequency of testing shall not exceed 1/300 Hz. The lateral force and lateral displacement shall be continuously recorded and plotted against each other. The bearing shall satisfy for each cycle the criteria for non-seismic effective stiffness and EDC shown in the Contract Plan and in table 1.

    b. Seismic Test as described in 13.2 (b) (4) for 15 cycles under vertical load equal to the average dead load (DL) plus the average seismic live load (LL) and the displacement amplitude shall be four and half (4.5) inch. The test shall be conducted over five (5) cycles followed by idle time, allowing for the bearing to cool down, and then repeating twice for a total of 15 cycles. The test shall be conducted at a frequency equal to the inverse of the effective period shown in the Contract Plans and in Table 1, however, the peak velocity need not exceed 10 in/sec. The bearing shall satisfy for each of the 5-cycle sub-tests the criteria for seismic effective stiffness and EDC (maximum and minimum values) shown in the Contract Plans and in Table 1. Testing under the described dynamic conditions may not be possible either due to significant limitations of available machines (e.g., machines of suppliers) or the low level of lateral forces and displacements by comparison to capacity of machines (e.g., SRMD machine at UC, San Diego). In that case, a compromise may be accepted by the Engineer in which the smaller Type 2 bearing may be tested under dynamic conditions as described herein. The larger Type 1 bearing may be tested quasi-statically and the results adjusted using the velocity property modification factor. This factor needs to be determined by testing of bearings Type 2.

3. One bearing or one pair of bearings (if tested in pairs) of either Type 1 or Type 2 shall be subjected to Wear and Fatigue Testing as described in the 1999 AASHTO Guide Specifications for Seismic Isolation Design, Article 13.1.2. The bearing (or bearings) shall

be compressed to load equal to the average deal load (DL) plus average live load (LL), displacement amplitude of one (1) inch and total movement (travel) of one (1) mile.

Following the Wear and Fatigue Test, the bearing (or bearings) shall be subjected to the thermal and seismic tests of item two (2) above and satisfy the criteria of the Contract Plans and of Table B-1. The Wear and Fatigue Test may be waived if the test had been previously conducted on similar size bearings and test data are available. Tests on rubber coupons or on bearings, without a lead core are not acceptable.

Specimens for all prototype tests shall remain stable and without splits or fractures under all loading conditions.

The Contractor shall perform any additional physical tests as directed by the Engineer in the presence of the Engineer, to demonstrate that the requirements shown in the Contract Plans for hysteretic behavior are satisfied. The Contractor shall submit to the Engineer for approval a written procedure for performing the additional physical test at least 14 days prior to the start of prototype tests.

If a bearing that is prototype tested fails to meet any of the acceptance criteria, said bearing shall be rejected. If rejected, the Contractor shall modify the bearing design or manufacturing procedures and submit revised working drawings, which include the modifications, and shall repeat the prototype tests on another bearing from the same design. Bearing prototype testing operations shall not begin until the Engineer has accepted the revised working drawings in writing. No extension of time or compensation will be made for modifying working drawings or supplemental calculations for re-submittal and review of working drawings and supplemental calculations due to rejection of a proposed bearing system, and designing and testing additional systems.

B2.3 Production (Proof) Testing

Prior to installation of any bearing, the bearings shall be proof tested and evaluated at an approved laboratory in the presence of the Engineer, unless otherwise directed. The tests may be performed on individual bearings or on pairs of bearings of the same size, at the Contractor's option.

All bearings shall be proof tested as follows:

1. *Proof Compression Test:* A five (5)-minute sustained proof load test on each production bearing shall be required. The compressive load for the test shall be 1.5 times the sum of the maximum dead load plus maximum live load (DL+LL) shown in the Contract Plans and in table 1. If bulging suggests poor laminate bond or the bearing demonstrates other signs of distress, the bearing will be rejected.
2. *Proof Combined Compression and Shear Test:* Five (5) fully reversed cycles of loading at displacement amplitude equal to 4.5 inch. The compressive load for the test shall be one (1.0) times the average dead load plus the average seismic live load shown in the Contract Plans and in table 1. Each bearing shall satisfy the criteria for seismic effective stiffness

and EDC (maximum for first cycle and minimum for fifth cycle) shown in the Contract Plans and in table B-1.

Proof tested bearings shall remain stable and without splits, fractures, or other unspecified distress under all loading conditions.

Table B-1. Isolator Performance Criteria

BEARING TYPE	**Type 1**	**Type 2**
Min. Vertical Compression Stiffness (kip/in)	13,000	6,500
Min. Non-Seismic Effective Stiffness (kip/in) at displ. = 3 in	22	16
Max. Non-Seismic Effective Stiffness (kip/in) at displ. = 3 in	30	22
Min. Non-Seismic EDC (kip-in) at displ. = 3 in	300	200
Max. Non-Seismic EDC (kip-in) at displ. = 3in	440	350
Seismic Effective Stiffness (kip/in) at displ. = 4.5 in		
First Cycle (maximum value)	42	32
Fifth Cycle (minimum value)	23	16
Seismic EDC (kip-in) at displ. = 4.5 in		
First Cycle (Maximum value)	1,950	1,540
Fifth Cycle (Minimum value)	900	700
Vertical Compressive Load (kip)		
Max. DL	1,725	725
Average DL	1,300	520
Max. LL	555	340
Average LL	480	270
Average Seismic LL	240	135
Max. Seismic Down	370	150
Effective Period (sec)	1.8	1.8

Notes: 1. Non-seismic conditions are defined as those for which the frequency does not exceed 1/300 Hz, or equivalently, the velocity in a constant velocity test does not exceed 0.04 in/sec.
2. Seismic conditions are defined as those for which the frequency equals to the inverse of the effective period, or the peak velocity in a sinusoidal test is not less than 10 in/sec.
3. Vertical stiffness to be measured in experiment under quasi-static conditions.

The material herein is based upon work supported in whole or in part by the Federal Highway Administration, New York State and other sponsors. Opinions, findings, conclusions or recommendations expressed in this publication do not necessarily reflect the views of these sponsors or the Research Foundation of the State of New York.

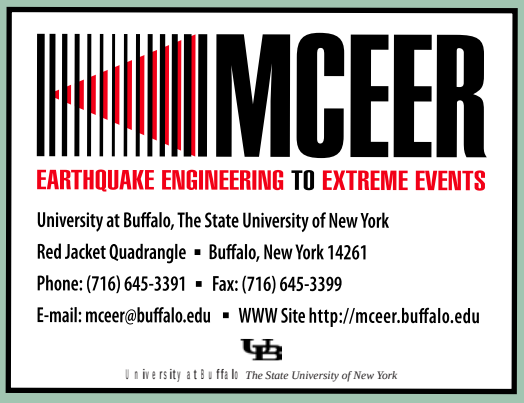
MCEER
EARTHQUAKE ENGINEERING TO EXTREME EVENTS
University at Buffalo, The State University of New York
Red Jacket Quadrangle ▪ Buffalo, New York 14261
Phone: (716) 645-3391 ▪ Fax: (716) 645-3399
E-mail: mceer@buffalo.edu ▪ WWW Site http://mceer.buffalo.edu
University at Buffalo The State University of New York